PROGRAMA DE DOCTORADO EN INGENIERÍA QUÍMICA Y AMBIENTAL

TESIS DOCTORAL:

Innovative technologies for biogas upgrading

Presentada por **David Fernando Marín De Jesus** para optar al grado de
Doctor por la Universidad de Valladolid

Dirigida por:
Dr. Raúl Muñoz Torre
Dra. Raquel Lebrero Fernández

Resumen

El biogás procedente de la digestión anaerobia de aguas residuales o residuos sólidos orgánicos representa una fuente de energía renovable importante para mitigar el uso de los combustibles fósiles. La purificación de biogás es necesaria antes de su utilización como combustible para vehículos o su inyección en las redes de gas natural. En este contexto, existen diversas normativas internacionales que establecen las concentraciones máximas y mínimas para cada componente del biometano permitidas en función de su aplicación final. Actualmente se dispone de una gran variedad de tecnologías físico-químicas y biológicas comerciales para eliminar el CO_2 y el H_2S del biogás. Sin embargo, la mayoría de estas tecnologías deben ser implementadas secuencialmente para eliminar el H_2S, el CO_2 y contaminantes traza como los siloxanos o los contaminantes orgánicos volátiles. En este sentido, esta tesis se centra en el estudio de nuevas tecnologías que permitan la remoción simultánea de H_2S y CO_2 del biogás en un proceso de una sola etapa, de una forma sostenible y con bajos costes de operación.

El estado del arte de las tecnologías de tratamiento de biogás se presenta en la sección de **Introduction**. Los objetivos, estrategias y desarrollo seguidos en esta tesis se resumen en la sección **Aims and Scope**.

En el **Capítulo 1**, la bioconversión de biogás en biometano junto con el tratamiento simultáneo de digestato se evaluó durante los meses de verano en un fotobiorreactor exterior de algas-bacterias del tipo high rate algal pond (HRAP) interconectado a una columna de absorción (AC) externa de CO_2-H_2S mediante la recirculación del caldo de cultivo. La eficiencia de eliminación del CO_2 osciló entre el 50 y el 95%, dependiendo de la alcalinidad del caldo de cultivo y de las condiciones ambientales, mientras que se logró una eliminación completa del H_2S independientemente de las condiciones operacionales. Se registró una concentración máxima de CH_4 del 94%, con una desorción limitada de O_2 y N_2, en el biometano para ratios líquido-biogás (L/G) en la AC de 1 y 2. La operación del proceso a una productividad constante de biomasa de 15 g m^{-2} d^{-1} (controlada mediante la purga del sedimentador) y la minimización de la generación de efluentes permitieron altas recuperaciones de carbono y nutrientes en la biomasa cosechada (C = 66±8%, N = 54±18%, P ≈ 100% y S = 16±3%). Por último, la baja diversidad observada

en la estructura de la población de microalgas se debió muy probablemente a las extremas condiciones ambientales y operacionales impuestas.

En el **Capítulo 2** se evaluó la influencia del tipo de difusor y la relación L/G en el rendimiento de mejora del biogás en un fotobiorreactor exterior del tipo HRAP. Se evaluaron cuatro tipos diferentes de difusores para mejorar la calidad del biometano (metálico de 2 μm, de piedra porosa, y dos membranas cerámicas tubulares de 0.2 y 0.4 μm). Cada tipo de difusor se probó de forma independiente utilizando tres relaciones L/G diferentes (0.5, 1 y 2). No se registró ninguna diferencia significativa en las concentraciones de CH_4 del biometano (> 93.0%) al trabajar con los diferentes tipos de difusores con relaciones L/G > 1. El difusor de biogás metálico fue el único que proporcionó concentraciones de CH_4 superiores al 94.0% a una relación L/G de 0.5. El aumento de la relación L/G conllevó un mayor stripping del N_2 y O_2 disuelto al biogás, lo que compensó la disminución en la concentración de CO_2 debido al mayor valor de pH de la solución en la columna de absorción. Un análisis de varianza (ANOVA) de los resultados obtenidos confirmó que tanto el tipo de difusor de biogás como la relación L/G determinan significativamente la calidad del biogás mejorado.

En los **Capítulos 3 y 4** se evaluó por primera vez la influencia de la variación estacional en el tratamiento del biogás junto con el tratamiento del digestato en un fotobiorreactor exterior de algas-bacterias. En el **Capítulo 3**, las variaciones anuales en la calidad del biogás tratado y la eficiencia del tratamiento del digestato se evaluaron en un HRAP exterior interconectado a una AC externa a través de un sedimentador cónico. Las concentraciones de CO_2 en el biogás tratado oscilaron entre 0.7% en Agosto y 11.9% en Diciembre, mientras que se alcanzó una eliminación completa de H_2S independientemente del mes de operación. Las concentraciones de CH_4 variaron entre el 85.2% en Diciembre y el 97.9% en Junio, con una limitada desorción de O_2 y N_2 en el biogás tratado debido a la baja relación L/G de recirculación en la AC. Por último, la diversidad de microalgas se redujo considerablemente a lo largo del año debido a la creciente salinidad del caldo de cultivo del HRAP, debido al modo de operación del proceso (en ausencia de efluente). Por otra parte, en el **Capítulo 4** se evaluó la influencia de las variaciones diarias y estacionales de las condiciones ambientales en la calidad del biometano. La elevada alcalinidad en el caldo de cultivo dio lugar a una composición

constante de biometano durante el día, independientemente del mes de operación, mientras que la elevada actividad de las algas durante primavera y verano potenció un aumento en la calidad del biometano. Las concentraciones de CO_2 en el biogás tratado oscilaron entre el 0.1% en Mayo y el 11.6% en Diciembre, mientras que se logró una completa eliminación de H_2S independientemente del mes de operación. La desorción de N_2 y O_2 al biogás tratado se mantuvo baja debido a la relación L/G de 1 de operación de la AC. Finalmente, la concentración de CH_4 en el biogás tratado osciló entre el 85.6% en Diciembre y el 99.6% en Agosto.

En el **Capítulo 5** se evaluaron tres estrategias de operación innovadoras para mejorar la calidad del biometano en condiciones ambientales desfavorables y sin aporte externo de alcalinidad en un fotobiorreactor exterior del tipo HRAP interconectado a una AC externa: i) el uso de un invernadero durante condiciones invernales, ii) una desorción directa del CO_2 en el HRAP mediante stripping con aire durante condiciones invernales y iii) el uso del digestato como agua de reposición durante las condiciones de verano. Las concentraciones de CO_2 en el biometano oscilaron entre 0.4% y 6.1% durante la operación con invernadero, entre 0.3% y 2.6% cuando se inyectó aire en el HRAP y entre 0.4% y 0.9% utilizando digestato como agua de reposición. El H_2S fue eliminado completamente en todas las estrategias probadas. Por otro lado, las concentraciones de CH_4 en el biometano oscilaron entre 89.5% y 98.2%, entre 93.0% y 98.2% y entre 96.3% y 97.9%, cuando se aplicaron las estrategias i), ii) y iii), respectivamente. El invernadero fue capaz de mantener una productividad algal de 7.5 g m^{-2} d^{-1} en invierno bajo clima continental, mientras que la desorpción directa de CO_2 con aire aumentó el pH, lo que favoreció una eliminación efectiva de CO_2 y H_2S. Por último, las altas tasas de evaporación en verano permitieron mantener altas concentraciones de carbono inorgánico en el caldo de cultivo mediante el uso de digestato como agua para compensar evaporación, lo que proporcionó una mejora en la calidad del biometano.

En el **Capítulo 6**, la influencia del ratio L/G y la alcalinidad en el rendimiento del tratamiento de biogás fueron evaluadas en un fotobiorreactor exterior horizontal tubular semi-cerrado de 11.7 m^3 interconectado a una AC de 45 L. Las concentraciones de CO_2 en el biometano tratado oscilaron entre <0.1 y 9.6% a una relación L/G de 2.0 y 0.5, respectivamente, con concentraciones máximas de CH_4 de 89.7% a una relación L/G de

1.0. Además, se observó una mayor eliminación de CO_2 (que conllevó una disminución de la concentración de CO_2 de 9.6 a 1.2%) y, por consiguiente un mayor contenido de CH_4 (aumentando de 88.0 a 93.2%), al aumentar la alcalinidad del caldo de cultivo en la AC de 42 ± 1 mg L^{-1} a 996 ± 42 mg IC L^{-1}. El H_2S se eliminó completamente independientemente del L/G o alcalinidad en la AC. La operación del fotobiorreactor en continuo con los parámetros de funcionamiento optimizados resultó en concentraciones de CO_2 (<0.1%-1.4%), H_2S (<0.7 mg m^{-3}) y CH_4 (94.1%-98.8%) acordes a normativas internacionales para la inyección de biometano en redes de gas natural.

En el **Capítulo 7** se evaluó el potencial de las bacterias fototróficas púrpuras (PPB) para el tratamiento simultáneo de aguas residuales de la cría de cerdo (PWW) y biogás en fotobiorreactores cerrados. La dilución de PWW se identificó como un parámetro clave en la eficiencia del tratamiento de las aguas residuales y en la calidad del biometano generado en fotobiorreactores de PPB bajo irradiación infrarroja. La dilución del agua residual cuatro veces conllevó las remociones de carbono orgánico total (TOC) y de nitrógeno total más eficientes (78% y 13%, respectivamente), con concentraciones de CH_4 del 90.8%. Se investigó la influencia de la concentración de fósforo (adición de 50 mg L^{-1} de $P-PO_4^{3-}$) en el tratamiento simultaneo de PWW y biogás con PPB. Se obtuvieron remociones de TOC de $\approx$ 60% y concentraciones de CH_4 de $\approx$ 90.0% independientemente del aporte de fósforo. Por último, el uso de PPB y consorcios alga-bacteria permitió obtener concentraciones de CH_4 en el biogás tratado de 93.3% y 73.6%, respectivamente, lo que confirmó el potencial de las PPB para el tratamiento simultáneo de biogás y PWW.

Por último, en el **Capítulo 8** se evaluó el potencial de un nuevo proceso basado en el uso de una solución de Fe/EDTA/carbonatada para la eliminación simultánea del H_2S y el CO_2 del biogás en una columna de absorción de 1.8 L interconectada a una columna de regeneración de 2.0 L. Este trabajo evaluó la influencia de la molaridad de la solución Fe/EDTA (M), la concentración de carbonato (IC) y los flujos de biogás (B), aire (A) y líquido (L) en el rendimiento del tratamiento de biogás utilizando un diseño experimental Taguchi $L_{16}(4^5)$. El ANOVA demostró que la molaridad de la solución de Fe/EDTA fue un factor significativo determinante en la concentración de H_2S. La concentración de carbono inorgánico impactó en las concentraciones de CO_2, N_2 y CH_4, y los flujos de

biogás y de líquido de recirculación afectaron el contenido de CO_2, O_2, N_2 y CH_4. Finalmente, el flujo de aire en la columna de regeneración impactó en las concentraciones de CO_2, H_2S, N_2 y CH_4. La optimización del proceso mediante el análisis del efecto de la interacción entre M e IC proporcionó las condiciones óptimas para cada factor de control. El funcionamiento en continuo del proceso de purificación de biogás con niveles de M de 0.05 M, IC de 10000 mg L^{-1}, y flujos de B, A y L de 10 mL min^{-1}, 1000 mL min^{-1} y 30 mL min^{-1}, respectivamente, proporcionaron una concentración de CH_4 de 97.4% en el biogás tratado, con niveles muy bajos de CO_2, O_2, N_2 y H_2S (1.4, 0.29, 0.97 y 0%, respectivamente), lo que cumple con la mayoría de las normativas internacionales sobre biometano.

Los resultados obtenidos en la presente tesis confirmaron el potencial del proceso fotosintético de purificación de biogás en condiciones exteriores como una herramienta sostenible, eficiente y de bajo coste para el tratamiento de biogás. Además, esta tesis doctoral proporcionó dos pruebas de concepto de nuevas tecnologías físico-químicas y biológicas para la purificación de biogás.

Abstract

The biogas from the anaerobic digestion of wastewaters or organic solid waste represents a key renewable energy vector in order to mitigate the use of fossil fuels. Biogas upgrading is required prior use as a vehicle fuel or injection into natural gas networks. In this context, several international regulations exist setting the maximum and minimum allowed concentrations of each biomethane component depending on its final application. Multiple physical-chemical and biological technologies are nowadays commercially available in order to remove CO_2 and H_2S from biogas. However, most of these technologies must be sequentially implemented to remove both H_2S, CO_2 and trace contaminants such as siloxanes or volatile organic contaminants. In this sense, this thesis focuses on the study of new technologies supporting the simultaneously removal of H_2S and CO_2 from biogas in a single step process, in a sustainable manner and with low operating costs.

The state-of-the-art of biogas upgrading technologies is presented in the **Introduction** section. The objectives, approach and strategies followed in this thesis are summarized in the **Aims and Scope** section.

In **Chapter 1**, the bioconversion of biogas to biomethane coupled to centrate treatment was evaluated during summer time in an outdoors pilot scale high rate algal pond (HRAP) interconnected to an external CO_2-H_2S absorption column (AC) via settled broth recirculation. CO_2-removal efficiencies ranged from 50 to 95% depending on the alkalinity of the cultivation broth and environmental conditions, while a complete H_2S removal was achieved regardless of the operational conditions. A maximum CH_4 concentration of 94%, along with a limited O_2 and N_2 stripping, were recorded in the upgraded biogas at recycling liquid-to-biogas (L/G) ratios in the AC of 1 and 2. Process operation at a constant biomass productivity of 15 g m^{-2} d^{-1} (controlled via settler waste) and the minimization of effluent generation supported high carbon and nutrient recoveries in the harvested biomass (C = 66±8%, N = 54±18%, P ≈ 100% and S = 16±3%). Finally, the low diversity in the structure of the microalgae population was likely due to harsh environmental and operational conditions imposed.

In **Chapter 2**, the influence of the diffuser type and L/G ratio on biogas upgrading performance in an outdoor pilot scale HRAP was evaluated. Four different types of biogas diffusers (metallic of 2 μm, porous stone, and two ceramic tubular membranes of 0.2 and 0.4 μm) were evaluated to improve the quality of biomethane. Each type of diffuser was tested independently using three different L/G ratios (0.5, 1 and 2). No significant difference was recorded in the CH_4 concentrations of biomethane (i.e. > 93.0%) working with the different types of diffusers at L/G ratios > 1. Only the metallic biogas diffuser supported CH_4 concentrations higher than 94.0% at a L/G ratio of 0.5. The increase in L/G ratio induced the stripping of the dissolved N_2 and O_2 into the biogas, which compensated the decrease in CO_2 concentration mediated by the higher pH value of the scrubbing solution in the absorption column. An analysis of variance (ANOVA) of the results here obtained confirmed that both the type of biogas diffuser and the L/G ratio significantly determined the quality of the upgraded biogas.

Chapters 3 and 4 evaluated for the first time the influence of seasonal variation on biogas upgrading coupled with digestate treatment in an outdoors pilot scale algal-bacterial photobioreactor. In **Chapter 3**, the yearly variations of the quality of the upgraded biogas and the efficiency of digestate treatment were evaluated in an outdoors pilot scale HRAP interconnected to an external AC via a conical settler. CO_2 concentrations in the upgraded biogas ranged from 0.7% in August to 11.9% in December, while a complete H_2S removal was achieved regardless of the operational month. CH_4 concentrations ranged from 85.2% in December to 97.9% in June, with a limited O_2 and N_2 stripping in the upgraded biogas mediated by the low recycling L/G ratio in the AC. Finally, microalgae diversity was severely reduced throughout the year likely due to the increasing salinity in the cultivation broth of the HRAP induced by process operation in the absence of effluent. On the other hand, in **Chapter 4**, the influence of the daily and seasonal variations of environmental conditions on biomethane quality was evaluated. The high alkalinity in the cultivation broth resulted in a constant biomethane composition during the day regardless of the monitored month, while the high algal-bacterial activity during spring and summer boosted a superior biomethane quality. CO_2 concentrations in the upgraded biogas ranged from 0.1% in May to 11.6% in December, while a complete H_2S removal was always achieved regardless of the month. A limited N_2 and O_2 stripping from the scrubbing cultivation broth was recorded in the upgraded biogas at a recycling L/G ratio in the AC

of 1. Finally, CH_4 concentration in the upgraded biogas ranged from 85.6% in December to 99.6% in August.

In **Chapter 5**, three innovative operational strategies to improve the quality of biomethane under unfavorable environmental conditions and without external alkalinity supplementation were evaluated in an outdoors pilot scale HRAP interconnected to an external AC: i) the use of a greenhouse during winter conditions, ii) a direct CO_2 stripping in the HRAP via air stripping during winter conditions and iii) the use of digestate as make-up water during summer conditions. CO_2 concentrations in the biomethane ranged from 0.4% to 6.1% using the greenhouse, from 0.3% to 2.6% when air was injected in the HRAP and from 0.4% to 0.9% using digestate as make up water. H_2S was completely removed under all strategies tested. On the other hand, CH_4 concentrations in biomethane ranged from 89.5% to 98.2%, from 93.0% to 98.2% and from 96.3% to 97.9%, when implementing strategies i), ii) and iii), respectively. The greenhouse was capable of maintaining microalgae productivities of 7.5 g m^{-2} d^{-1} during winter under continental weather conditions, while mechanical CO_2 stripping increased the pH in order to support an effective CO_2 and H_2S removal. Finally, the high evaporation rates during summer conditions allowed maintaining high inorganic carbon concentrations in the cultivation broth using centrate as make-up water, which provided a cost effective biogas upgrading.

In **Chapter 6**, the influence of L/G ratios and alkalinity on the biogas upgrading performance was evaluated in a 11.7 m^3 outdoors horizontal semi-closed tubular photobioreactor interconnected to a 45 L AC. CO_2 concentrations in the upgraded biomethane ranged from <0.1 to 9.6% at L/G of 2.0 and 0.5, respectively, with maximum CH_4 concentrations of 89.7% at a L/G of 1.0. Moreover, an enhanced CO_2 removal (mediating a decrease in CO_2 concentration from 9.6 to 1.2%), and therefore higher CH_4 contents (increasing from 88.0 to 93.2%), were observed when increasing the alkalinity of the AC cultivation broth from 42±1 mg L^{-1} to 996±42 mg IC L^{-1}. H_2S was completely removed regardless of the L/G or the alkalinity in AC. The continuous operation of the photobioreactor with optimized operating parameters resulted in contents of CO_2 (<0.1%- 1.4%), H_2S (<0.7 mg m^{-3}) and CH_4 (94.1%-98.8%) complying with international regulations for biomethane injection into natural gas grids.

In **Chapter 7**, the potential of purple phototrophic bacteria (PPB) for the simultaneous treatment of piggery wastewater (PWW) and biogas upgrading was evaluated batchwise in gas-tight photobioreactors. PWW dilution was identified as a key parameter determining the efficiency of wastewater treatment and biomethane quality in PPB photobioreactors illuminated with infrared radiation. Four times diluted PWW supported the most efficient total organic carbon (TOC) and total nitrogen removals (78% and 13%, respectively), with CH_4 concentrations of 90.8%. The influence of phosphorous concentration (supplementation of 50 mg L^{-1} of $P-PO_4^{3-}$) on PPB-based PWW treatment coupled to biogas upgrading was investigated. TOC removals of $\approx$ 60% and CH_4 concentrations of $\approx$ 90.0% were obtained regardless of phosphorus supplementation. Finally, the use of PPB and algal-bacterial consortia supported CH_4 concentrations in the upgraded biogas of 93.3% and 73.6%, respectively, which confirmed the potential PPB for biogas upgrading coupled to PWW treatment.

Finally, **Chapter 8** evaluated the potential of a novel Fe/EDTA/carbonate-based scrubbing process for the simultaneous removal of H_2S and CO_2 from biogas in a 1.8 L absorption column interconnected to a 2.0 L air-aided regeneration column. This work evaluated the influence of Fe/EDTA molarity (M), carbonate concentration (IC), and biogas (B), air (A) and liquid (L) flow rates on biogas upgrading performance using a Taguchi $L_{16}(4^5)$ experimental design. The ANOVA demonstrated that the molarity of the Fe/EDTA solution was a significant factor influencing H_2S concentration. The inorganic carbon concentration impacted on the concentrations of CO_2, N_2 and CH_4, and the biogas and recycling liquid flow rates affected CO_2, O_2, N_2 and CH_4 content. Finally, the air flow rate in the regeneration column impacted on CO_2, H_2S, N_2 and CH_4 concentrations. Process optimization via analysis of the effect of the interaction between M and IC provided the optimal conditions for each control factor. Continuous biogas upgrading operation at M of 0.05 M, IC of 10000 mg L^{-1}, and B, A and L flow rates of 10 mL min^{-1}, 1000 mL min^{-1} and 30 mL min^{-1}, respectively, provided a CH_4 concentration of 97.4% in the upgraded biogas with very low levels of CO_2, O_2, N_2 and H_2S (1.4, 0.29, 0.97 and 0%, respectively), which fulfilled with most international biomethane regulations.

The results obtained in the present thesis confirmed the potential of photosynthetic biogas upgrading under outdoors conditions as a cost-effective and sustainable tool for the

upgrading of biogas. In addition, this thesis provided two proofs of concept of new physical/chemical and biological technologies for biogas upgrading.

List of publications

The following publications are presented as part of the present thesis. All of them are published in international journals indexed in Journal Citation Reports.

Paper I. Esther Posadas, **David Marín**, Saúl Blanco, Raquel Lebrero, Raúl Muñoz (2017) *Simultaneous biogas upgrading and centrate treatment in an outdoors pilot scale high rate algal pond*. Bioresource Technology 232: 133-141.

Paper II. **David Marín**, Alessandro A. Carmona-Martínez, Raquel Lebrero, Raúl Muñoz (2020) *Influence of the diffuser type and liquid-to-biogas ratio on biogas upgrading performance in an outdoors pilot scale high rate algal pond*. Fuel 275: 117999.

Paper III. **David Marín**, Esther Posadas, Patricia Cano, Victor Pérez, Saúl Blanco, Raquel Lebrero, Raúl Muñoz (2018) *Seasonal variation of biogas upgrading coupled with digestate treatment in an outdoors pilot scale algal-bacterial photobioreactor*. Bioresource Technology 263: 58-66.

Paper IV. **David Marín**, Esther Posadas, Patricia Cano, Víctor Pérez, Raquel Lebrero, Raúl Muñoz (2018) *Influence of the seasonal variation of environmental conditions on biogas upgrading in an outdoors pilot scale high rate algal pond*. Bioresource Technology 255: 354-358.

Paper V. **David Marín**, Alessandro A. Carmona-Martínez, Saúl Blanco, Raquel Lebrero, Raúl Muñoz (2021) *Innovative operational strategies in photosynthetic biogas upgrading in an outdoors pilot scale algal-bacterial photobioreactor*. Chemosphere 264: 128470.

Paper VI. **David Marín**, Antonio Ortíz, Rubén Díez-Montero, Enrica Uggetti, Joan García, Raquel Lebrero, Raúl Muñoz (2019) *Influence of liquid-to-biogas ratio and alkalinity on the biogas upgrading performance in a demo scale algal-bacterial photobioreactor*. Bioresource Technology 280: 112-117.

Paper VII.   **David Marín**, Esther Posadas, Dimas García, Daniel Puyol, Raquel Lebrero, Raúl Muñoz (2019) *Assessing the potential of purple phototrophic bacteria for the simultaneous treatment of piggery wastewater and upgrading of biogas*. Bioresource Technology 281: 10-17.

Paper VIII. **David Marín**, Marisol Vega, Raquel Lebrero, Raúl Muñoz (2020) *Optimization of a novel chemical scrubbing process based on a Fe-EDTA-carbonate based solvent for the simultaneous removal of CO_2 and H_2S from biogas*. Journal of Water Process Engineering 37: 101476.

Contribution to the papers included in the thesis

Paper I. In this work, I was responsible of the start-up and operation of the experimental set-up in collaboration with Dr. Esther Posadas under the supervision of Dr. Raquel Lebrero and Dr. Raúl Muñoz. I performed the results evaluation and part of the manuscript writing in collaboration with Dr. Esther Posadas under the supervision of Dr. Raquel Lebrero and Dr. Raúl Muñoz. Dr. Saúl Blanco was responsible of the characterization of the microalgal populations, where I contributed in the data analysis and discussion.

Paper II. In this work, I was responsible of the design, start-up and operation of the experimental set-up under the supervision of Dr. Raquel Lebrero and Dr. Raúl Muñoz. I performed the mass balance calculations, results evaluation and manuscript writing under the supervision of Dr. Alessandro Carmona, Dr. Raquel Lebrero and Dr. Raúl Muñoz.

Paper III. In this work, I was responsible of the design, start-up and operation of the experimental set-up in collaboration with Eng. Patricia Cano, MSc Eng. Victor Pérez and Dr. Esther Posadas under the supervision of Dr. Raquel Lebrero and Dr. Raúl Muñoz. I performed the mass balance calculations, results evaluation and manuscript writing under the supervision of Dr. Esther Posadas, Dr. Raquel Lebrero and Dr. Raúl Muñoz. Dr. Saúl Blanco was responsible of the characterization of the microalgal populations, where I contributed in the data analysis and discussion.

Paper IV. In this work, I was responsible of the design, start-up and operation of the experimental set-up in collaboration with Eng. Patricia Cano, MSc Eng. Victor Pérez and Dr. Esther Posadas under the supervision of Dr. Raquel Lebrero and Dr. Raúl Muñoz. I performed the mass balance calculations, results evaluation and manuscript writing under the supervision of Dr. Esther Posadas, Dr. Raquel Lebrero and Dr. Raúl Muñoz.

Paper V. In this work, I was responsible of the design, start-up and operation of the experimental set-up under the supervision of Dr. Raquel Lebrero and Dr. Raúl Muñoz. I performed the mass balance calculations, results evaluation and manuscript writing under the supervision of Dr. Alessandro Carmona, Dr. Raquel Lebrero and Dr. Raúl Muñoz. Dr.

Saúl Blanco was responsible of the characterization of the microalgal populations, where I contributed in the data analysis and discussion.

Paper VI. In this work, I was responsible of the start-up and operation of the experimental set-up in collaboration with MSc Eng. Antonio Ortíz under the supervision of Dr. Enrica Uggetti (Universitat Politècnica de Catalunya-BarcelonaTech), Dr. Rubén Díez (Universitat Politècnica de Catalunya-BarcelonaTech), Dr. Joan García (Universitat Politècnica de Catalunya-BarcelonaTech), Dr. Raquel Lebrero and Dr. Raúl Muñoz. I performed the mass balance calculations, results evaluation and manuscript writing under the supervision of Dr. Raquel Lebrero and Dr. Raúl Muñoz. Part of this work was carried out at the Agròpolis experimental campus of the Universitat Politècnica de Catalunya-BarcelonaTech (Catalunya, Spain).

Paper VII. In this work, I was responsible of the design, start-up and operation of the experimental set-up in collaboration with Dr. Dimas García and Dr. Esther Posadas under the supervision of Dr. Raquel Lebrero and Dr. Raúl Muñoz. I performed the mass balance calculations, results evaluation and manuscript writing under the supervision of Dr. Daniel Puyol, Dr. Raquel Lebrero and Dr. Raúl Muñoz.
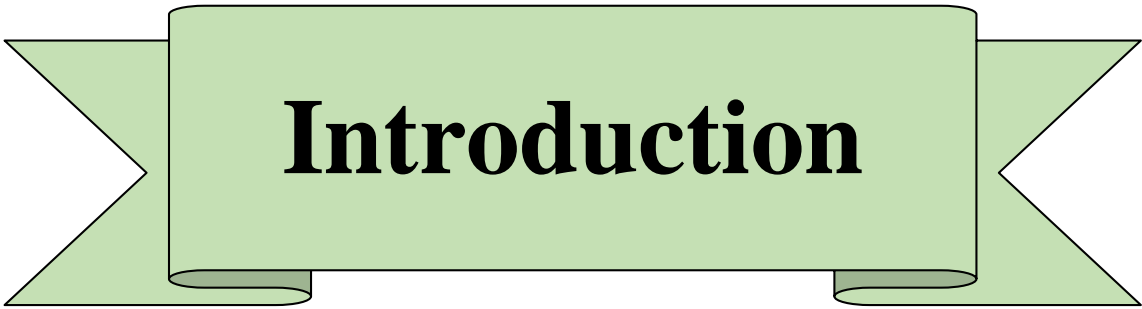
Paper VIII. In this work, I was responsible of the design, start-up and operation of the experimental set-up under the supervision of Dr. Raquel Lebrero and Dr. Raúl Muñoz. I performed the mass balance calculations, results evaluation and manuscript writing under the supervision of Dr. Marisol Vega, Dr. Raquel Lebrero and Dr. Raúl Muñoz. Dr. Marisol Vega was responsible of the statistical analysis.

Introduction

1.1 Biogas: current global situation

Biogas from the anaerobic digestion of wastewater or organic solid waste represents nowadays an important and growing renewable energy vector that can mitigate the greenhouse gas emissions derived from the massive use of fossil fuels needed to drive today's society worldwide (Herrmann et al., 2016). Biogas from anaerobic digestion has a typical composition of CH_4 (35-65%), CO_2 (25-60%), CO (<0.6%), H_2S (0.005-2%), N_2 (0-2%), NH_3 (<1%), H_2O (5-10%), O_2 (0-1%), siloxanes (0-0.02%) and halogenated hydrocarbons (<0.6%), where the majority of these compounds are impurities that need to be removed (Ryckebosch et al., 2011). For instance, CO_2 directly affects the specific calorific value of biogas, H_2S causes corrosion in pipelines, engines and storage structures, and high concentrations of O_2 involve explosion hazards.

Nowadays, biogas can be used in multiple industrial and domestic applications to generate steam or electricity in turbines, internal combustion engines or fuel cells (prior reforming), injected into natural gas networks or used as a vehicle fuel (Andriani et al., 2014; Muñoz et al., 2015). The conversion of biogas into biomethane is required prior its use in the industrial sector, in this sense, biomethane can be described as the product obtained from the process of separating unwanted components in biogas such as CO_2 to increase the total methane content and meet natural gas standards (European Biogas Association, 2019a). The relevance of biogas production in the EU energy sector has increased significantly over the past years as a result of the need to reduce current imports of natural gas from Russia, Algeria or the Middle East region. Indeed, the number of biogas plants has increased from 6227 in 2009 to 18202 by the end of 2018, while biomethane production capacity has increased from 752 GWh by 2011 to 19352 GWh by the end of 2017 (Figures 1 and 2) (European Biogas Association, 2019b).
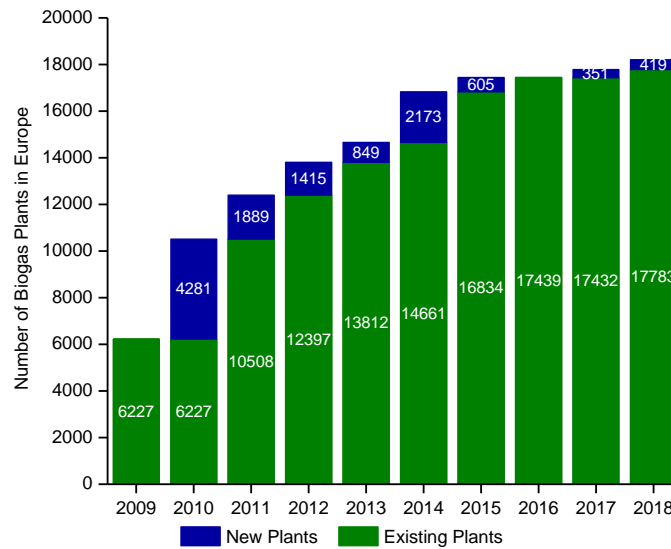
Figure 1. Time course of the number of biogas plants in Europe (Source: European Biogas Association, 2019)
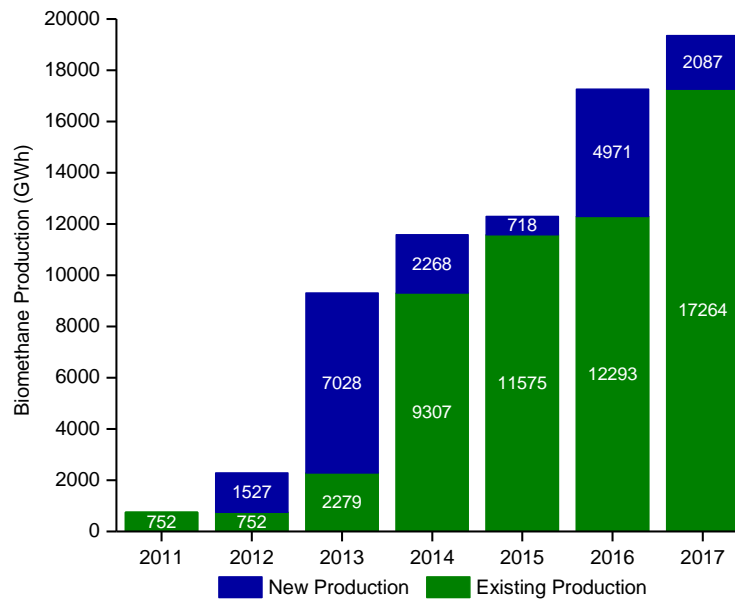
Figure 2. Time course of the biomethane production capacity (Source: European Biogas Association, 2019)

The removal of biogas impurities (i.e. biogas upgrading) is mandatory prior use as a vehicle fuel or injection into natural gas networks. In this context, several international regulations establish the maximum and minimum concentrations allowed for each biomethane component depending on its final application. Table 1 summarizes the technical specifications required for injection of biogas into natural gas grids and use as a vehicle fuel in different countries. Table 2 summarizes the specifications of biomethane according to the recent European Standard EN 16723.

4

In order to fulfill the required standards, multiple physical-chemical and biological technologies are nowadays commercially available to remove CO_2 and H_2S from biogas. Most of these commercial technologies must be sequentially implemented to eliminate both H_2S and CO_2, together with other trace contaminants such as siloxanes or volatile organic contaminants. This results in complex and costly processes (both in terms of operating and investment costs). In addition, physical-chemical technologies typically exhibit high environmental impacts derived from the massive energy use and the discharge into the open atmosphere of the CO_2 separated from biogas (Tippayawong and Thanompongchart, 2010).

Table 1. Technical specifications required for injection of biogas into natural gas grids and use as a vehicle fuel (Awe et al., 2017; European Committee for Standardization, 2018, 2017; Ministerio para la Transición Ecológica, 2018; Muñoz et al., 2015; Persson et al., 2006; Rodero et al., 2018a; Ryckebosch et al., 2011)

Component	Unit					Country					
		Austria	Belgium	Chile	Czech Republic	France	Germany	Netherlands	Spain	Sweden	Switzerland
CH_4	% vol	≥ 96	≥ 85	> 88	≥ 95	≥ 86	-	> 80	> 90	≥ 97	≥ 96
CO_2	% vol	≤ 3	≤ 2.5	-	≤ 5	≤ 2.5	≤ 6	≤ 6	< 2	≤ 3	≤ 6
O_2	% vol	≤ 0.5	-	< 1	≤ 0.5	≤ 0.01	< 3	< 0.5	< 0.3	≤ 1	≤ 0.5
CO	% vol	-	≤ 0.2	-	-	≤ 2	-	≤ 1	< 2	-	-
H_2	% vol	≤ 4	≤ 0.1	-	-	≤ 6	≤ 5	< 12	< 5	≤ 0.5	≤ 4
H_2S	mg Nm^{-3}	< 5	≤ 5	-	< 7	< 5	< 5	≤ 5	-	< 15.2	< 5
Sulfur	mg Nm^{-3}	< 10	< 30	< 35	< 30	< 75	< 30	< 45	-	< 23	< 30
Siloxanes	mg Nm^{-3}	≤ 10	-	-	≤ 6 mg Si m^{-3}	-	-	< 5 ppm_v	< 10	-	-
NH_3	mg Nm^{-3}	Free	≤ 3	-	Free	< 3	< 20	≤ 3	< 3	≤ 20	≤ 20
Mercaptans	mg Nm^{-3}	≤ 6	≤ 6	-	≤ 5	≤ 6	≤ 6	≤ 10	-	-	≤ 5 ppm_v
Water dew point	ºC	≤ -8 (40 bar)	-	-	≤ -10	≤ -5 (P_{max})	Ground Temperature	< -10 (8 bar)	< -8	$\leq T_{amb}-5$	≤ -8 (P_{max})

Table 2. Technical specifications of biomethane for use as automotive fuel according to the recent European Standard EN 16723 (European Committee for Standardization, 2018, 2017)

Component	Unit	Normal Methane Number Grade	High Methane Number Grade
Methane Number	Index	> 65	> 80
CO	% vol	< 0.1	< 0.1
H_2	% vol	< 2	< 2
O_2	% vol	< 1	< 1
H_2S	mg Nm^{-3}	< 5	< 5
NH_3	mg Nm^{-3}	< 10	< 10
Total volatile silicon	mg Nm^{-3}	< 0.5	< 0.5
Amines	mg Nm^{-3}	< 10	< 10
Dust impurities	-	Free	Free

1.2 Physical/Chemical biogas upgrading technologies

1.2.1 CO_2 removal technologies

The concentration of CO_2 in biogas is typically reduced nowadays by physical/chemical technologies, which so far are the only systems commercially available. The most popular physical/chemical technologies are pressure swing adsorption, water/chemical/organic scrubbing, membrane separation and cryogenic separation (Angelidaki et al., 2018; Muñoz et al., 2015; Rodero et al., 2018). Figure 3 shows the percentage of existing plants of physical/chemical technologies in the EU.
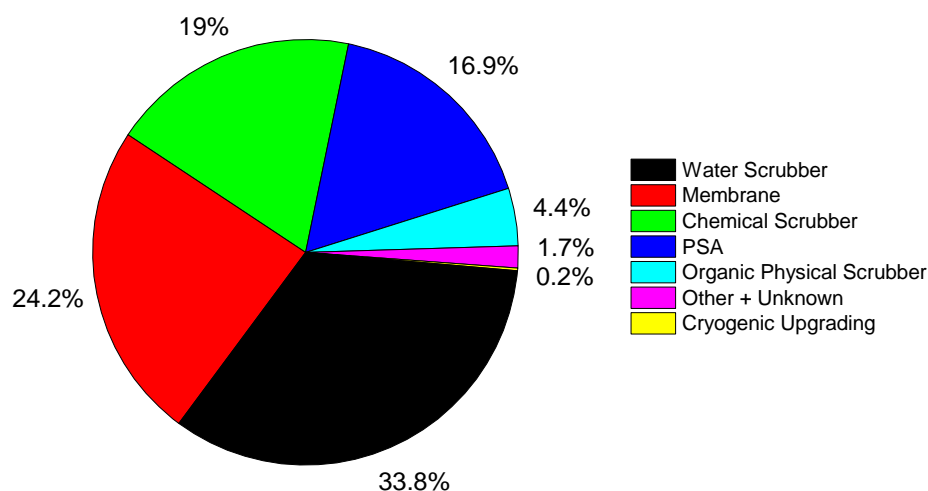

Figure 3. Percentage of existing plants of physical/chemical technologies for CO_2 removal in the EU (Source: Wall et al., 2018)

Pressure swing adsorption

This process is based on the adsorption of CO_2, under a sequence of pressure changes, by a selective porous adsorbent with a defined surface area that supports the preferential adsorption of CO_2 molecules over CH_4 molecules due to their higher affinity for the selected porous adsorbent (Figure 4). The adsorbent materials used in this technology can be activated alumina, activated carbon, polymeric sorbents, silica gel or zeolite (Angelidaki et al., 2018; Augelletti et al., 2017; Muñoz et al., 2015; Rodero et al., 2018; Ryckebosch et al., 2011). This process is considered a versatile mature technology due to its multiple design and operating parameters such as the type of adsorbent material, column size, operating pressure, cycle steps and use of single or multiple bed process (Augelletti et al., 2017). CH_4 concentrations up to 96-98% in the upgraded biogas have been reported at industrial scale (Angelidaki et al., 2018; Bauer et al., 2013).
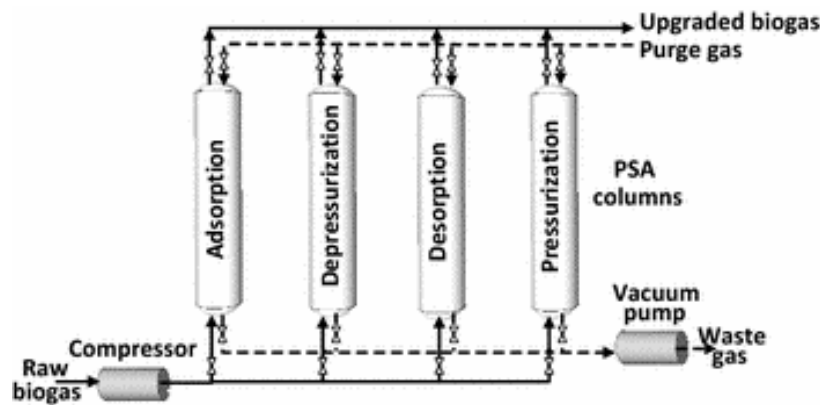

Figure 4. Biogas upgrading by pressure swing adsorption (Source: Muñoz et al., 2015)

Water scrubbing

This process is still the most commonly used technology for the upgrading of biogas worldwide. It is based on the removal of CO_2 from biogas due to the higher aqueous solubility of CO_2 compared with that of CH_4 (Henry´s law constant = $H_{CO2} \approx 0.83$ versus $H_{CH4} \approx 0.03$ at 25.0 ºC; where H = liquid-phase concentration / gas-phase concentration (C_L/C_G)). Thus, H_{CO2} is approximately twenty-six times higher than H_{CH4} (Sander, 2015). The absorption of CO_2 from raw biogas is carried out in a single-pass scrubber using pressurized water followed by a two-stage stripping process for water regeneration, where CO_2 is finally stripped out from the water in a desorption column aided with air at atmospheric pressure (Figure 5) (Angelidaki et al., 2018; Bauer et al., 2013; Persson et al., 2006; Rodero et al., 2018a; Sander, 2015). CH_4 concentrations in the upgraded biogas

in pressurized water scrubbers can reach values higher than 96%, along with CO_2 concentrations below 2% (Bauer et al., 2013).
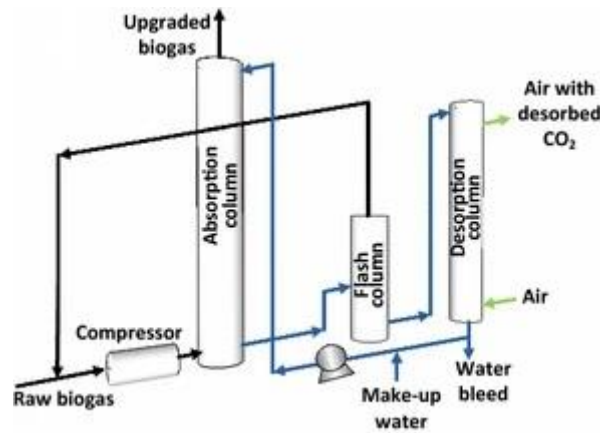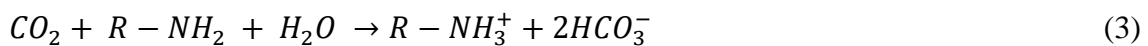

Figure 5. Biogas upgrading by water scrubbing (Source: Muñoz et al., 2015)

Chemical scrubbing

Chemical scrubbing is based on the selective absorption of CO_2 using a chemical-based solution as CO_2 absorbent, which maximizes the capacity of CO_2 removal from biogas. The most common chemicals used in chemical scrubbers are alkanol amines or alkali aqueous solutions (KOH, K_2CO_3, NaOH, $Fe(OH)_3$ or $FeCl_3$) (Angelidaki et al., 2018; Awe et al., 2017; Bauer et al., 2013; Rodero et al., 2018). Figure 6 shows a diagram of the biogas upgrading process by chemical scrubbing. The chemical reactions involved in this process are described by equations (1) to (3):

$$CO_2 + 2OH^- \rightarrow CO_3^{2-} + H_2O \tag{1}$$
$$CO_2 + CO_3^{2-} + H_2O \rightarrow 2HCO_3^- \tag{2}$$
$$CO_2 + R - NH_2 + H_2O \rightarrow R - NH_3^+ + 2HCO_3^- \tag{3}$$

CH_4 concentrations up to 96-99% in the upgraded biogas have been reported in literature along with CH_4 losses lower than 0.1% (Angelidaki et al., 2018; Bauer et al., 2013; Ryckebosch et al., 2011).

Figure 6. Biogas upgrading by chemical scrubbing (Source: Muñoz et al., 2015)

Organic scrubbing

This process is similar to water scrubbing. However, water is substituted by methanol or polyethylene glycol as absorbents due to their higher affinity for CO_2 compared to the former, likely resulting in a reduction in the investment and operating costs of biogas purification (Muñoz et al., 2015; Petersson and Wellinger, 2009; Ryckebosch et al., 2011). Figure 7 shows a diagram of the biogas upgrading process by organic scrubbing. CH_4 concentrations up to 96-98% in the upgraded biogas have been reported in literature along with CH_4 losses lower than 2% (Angelidaki et al., 2018; Bauer et al., 2013; Ryckebosch et al., 2011; Sun et al., 2015).
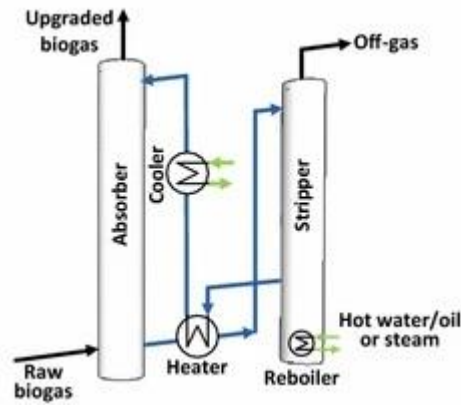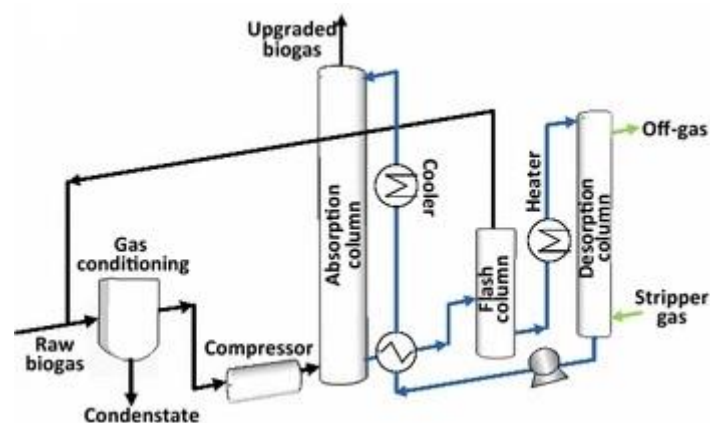

Figure 7. Biogas upgrading by organic scrubbing (Source: Muñoz et al., 2015)

Membrane separation

CO_2 removal from biogas is based on the enhanced permeability of this compound through the membrane material compared to CH_4. The most common materials used in membrane manufacture are polymers. An ideal membrane should have a large permeability difference between CH_4 and CO_2 in order to minimize CH_4 losses and efficiently purify the biogas. The process can be performed either by gas:gas separation or gas:liquid separation (Figure 8). CH_4 concentrations of up to 98-99% in the upgraded biogas have been reported in literature in gas:liquid units and up to 92-94% in gas:gas units (Angelidaki et al., 2018; Bauer et al., 2013; Beil and Beyrich, 2013; Muñoz et al., 2015; Ryckebosch et al., 2011).
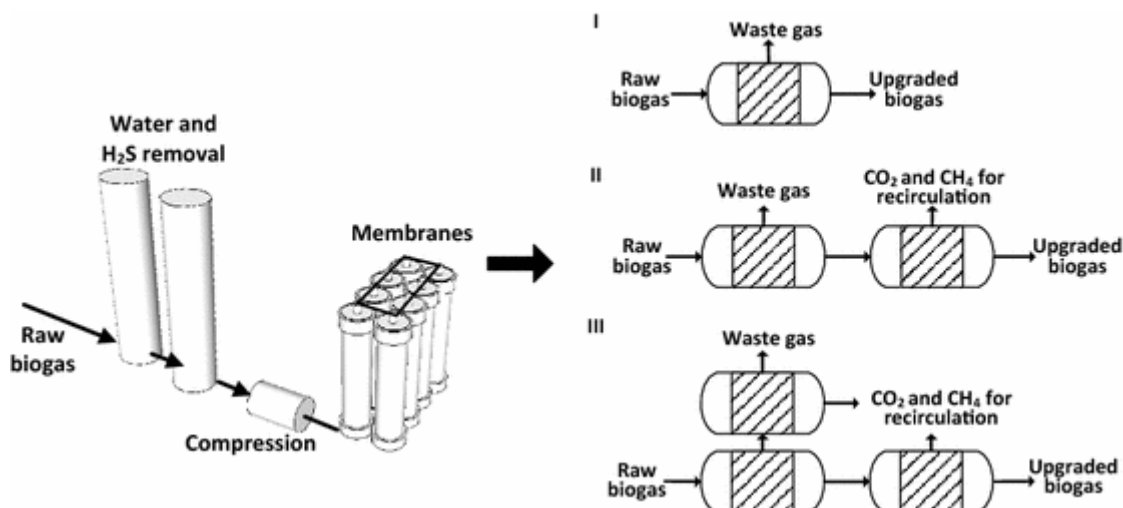
Figure 8. Biogas upgrading by membrane separation using gas:gas units with i) single-pass membrane unit, ii) multiple stage membrane units with internal recirculation of permeate and iii) internal recirculation of retentates (Source: Muñoz et al., 2015)

Cryogenic separation

Cryogenic processes apply low temperatures to biogas in order to achieve the separation of biogas components based on their different condensation points (Figure 9). In this context, the condensation point at atmospheric pressure for H_2S is -60 °C, for CO_2 -78 °C, for CH_4 -161 °C, for O_2 -183 °C and for N_2 -196 °C. Up to 97-98% of CH_4 in the upgraded biogas have been reported in literature with CH_4 losses lower than 2% (Angelidaki et al., 2018; Awe et al., 2017; Bauer et al., 2013; Muñoz et al., 2015; Rodero et al., 2018).

Figure 9. Biogas upgrading by cryogenic separation (Adapted from: Awe et al., 2017)

Table 3 summarizes the main advantages and disadvantages of the physical/chemical CO_2 removal technologies discussed in this section.

Table 3. Advantages and disadvantages of physical/chemical CO_2 removal technologies (Angelidaki et al., 2018; Augelletti et al., 2017; Bauer et al., 2013; Muñoz et al., 2015; Rodero et al., 2018).
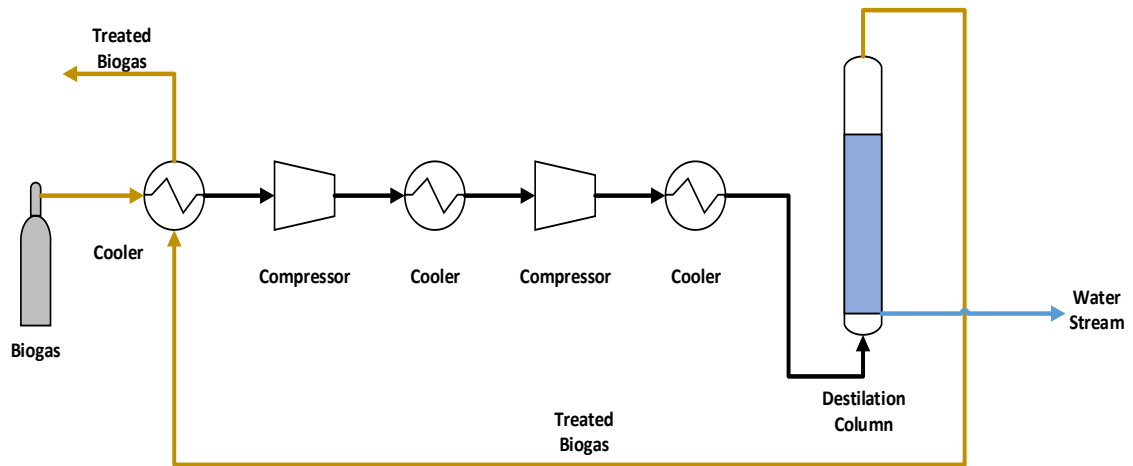
Technology	Advantages	Disadvantages
Pressure swing adsorption	• Low energy and capital investment cost	• H_2S and siloxanes have to be removed prior injection of the biogas in this technology • High operating pressure (3-10 bar)
Water scrubbing	• Low cost water supply	• High operating pressure (6-10 bar) • Possible elemental sulfur accumulation • Prior H_2S removal is highly recommended
Chemical scrubbing	• Low pressure needed	• High energy requirements for solvent regeneration • Prior H_2S removal is highly recommended • Corrosion
Organic scrubbing	• Reduction in investment and operating costs	• High operating pressure (4-10 bar) • Prior H_2S removal is highly recommended • H_2O needs to be removed
Membrane separation	• High lifetime of membranes (5-10 years)	• High operating pressure (5-8 bar) • Particles and siloxanes removal required
Cryogenic separation	• Simultaneous H_2S removal	• Low operating temperatures (up to -196 ºC) • High energy requirements • High investment and operation costs

1.2.2 H₂S removal technologies

Physical/chemical technologies are commonly used nowadays for the removal of H_2S from raw biogas, although biotechnological alternatives also exist at commercial scale (further developed in section 1.3.2). The most popular physical/chemical technologies are adsorption onto activated carbon, adsorption using iron oxide or hydroxide, membrane separation, absorption and in-situ precipitation in the digester via iron salt addition (Muñoz et al., 2015; Petersson and Wellinger, 2009).

Adsorption on activated carbon

H_2S removal by activated carbon filtration can be carried out either by simple physical adsorption onto the carbon surface or by catalytic conversion, where H_2S is converted into sulfur and water (Figure 10). The latter mechanism requires high temperature (50-70 ºC) and pressure (7-8 bar), and the addition of 4-6 % of air in the biogas to support the partial oxidation of H_2S to S (Eq. 4) (Ryckebosch et al., 2011). The lifetime of the activated carbon ranges from 4000 to 8000 hours depending on the H_2S loading rate applied to the filter (Wellinger and Lindberg, 2005), a regeneration or replacement of the carbon being necessary after carbon saturation.
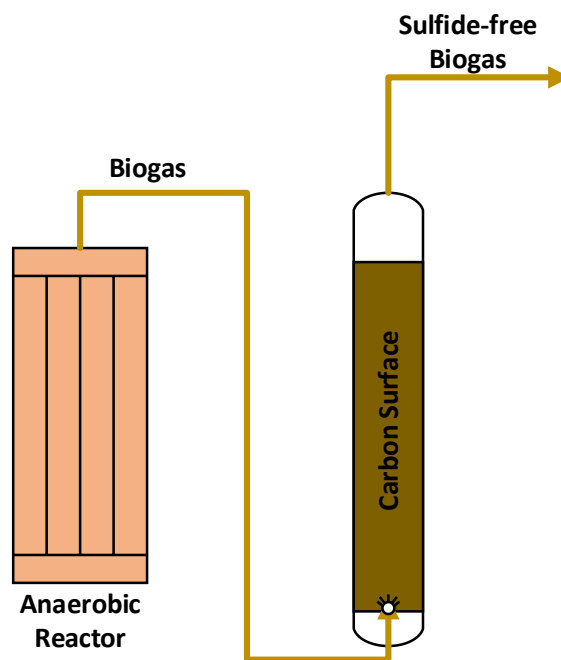
$$2H_2S + O_2 \rightarrow 2S + 2H_2O \tag{4}$$

Figure 10. Biogas upgrading by adsorption on activated carbon (Adapted from: Kanjanarong et al., 2017)

Adsorption using iron oxide or hydroxide

Process operation is based on the selective adsorption of H_2S in adsorbent modules operated in parallel using an adsorption-regeneration configuration. These modules contain an organic packing material impregnated with iron oxide (Fe_2O_3), iron hydroxide ($Fe(OH)_3$) or zinc oxide (ZnO) that retains H_2S during biogas circulation (Abatzoglou and Boivin, 2009; Iovane et al., 2014; Muñoz et al., 2015). The chemical reactions involved in H_2S oxidation and adsorbent regeneration are described by equations (5) to (7):

$$Fe_2O_3 + 3H_2S \rightarrow Fe_2S_3 + 3H_2O \qquad (5)$$
$$2Fe(OH)_3 + 3H_2S \rightarrow Fe_2S_3 + 6H_2O \qquad (6)$$
$$2Fe_2S_3 + 3O_2 \rightarrow 2Fe_2O_3 + 6S \qquad (7)$$

The two first reactions are endothermic and need a moderate temperature between 25 and 50 ºC to occur, while the third reaction is exothermic and temperature is not controlled. Adsorption using iron oxide or hydroxide operates at a biogas residence time ranging from 1 to 15 min and can support inlet concentrations of H_2S down to 100 ppm_v (Muñoz et al., 2015; Ryckebosch et al., 2011). This physical/chemical technology is widely implemented because it is efficient (reductions of 99% are typically reported) and exhibits moderate operating costs (Iovane et al., 2014; Rutledge, 2005).

Membrane separation

H_2S can be removed from biogas by permeation (along with CO_2) through a semipermeable membrane that retains CH_4. Similarly to the membrane systems for CO_2 separation, H_2S removal can be carried out at high pressure in gas:gas modules or at low pressure in gas:liquid modules with a CO_2 absorbent on the other side of the membrane (Iovane et al., 2014). For biogas containing H_2S concentrations of 2%, removal efficiencies of 98% (Ryckebosch et al., 2011) and for biogas with an initial H_2S concentrations of 0.2%, removal efficiencies of 58-94 % have been reported, working at pressure membrane betwwen 3.7 and 7.6 bar (Iovane et al., 2014).
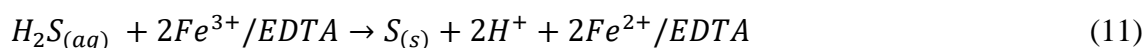
In-situ precipitation

Addition of Fe^{2+} or Fe^{3+} ions in the form of $FeSO_4$, $FeCl_3$ and $FeCl_2$ salts into the organic feed or directly into the digester represents an efficient mechanism for the control of H_2S concentration in biogas. These ions react with the dissolved H_2S generating the insoluble forms FeS and/or elemental S following the reactions shown in equations (8) and (9) (Muñoz et al., 2015; Petersson and Wellinger, 2009; Ryckebosch et al., 2011):

$$Fe^{2+} + S^{2-} \rightarrow FeS \tag{8}$$
$$2Fe^{3+} + 3S^{2-} \rightarrow 2FeS + S \tag{9}$$

This method is efficient to reduce H_2S concentration in moderate to high strength biogas, but cannot decrease H_2S levels below 100-150 ppm_v. While its operation is simple and the investment costs are low, the widespread use of this technology is limited by the high operating cost derived from the purchase of the iron salts (Persson et al., 2006).

1.2.3 Absorption by Fe/EDTA solution

The use of an absorption-stripping process based on an aqueous solution of Fe-EDTA represents an innovative physicochemical technology capable of simultaneously removing H_2S and CO_2 from biogas (Awe et al., 2017). Fe^{3+}-EDTA solutions support a cost-effective H_2S oxidation to elemental sulfur, which is a solid residue that can be disposed of safely and easily (Demmink and Beenackers, 1998; Frare et al., 2010). According to Wubs and Beenackers (1993), the absorption and oxidation of H_2S with Fe-EDTA is described by equations (10) and (11), where the first step is the physical absorption and mass transfer of H_2S from the biogas into the aqueous phase:

$$H_2S_{(g)} \leftrightarrow H_2S_{(aq)} \tag{10}$$
$$H_2S_{(aq)} + 2Fe^{3+}/EDTA \rightarrow S_{(s)} + 2H^+ + 2Fe^{2+}/EDTA \tag{11}$$

The precipitated sulfur generated in the absorption column can be removed using an appropriate solid–liquid separation technique, such as filtration or sedimentation. The Fe^{2+}/EDTA resulting from H_2S oxidation to $S_{(s)}$ can be regenerated into its active ferric form (Fe^{3+}/EDTA) by oxidation with the air used for CO_2 stripping (equations 12 and 13) in a separate column interconnected to the absorption column (Figure 11). The typical

operational conditions for this process are temperature ranging from 20 to 60 ºC and pH of 6-9 (Demmink et al., 1994; Wubs and Beenackers, 1993).
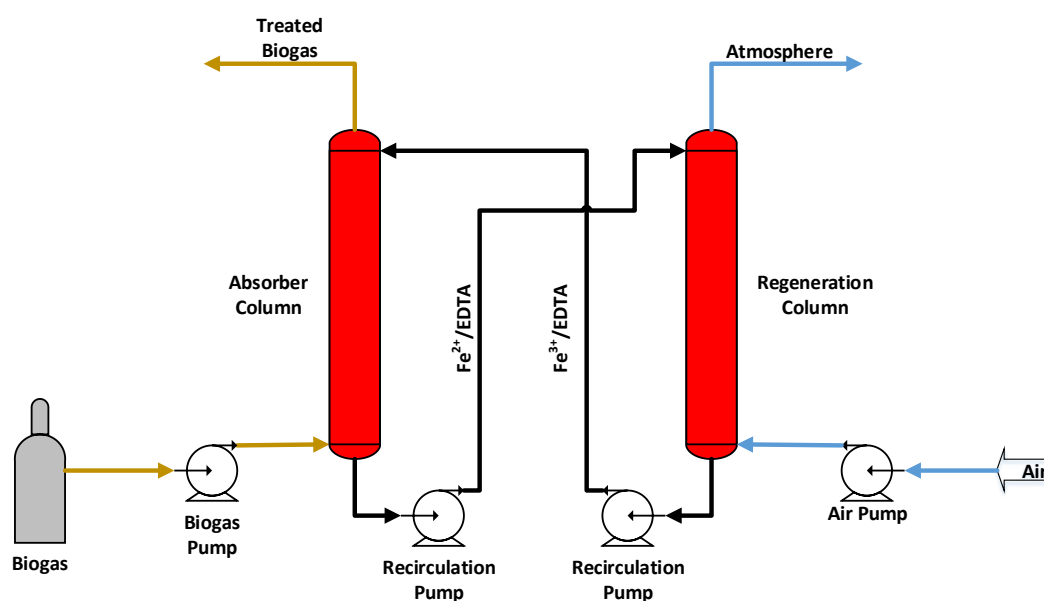
$$O_{2\,(g)} \leftrightarrow O_{2\,(aq)} \tag{12}$$

$$O_{2\,(aq)} + 4Fe^{2+}/EDTA + 2H_2O \rightarrow 4Fe^{3+}/EDTA + 4OH^- \tag{13}$$
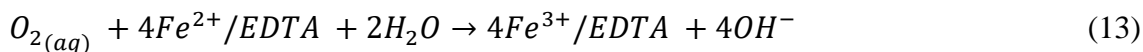
Figure 11. Experimental set-up for H$_2$S absorption by Fe/EDTA (Adapted from: Schiavon Maia et al., 2017)

This technology has been studied in recent years in order to elucidate the potential of Fe^{3+}/EDTA to remove H$_2$S from biogas. In this regard, Horikawa et al, (2004) investigated the purification of biogas using a 0.2 M Fe/EDTA aqueous solution in a system composed of an absorption and a regeneration column with a total volume of 0.82 L and operated with a biogas flow rate of 1000 mL min^{-1} and a liquid flow rate of 83 mL min^{-1}. Under these operational conditions, H$_2$S removal efficiencies (REs) of 90% and CO$_2$-REs ranging from 4.0 to 16.0% were recorded. Similarly, Schiavon Maia et al, (2017) studied the removal of H$_2$S in a similar absorption-regeneration system using a 0.2 M Fe/EDTA solution at biogas and liquid flow rates of 340 mL min^{-1}. Under these operational conditions H$_2$S-REs of 91% were consistently achieved.

Despite the optimization of this technology for the removal of H$_2$S and its promising results, the optimization of the operational conditions to support a simultaneous removal

of CO_2 and H_2S has not been conducted so far. In this sense, the use of a novel Fe/EDTA/carbonate-based scrubbing process (solution of Fe/EDTA enriched with HCO_3^- and CO_3^{2-}) at a high pH value (9.0-10.0) can mediate a rapid and effective CO_2 capture at ambient pressure and allow an air-aided CO_2 desorption. This hypothesis justifies the research, development and validation of the experiment that will be presented in this thesis (Chapter 8).

Table 4 summarizes the main advantages and disadvantages of the physical/chemical H_2S removal technologies discussed in this section.

Table 4. Advantages and disadvantages of physical/chemical H_2S removal technologies from raw biogas (Adapted from Rodero et al., 2018).

| Technology	Advantages	Disadvantages
Adsorption on activated carbon	• High H_2S removal efficiencies	• High temperature is needed for carbon regeneration • Short lifetime of the activated carbon
Adsorption using iron oxide or hydroxide	• Removal efficiencies >99% • Low operating costs	• Temperature must be controlled
Membrane separation	• Simultaneous CO_2 removal • High H_2S removal efficiencies	• Inlet H_2S concentrations in the biogas below <2%
In-situ precipitation	• Low investment cost • Efficient at high H_2S concentrations	• H_2S in treated biogas >100 –150 ppm_v • High operating costs
Absorption by Fe/EDTA solution	• High H_2S removal efficiencies	• Simultaneous removal of CO_2 has not been tested

1.3 Biological biogas upgrading technologies

1.3.1 CO₂ removal technologies

The concentration of CO_2 in biogas can be also reduced biologically, although no biological technologies are commercially available nowadays. The most popular biological technologies under current investigation are chemoautotrophic biogas upgrading and photosynthetic biogas upgrading (Angelidaki et al., 2018; Muñoz et al., 2015; Rodero et al., 2018a).

Chemoautotrophic biogas upgrading

The chemoautotrophic biogas upgrading process is based on the action of hydrogenotrophic methanogens to transform CO_2 into CH_4 using H_2 as an electron donor according to equation 14 (Rittmann, 2015).

$$4H_2 + CO_2 \rightarrow CH_4 + 2H_2O \tag{14}$$
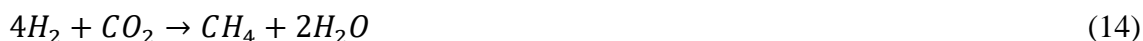
One drawback of this technology is the limited bioconversion of CO_2 to CH_4 due to the low aqueous solubility of H_2, which typically limits the gas-water H_2 mass transfer rates and decreases the efficiency of CH_4 production at the expenses of an enhanced biomass formation (Strevett et al., 1995). Another important problem of this technology is that electricity production from fossil fuels is typically necessary in order to obtain H_2. Therefore, the production of H_2 using renewables energies remains the key factor to maintain the sustainability of this process. H_2 must be produced from water electrolysis using the surplus of solar or wind energy, which can be regarded as an energy storage technology (Angelidaki et al., 2018; Muñoz et al., 2015; Rodero et al., 2018).

Several investigations have been conducted to date in order to understand chemoautotrophic biogas upgrading. For instance, Luo and Angelidaki (2012) reached CH_4 concentrations of 90-95% in thermophilic stirred tank reactors (STR) sparged with a synthetic mixture of H_2:CH_4:CO_2 (60:25:15) at a gas residence time (GRT) ranging from 1 to 8 h. Wang et al., (2013) achieved CH_4 concentrations between 90-99% in a mesophilic sewage sludge STR digester with *in-situ* coke gas addition (92% H_2: 8% CO) via bubbleless membranes at a GRT between 13 and 22 h, while Burkhardt and Busch (2013) reached CH_4 concentrations between 94-98% in a mesophilic biotrickling filter

with random packing and internal gas recycling supplied with synthetic CO_2:H_2 mixtures at a GRT between 2 and 10 h.

1.3.2 H$_2$S removal technologies

The concentration of H_2S in biogas can be reduced by biological oxidation to sulphate or elemental sulfur. The most popular biological technologies are *in-situ* microaerobic H_2S removal and biotrickling filtration of H_2S (Muñoz et al., 2015; Rodero et al., 2018).

In-situ *microaerobic H$_2$S removal*

Sulfur oxidizing bacteria are responsible for the partial oxidation of H_2S in anaerobic digesters under microaerobic conditions induced by a controlled O_2 dosing. The limited oxygen availability supports the oxidation of H_2S to elemental sulfur instead of SO_4^{2-}, bioreaction that is used to provide energy to these lithoautotrophic microbes. This process is described by equations (15) to (17) according to Janssen et al., (1995) and Madigan et al., (2009).

$$2HS^- + O_2 \rightarrow 2S^0 + 2OH^- \tag{15}$$
$$2HS^- + 4O_2 \rightarrow 2SO_4^{2-} + 2H^+ \tag{16}$$
$$2HS^- + 2O_2 \rightarrow S_2O_3^{2-} + H_2O \tag{17}$$

In this process, sulfur oxidizing bacteria employ O_2 as an electron acceptor (Tang et al., 2009). Sulfur oxidizing bacteria typically grow in the headspace of the anaerobic digester due to the absence of alternative biomass attachment structures in the digester, creating superimposed layers of elemental S that act as a support material to facilitate O_2 transfer and microbial growth (Díaz et al., 2011; Kobayashi et al., 2012). H_2S-REs higher than 97% are typically recorded in mesophilic digesters of wastewater treatment plant sludge (Díaz et al., 2011, 2010; Jenicek et al., 2008; Ramos et al., 2014; Ramos and Fdz-Polanco, 2014).

Biotrickling filtration of H$_2$S

This process consists of a bed column packed with structured or random materials such as polyurethane foam or pall rings, supporting an effective biofilm growth. These columns operate with a recirculating aqueous phase containing the essential nutrients

required for sulfur oxidizing bacteria growth (Figure 12) (Fortuny et al., 2011; Muñoz et al., 2015; Rodero et al., 2018). Similar to microaerobic anaerobic digestion, this process is based on the action of sulfur oxidizing bacteria capable of using H_2S as energy source and O_2 as an electron acceptor, as described by equations (18) and (19) (Gabriel et al., (2013)):

$$H_2S + 0.5O_2 \rightarrow S + H_2O \tag{18}$$
$$H_2S + 2O_2 \rightarrow SO_4^{2-} + 2H^+ \tag{19}$$

Nitrate can be also used as electron acceptor to support the partial or complete oxidation of H_2S according to equations (20) and (21) (Lebrero et al., 2016):

$$5H_2S + 2NO_3^- \rightarrow 5S^0 + N_2 + 4H_2O + 2OH^- \tag{20}$$
$$5H_2S + 8NO_3^- \rightarrow 5SO_4^{2-} + 4N_2 + 4H_2O + 2H^+ \tag{21}$$
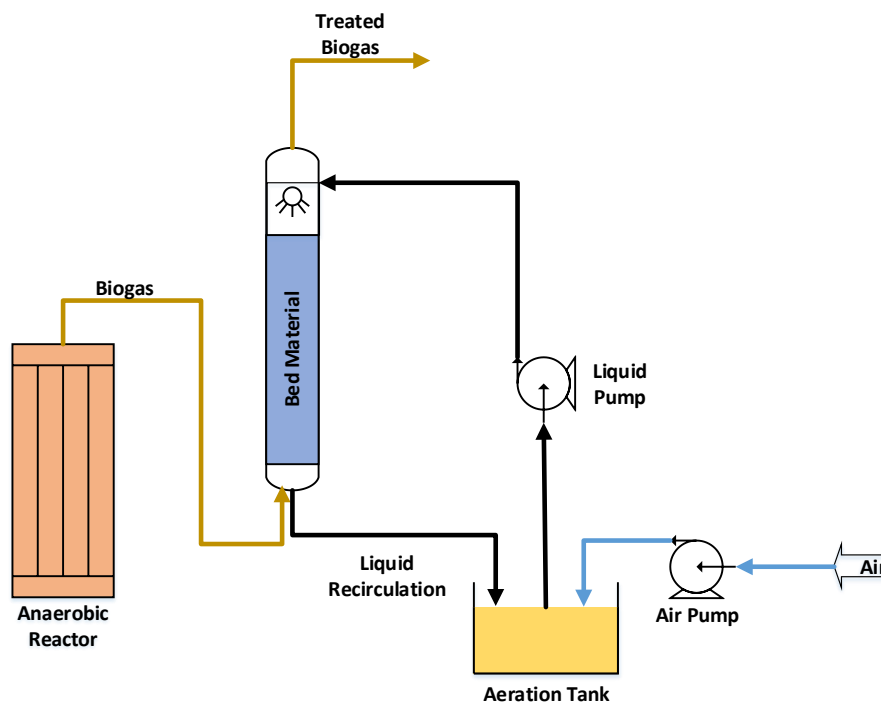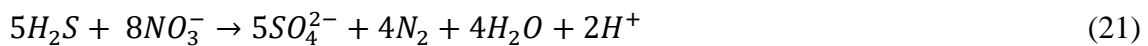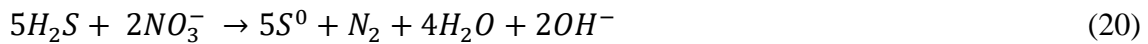

Figure 12. Biogas upgrading by biotrickling filtration (Adapted from: Khoshnevisan et al., 2017)
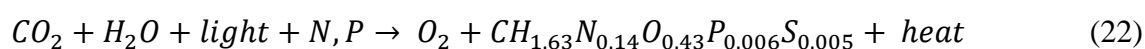
An important operational problem in this technology is the accumulation of elemental sulfur and the explosion risks if O_2 is present at high concentrations. The optimal ranges of temperature and pH for H_2S abatement in biotrickling filters are 28-35 ℃ and 2-4,

respectively (Fernández et al., 2014; Montebello et al., 2013; Muñoz et al., 2015). H_2S-REs of 99% have been recorded using an aerobic biotrickling filter packed with metallic pall rings (Montebello et al., 2012) at a GRT of 3 min, while aerobic biotrickling filters packed with HD-QPAC can achieve H_2S-REs of 98% at GRTs of 2-3 min (Fortuny et al., 2011). Similarly, Fernández et al., (2014) achieved H_2S-REs of 99% at a GRT of 2.4-3.4 min, working in an anoxic biotrickling filter packed with polyurethane foam, using $Ca(NO_3)_2$, KNO_3 and $NaNO_3$ as electron acceptor.

1.3.3 Simultaneous H_2S and CO_2 removal in algal-bacterial processes

Despite the large portfolio of physical-chemical and biological biogas upgrading technologies existing nowadays, none of them provide a simultaneous CO_2 and H_2S removal. Therefore, an integral biogas upgrading requires the sequential implementation of technologies to remove H_2S and CO_2, which significantly increases the initial investment and operational cost of the process (nowadays accounting for ~ 30% of the biomethane price (Stürmer et al., 2020)). In this context, algal-bacterial processes have recently emerged as an environmentally friendly and cost-efficient alternative to remove CO_2 and H_2S from raw biogas in a single-step process at low operating costs and with limited environmental impacts (Bahr et al., 2014; Bose et al., 2019; Nagarajan et al., 2019; Yan et al., 2016).

This technology is based on the simultaneous fixation of CO_2 by microalgae using solar energy and the aerobic oxidation of H_2S into SO_4^{2-} by sulfur oxidizing bacteria mediated by the elevated dissolved oxygen concentration present in the photobioreactor cultivation broth as a result of photosynthetic activity (Figure 13) (Bahr et al., 2014; Posadas et al., 2015; Serejo et al., 2015; Toledo-Cervantes et al., 2016). The CO_2 is converted into microalgae biomass through oxygenic photosynthesis using the electrons released during water photolysis, a process that can be described by equation (22) (Muñoz et al., 2015). Meanwhile, the mechanism of the oxidation of H_2S into SO_4^{2-} can be described by equation (23) (Syed et al., 2006).

$$CO_2 + H_2O + light + N,P \rightarrow O_2 + CH_{1.63}N_{0.14}O_{0.43}P_{0.006}S_{0.005} + heat \qquad (22)$$

$$H_2S + CO_2 + N,P + O_2 \rightarrow biomass + S/SO_4^{2-} + H_2O \qquad (23)$$
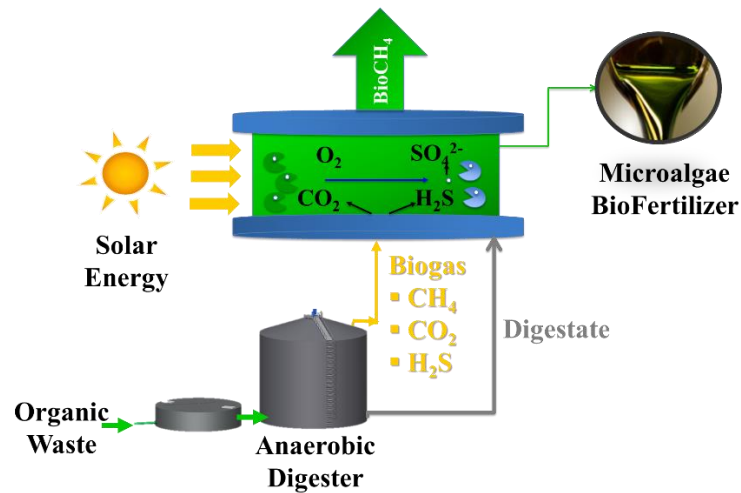
Figure 13. Fundamentals of photosynthetic biogas upgrading process (Adapted from Bahr et al., 2014)

CO_2 absorption from biogas into the aqueous cultivation broth of the photobioreactor is required prior removal by microalgal photosynthesis. Similarly, the transport of H_2S from biogas to the algal-bacterial cultivation broth is necessary prior H_2S oxidation into SO_4^{2-} (Posadas et al., 2015; Rodero et al., 2018). CO_2 removal represents the main bottleneck of the upgrading process due to the higher aqueous solubility of H_2S compared with that of CO_2. Indeed, H_{H2S} is approximately three times higher than H_{CO2} (Henry´s law constant $H_{H2S} \approx 2.45$ versus $H_{CO2} \approx 0.83$ at 25.0 ºC) (Sander, 2015).

The need to provide nutrients to algal-bacterial processes is an important operational issue determining both the economic and environmental sustainability of the process. All nutrients needed during photosynthetic biogas upgrading can be obtained through the treatment of domestic wastewater, agricultural wastewater or digestate from the anaerobic digester. For instance, Rodero et al., (2018b) used real digestate from Valladolid wastewater treatment plant as nutrient source with a composition of: inorganic carbon (IC) = 459 ± 83 mg L^{-1}, total nitrogen (TN) = 576 ± 77 mg L^{-1} and S-SO_4^{2-} = 4.7 ± 3.4 mg L^{-1}. Uggetti et al., (2018) worked with agricultural wastewater as a nutrient source with a composition of: total organic carbon (TOC) = 131 ± 80 mg L^{-1}, IC = 36 ± 10 mg L^{-1}, TN = 15 ± 7 mg L^{-1}, N-NH_4^+ = 3.8 ± 3.4 mg L^{-1}, N-NO_2^- = 0.9 ± 1.4 mg L^{-1}, N-NO_3^- = 8.4 ± 2.1 mg L^{-1} and P-PO_4^{3-} = 0.8 ± 1.1 mg L^{-1}.

There are two types of algal photobioreactors commercially available nowadays for industrial applications: closed photobioreactors and open photobioreactors. Tubular

photobioreactor (TPBRs) are the most popular closed systems. TPBRs typically consist of a set of tubes with an optimum diameter from 3 to 12 cm and with an internal liquid velocity controlled by centrifugal pumps ranging between 20 and 100 cm s^{-1} (Christenson and Sims, 2011). This configuration supports high growth rates of microalgae due to the high photosynthetic efficiencies as a result of its high illuminated area per volume ratio, which makes them ideal for mass microalgae cultivation. Operating parameters such as temperature, internal velocity and light irradiance can be tailored to the optimal values in order to maximize microalgae productivity, although temperature control can be technically difficult and economically non-feasible (Pulz, 2001). The main disadvantages of TPBRs are the risk of biofouling in the internal wall of the tubes (which can ultimately block light penetration) and the high operational costs in order to operate under optimal conditions (Béchet et al., 2010). A TPBRs interconnected to a biogas absorption column (AC) via mixing chamber is represented in Figure 14.
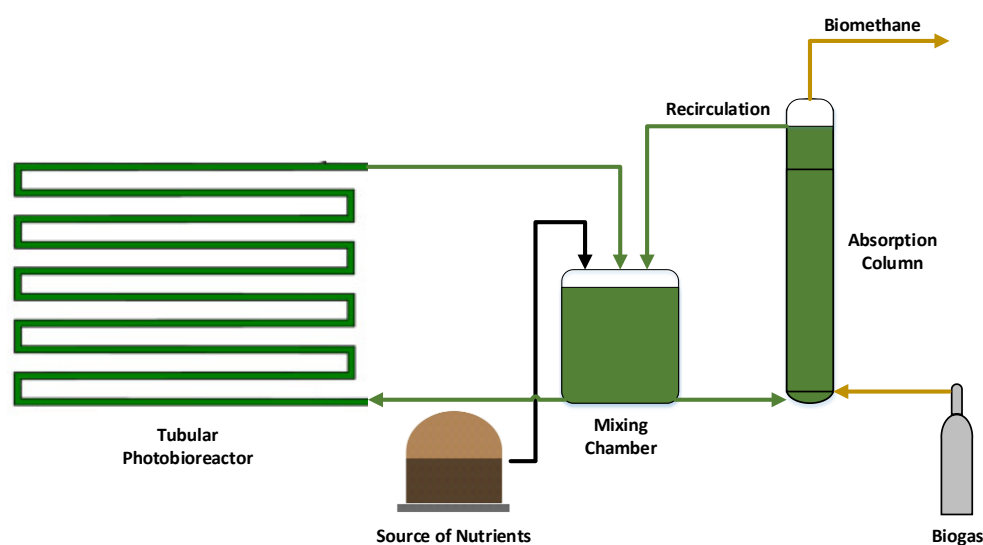
Figure 14. Biogas upgrading in a TPBR interconnected to a biogas scrubbing bubble column (Adapted from Oliva et al., 2019; Toledo-Cervantes et al., 2018)

Several investigations have been conducted to date in order to understand photosynthetic biogas upgrading in this type of closed photobioreactor under indoors conditions (Table 4). For instance, Converti et al., (2009) reached CO_2-REs of 100% in an enclosed tubular photobioreactor of 1 L inoculated with *Spirulina platensis*. Meanwhile, a 100% of H_2S-Res and CO_2-REs ranging between 94 and 97% where obtained by Mann et al., (2009) in an photobioreactor of 0.45 L inoculated with *Chlorella vulgaris*. Finally, Toledo-

Cervantes et al., (2018) works in a system that use a 60 L mixing chamber for interconnect the photobioreactor of 45.5 L, inoculated with *Acutodesmus obliquus,* to a 3.5 L AC, this variation in the system resulted in H_2S-REs of 98%, CO_2-REs of 91% and CH_4 concentrations of 83%.

Conversely, open photobioreactors, and more specifically high rate algal ponds (HRAPs) are the most common photobioreactor configuration implemented for biogas upgrading due to their cost-competitiveness and environmental sustainability. Their operating costs account for $0.03 \in (Nm^3)^{-1}$ treated biogas with an energy demand of 0.08 kW-h $(Nm^3)^{-1}$ treated biogas (Toledo-cervantes et al., 2017). HRAPs are interconnected to a biogas AC via an external liquid recirculation from a settler (Figure 15). The implementation of a settler between the HRAP and the AC allows for biogas scrubbing with a biomass free cultivation broth, which prevents the clogging and malfunctioning of the AC. The settled biomass is harvested from the bottom of the settler in order to ensure a constant biomass productivity in the HRAP. The main disadvantages of this photobioreactor configuration are the large land area needed to support an effective CO_2 fixation and the high water evaporation rates (Alcántara et al., 2015).
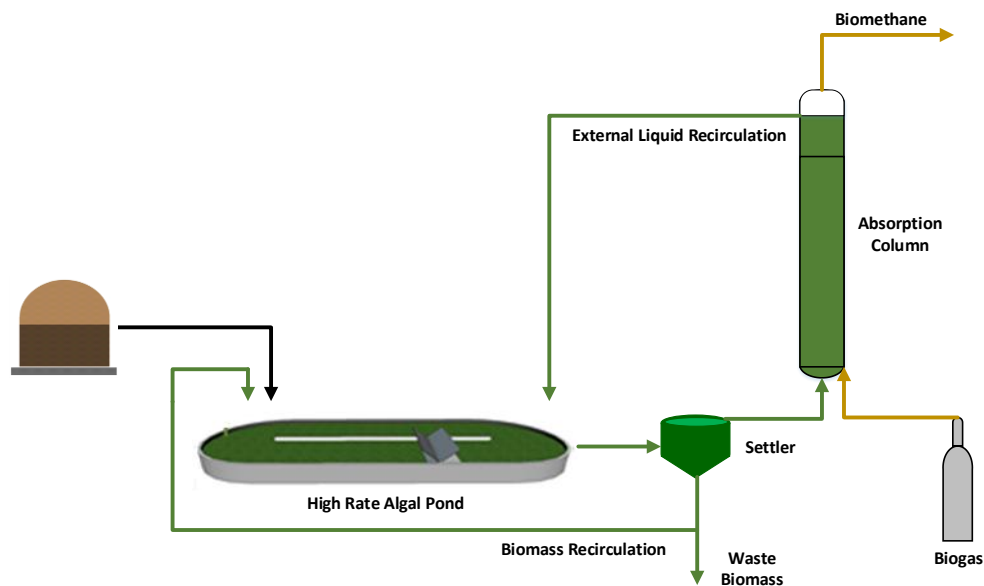

Figure 15. Biogas upgrading process in a HRAP interconnected to a biogas scrubbing bubble column (Adapted from Bahr et al., 2014)

Several investigations have been carried out to date to elucidate the potential of photosynthetic biogas upgrading in an open HRAP interconnected to an AC (Alcántara et al., 2015; Bahr et al., 2014; Posadas et al., 2016, 2015; Rodero et al., 2019, 2018b; Serejo et al., 2015; Toledo-Cervantes et al., 2017, 2016) (Table 4). For instance, Bahr et al., (2014) reached H_2S-REs of 100% and CO_2-REs ranging from 62 to 98% in a 180 L HRAP interconnected to a 0.8 L AC inoculated with *Spirulina platensis*. Meier et al., (2015) attained CO_2-REs of 93% and O_2 concentrations of 1.2% in an open photobioreactor of 75 L interconnected to a 0.7 L AC inoculated with *Nannochloropsis gaditana*. Finally, the use of a HRAP of 180 L interconnected to a 2.5 L AC has been developed in recent years. Serejo et al., (2015) reported H_2S-REs of 100% with CO_2-REs of 80% and CH_4 concentrations of 88% inoculated with *Chlorella vulgaris*. Toledo-Cervantes et al., (2017) reached H_2S-REs of 100% with CO_2-REs higher than 95% and CH_4 concentrations of 96% inoculated with *Mychonastes homosphaera*. Rodero et al., (2019) reached H_2S-REs of 100% with CO_2-REs of 95% and CH_4 concentrations higher than 95% operated with an automatic control system.

Despite the rapid optimization of this technology in the past years and the promising results obtained so far, most studies have been conducted under indoors conditions (constant temperature and radiation) and at pilot scale, which limits the widespread implementation of this technology. In this context, the evaluation of the performance of photosynthetic biogas upgrading under outdoors conditions is required in order to understand the influence of the seasonal and diurnal variations of light irradiance, the number of sun hours and the temperature on the quality of the upgraded biogas. Similarly, the validation of this technology at semi-industrial scale in order to promote its acceptance by the industrial sector is a must. These limitations justify the research, development and validation of outdoors experiments that will be presented in this thesis (Chapters 1 to 6).

Table 5. Indoors experimental studies for biogas upgrading in different microalgal photobioreactors (Adapted from Angelidaki et al., 2018; Muñoz et al., 2015; Rodero et al., 2018)

Type of photobioreactor	Microalgae species	Raw biogas composition (%)	CO_2-REs (%)	H_2S (%)	O_2 (%)	CH_4 (%)	Reference
Algal pond of 15 L with a biolift absorption unit	*Chlorella vulgaris*	CH_4: 55-71 CO_2: 44-48 H_2S: < 1	74-95	0.3-0.4	-	88-97	Conde et al., (1993)
Enclosed tubular photobioreactor of 1 L	*Spirulina platensis*	CH_4: 70-72 CO_2: 17-19	100	-	10-24	-	Converti et al., (2009)
Enclosed tubular photobioreactor of 0.45 L	*Chlorella vulgaris*	CH_4: 58 CO_2: 41 H_2S: 0.05	94-97	0	18-23	50-53	Mann et al., (2009)
Glass bubble columns of 0.4-0.6 L	*Chlorella vulgaris*	CH_4: 38-80 CO_2: 19-62 H_2S: 0.2	-	-	< 3.5	-	Doušková et al., (2010)
HRAP of 180 L interconnected to a 0.8 L bubble column	*Spirulina platensis*	CO_2: 30 H_2S: 0.5 N_2: 69.5	62-98	0	< 1	-	Bahr et al., (2014)

Table 5. Continued

Type of photobioreactor	Microalgae species	Raw biogas composition (%)	CO$_2$-REs (%)	H$_2$S (%)	O$_2$ (%)	CH$_4$ (%)	Reference
Enclosed tubular photobioreactor of 5.3 L	*Scenedesmus obliquus*	CH$_4$: 50-60 CO$_2$: 40-50	90	-	-	-	Thiansathit et al., (2015)
HRAP of 180 L interconnected to a 2.5 L absorption column	*Planktolynga brevicellularis* *Stigeoclonium tenue* *Limnothrix planktonica*	CH$_4$: 70 CO$_2$: 29.5 H$_2$S: 0.5	72-79	0	0.7-1.2	81	Posadas et al., (2015)
HRAP of 180 L interconnected to a 2.5 L absorption column	*Chlorella vulgaris*	CH$_4$: 70 CO$_2$: 29.5 H$_2$S: 0.5	80	0	< 2	88	Serejo et al., (2015)
HRAP of 180 L interconnected to a 2.5 L absorption column	*Phormidium sp.* *Oocystis* *Microspora sp.*	CO$_2$: 30 N$_2$: 70	55	-	-	-	Alcántara et al., (2015)
Open photobioreactor of 75 L interconnected to a 0.7 L absorption column	*Nannochloropsis gaditana*	CH$_4$: 72 CO$_2$: 28	93	-	1.2	-	Meier et al., (2015)

Table 5. Continued

Type of photobioreactor	Microalgae species	Raw biogas composition (%)	CO$_2$-REs (%)	H$_2$S (%)	O$_2$ (%)	CH$_4$ (%)	Reference
HRAP of 180 L interconnected to a 2.5 L absorption column	*Microspora sp.* *Scenedesmus* *Synechocystis aquatilis* *Woronichinia sp.*	CO$_2$: 30 N$_2$: 70	40-100	-	2-20	-	Posadas et al., (2016)
HRAP of 180 L interconnected to a 2.5 L absorption column	*Geitlerinema sp.* *Staurosira sp.* *Stigeoclonium tenue*	CH$_4$: 70 CO$_2$: 29.5 H$_2$S: 0.5	100	0	0.03	97	Toledo-Cervantes et al., (2016)
Enclosed photobioreactor of 16.9 L	*Scenedesmus sp.*	CH$_4$: 73 CO$_2$: 25 H$_2$S: 1	67	0	18	65	Prandini et al., (2016)
Open photobioreactor of 50 L interconnected to a 0.3 L absorption column	*Chlorella sorokiniana*	CH$_4$: 65 CO$_2$: 32	90	-	< 1	< 4	Meier et al., (2017)
HRAP of 180 L interconnected to a 2.5 L absorption column	*Mychonastes homosphaera*	CH$_4$: 70 CO$_2$: 29.5 H$_2$S: 0.5	≥ 95	0	< 1	96	Toledo-Cervantes et al., (2017)

Table 5. Continued

Type of photobioreactor	Microalgae species	Raw biogas composition (%)	CO$_2$-REs (%)	H$_2$S (%)	O$_2$ (%)	CH$_4$ (%)	Reference
HRAP of 25 L interconnected to a 0.35 L absorption column	-	CO$_2$: 30 H$_2$S: 0.5 N$_2$: 69.5	89-94	0	-	-	Franco-Morgado et al., (2017)
HRAP of 180 L interconnected to a 2.5 L absorption column	-	CH$_4$: 70 CO$_2$: 29.5 H$_2$S: 0.5	98-99	0-0.02	-	99	Rodero et al., (2018)
Tubular photobioreactor of 45.5 L interconnected to a 3.5 L absorption column using a 60 L mixing chamber	*Acutodesmus obliquus*	CH$_4$: 70 CO$_2$: 29.5 H$_2$S: 0.5	91	0.01	7.1	83	Toledo-Cervantes et al., (2018)
HRAP of 180 L interconnected to a 2.5 L absorption column coupled to an automatic control system	-	CH$_4$: 70 CO$_2$: 29.5 H$_2$S: 0.5	95	0	-	> 95	Rodero et al., (2019)

1.3.4 Purple phototrophic bacteria processes

Purple phototrophic bacteria (PPB) have emerged as a promising technology platform for wastewater treatment based on their ability to assimilate a higher fraction of the carbon, nitrogen and phosphorous present in wastewater compared to their aerobic and anaerobic counterparts (Hiraishi et al., 1991; Khatipov et al., 1998; Takabatake et al., 2004). More than twenty genera of PPB have been identified to date, *Rhodobacter* or *Rhodopseudomonas* being the dominant genera (Table 6). PPB are a physiologically versatile group that can grow well both phototrophically and in darkness. Pigments and photocomplexes are very similar in the different species of PPB, which suggests that the acquisition of phototrophic capacity occurred by lateral gene transfer (Madigan and Jung, 2009). Most PPB grow optimally in media containing readily biodegradable organic compounds and ammonia as nitrogen source (Madigan and Jung, 2009). In this sense, PPB have attracted an increasing interest in recent years as a platform for resource recovery from wastewaters (Puyol et al., 2017).

Table 6. Genera of phototrophic purple bacteria typically found in wastewater treatment processes (Adapted from Madigan and Jung, 2009)

Taxonomy/Phylogeny	Genus	Morphology
	Rhodobaca	Cocci to short rods
	Rhodobacter	Rods
	Rhodovulum	Rods-Cocci
	Rhodopseudomonas	Budding rods
	Rhodoblastus	Budding rods
	Blastochlorts	Budding rods
	Rhodomicrobium	Budding rods
Alphaproteobacteria	*Rhodobium*	Rods
	Rhodoolane	Rods
	Rhodoista	Spirilla
	Rhodospirillum	Spirilla
	Rhodospirillum	Spirilla
	Rhodopila	Cocci
	Rhodospira	Spirilla
	Rhodovibrio	Vibrio

Table 6. Continued

Taxonomy/Phylogeny	Genus	Morphology
	Rhodothallasium	Spirilla
Alphaproteobacteria	*Roseospira*	Spirilla
	Roseospirillum	Spirilla
	Rhodocyclus	Curled vibrios
Betaproteobacteria	*Rhodoferax*	Rods, vibrios
	Rubrivivax	Rods, curved rods

One of the most polluted wastewaters, with high concentrations of organic matter and nitrogen, is piggery wastewater, which renders them ideal to be treated with PPB (De Godos et al., 2009; García et al., 2017). The mechanism of N_2 fixation can be described by equation (24) (Madigan and Jung, 2009).

$$N_2 + 8H^+ + 8e^- \rightarrow 2NH_3 + H_2 \tag{24}$$

PPB can utilize infrared radiation as a source of energy, which reduces the power required by photon emission and allows a deeper light penetration into the cultivation broth (Hülsen et al., 2016, 2014). Another key advantage of PPB in comparison with other microorganisms is the lower influence of temperature on PPB metabolism, which makes them ideal microorganisms to support wastewater treatment under multiple weather conditions.

PPB can also be used for the upgrading of biogas. In this context, PPB exhibit a versatile metabolism capable of using H_2S in biogas or the organic matter present in wastewater as electron donor to reduce CO_2 from biogas without O_2 generation. The sulfur is thus oxidized to elemental sulfur, which is stored as granules within the cells. The unique metabolisms of PPB can support a cost-effective and environmentally friendly alternative for biogas upgrading. The mechanisms of CO_2 fixation and H_2S oxidation can be described by equations (25) and (26) (Mara, 2003).

$$21H_2S + 10CO_2 + 2NH_3 \rightarrow 2(C_5H_8O_2N) + 21S^0 + 16H_2O \tag{25}$$
$$21S^0 + 30CO_2 + 6NH_3 + 16H_2O \rightarrow 6(C_5H_8O_2N) + 21H_2SO_4 \tag{26}$$
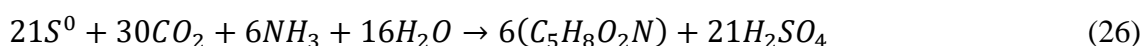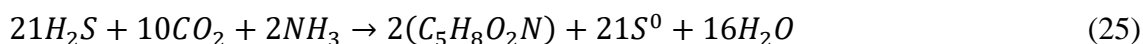
Hence, PPB-based photobioreactors can support the simultaneous treatment of piggery wastewater and the upgrading of biogas under infrared radiation. Indeed, purple photosynthetic bacteria can assimilate the CO_2 present in biogas in the Calvin cycle using the volatile fatty acids present in piggery wastewater as electron donors (McKinlay and Harwood, 2010; Vasiliadou et al., 2018). A diagram of the fundamentals of this innovative biotechnology is presented in Figure 16.
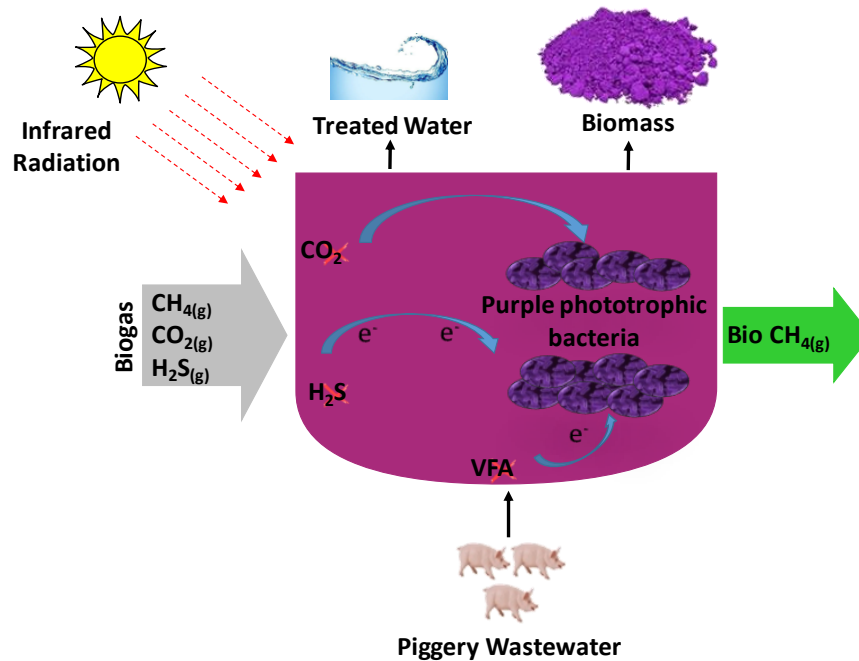

Figure 16. Fundamentals of biogas upgrading coupled with piggery wastewater treatment using purple phototrophic bacteria

Despite the potential of this technology for biogas upgrading, no proof of concept of the process has been reported in literature. This knowledge gap supports the research, development and validation of PPB-based photosynthetic biogas upgrading (Chapter 7).

1.4 References

1. Abatzoglou, N., Boivin, S., 2009. A review of biogas purification processes. Biofuels, Bioprod. Biorefining 42–71. https://doi.org/10.1002/bbb.117

2. Alcántara, C., García-encina, P.A., Muñoz, R., 2015. Evaluation of the simultaneous biogas upgrading and treatment of centrates in a high-rate algal pond through C , N and P mass balances 150–157. https://doi.org/10.2166/wst.2015.198

3. Andriani, D., Wresta, A., Atmaja, T.D., Saepudin, A., 2014. A Review on Optimization Production and Upgrading Biogas Through CO2 Removal Using Various Techniques. Appl. Biochem. Biotechnol. 172, 1909–1928. https://doi.org/10.1007/s12010-013-0652-x

4. Angelidaki, I., Treu, L., Tsapekos, P., Luo, G., Campanaro, S., Wenzel, H., Kougias, P.G., 2018. Biogas upgrading and utilization: Current status and perspectives. Biotechnol. Adv. 36, 452–466. https://doi.org/10.1016/j.biotechadv.2018.01.011

5. Augelletti, R., Conti, M., Annesini, M.C., 2017. Pressure swing adsorption for biogas upgrading. A new process configuration for the separation of biomethane and carbon dioxide. J. Clean. Prod. 140, 1390–1398. https://doi.org/10.1016/j.jclepro.2016.10.013

6. Awe, O.W., Zhao, Y., Nzihou, A., Minh, D.P., Lyczko, N., 2017. A Review of Biogas Utilisation, Purification and Upgrading Technologies. Waste and Biomass Valorization 8, 267–283. https://doi.org/10.1007/s12649-016-9826-4

7. Bahr, M., Díaz, I., Dominguez, A., González Sánchez, A., Muñoz, R., 2014. Microalgal-biotechnology as a platform for an integral biogas upgrading and nutrient removal from anaerobic effluents. Environ. Sci. Technol. 48, 573–581. https://doi.org/10.1021/es403596m

8. Bauer, F., Hulteberg, C., Persson, T., Tamm, D., 2013. Biogas upgrading – Review of commercial technologies. SGC Rapp. 270.

9. Béchet, Q., Shilton, A., Fringer, O.B., Muñoz, R., Guieysse, B., 2010. Mechanistic Modeling of Broth Temperature in Outdoor Photobioreactors. Environ. Sci. Technol. 44, 2197–2203. https://doi.org/10.1021/es903214u

10. Beil, M., Beyrich, W., 2013. Biogas upgrading to biomethane, in: Wellinger, A., Murphy, J., Baxter, D.B.T.-T.B.H. (Eds.), Woodhead Publishing Series in Energy. Woodhead Publishing, pp. 342–377. https://doi.org/https://doi.org/10.1533/9780857097415.3.342

11. Bose, A., Lin, R., Rajendran, K., O'Shea, R., Xia, A., Murphy, J.D., 2019. How to optimise photosynthetic biogas upgrading: a perspective on system design and microalgae selection. Biotechnol. Adv. 107444. https://doi.org/10.1016/j.biotechadv.2019.107444

12. Burkhardt, M., Busch, G., 2013. Methanation of hydrogen and carbon dioxide. Appl. Energy 111, 74–79. https://doi.org/https://doi.org/10.1016/j.apenergy.2013.04.080

13. Conde, J.L., Moro, L.E., Travieso, L., Sanchez, E.P., Leiva, A., Dupeirón, R., Escobedo, R., 1993. Biogas purification process using intensive microalgae cultures. Biotechnol. Lett. 15, 317–320. https://doi.org/10.1007/BF00128326

14. Converti, A., Oliveira, R.P.S., Torres, B.R., Lodi, A., Zilli, M., 2009. Biogas production and valorization by means of a two-step biological process. Bioresour. Technol. 100, 5771–5776. https://doi.org/10.1016/j.biortech.2009.05.072

15. De Godos, I., Blanco, S., García-encina, P.A., Becares, E., Muñoz, R., 2009. Bioresource Technology Long-term operation of high rate algal ponds for the bioremediation of piggery wastewaters at high loading rates. Bioresour. Technol. 100, 4332–4339. https://doi.org/10.1016/j.biortech.2009.04.016

16. Demmink, J.F., Beenackers, A.A.C.M., 1998. Gas Desulfurization with Ferric Chelates of EDTA and HEDTA: New Model for the Oxidative Absorption of Hydrogen Sulfide. Ind. Eng. Chem. Res. 37, 1444–1453. https://doi.org/10.1021/ie970427n

17. Demmink, J.F., Wubs, H.J., Beenackers, A.A.C.M., 1994. Oxidative Absorption of Hydrogen Sulfide by a Solution of Ferric Nitrilotriacetic Acid Complex in a Cocurrent Down Flow Column Packed with SMV-4 Static Mixers. Ind. Eng. Chem. Res. 33, 2989–2995. https://doi.org/10.1021/ie00036a013

18. Díaz, I., Lopes, A.C., Pérez, S.I., Fdz-Polanco, M., 2011. Determination of the optimal rate for the microaerobic treatment of several H2S concentrations in biogas from sludge digesters. Water Sci. Technol. 64, 233–238. https://doi.org/10.2166/wst.2011.648

19. Díaz, I., Lopes, A.C., Pérez, S.I., Fdz-Polanco, M., 2010. Performance evaluation of oxygen, air and nitrate for the microaerobic removal of hydrogen sulphide in biogas from sludge digestion. Bioresour. Technol. 101, 7724–

7730. https://doi.org/10.1016/j.biortech.2010.04.062

20. Doušková, I., Kaštánek, F., Maléterová, Y., Kaštánek, P., Doucha, J., Zachleder, V., 2010. Utilization of distillery stillage for energy generation and concurrent production of valuable microalgal biomass in the sequence: Biogas-cogeneration-microalgae-products. Energy Convers. Manag. 51, 606–611. https://doi.org/10.1016/j.enconman.2009.11.008

21. European Biogas Association, 2019a. Biogas Basics.

22. European Biogas Association, 2019b. EBA Annual Report 2019.

23. European Committee for Standardization, 2018. UNE EN 16723-2:2018 Natural gas and biomethane for use in transport and biomethane for injection in the natural gas network - Part 2: Automotive fuels specification [WWW Document]. URL https://www.en-standard.eu/une-en-16723-2-2018-natural-gas-and-biomethane-for-use-in-transport-and-biomethane-for-injection-in-the-natural-gas-network-part-2-automotive-fuels-specification/ (accessed 12.10.19).

24. European Committee for Standardization, 2017. UNE EN 16723-1:2017 Natural gas and biomethane for use in transport and biomethane for injection in the natural gas network - Part 1: Specifications for biomethane for injection in the natural gas network [WWW Document]. URL https://www.en-standard.eu/une-en-16723-1-2017-natural-gas-and-biomethane-for-use-in-transport-and-biomethane-for-injection-in-the-natural-gas-network-part-1-specifications-for-biomethane-for-injection-in-the-natural-gas-network/ (accessed 12.10.19).

25. Fernández, M., Ramírez, M., Gómez, J.M., Cantero, D., 2014. Biogas biodesulfurization in an anoxic biotrickling filter packed with open-pore polyurethane foam. J. Hazard. Mater. 264, 529–535. https://doi.org/10.1016/j.jhazmat.2013.10.046

26. Fortuny, M., Gamisans, X., Deshusses, M.A., Lafuente, J., Casas, C., Gabriel, D., 2011. Operational aspects of the desulfurization process of energy gases mimics in biotrickling filters. Water Res. 45, 5665–5674. https://doi.org/10.1016/j.watres.2011.08.029

27. Franco-Morgado, M., Alcántara, C., Noyola, A., Muñoz, R., González-Sánchez, A., 2017. A study of photosynthetic biogas upgrading based on a high rate algal pond under alkaline conditions: Influence of the illumination regime. Sci. Total Environ. 592, 419–425. https://doi.org/10.1016/j.scitotenv.2017.03.077

28. Frare, L.M., Vieira, M.G.A., Silva, M.G.C., Pereira, N.C., Gimenes, M.L., 2010. Hydrogen sulfide removal from biogas using Fe/EDTA solution: Gas/Liquid contacting and sulfur formation. Environ. Prog. Sustain. Energy 29. https://doi.org/10.1002/ep

29. Gabriel, D., Deshusses, M.A., Gamisans, X., 2013. Desulfurization of Biogas in Biotrickling Filters. Air Pollut. Prev. Control Bioreact. Bioenergy 513–523. https://doi.org/10.1002/9781118523360.ch22

30. García, D., Posadas, E., Grajeda, C., Blanco, S., Martínez-Páramo, S., Acién, G., García-Encina, P., Bolado, S., Muñoz, R., 2017. Comparative evaluation of piggery wastewater treatment in algal-bacterial photobioreactors under indoor and outdoor conditions. Bioresour. Technol. 245, 483–490. https://doi.org/10.1016/j.biortech.2017.08.135

31. Herrmann, C., Kalita, N., Wall, D., Xia, A., Murphy, J.D., 2016. Optimised biogas production from microalgae through co-digestion with carbon-rich co-substrates. Bioresour. Technol. 214, 328–337. https://doi.org/10.1016/j.biortech.2016.04.119

32. Hiraishi, A., Yanase, A., Kitamura, H., 1991. Polyphosphate Grown Accumulation under Different by Rhodobacter Environmental on the sphaeroides Conditions with Special Emphasis Phosphate Effect of External Concentrations. Bull. Japanese Soc. Microb. Ecol. 6, 25–32.

33. Horikawa, M.S., Rossi, F., Gimenes, M.L., Costa, C.M.M., Da Silva, M.G.C., 2004. Chemical absorption of H2S for biogas purification. Brazilian J. Chem. Eng. 21, 415–422. https://doi.org/10.1590/S0104-66322004000300006

34. Hülsen, T., Barry, E.M., Lu, Y., Puyol, D., Keller, J., Batstone, D.J., 2016. Domestic wastewater treatment with

purple phototrophic bacteria using a novel continuous photo anaerobic membrane bioreactor. Water Res. 100, 486–495. https://doi.org/10.1016/j.watres.2016.04.061

35. Hülsen, T., Batstone, D.J., Keller, J., 2014. Phototrophic bacteria for nutrient recovery from domestic wastewater. Water Res. 50, 18–26. https://doi.org/10.1016/j.watres.2013.10.051

36. Iovane, P., Nanna, F., Ding, Y., Bikson, B., Molino, A., 2014. Experimental test with polymeric membrane for the biogas purification from CO2 and H2S. Fuel 135, 352–358. https://doi.org/10.1016/j.fuel.2014.06.060

37. Janssen, A.J.H., Sleyster, R., van der Kaa, C., Jochemsen, A., Bontsema, J., Lettinga, G., 1995. Biological sulphide oxidation in a fed-batch reactor. Biotechnol. Bioeng. 47, 327–333. https://doi.org/10.1002/bit.260470307

38. Jenicek, P., Keclik, F., Maca, J., Bindzar, J., 2008. Use of microaerobic conditions for the improvement of anaerobic digestion of solid wastes. Water Sci. Technol. 58, 1491–1496. https://doi.org/10.2166/wst.2008.493

39. Kanjanarong, J., Giri, B.S., Jaisi, D.P., Oliveira, F.R., Boonsawang, P., Chaiprapat, S., Singh, R.S., Balakrishna, A., Khanal, S.K., 2017. Removal of hydrogen sulfide generated during anaerobic treatment of sulfate-laden wastewater using biochar: Evaluation of efficiency and mechanisms. Bioresour. Technol. 234, 115–121. https://doi.org/https://doi.org/10.1016/j.biortech.2017.03.009

40. Khatipov, E., Miyakea, M., Miyakec, J., Asadaa, Y., 1998. Accumulation of poly- L -hydroxybutyrate by Rhodobacter sphaeroides on various carbon and nitrogen substrates. FEMS Microbiol. Lett. 162, 39–45.

41. Khoshnevisan, B., Tsapekos, P., Alfaro, N., Díaz, I., Fdz-Polanco, M., Rafiee, S., Angelidaki, I., 2017. A review on prospects and challenges of biological H2S removal from biogas with focus on biotrickling filtration and microaerobic desulfurization. Biofuel Res. J. 4, 741–750. https://doi.org/10.18331/BRJ2017.4.4.6

42. Kobayashi, T., Li, Y.Y., Kubota, K., Harada, H., Maeda, T., Yu, H.Q., 2012. Characterization of sulfide-oxidizing microbial mats developed inside a full-scale anaerobic digester employing biological desulfurization. Appl. Microbiol. Biotechnol. 93, 847–857. https://doi.org/10.1007/s00253-011-3445-6

43. Lebrero, R., Toledo-Cervantes, A., Muñoz, R., del Nery, V., Foresti, E., 2016. Biogas upgrading from vinasse digesters: a comparison between an anoxic biotrickling filter and an algal-bacterial photobioreactor. J. Chem. Technol. Biotechnol. 91, 2488–2495. https://doi.org/10.1002/jctb.4843

44. Luo, G., Angelidaki, I., 2012. Integrated biogas upgrading and hydrogen utilization in an anaerobic reactor containing enriched hydrogenotrophic methanogenic culture. Biotechnol. Bioeng. 109, 2729–2736. https://doi.org/10.1002/bit.24557

45. Madigan, M.T., Jung, D.O., 2009. An Overview of Purple Bacteria: Systematics, Physiology, and Habitats BT - The Purple Phototrophic Bacteria, in: Hunter, C.N., Daldal, F., Thurnauer, M.C., Beatty, J.T. (Eds.), . Springer Netherlands, Dordrecht, pp. 1–15. https://doi.org/10.1007/978-1-4020-8815-5_1

46. Madigan, M.T., Martinko, J.M., Dunlap, P. V., Clark, D.P., 2009. Brock biology of microorganisms, 12th ed. Pearson Benjamin-Cummings, San Francisco.

47. Mann, G., Schlegel, M., Schumann, R., Sakalauskas, A., 2009. Biogas-conditioning with microalgae. Agron. Res. 7, 33–38.

48. Mara, D., 2003. Domestic Wastewater Treatment in Developing Countries. Earthscan, London.

49. McKinlay, J.B., Harwood, C.S., 2010. Carbon dioxide fixation as a central redox cofactor recycling mechanism in bacteria. Proc. Natl. Acad. Sci. 107, 11669–11675. https://doi.org/10.1073/pnas.1006175107

50. Meier, L., Barros, P., Torres, A., Vilchez, C., Jeison, D., 2017. Photosynthetic biogas upgrading using microalgae: Effect of light/dark photoperiod. Renew. Energy 106, 17–23. https://doi.org/10.1016/j.renene.2017.01.009

51. Meier, L., Pérez, R., Azócar, L., Rivas, M., Jeison, D., 2015. Photosynthetic CO2 uptake by microalgae: An attractive tool for biogas upgrading. Biomass and Bioenergy 73, 102–109. https://doi.org/10.1016/j.biombioe.2014.10.032

52. Ministerio para la Transición Ecológica, 2018. Resolución de 8 de octubre de 2018, de la Dirección General de

Política Energética y Minas, por la que se modifican las normas de gestión técnica del sistema NGTS-06, NGTS-07 y los protocolos de detalle PD-01 y PD-02. Boletín Of. del estado 102917–102948.

53. Montebello, A.M., Bezerra, T., Rovira, R., Rago, L., Lafuente, J., Gamisans, X., Campoy, S., Baeza, M., Gabriel, D., 2013. Operational aspects, pH transition and microbial shifts of a H2S desulfurizing biotrickling filter with random packing material. Chemosphere 93, 2675–2682. https://doi.org/10.1016/j.chemosphere.2013.08.052

54. Montebello, A.M., Fernández, M., Almenglo, F., Ramírez, M., Cantero, D., Baeza, M., Gabriel, D., 2012. Simultaneous methylmercaptan and hydrogen sulfide removal in the desulfurization of biogas in aerobic and anoxic biotrickling filters. Chem. Eng. J. 200–202, 237–246. https://doi.org/10.1016/j.cej.2012.06.043

55. Muñoz, R., Meier, L., Diaz, I., Jeison, D., 2015. A review on the state-of-the-art of physical/chemical and biological technologies for biogas upgrading. Rev. Environ. Sci. Bio/Technology 14, 727–759. https://doi.org/10.1007/s11157-015-9379-1

56. Nagarajan, D., Lee, D.-J., Chang, J.-S., 2019. Integration of anaerobic digestion and microalgal cultivation for digestate bioremediation and biogas upgrading. Bioresour. Technol. 290, 121804. https://doi.org/10.1016/j.biortech.2019.121804

57. Oliva, G., Ángeles, R., Rodríguez, E., Turiel, S., Naddeo, V., Zarra, T., Belgiorno, V., Muñoz, R., Lebrero, R., 2019. Comparative evaluation of a biotrickling filter and a tubular photobioreactor for the continuous abatement of toluene. J. Hazard. Mater. 380, 120860. https://doi.org/10.1016/j.jhazmat.2019.120860

58. Persson, M., Jönsson, O., Wellinger, A., 2006. Biogas Upgrading to Vehicle Fuel Standards and Grid Injection [WWW Document]. URL http://task37.ieabioenergy.com/files/daten-redaktion/download/publi-task37/upgrading_report_final.pdf (accessed 1.23.20).

59. Petersson, a., Wellinger, A., 2009. Biogas upgrading technologies–developments and innovations. IEA Bioenergy 20.

60. Posadas, E., Serejo, M.L., Blanco, S., Pérez, R., García-Encina, P.A., Muñoz, R., 2015. Minimization of biomethane oxygen concentration during biogas upgrading in algal-bacterial photobioreactors. Algal Res. 12, 221–229. https://doi.org/10.1016/j.algal.2015.09.002

61. Posadas, E., Szpak, D., Lombó, F., Domínguez, A., Díaz, I., Blanco, S., García-Encina, P.A., Muñoz, R., 2016. Feasibility study of biogas upgrading coupled with nutrient removal from anaerobic effluents using microalgae-based processes. J. Appl. Phycol. 28, 2147–2157. https://doi.org/10.1007/s10811-015-0758-3

62. Prandini, J.M., da Silva, M.L.B., Mezzari, M.P., Pirolli, M., Michelon, W., Soares, H.M., 2016. Enhancement of nutrient removal from swine wastewater digestate coupled to biogas purification by microalgae Scenedesmus spp. Bioresour. Technol. 202, 67–75. https://doi.org/10.1016/j.biortech.2015.11.082

63. Pulz, O., 2001. Photobioreactors: Production systems for phototrophic microorganisms. Appl. Microbiol. Biotechnol. 57, 287–293. https://doi.org/10.1007/s002530100702

64. Puyol, D., Batstone, D.J., Hülsen, T., Astals, S., Peces, M., Krömer, J.O., 2017. Resource Recovery from Wastewater by Biological Technologies: Opportunities, Challenges, and Prospects . Front. Microbiol. .

65. Ramos, I., Fdz-Polanco, M., 2014. Microaerobic control of biogas sulphide content during sewage sludge digestion by using biogas production and hydrogen sulphide concentration. Chem. Eng. J. 250, 303–311. https://doi.org/10.1016/j.cej.2014.04.027

66. Ramos, I., Pérez, R., Reinoso, M., Torio, R., Fdz-Polanco, M., 2014. Microaerobic digestion of sewage sludge on an industrial-pilot scale: The efficiency of biogas desulphurisation under different configurations and the impact of O2 on the microbial communities. Bioresour. Technol. 164, 338–346. https://doi.org/10.1016/j.biortech.2014.04.109

67. Rittmann, S.K.-M.R., 2015. A Critical Assessment of Microbiological Biogas to Biomethane Upgrading Systems BT - Biogas Science and Technology, in: Guebitz, G.M., Bauer, A., Bochmann, G., Gronauer, A., Weiss, S. (Eds.), . Springer International Publishing, Cham, pp. 117–135. https://doi.org/10.1007/978-3-319-21993-6_5

68. Rodero, M. del R., Carvajal, A., Castro, V., Navia, D., de Prada, C., Lebrero, R., Muñoz, R., 2019. Development of a control strategy to cope with biogas flowrate variations during photosynthetic biogas upgrading. Biomass and Bioenergy 131, 105414. https://doi.org/10.1016/j.biombioe.2019.105414

69. Rodero, R., Ángeles, R., Marín, D., Díaz, I., Colzi, A., Posadas, E., Lebrero, R., Muñoz, R., 2018a. Biogas Purification and Upgrading Technologies, in: Tabatabaei, M., Ghanavati, H. (Eds.), Biogas: Fundamentals, Process, and Operation. Springer International Publishing, pp. 239–276. https://doi.org/10.1007/978-3-319-77335-3

70. Rodero, R., Posadas, E., Toledo-Cervantes, A., Lebrero, R., Muñoz, R., 2018b. Influence of alkalinity and temperature on photosynthetic biogas upgrading efficiency in high rate algal ponds. Algal Res. 33, 284–290. https://doi.org/10.1016/j.algal.2018.06.001

71. Rutledge, B., 2005. California Biogas Industry Assessment White Paper [WWW Document]. URL https://calstart.org/wp-content/uploads/2018/10/California-Biogas-Industry-Assessment.pdf (accessed 1.23.20).

72. Ryckebosch, E., Drouillon, M., Vervaeren, H., 2011. Techniques for transformation of biogas to biomethane. Biomass and Bioenergy 35, 1633–1645. https://doi.org/10.1016/j.biombioe.2011.02.033

73. Sander, R., 2015. Compilation of Henry 's law constants (version 4.0) for water as solvent 4399–4981. https://doi.org/10.5194/acp-15-4399-2015

74. Schiavon Maia, D.C., Niklevicz, R.R., Arioli, R., Frare, L.M., Arroyo, P.A., Gimenes, M.L., Pereira, N.C., 2017. Removal of H2S and CO2 from biogas in bench scale and the pilot scale using a regenerable Fe-EDTA solution. Renew. Energy 109, 188–194. https://doi.org/10.1016/j.renene.2017.03.023

75. Serejo, M.L., Posadas, E., Boncz, M.A., Blanco, S., García-Encina, P., Muñoz, R., 2015. Influence of biogas flow rate on biomass composition during the optimization of biogas upgrading in microalgal-bacterial processes. Environ. Sci. Technol. 49, 3228–3236. https://doi.org/10.1021/es5056116

76. Strevett, K.A., Vieth, R.F., Grasso, D., 1995. Chemo-autotrophic biogas purification for methane enrichment: mechanism and kinetics. Chem. Eng. J. Biochem. Eng. J. 58, 71–79. https://doi.org/https://doi.org/10.1016/0923-0467(95)06095-2

77. Stürmer, B., Kirchmeyr, F., Kovacs, K., Hofmann, F., Collins, D., Claire, I., Stambasky, J., Proietti, S., Loriana, P., 2020. Technical-economic analysis for determining the feasibility threshold for tradable biomethane certificates. pp. 1–24.

78. Sun, Q., Li, H., Yan, J., Liu, L., Yu, Z., Yu, X., 2015. Selection of appropriate biogas upgrading technology-a review of biogas cleaning, upgrading and utilisation. Renew. Sustain. Energy Rev. 51, 521–532. https://doi.org/10.1016/j.rser.2015.06.029

79. Syed, M., Soreanu, G., Falletta, P., Béland, M., 2006. Removal of hydrogen sulfide from gas streams using biological processes - A review. Can. Biosyst. Eng. 48, 2.1-2.14.

80. Takabatake, H., Suzuki, K., Ko, I.-B., Noike, T., 2004. Characteristics of anaerobic ammonia removal by a mixed culture of hydrogen producing photosynthetic bacteria. Bioresour. Technol. 95, 151–158. https://doi.org/10.1016/j.biortech.2003.12.019

81. Tang, K., Baskaran, V., Nemati, M., 2009. Bacteria of the sulphur cycle: An overview of microbiology, biokinetics and their role in petroleum and mining industries. Biochem. Eng. J. 44, 73–94. https://doi.org/10.1016/j.bej.2008.12.011

82. Thiansathit, W., Keener, T.C., Khang, S.J., Ratpukdi, T., Hovichitr, P., 2015. The kinetics of Scenedesmus obliquus microalgae growth utilizing carbon dioxide gas from biogas. Biomass and Bioenergy 76, 79–85. https://doi.org/10.1016/j.biombioe.2015.03.012

83. Tippayawong, N., Thanompongchart, P., 2010. Biogas quality upgrade by simultaneous removal of CO2 and H2S in a packed column reactor. Energy 35, 4531–4535. https://doi.org/10.1016/j.energy.2010.04.014

84. Toledo-cervantes, A., Estrada, J.M., Lebrero, R., Muñoz, R., 2017. A comparative analysis of biogas upgrading

technologies : Photosynthetic vs physical / chemical processes. Algal Res. 25, 237–243. https://doi.org/10.1016/j.algal.2017.05.006

85. Toledo-Cervantes, A., Madrid-Chirinos, C., Cantera, S., Lebrero, R., Muñoz, R., 2017. Influence of the gas-liquid flow configuration in the absorption column on photosynthetic biogas upgrading in algal-bacterial photobioreactors. Bioresour. Technol. 225, 336–342. https://doi.org/10.1016/j.biortech.2016.11.087

86. Toledo-Cervantes, A., Morales, T., González, Á., Muñoz, R., Lebrero, R., 2018. Long-term photosynthetic CO_2 removal from biogas and flue-gas: Exploring the potential of closed photobioreactors for high-value biomass production. Sci. Total Environ. 640–641, 1272–1278. https://doi.org/10.1016/j.scitotenv.2018.05.270

87. Toledo-Cervantes, A., Serejo, M.L., Blanco, S., Pérez, R., Lebrero, R., Muñoz, R., 2016. Photosynthetic biogas upgrading to bio-methane: Boosting nutrient recovery via biomass productivity control. Algal Res. 17, 46–52. https://doi.org/10.1016/j.algal.2016.04.017

88. Uggetti, E., García, J., Álvarez, J.A., García-Galán, M.J., 2018. Start-up of a microalgae-based treatment system within the biorefinery concept: From wastewater to bioproducts. Water Sci. Technol. 78, 114–124. https://doi.org/10.2166/wst.2018.195

89. Vasiliadou, I.A., Berná, A., Manchon, C., Melero, J.A., Martinez, F., Esteve-Nuñez, A., Puyol, D., 2018. Biological and bioelectrochemical systems for hydrogen production and carbon fixation using purple phototrophic bacteria. Front. Energy Res. 6, 1–12. https://doi.org/10.3389/fenrg.2018.00107

90. Wall, D.M., Dumont, M., Murphy, J.D., 2018. Green gas - Facilitating a future green gas grid through the production of renewable gas, IEA Bioenergy Task 37.

91. Wang, W., Xie, L., Luo, G., Zhou, Q., Angelidaki, I., 2013. Performance and microbial community analysis of the anaerobic reactor with coke oven gas biomethanation and in situ biogas upgrading. Bioresour. Technol. 146, 234–239. https://doi.org/10.1016/j.biortech.2013.07.049

92. Wellinger, A., Lindberg, A., 2005. Biogas upgrading and utilisation. IEA Bioenergy Task 24: Energy from biological conversion of organic waste.

93. Wubs, H.J., Beenackers, A.A.C.M., 1993. Kinetics of H2S absorption into aqueous ferric solutions of edta and hedta. Ind. Eng. Chem. Res. 32, 2580–2594. https://doi.org/10.1021/ie00023a022

94. Yan, C., Muñoz, R., Zhu, L., Wang, Y., 2016. The effects of various LED (light emitting diode) lighting strategies on simultaneous biogas upgrading and biogas slurry nutrient reduction by using of microalgae Chlorella sp. Energy 106, 554–561. https://doi.org/10.1016/j.energy.2016.03.033

Aims and Scope

2.1 Justification

The increase in the production of biogas from the anaerobic digestion of wastewater or organic solid waste represents an opportunity to reduce the consumption of fossil fuels in activities such as steam generation, electricity generation, heating or transportation. Despite the widespread use of biogas for industrial heat and electricity generation on-site (prior desulfurization), a biogas upgrading process is required prior use as a vehicle fuel or injection into natural gas networks. In this context, multiple physical-chemical and biological technologies are nowadays commercially available in order to remove CO_2 and H_2S from biogas. Most of these commercial technologies must be sequentially implemented to remove both H_2S, CO_2 and trace contaminants such as siloxanes or volatile organic contaminants. This results in complex and costly processes, which ultimately increases the price of biomethane. In addition, physical-chemical technologies typically exhibit high environmental impacts derived from the intensive energy use and the discharge into the open atmosphere of the CO_2 separated from biogas. Therefore, the engineering of new technologies capable of providing the simultaneously removal of H_2S and CO_2 from biogas in a single step process is required. In this context, algal-bacterial processes have recently emerged as an environmentally friendly and cost-efficient alternative to remove CO_2 and H_2S from raw biogas in a single-step process at low operating costs and with limited environmental impacts. Several investigations have been carried out in algal-bacterial photobioreactors (closed and open systems) under indoors conditions (under constant temperature and radiation) and at pilot scale, which limits the widespread implementation of this technology. In this context, the evaluation of the performance of photosynthetic biogas upgrading under outdoors conditions is required in order to understand the influence of the seasonal and diurnal variations of light irradiance, the number of sun hours and temperature on the quality of the upgraded biogas. Similarly, the validation of this technology at semi-industrial scale in order to promote its acceptance by the industrial sector is necessary.

On the other hand, purple phototrophic bacteria (PPB) have emerged as a promising biological technology platform for wastewater treatment and for the upgrading of biogas. In this context, PPB exhibit a versatile metabolism capable of using the H_2S in biogas or the organic matter present in the wastewater as electron donor to reduce CO_2 from biogas without O_2 generation. The sulfur is thus oxidized to elemental sulfur (S^0), which is stored

as granules within the cells. The unique metabolism of PPB can support a cost-effective and environmentally friendly biotechnology for biogas upgrading. Despite the potential of this technology, no proof of concept of the process has been reported in literature. This knowledge gap supports the research, development and validation of PPB-based photosynthetic biogas upgrading presented in this thesis.

Finally, the use of an absorption-stripping process based on an aqueous solution of Fe-EDTA represents an innovative physicochemical technology capable of simultaneously removing H_2S and CO_2 from biogas with a minimum reagent demand. This technology has been studied in recent years in order to elucidate the potential of Fe^{3+}/EDTA to remove H_2S from biogas, where H_2S is oxidized into elemental sulfur. Despite the successful performance of this technology for the removal of H_2S, the optimization of the operational conditions to support a simultaneous removal of CO_2 and H_2S has not been conducted so far. In this sense, the engineering of a novel Fe/EDTA/carbonate-based scrubbing process (solution of Fe/EDTA enriched with HCO_3^- and CO_3^{2-}) at a high pH value (9.0-10.0) can mediate a rapid and effective CO_2 capture at ambient pressure and allow an air-aided CO_2 desorption during Fe^{2+} regeneration. This hypothesis justifies the research, development and validation of this novel technology.

2.2 Main Objectives

The overall objective of the present thesis was the development of innovative technologies in order to overcome the current limitations of physicochemical and biological technologies devoted to the upgrading of biogas into biomethane. This goal will be addressed using a multidisciplinary approach involving both photosynthetic systems and absorption-desorption units supported by chemical oxidation. More specifically, the individual goals to achieve this overall objective were:

1.   The study of biogas upgrading in algal-bacterial photobioreactors under outdoors conditions.

2.   The assessment of the influence of the seasonal and diurnal variations of light irradiance, the number of sun hours and temperature on the quality of the upgraded biogas.

3.   The validation of photosynthetic biogas upgrading at semi-industrial scale in order to promote its acceptance by the industrial sector.

4.   The study of the potential and limitations of PPB for the upgrading of biogas coupled to piggery wastewater treatment.

5.   The study of a novel Fe/EDTA/carbonate-based scrubbing process for the simultaneous removal of H_2S and CO_2 from biogas.

2.3 Development of the thesis

In order to fulfill with the specific objectives above cited, eight experiments were conducted along this 4-y thesis. More specifically:

The first and second objective were accomplished in **Chapters 1, 2, 3, 4 and 5**. First, the bioconversion of biogas to biomethane coupled to centrate treatment during summer time was evaluated in an outdoors pilot scale high rate algal pond (HRAP) interconnected to an external absorption column (AC) via settled broth recirculation (**Chapter 1**). Then (**Chapter 2**) the influence of the diffuser type and liquid-to-biogas (L/G) ratio on biogas upgrading performance in an outdoors pilot scale HRAP was evaluated. In addition, the influence of seasonal environmental variations on biogas upgrading coupled with digestate treatment in an outdoors pilot scale HRAP was herein evaluated for the first time (**Chapters 3 and 4**). Finally, three innovative operational strategies to improve the quality of biomethane during unfavorable environmental conditions and to prevent an external alkalinity supplementation were evaluated in an outdoors pilot scale HRAP interconnected to an external AC (**Chapter 5**).

The third objective was accomplished in **Chapter 6**, where the influence of L/G ratios and alkalinity on biogas upgrading performance was evaluated in a 11.7 m^3 outdoors horizontal semi-closed tubular photobioreactor interconnected to a 45 L AC.

Chapter 7 addressed the fourth objective by evaluating the potential of PPB for the simultaneous treatment of piggery wastewater and biogas upgrading in gas-tight batch photobioreactors under infrared radiation.

Finally, the fifth objective was accomplished in **Chapter 8**, where the potential and limitations of a novel Fe/EDTA/carbonate-based scrubbing process for the simultaneous removal of H_2S and CO_2 from biogas were evaluated in an absorption column interconnected to an air-aided regeneration column.

Chapter 1

Simultaneous biogas upgrading and centrate treatment in an outdoors pilot scale high rate algal pond

Esther Posadas, David Marín, Saúl Blanco, Raquel Lebrero, Raúl Muñoz. Bioresource Technology 232 (2017) 133-141

Simultaneous biogas upgrading and centrate treatment in an outdoors pilot scale high rate algal pond

Esther Posadas[1], David Marín[1, 3], Saúl Blanco[2], Raquel Lebrero[1], Raúl Muñoz[1,*]

[1] Department of Chemical Engineering and Environmental Technology, Valladolid University, Dr. Mergelina, s/n, 47011, Valladolid, Spain.

[2] Department of Biodiversity and Environmental Management, University of León, 24071 León, Spain.

[3] Universidad Pedagógica Nacional Francisco Morazán, Boulevard Centroamérica, Tegucigalpa, Honduras.

[*] Corresponding author: mutora@iq.uva.es

Abstract

The bioconversion of biogas to biomethane coupled to centrate treatment was evaluated in an outdoors pilot scale high rate algal pond interconnected to an external CO_2-H_2S absorption column (AC) via settled broth recirculation. CO_2-removal efficiencies ranged from 50 to 95% depending on the alkalinity of the cultivation broth and environmental conditions, while a complete H_2S removal was achieved regardless of the operational conditions. A maximum CH_4 concentration of 94% with a limited O_2 and N_2 stripping was recorded in the upgraded biogas at recycling liquid/biogas ratios in the AC of 1 and 2. Process operation at a constant biomass productivity of 15 g m^{-2} d^{-1} and the minimization of effluent generation supported high carbon and nutrient recoveries in the harvested biomass (C = 66±8%, N= 54±18%, P≈100% and S =16±3%). Finally, a low diversity in the structure of the microalgae population was promoted by the environmental and operational conditions imposed.

Keywords: algal-bacterial symbiosis, biogas upgrading, biomethane, microalgae, outdoors conditions, wastewater treatment.

1. Introduction

Biogas from the anaerobic digestion of organic solid waste and wastewater represents a renewable energy source with a significant potential to reduce the current world´s fossil fuel dependence (Hermann et al., 2016). Biogas can be used as a fuel for the on-site generation of domestic heat or steam and electricity in industry, as a substrate in fuel cells or as a substitute of natural gas prior to upgrading (Andriani et al., 2014; Muñoz et al., 2015). For instance, the use of this biofuel in the European Union during 2014 supported

a production of electricity and heat of $2.82 \cdot 10^5$ TJ and $1.16 \cdot 10^5$ TJ, respectively (EBA, 2016). Biogas conversion to biomethane is highly recommended due to the high concentration of impurities present in the raw biogas: CO_2 (25-60%), CO (<0.6%), H_2S (0.005-2%), N_2 (0-2%), NH_3 (<1%), H_2O (5-10%), O_2 (0-1%), siloxanes (0-0.02%) and halogenated hydrocarbons (VOC <0.6%) (Ryckebosch et al., 2011). In fact, biogas upgrading is a mandatory step required prior biomethane injection into natural gas grids or use as a vehicle fuel, which must provide concentrations of CH_4 ≥95%, CO_2 ≤2%, O_2≤0.3% and negligible amounts of H_2S according to most international regulations (Muñoz et al., 2015). In this context, the removal of CO_2 from raw biogas would contribute to reduce the transportation costs and to increase the calorific value of biomethane, while the removal of H_2S would limit the corrosion in pipelines, boilers, engines, etc. (Posadas et al., 2015a).

Several physical-chemical and biological technologies are nowadays available at commercial scale to remove CO_2 and H_2S from biogas. Pressure swing adsorption, amine/water/organic scrubbing or membrane separation are typically applied to remove CO_2, while activated carbon filtration, chemical precipitation or anoxic/aerobic biotrickling filtration provide satisfactory levels of H_2S removal (Mann et al., 2016; Toledo-Cervantes et al., 2016; Muñoz et al., 2015). However, these H_2S and CO_2 removal technologies must be sequentially implemented to remove both biogas contaminants, which makes physical-chemical biogas upgrading a costly and complex two-stage process (Muñoz et al., 2015). The few technologies supporting a simultaneous removal of CO_2 and H_2S from low S-strength biogas (i.e. chemical scrubbing) exhibit high environmental impacts and operating costs (Tippayawong and Thanompongchart, 2010). In this context, algal-bacterial photobioreactors have recently emerged as an environmentally friendly and cost-efficient alternative to remove CO_2 and H_2S from raw biogas in a single-step process (Bahr et al., 2014; Yan et al., 2016).

Photosynthetic biogas upgrading in algal-bacterial photobioreactors is based on the simultaneous fixation of CO_2 by microalgae and oxidation of H_2S to SO_4^{2-} by sulfur oxidizing bacteria or chemical reactions, the latter supported by the high dissolved oxygen (DO) concentrations present in the cultivation broth (Posadas et al., 2015a; Toledo-Cervantes et al., 2016). The economic and environmental sustainability of this

process can be boosted via integration of biogas upgrading with the recovery of nutrients from digestate in the form of a valuable algal-bacterial biomass (Serejo et al., 2015; Posadas et al., 2015a, 2016; Toledo-Cervantes et al., 2016; Yan et al., 2016).

Several investigations aiming at integrating photosynthetic biogas upgrading with digestate treatment have been recently carried out in indoors high rate algal ponds (HRAPs) interconnected to biogas absorption columns (AC) under artificial illumination (Bahr et al. 2014; Alcántara et al., 2015; Posadas et al. 2015a, 2016; Serejo et al. 2015; Meier et al. 2015; Toledo-Cervantes et al. 2016, 2017). Despite the rapid optimization of this technology (Toledo-Cervantes et al., 2016, 2017), the constant temperature (often in the optimum range) and radiation (often too low compared to solar radiation) prevailing under laboratory conditions still hinder the complete understanding of a process designed to be ultimately implemented outdoors under solar radiation. Therefore, the evaluation of the performance of photosynthetic biogas upgrading under outdoors conditions is crucial to understand the influence of the diurnal variations of light irradiance and temperature on the quality of the upgraded biogas. Similarly, process operation to minimize the desorption of O_2 and N_2 from the cultivation broth to the upgraded biogas, and to maximize nutrient recovery from digestates, must be optimized to the particular conditions prevailing during outdoors operation.

Despite the remarkable environmental advantages of using digestates as a nutrient source during biogas upgrading, their high nutrients content results in high biomass concentrations in the HRAPs (7-50 g L^{-1}) and the need to operate the process at low digestates flowrates (Toledo-Cervantes et al., 2016). This severely decreases the photosynthetic efficiency of the system as a result of mutual shading and entails a net consumption of water to compensate evaporation losses (Posadas et al., 2016). In this context, all studies carried out to date set the make-up water input to maintain similar effluent and influent flowrates in order to guarantee a constant biomass output, which resulted in the generation of effluents with residual nutrient concentrations (Toledo-Cervantes et al., 2016; Posadas et al., 2016). On this basis, there is an urgent need to develop novel photobioreactor designs and operational strategies to minimize effluent generation while maintaining high microalgae productivities using digestates as a nutrient source.

This work aimed at evaluating the potential of a novel pilot scale HRAP interconnected to an AC via recirculation of the settled cultivation broth under outdoors conditions during the simultaneous upgrading of biogas and treatment of centrate. Process performance was evaluated under pseudo-steady state conditions at different alkalinity levels and make-up water supply regimes from June to October. Under each operational stage, process performance was also assessed during one diurnal cycle of temperature and radiance. A novel strategy decoupling biomass productivity from the effluent flowrate via control of the biomass wastage from the settler was applied to maximize the recovery of carbon and nutrients from biogas and centrate in the form of harvested biomass. Finally, the influence of the recycling liquid/biogas (L/G) ratio in the AC on the efficiency of biogas upgrading was also evaluated during a 24 h diurnal cycle.

2. Materials and methods

2.1 Biogas and centrate

A synthetic biogas mixture, composed of CO_2 (29.5%), H_2S (0.5%) and CH_4 (70%), was used as a model biogas (Abello Linde; Spain). Centrate was obtained from the centrifuges dehydrating the anaerobically digested sludge of Valladolid wastewater treatment plant and stored at 4 ºC prior to use. Centrate composition along the experimental period was subjected to the typical variations of real wastewaters: total organic carbon (TOC) = 70 ± 8 mg L^{-1}, inorganic carbon (IC) = 522 ± 40 mg L^{-1}, total nitrogen (TN) = 580 ± 102 mg L^{-1}, $N\text{-}NH_4^+$ = 553 ± 67 mg L^-, $P\text{-}PO_4^{3-}$ = 34 ± 7 mg L^{-1} and SO_4^{2-} = 9 ± 9 mg L^{-1}.

2.2 Experimental set-up

The pilot plant was located outdoors at the Department of Chemical Engineering and Environmental Technology of Valladolid University (41.39º N, 4.44º W). The experimental set-up consisted of a 180 L HRAP with an illuminated surface of 1.20 m² (length = 170 cm; width = 82 cm; depth =15 cm) and two water channels divided by a central wall and baffles in each side of the curvature. The HRAP was interconnected to an external 2.5 L bubble absorption column (internal diameter = 4.4 cm; height = 165 cm) provided with a metallic gas diffuser (2 μm pore size) located at the bottom of the column. The HRAP and AC were interconnected via external liquid recirculation of the supernatant of the algal-bacterial cultivation broth from an 8 L settler located at the outlet of the HRAP (Fig. 1). The internal recirculation velocity of the cultivation broth in the

HRAP was ≈ 20 cm s^{-1}, which was provided by the continuous rotation of a 6-blade paddlewheel.
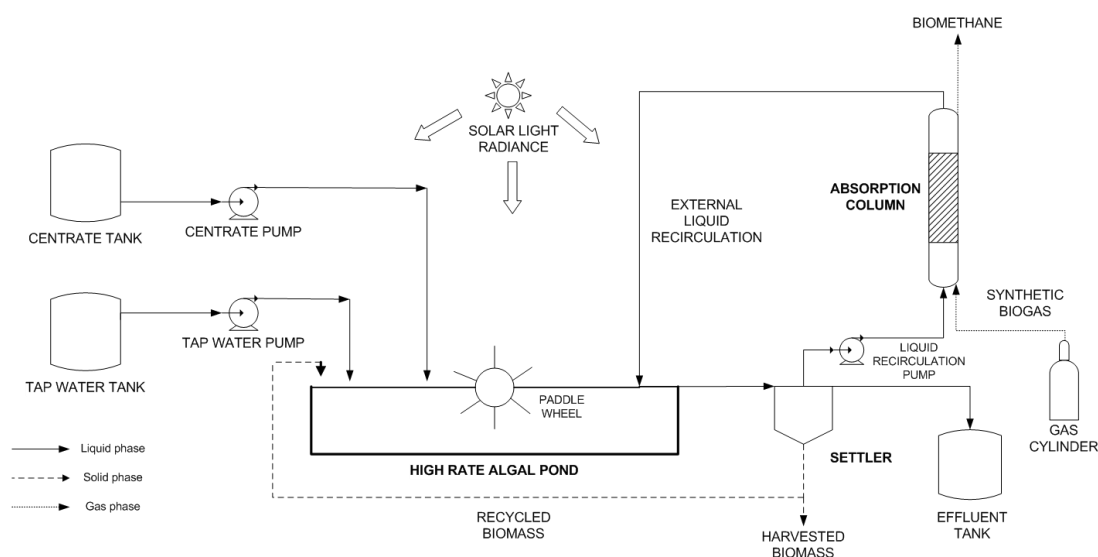

Figure 1. Schematic diagram of the outdoors experimental set-up used for the continuous upgrading of biogas.

2.3 Operational conditions and sampling procedures

Process operation was carried out from June 29th to October the 4th 2016. Based on a previous study conducted by Norvill et al. (2017) in a similar HRAP treating urban wastewater at 4 days of hydraulic retention time (HRT) in the same location, a constant biomass productivity of 15 g m^{-2} d^{-1} was set throughout the 92 days of operation. The required C, N and P input to maintain this biomass productivity was 9.7 g C d^{-1}, 1.9 g N d^{-1} and 0.2 g P d^{-1}, assuming a C, N and P biomass content of 45, 9 and 1%, respectively (Posadas et al., 2015b). This required a centrate flow rate of 3.2 L d^{-1} (considering an IC and N-NH$_4^+$ stripping of 20%, and the absence of P removal by precipitation; Posadas et al. (2013)) and a biogas flow rate of 74.9 L d^{-1} (assuming an average CO$_2$ removal efficiency in the AC of 80% based on Posadas et al. (2015a)). The recycling liquid/biogas (L/G) ratio in the AC was fixed at 0.5 according to Toledo-Cervantes et al. (2016). The liquid and biogas residence time in the AC under these operational conditions were 96 and 48 min, respectively. The settled biomass in the settler was continuously recirculated to the HRAP at a flow rate of 7.2 L d^{-1}. This, together with the external recycling, resulted in a HRT in the settler of 4.4 h. This process configuration has been shown to increase the settleability of the algal-bacterial biomass, while avoiding biomass degradation in the

settler (Valigore et al., 2012; Park et al., 2011, 2013). Biomass harvesting was performed by daily removing the required settled biomass volume according to its total suspended solids (TSS) concentration in order to maintain the above mentioned biomass productivity.

The HRAP was initially filled with tap water (IC = 550 mg L^{-1}) and inoculated to an initial concentration of 210 mg TSS L^{-1} with *Chlorella* sp. from a HRAP treating centrate at the Department of Chemical Engineering and Environmental Technology of Valladolid University (Spain). The system was inoculated on June 29th, and after 5 d of inoculum acclimation batchwise, three different operational conditions were tested (corresponding to stages I, II and III) to optimize the simultaneous outdoors biogas upgrading and centrate treatment from a technical and environmental view point (Table 1).

Table 1. Environmental and operational parameters during the three operational stages.

PARAMETER	STAGE		
	I	II	III
Date	05/07 - 08/08	09/08 – 06/09	07/09 – 04/10
Average temperature (ºC)	23.8 ± 6.7	23.5 ± 6.4	20.0 ± 6.7
Average PAR (µmol m^{-2} s^{-1})	1427 ± 65	1258 ± 140	946 ± 174
Number of sun hours (h)	12 ± 1	11 ± 1	9 ± 1
IC$_{influent}$ (mg L^{-1})	522 ± 40	2009 ± 135	2040 ± 120
Effluent from the settler (L d^{-1})	0.6	0.8	No effluent

Stage I (reference state) was conducted at a centrate IC concentration of 522 ± 40 mg C L^{-1}. During stages II and III, the IC concentration of the centrate was increased up to 2024±124 mg C L^{-1} by addition of NaHCO$_3$ and Na$_2$CO$_3$, which increased the pH of the centrate from 8.38±0.33 in stage I to 9.94±0.09 and 10.06±0.13 in stages II and III, respectively (Table 1). Tap water was fed to the HRAP in stages I and II to compensate evaporation losses and maintain an effluent flowrate of 0.6±0.4 and 0.8±0.4 L d^{-1}, respectively, thus minimizing the loss of carbon, nutrients and fresh water. The effluent

from the system was returned to the HRAP in stage III to minimize the supply of $NaHCO_3$ and Na_2CO_3, with a subsequent decrease in the supply of make-up water. Each operational stage was maintained for approximately one month, where temperature, solar radiation and number of sun hours remained approximately constant (Table 1). The results obtained for the liquid phase throughout the three operational stages were provided as average values along with their corresponding standard deviation from measurements recorded for four consecutive days during each steady state.

The ambient and cultivation broth temperatures, influent and effluent flowrates, DO and pH in the cultivation broth, and the photosynthetic active radiation (PAR) were daily monitored. Gas samples of 100 µL of the raw and upgraded biogas were drawn twice a week to monitor the concentrations of CO_2, H_2S, CH_4, O_2 and N_2. The inlet and outlet biogas flowrates in the AC were also measured to accurately determine both CO_2 and H_2S removals, and CH_4 losses by absorption. Liquid samples of 100 mL from the centrate and the treated effluent after settling were withdrawn twice a week to monitor the pH, TSS concentration, and concentrations of dissolved TOC, IC, TN, $N-NH_4^+$, $N-NO_2^-$, $N-NO_3^-$, $P-PO_4^{3-}$ and SO_4^{2-} following sample filtration through 0.20 µm nylon filters. Likewise, liquid samples of 25 mL were drawn from the cultivation broth and from the bottom of the settler twice a week to monitor the algal-bacterial TSS concentration. The algal-bacterial biomass harvested from the settler under steady state was washed three times with distilled water and dried for 24 hours at 105 ºC to determine its elemental composition (C, N, P and S). Process monitoring and biomass harvesting were always conducted at 9:00 a.m. along the entire experimental period.

At the end of each operational stage, the outdoors temperature and PAR, along with the temperature, DO concentration and pH in the HRAP, settler and AC were measured every 30 minutes during one entire diurnal cycle from one hour prior to dawn to one hour after sunset. The composition and flowrate of the upgraded biogas were recorded every hour, and the concentrations of TOC, IC and TN in the HRAP, settler and AC were analyzed every 2 hours.

2.4 Influence of the L/G ratio on the quality of the upgraded biogas

L/G ratios ranging from 0.5 to 5 were tested at the end of stage III (4th - 7th October) to optimize the quality of the upgraded biogas. A biogas flowrate of 74.9 L d^{-1} was maintained while the liquid flowrates were set at 37.5, 74.9, 149.8 and 374.5 L d^{-1} (providing L/ G ratios of 0.5, 1, 2 and 5, respectively). Each L/G ratio was maintained for 12 h during one-day diurnal cycle. The ambient temperature and PAR, along with the temperature, DO and pH in the HRAP, settler and AC, and the composition and flowrate of the upgraded biogas, were measured every two hours from one hour prior to dawn to one hour after sunset.

2.5 Analytical procedures

The monthly average ambient temperatures, PARs and number of sun hours were provided by the official AEMET meteorological station located at the University of Valladolid. CO_2, H_2S, CH_4, O_2 and N_2 gas concentrations were determined using a Varian CP-3800 GC-TCD (Palo Alto, USA) according to Posadas et al. (2015a). Temperature and DO concentration were determined using an OXI 330i oximeter (WTW, Germany). An Eutech Cyberscan pH 510 (Eutech instruments, The Netherlands) was used for pH determination. The PAR was measured with a LI-250A light meter (LI-COR Biosciences, Germany). The concentrations of dissolved TOC, IC and TN were measured using a Shimadzu TOC-VCSH analyzer (Japan) coupled with a TNM-1 chemiluminescence module. $N-NH_4^+$ concentration was determined with an ammonium specific electrode Orion Dual Star (Thermo Scientific, The Netherlands). The concentrations of $N-NO_3^-$, $N-NO_2^-$, $P-PO_4^{3-}$ and SO_4^{2-} were quantified by HPLC-IC according to Posadas et al. (2013). All analyses were carried out according to Standard Methods (APHA, 2005).

The determination of the C, N and S content of the algal-bacterial biomass was conducted in a LECO CHNS-932 analyzer, while phosphorus content was determined spectrophotometrically after acid digestion in a microwave according to Standard Methods (APHA, 2005). The identification, quantification and biometry measurements of the microalgae assemblage under steady state were performed by microscopic examination (OLYMPUS IX70, USA) of biomass samples (fixed with lugol acid at 5% and stored at 4 ºC prior to analysis) according to Sournia (1978).

3. Results and discussion

3.1. Environmental parameters

The average ambient temperature, PAR and number of sun hours slightly decreased from stage I (July) to stage III (September), which is inherent to outdoors environmental conditions in European latitudes (Table 1). Despite these variations, the climatological conditions were comparable throughout the three experimental stages, which allowed for a fair comparison of the influence of operational conditions on process performance.

The DO concentration, temperature and pH in the cultivation broth of the HRAP during a diurnal cycle at the end of each operational stage were directly correlated with the ambient temperature and light radiance (Fig. A.1-A.4). Hence, the DO concentration in the HRAP during steady state in stages I, II and III fluctuated from 1.4 to 15.6, 1.3 to 16.7 and 0.9 to 13.2 mg O_2 L^{-1}, respectively (Fig. A.2). Microalgae activity was not inhibited at such low-moderate DO concentrations, since pernicious effects on photosynthesis are typically encountered above 25 mg O_2 L^{-1} (Molina et al., 2001). The average temperature and pH in the cultivation broth of the HRAP under steady state during stages I, II and III were 25±6, 25±6 and 19±5°C, and 8.9±0.4, 10.0±0.0 and 9.9±0.0, respectively (Fig. A.3 and A.4). The higher pH recorded in stages II and III was attributed to the higher pH of the centrate fed to the system compared with that used during stage I. Moreover, the lower buffer capacity of the cultivation broth in this first operational stage (Table 1; Fig. A.5) resulted in significant variations of the pH along the day (from 8.3 to 9.4), which confirmed the key role of alkalinity for pH control in algal-bacterial photobioreactors (Posadas et al., 2013). The lower pH values recorded in the AC compared to those in the HRAP, regardless of the operational stage, were due to the acidification of the recycling broth caused by the absorption of CO_2 and H_2S (Posadas et al., 2016) (Fig. A.4). Despite these sharp daily variations in temperature, DO and pH, all parameters remained in the acceptable range to support microbial activity (Posadas, 2016).

Finally, the evaporation rates during stages I, II and III accounted for 7±2 L, 9±1 and 3±2 L m^{-2} d^{-1}, respectively (Fig. A.6). The highest evaporation rate here recorded was ~1.5 times higher than the maximum predicted for an arid area by Guieysse et al. (2013). These high values were attributed to the high temperatures and turbulence in the HRAP as a result of the typical oversizing of the motor of the paddlewheel in lab scale-pilot systems

(Posadas et al., 2015c; Guieysse et al., 2013). In this context, the scale-up of this experimental set-up will likely entail lower evaporation rates.

3.2 Biogas upgrading

The composition of the biomethane obtained during stage I significantly varied depending on the daily fluctuations in the environmental conditions compared to stages II and III, where the concentration of all biogas components remained approximately constant mainly as a consequence of the higher alkalinity into the medium (Fig. 2). CH_4 concentrations in the upgraded biogas during stage I ranged from 72 to 93 %, while the removal efficiencies (REs) of CO_2 and H_2S ranged from 50 to 75 % and from 91 to 100%, respectively. Average CH_4 concentrations of 90±2 % and 91±1 % were recorded in the upgraded biogas during stages II and III, respectively, along with CO_2-REs of 86±4% and a complete H_2S removal regardless of the operational conditions (Fig. 2). These results also showed that the absence of effluent in stage III did not influence the quality of the upgraded biogas. O_2 and N_2 concentrations in the biomethane during the three operational stages ranged from 0.1 to 2.0% and from 0.6 to 5.0%, respectively, depending on the pH of the cultivation broth and on the alkalinity (Fig. 2c). These values were only slightly higher than those reported by Toledo-Cervantes et al. (2016) during the indoors operation of a similar process at a L/G ratio of 1, which validated the results obtained under laboratory conditions. CH_4 absorption in the AC was negligible, with average losses of 2.2±1.2% (on a mass basis) along the three operational stages. The biomethane composition obtained was both compliant with the regulations for injection into natural gas grids in some countries in Europe (i.e. Belgium and The Netherlands) and Latin-America (i.e. Chile), and suitable for use as autogas (Muñoz et al., 2015).

The main fluctuations in the composition of the upgraded biogas were recorded during stage I, which were attributed to the influence of the diurnal variations in radiation and temperature under process operation with a low ionic strength cultivation broth. In this context, the concentrations of CH_4, CO_2, H_2S, O_2 and N_2 in the upgraded biogas ranged from 70.5 to 86.8%, 8.8 to 24.7%, 0 to 0.1%, 0.7 to 1.1% and 2.6 to 4.2%, respectively, during the diurnal cycle evaluated in stage I (Fig. 3). The increase in the alkalinity of the cultivation broth during stages II and III (from 267±56 mg IC L^{-1} in stage I to 2174±253 and 2660±48 mg IC L^{-1} during stages II and III, respectively) reduced the variability in

the composition of the upgraded biogas. In this sense, CH_4, CO_2, O_2 and N_2 concentrations in stage II ranged from 87 to 92%, 5 to 9%, 0 to 1% and 1 to 3%, respectively, while in stage III these concentrations varied from 85 to 93%, 4 to 12%, 0 to 2% and 1 to 3%, respectively (Fig. 3). H_2S was completely removed in both stages.
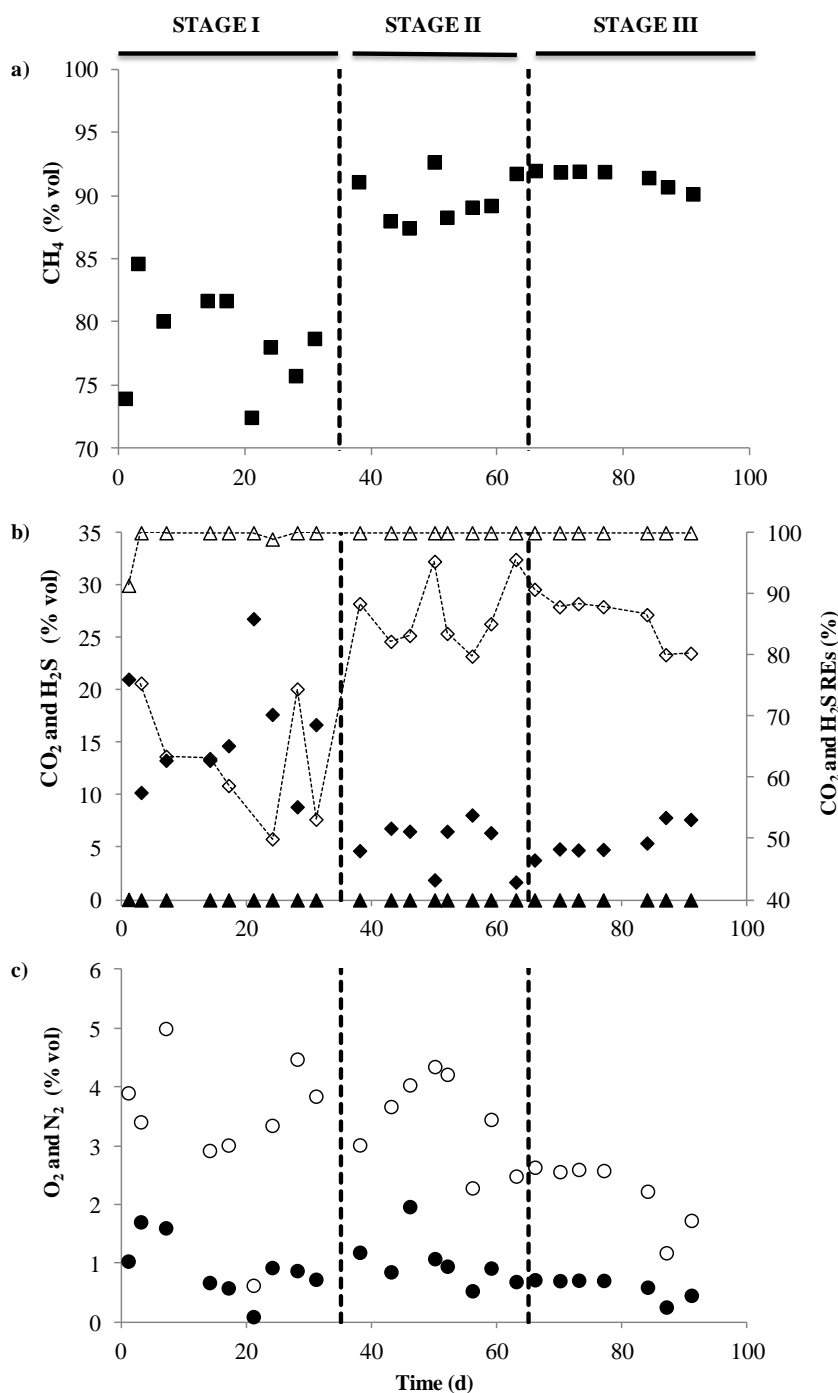

Figure 2. Time course of the concentration of (a) CH_4 (■), (b) CO_2 (♦) and H_2S (▲), and (c) O_2 (●) and N_2 (○) in the upgraded biogas. The removal efficiencies of CO_2 (◊) and H_2S (Δ) are also displayed in figure 2b.
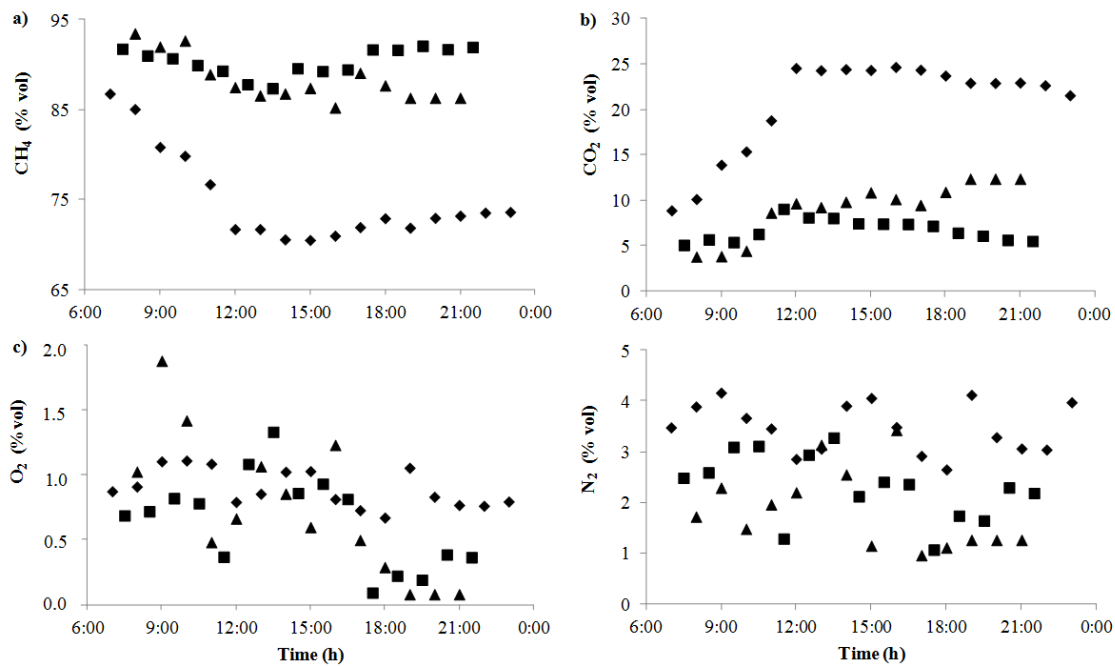
Figure 3. Time course of the concentration of (a) CH_4, (b) CO_2, (c) O_2 and (d) N_2 in the upgraded biogas during the diurnal cycle evaluated in stages I (♦), II (■) and III (▲).

The highest CO_2-REs, which entailed also the highest CH_4 concentrations in the upgraded biogas, were recorded at the lowest ambient temperature regardless of the operational stage as a result of the higher solubility of CO_2 (Sander, 1999). A 60% decrease in CO_2 solubility is expected when temperature increases from 10 to 40°C (Sander, 1999). However, the high CO_2 concentration gradient supported by the high alkalinity of the cultivation broth in stages II and III compensated the decrease in CO_2 solubility mediated by the 30 °C temperature increase (Fig. A.3). The correlation between the temperature of the cultivation broth in the settler and the CO_2 concentration in the upgraded biogas was only significant during stage I (Fig. 4). This result suggested that CO_2 absorption in a low alkalinity media is controlled by the influence of the temperature on the aqueous solubility of CO_2 (according to the Henry´s Law constant) (Sander, 1999). However, the influence of the temperature on the concentration of O_2 or N_2 in the upgraded biogas was negligible likely due to their limited aqueous solubility. These results confirmed the high influence of the ionic strength of the recycling cultivation broth on the quality of the upgraded biogas (Bahr et al. 2014). The higher CO_2-REs recorded in stages II and III compared to stage I were likely mediated by the pH increase in the cultivation broth, which significantly enhanced the CO_2 concentration gradient (Bahr et al. 2014; Toledo-Cervantes et al. 2016). The CO_2-REs here reported were always higher than those

recorded by Bahr et al. (2014) during simultaneous biogas upgrading and centrate treatment (≈40%), and similar to those obtained by Serejo et al. (2015), who reported an average CO_2-RE of ≈80% at a L/G ratio of 10 during the upgrading of biogas combined with the treatment of diluted anaerobically digested vinasse.
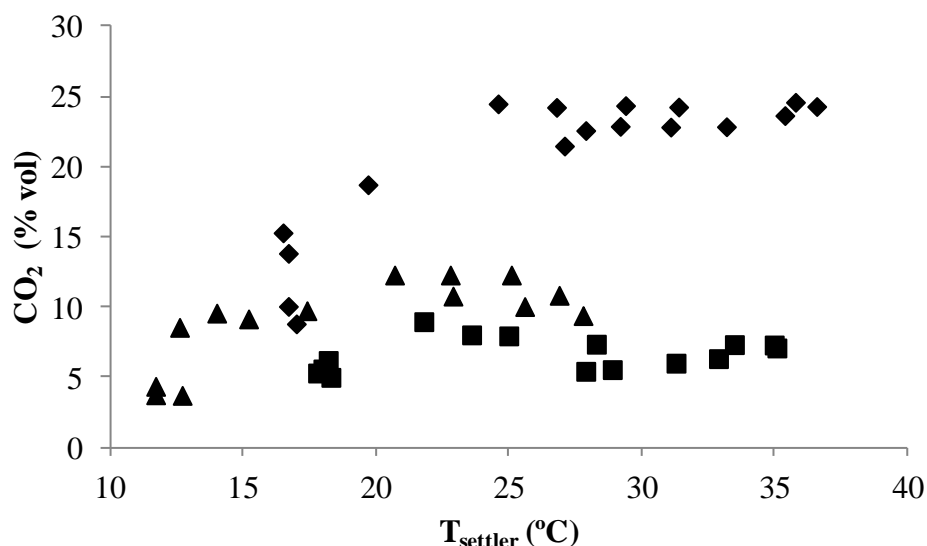

Figure 4. Influence of the temperature in the settler on the CO_2 concentration in the upgraded biogas during stages I (♦), II (■) and III (▲).

The high aqueous solubility of H_2S (three times higher than that of CO_2) resulted in high H_2S-REs, comparable to those recorded in previous studies carried out under laboratory conditions (Bahr et al., 2014; Posadas et al., 2015a; Serejo et al., 2015; Toledo-Cervantes et al., 2016; Lebrero et al., 2016). A complete H_2S removal was observed in stages II and III due to the higher pH of the cultivation broth (Fig. 2b), which was in agreement with the results obtained by Bahr et al. (2014). H_2S oxidation ratios (defined as the ratio between the mass of S-SO_4^{2-} in the HRAP cultivation broth and the mass of H_2S absorbed in the AC) of 36±13, 47±9 and 47±7 % were recorded during stages I, II and III, respectively. In this sense, an incomplete H_2S oxidation to SO_4^{2-} was also observed by Toledo-Cervantes et al. (2016) and Lebrero et al. (2016) likely due to the low O_2 concentration in the absorption column. Despite the fact that the highest DO concentrations were achieved during stage I, the lowest H_2S oxidation ratio recorded in this period was associated to the effect of the temperature on the solubility of the H_2S in a low ionic strength medium and therefore, to the limited H_2S mass transfer efficiency from the biogas to the liquid phase. The higher effluent flowrate and lower water

evaporation rates (entailing a lower accumulation of $S-SO_4^2$ in the cultivation broth) during stage I could also explain the lower oxidation ratio recorded.

3.3 Influence of the L/G ratio on the quality of the upgraded biogas

The similar PAR and outdoor temperatures recorded during the five consecutive days of this study allowed an unbiased comparison of the influence of the L/G ratio on biomethane composition (Fig. A. 7). In fact, similar DO concentrations and temperature profiles were recorded in the HRAP regardless of the tested L/G ratio (Fig. A. 8), although the pH of the cultivation broth in the HRAP and AC varied depending on the L/G ratio tested (Figs. A.8-A.10). Thus, the daily average pH of the cultivation broth in the AC was 8.8 ± 0.1, 9.4 ± 0.1, 9.6 ± 0.1 and 9.8 ± 0.8 at L/G ratios of 0.5, 1, 2 and 5, respectively (Fig. A.9). This pH increase at higher L/G ratios was attributed to the lower CO_2 transferred per volume of recycling cultivation both, which prevented the acidification of the broth in the AC.

L/G ratios > 1 supported a significant decrease in CO_2 concentration in the upgraded biogas, which ranged from 1.8 to 3.7% and corresponded to CO_2-REs $\approx 95\%$ (Fig. 5b).

The increase in pH in the cultivation broth of the AC at increasing L/G ratios supported higher CO_2 concentrations gradient between the biogas and liquid phase, which enhanced CO_2-REs (Posadas et al., 2016). In this current particular study, the maximum CO_2 mass transfer capacity was achieved at a L/G ratio of 1. In this context, Serejo et al. (2015) recorded a maximum CO_2 mass transfer (CO_2-RE of $95\pm2\%$) at a L/G ratio of 15, pH of 8 and IC concentrations $\approx$80 mg L^{-1}, respectively. On the other hand, Toledo-Cervantes et al. (2016) recorded a CO_2-RE of $98.8\pm0.2\%$ regardless of the tested L/G (0.5-60) at a pH of 10 and IC concentration $\approx$4000 mg L^{-1}. These studies confirmed the key role of the alkalinity of the recycling cultivation broth on the biogas upgrading efficiency compared to other operational parameters.

H_2S was completely removed regardless of the tested ratio likely due to its high aqueous solubility (Bahr et al., 2014; Serejo et al., 2015). The O_2 and N_2 concentration in the upgraded biogas only increased significantly at a L/G ratio of 5 (up to 5.5% and 12.8%, respectively) (Fig. 5c, 5d). Indeed, the increase in the L/G ratio mediated a higher

desorption of O_2 and N_2 from the recycling, which negatively impacted the final concentration of CH_4 in the upgraded biogas. In this context, the maximum CH_4 concentration (94%) was obtained at L/G ratios of 1 and 2 (Fig. 5a).
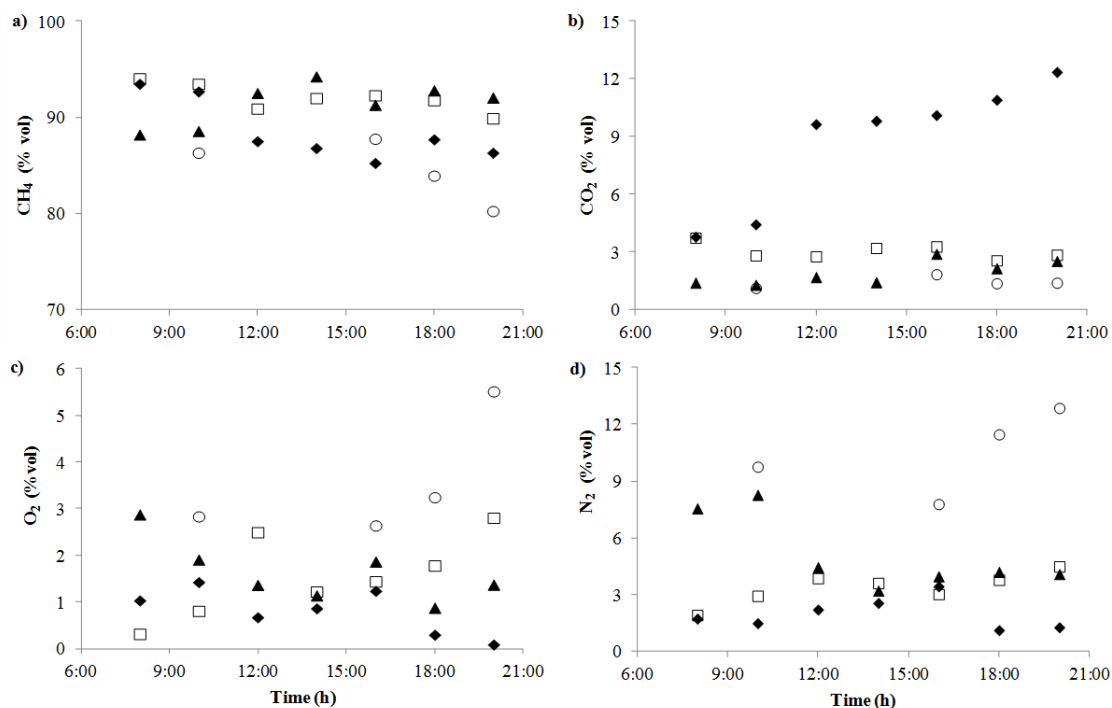

Figure 5. Time course of the concentration of (a) CH_4, (b) CO_2, (c) O_2 and (d) N_2 in the upgraded biogas at L / G ratios of 0.5 (♦), 1 (□), 2 (▲) and 5 (○).

3.4 Wastewater treatment performance

The wastewater treatment efficiency of the HRAP was evaluated under pseudo-steady state at the three operational stages evaluated (Fig. 6; Figs. A11-A12).

The TOC effluent concentrations, which ranged from14 to 85 mg L^{-1}, were similar to the influent TOC concentrations due to the low biodegradability of the centrate, the concentration effect caused by the high water evaporation rates in the HRAP and the low or negligible effluent flowrates (Posadas et al., 2013; 2015c) (Fig. 6a). Despite the low DO concentrations recorded in the cultivation broth (<2 mg O_2 L^{-1}) in the early morning could have partially limited organic matter oxidation (Metcalf and Eddy, 2003), the removals of TOC estimated by mass balance calculations ranged from 59±7% (stage III) to 74±7% (stage I) (Table 2) (Fig. A.3).

Table 2. Steady state removal efficiencies of total organic carbon, total inorganic carbon, total nitrogen, ammonium and phosphorus during the three operational stages.

STAGE	Removal efficiencies (%)				
	TOC	TIC	TN	$N-NH_4^+$	$P-PO_4^{3-}$
I	74±7	95±1	86±4	100±0	92±2
II	57±6	72±8	87±4	100±0	84±5
III	59±7	75±7	80±8	99±1	85±5

The TIC-REs in stage I were higher than those recorded in stages II and III as a result of the higher inorganic carbon feeding and $C-CO_2$ REs in the AC during these latter stages (Table 2). Therefore, only 65±6 and 66±8% of the total carbon removed in stages II and III was recovered in the harvested biomass, while a 97±1% carbon recovery was observed during stage I (Table 3). Despite the higher pH values should have promoted lower IC removals by stripping based on the limited CO_2 aqueous equilibrium concentration, the lower IC loading during stage I resulted in a lower fraction of C removed by stripping (Table 3) (Posadas et al., 2013) (Fig. 6b).

Similar TN-REs of 86±4, 87±4 and 80±4% were recorded during stages I, II and III, respectively, while a complete $N-NH_4^+$ removal occurred during the entire experimental period (Table 2; Fig. 6c, 6d). Nitrification was not inhibited by the high pH values prevailing during stages II and III or the low DO concentrations (<1 mg O_2 L^{-1}) present in the first hours in the morning (Fig. A.3). $N-NO_2^-$ concentrations were low compared to $N-NO_3^-$ despite temperatures higher than 28ºC were always recorded close to midday, which are known to promote the partial oxidation of $N-NH_4^+$ (Fig. 6e; Figs. A.2-A.3) (Metcalf and Eddy, 2003). The oxidation ratios (referred to [$N-NO_3^-$+ $N-NO_2^-$] mass outputs compared to TN mass input, Posadas et al. (2015a)) were 11±2, 13±4 and 19±8% during stages I, II and III, respectively. The high nitrification activity, together with the high evaporation rates, induced an increase in $N-NO_3^-$ concentration in the cultivation broth up to 148 mg L^{-1} in stage I, 198 mg L^{-1} in stage II and 293 mg L^{-1} in stage III, this latter increase mediated by the absence of effluent from the HRAP (Fig. 6f). The nitrogen recovered in the harvested biomass accounted for 65±3, 54±18 and 76±19% of the total nitrogen removed during stages I, II and III, respectively (Table 3). These values were considerably higher than those recorded by Posadas et al. (2015a) (45±7%) and Toledo-Cervantes et al. (2017) (19±13% and 36±18%) in a similar indoors experimental set-up

during the simultaneous treatment of biogas and digestates as a result of the lower microalgae productivities in those studies.
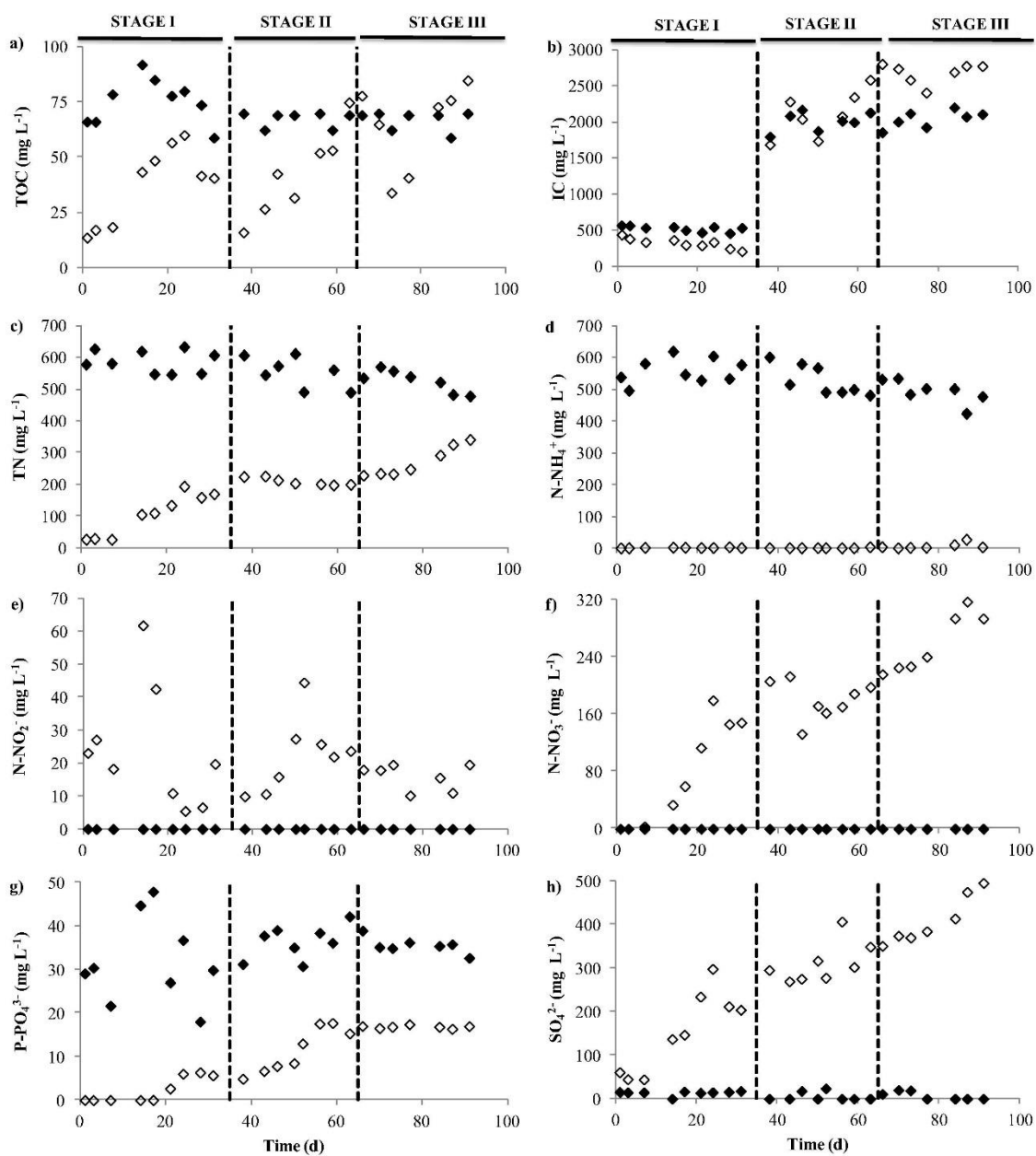

Figure 6. Time course of the influent (♦) and effluent (◊) concentrations of (a) TOC, (b) IC, (c) TN, (d) N-NH$_4^+$, (e) N-NO$_2^-$, (f) N-NO$_3^-$, (g) P-PO$_4^{3-}$ and (h) SO$_4^{2-}$ throughout the three operational stages.

Table 3. Carbon and nutrient recovery via biomass assimilation estimated from the carbon and nutrients removal, and the biomass elemental composition of the harvested biomass during stages I, II and III.

STAGE	Carbon and nutrient recovery as biomass (%)				Biomass elemental composition (%)			
	C	N	P	S	C	N	P	S
I	97±1	65±3	100±0	26±5	41.1	6.7	1.1	0.4
II	65±6	54±18	91±9	17±3	35.8	5.7	0.7	0.2
III	66±8	76±19	99±1	16±3	37.8	6.5	0.8	0.2

High P-PO$_4$$^{3-}$ REs of 92±2, 84±5 and 85±5% were recorded during stages I, II and III, respectively (Table 2). The higher P-RE in stage I was likely mediated by the higher P content of the harvested biomass (Table 3). In this regard, P-PO$_4$$^{3-}$ concentration in the cultivation broth increased up to 6 mg L^{-1} in stage I, 15 mg L^{-1} in stage II and 17 mg L^{-1} in stage III. These increasing P-PO$_4$$^{3-}$ concentration were also supported by the evaporation rate and the low or negligible effluent flowrates (Fig. 6g). A P mass balance revealed than approximately 100% of the P removed was recovered in the harvested biomass, despite high pH values are known to promote PO$_4$$^{3-}$ precipitation (Cai et al., 2013) (Table 3).

Finally, H$_2$S oxidation supported an increase in SO$_4$$^{2-}$ concentration in the cultivation broth of the HRAP from 60 to 495 mg L^{-1} through the 92 operational days, also triggered by the high evaporation rates and low effluent flowrates (Fig. 6h). The fraction of H$_2$S not fully oxidized to sulphate would have remained as S-intermediates in the liquid phase (S°, thiosulfate or sulfite) (Toledo-Cervantes et al., 2016). This was confirmed by the observation of S° accumulation on the walls and diffuser of the AC during stage I (Photograph 1, appendix), while a S mass balance revealed that only 26±5, 17±3 and 16±3% of the S removed was recovered in the harvested biomass during stages I, II and III, respectively (Table 3). Further analyses to determine the actual sulfur compounds present in the cultivation broth are required.

3.5 Concentration and composition of the algal-bacterial biomass

The steady state biomass concentrations in the HRAP during stages I, II and III averaged 660±17, 1078±84 and 665±79 mg TSS L^{-1} (Fig. A. 13). The operational strategy here evaluated based on the control of biomass productivity via regulation of the settled

biomass wastage rate successfully maintained the concentration of algal-bacterial biomass below light limiting values. At this point it should be stressed that the theoretical biomass concentration generated based on the centrate composition would be ≈2000 mg TSS L^{-1} (with P as the limiting nutrient). The good settling characteristics of the algal-bacterial (supporting TSS-REs in the settler of 80±9%) were likely promoted by the short HRT in the settler and the continuous recirculation of the settled biomass, which boosted the enrichment of rapidly settling algal-bacterial flocs (Valligore et al., 2011; Park et al., 2011).

The elemental composition of the harvested biomass remained within the typical range reported in literature, regardless of the operational stage (Posadas et al., 2016; Bi et al., 2013). C, N and P content in the biomass decreased from stage I to stage II and slightly increased in stage III (Table 3). The different C/N/P (g/g/g) ratios present in the cultivation broth of the HRAP (100/39/2, 100/6/1 and 100/12/1 during stages I, II and III, respectively) could have influenced this final biomass composition, despite the C/N ratio in the harvested biomass remained always at the optimum value of 6 regardless of the operational conditions (Serejo et al., 2015). The main differences were recorded in the S content, which decreased from 0.4% in stage I to 0.2% in stages II and III (Table 3). The higher S content in the biomass was recorded concomitantly with the occurrence of S precipitation (Photograph 1, appendix), and was attributed to the likely S absorption into the biomass.

The inoculated *Chlorella* sp. was gradually replaced by *Chloroidium saccharophilum*s (*Chlorella saccharophila)* during stage I. *Chloroidium saccharophilum* was the dominant microalga species during stage I (94%) and stage III (100 %), while *Pseudanabaena* sp. accounted for 6% and 54% of the total number of microalgae cells in stages I and II, respectively (Fig. A.14). *Pseudanabaena* sp. has been consistently found in a similar indoors experimental set-up during the simultaneous upgrading of biogas and digested vinasse treatment (Posadas et al. 2015a; Serejo et al. 2015). The lower microalgae diversity recorded outdoors compared to that observed under laboratory conditions in a similar experimental set-up was likely due to i) the recirculation of the settled biomass and ii) the high alkalinity in the cultivation broth in stages II and III (Serejo et al., 2015; Posadas et al., 2015a; Toledo-Cervantes et al., 2016, 2017; Park et al., 2011).

4. Conclusions

This work constitutes the first proof-of-concept study of photosynthetic biogas upgrading coupled with centrate treatment at pilot scale under outdoors conditions. The feasibility of a zero-effluent process operation was also demonstrated. Temperature played a key role on the efficiency of biogas upgrading at low-to-medium alkalinities, while high alkalinities enhanced process robustness against daily temperature variations. Process operation at L/G ratios of 1-2 provided a biomethane complying with most international regulations. A consistent centrate treatment was achieved regardless of the operational conditions, while the decoupling of biomass productivity from the HRT allowed high recoveries of C, N and P.

Acknowlegments

References

1. Alcántara C., García-Encina P., Muñoz R., 2015. Evaluation of simultaneous biogas upgrading and treatment of centrates in a HRAP through C, N and P mass balances. Water Sci. Technol. 72, 150-157.

2. Andriani D., Wresta A., Atmaja T., Saepudin A., 2014. A review on optimization production and upgrading biogas through CO_2 removal using various techniques. Appl. Biochem. Biotechnol. 172, 1909–1928.

3. APHA; AWWA; WEF. Standard Methods for the Examination of Water and Wastewater; 21st ed.; Washington, 2005.

4. Bahr M., Díaz I., Domínguez A., González Sánchez A., Muñoz R., 2014. Microalgal-biotechnology as a platform for integral biogas upgrading and nutrient removal from anaerobic effluents. Environ. Sci. Technol. 48, 573-581.

5. Bi Z., He B. B., 2013. Characterization of microalgae for the purpose of biofuel production. Transactions of the ASABE, Vol. 56 (4), 1529-1539.

6. Cai T., Park S.Y., Li Y., 2013. Nutrient recovery from wastewater streams by microalgae: Status and prospects. Renew. Sust. Energ. Rev. 19, 360-369.

7. European Biogas Association (EBA): ATBEST International Conference 7-8 September (2016), Linköping by Arthur Wellinger.

8. Guieysse B., Béchet Q., Shilton A., 2013. Variability and uncertainty in water demand and water footprint assessments of fresh algae cultivation based on case studies from five climatic regions. Bioresour. Technol. 128, 317–323.

9. Herrmann C., Kalita N., Wall D., Xia A., Murphy J. D., 2016. Optimised biogas production from microalgae through co-digestion with carbon-rich co-substrates. Bioresour. Technol. 214, 328-337.

10. Lebrero R., Toledo-Cervantes, Muñoz R., Del Nery V., Foresti E., 2016. Biogas upgrading from vinasse digesters: a comparison between ananoxic biotrickling filter and an algal-bacterial photobioreactor. J. Chem. Technol. Biotechnol. 91 (9), 2488-2495.

11. Mann G., Schlegel M., Kanswohl N., Schumann R., 2016. Experimental system for the prevention of O_2– and air contamination during biogas upgrading with phototrophic microalgae. Appl. Agric. Forestry. Res. DOI: 10.3220/LBF1471268642000.

12. Meier L., Pérez R., Azócar L., Rivas M., Jeison D. 2015. Photosynthetic CO_2 uptake by microalgae: an attractive tool for biogas upgrading. Biomass Bioenerg. 73, 102-109.

13. Metcalf, Eddy, 2003. Wastewater Engineering and Reuse, 4th ed., New York, Mc. GrawHill.

14. Molina E., Fernández J. M., Acién F. G., Chisti Y., 2001. Tubular photobioreactors design for algal cultures. J. Biotechnol. 92, 113-131.

15. Muñoz R., Meier L., Díaz I, Jeison D., 2015. A review on the state-of-the-art of physical/chemical and biological technologies for biogas upgrading. Rev. Environ. Sci. Biotechnol. 14, 727–759.

16. Norvill Z., Toledo-Cervantes A., Blanco S., Shilton A., Guieysse B., Muñoz R., 2017. Photodegradation and sorption govern tetracycline removal during wastewater treatment in algal ponds. Bioresour. Technol. (submitted for publication).

17. Park J.B.K., Craggs R.J., Shilton A.N., 2013. Enhancing biomass energy yield from pilot-scale high rate algal ponds with recycling. Water Res. 47 (13), 4422-4432.

18. Park J.B.K., Craggs R.J., Shilton A.N., 2011. Recycling algae to improve species control and harvest efficiency from a high rate algal pond. Water Res. 45 (20), 6637-6649.

19. Posadas, 2016. Innovative algal-bacterial processes for wastewater treatment: a further step towards full scale implementation: http://uvadoc.uva.es/handle/10324/18777.

20. Posadas E., García-Encina P. A., Soltau A., Domínguez A., Díaz I., Muñoz R., 2013. Carbon and nutrient removal from centrates and domestic wastewater using algal-bacterial biofilm bioreactors. Bioresour. Technol. 139, 50-58.

21. Posadas E., Morales M. M., Gómez C., Acién F. G., Muñoz R., 2015b. Influence of pH and CO_2 source on the performance of microalgae-based secondary domestic wastewater treatment in outdoors pilot raceways. Chem. Eng. J. 265, 239-248.

22. Posadas E., Muñoz A., García-González M.-C., Muñoz R., García-Encina P. A., 2015c. A case study of a pilot high rate algal pond for the treatment of fish farm and domestic wastewaters, J. Chem. Technol. Biotechnol. 90 (6), 1094-1101.

23. Posadas E., Serejo M., Blanco S., Pérez R., García-Encina P.A., Muñoz R., 2015a. Minimization of biomethane oxygen concentration during biogas upgrading in algal–bacterial photobioreactors. Algal Res. 12, 221-229.

24. Posadas E., Szpak D., Lombó F., Domínguez A., Díaz I., Blanco S., García-Encina P., Muñoz R., 2016. Feasibility study of biogas upgrading coupled with nutrient removal from anaerobic effluents using microalgae-based processes. J. Appl. Phycol. 28 (4), 2147-2157.

25. Ryckebosch E., Drouillon M., Vervaeren H., 2011.Techniques for transformation of biogas to biomethane. Biomass Bioenerg. 35 (5), 1633-1645.

26. Sander R., 1999. Compilation of Henry's Law Constants for Inorganic and Organic Species of Potential importance in Environmental Chemistry (Last access: 30.11.2016): http://www.mpchmainz.mpg.de/sander/res/henry.html

27. Serejo M., Posadas E., Boncz M., Blanco S., Garcia-Encina PA., Muñoz R., 2015. Influence of biogas flow rate on biomass composition during the optimization of biogas upgrading in microalgal-bacterial processes. Environ. Sci. Technol. 49 (5), 3228-3236.

28. Sournia A., Phytoplanton Manual. Museum National d' Historie Naturelle, París, United Nations Educational, Scientific and Cultural Organization (Unesco), 1978.

29. Toledo-Cervantes A., Madrid-Chirinos C., Cantera S., Lebrero R., Muñoz R., 2017. Influence of the gas-liquid flow configuration in the absorption column on photosynthetic biogas upgrading in algal-bacterial photobioreactors. Bioresour. Technol. 225, 336-342.

30. Toledo-Cervantes A., Serejo M., Blanco S., Pérez R., Lebrero R., Muñoz R., 2016. Photosynthetic biogas upgrading to bio-methane: Boosting nutrient recovery via biomass productivity control. Algal Res. 17, 46-52.

31. Tippayawong N., Thanompongchart P., 2010. Biogas quality upgrade by simultaneous removal of CO_2 and H_2S in a packed column reactor. Energy 35 (12), 4531-4535.

32. Valigore J. M., Gostomski P. A. , Wareham D. G. , O'Sullivan A. D., 2012. Effects of hydraulic and solids retention times on productivity and settleability of microbial (microalgal-bacterial) biomass grown on primary treated wastewater as a biofuel feedstock. Water Res. 46, 2957-2964.

33. Yan C., Muñoz R., Zhu L., Wang Y. (2016). The effects of various LED (light emittion diode) lighting strategies on simultaneous biogas upgrading and biogas slurry nutrient reduction by using of microalgae *Chlorella* sp. Energy 106, 554-561

Supplementary material

Simultaneous biogas upgrading and centrate treatment in an outdoors pilot scale high rate algal pond

Esther Posadas[1], David Marín[1, 3], Saúl Blanco[2], Raquel Lebrero[1], Raúl Muñoz[1,*]

[1] Department of Chemical Engineering and Environmental Technology, Valladolid University, Dr. Mergelina, s/n, 47011, Valladolid, Spain.

[2] Department of Biodiversity and Environmental Management, University of León, 24071 León, Spain.

[3] Universidad Pedagógica Nacional Francisco Morazán, Boulevard Centroamérica, Tegucigalpa, Honduras.

* Corresponding author: mutora@iq.uva.es

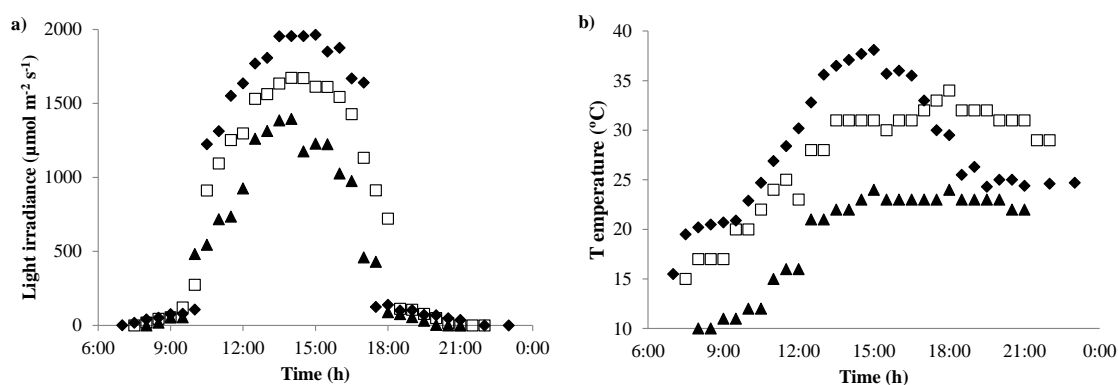## 1. Evolution of the PAR and ambient temperature

Figure A.1. Time course of (a) light radiance and ambient (b) temperature during one diurnal cycle under steady state in stage I (♦), stage II (□) and stage III (▲).

2. Evolution of the dissolved oxygen, temperature and pH in the HRAP, AC and settler
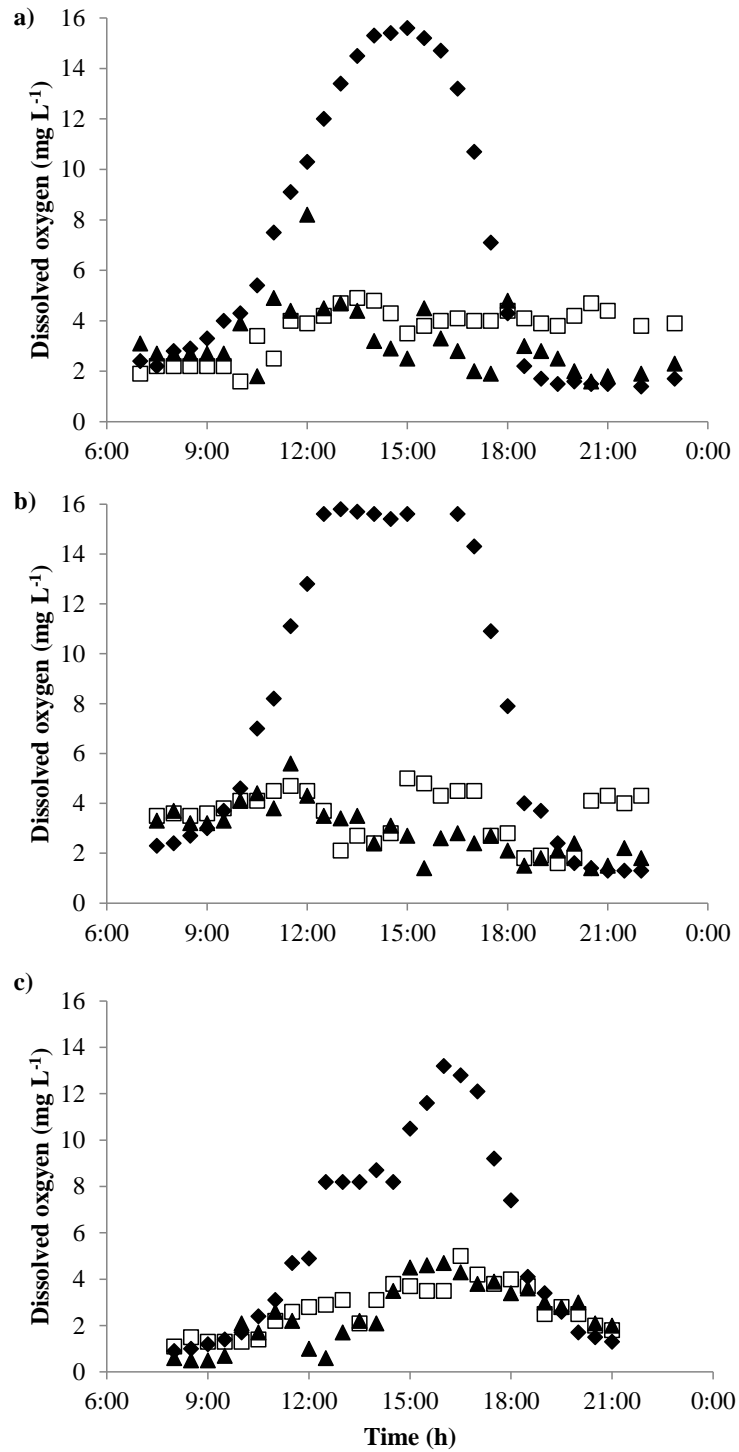

Figure A.2. Time course of dissolved oxygen concentration in the HRAP (♦), AC (□) and settler (▲) during stages (a) I, (b) II and (c) III.

The higher temperatures in the settler and AC at midday were likely due to their enclosed design, while the open nature of the HRAP allowed heat exchange with the atmosphere and water evaporation contributed to temperature control (Murphy and Berberog, 2012).

Figure A.3. Time course of the temperature in the cultivation broth of the HRAP (♦), AC (□) and settler (▲) during stages (a) I, (b) II and (c) III under steady state.

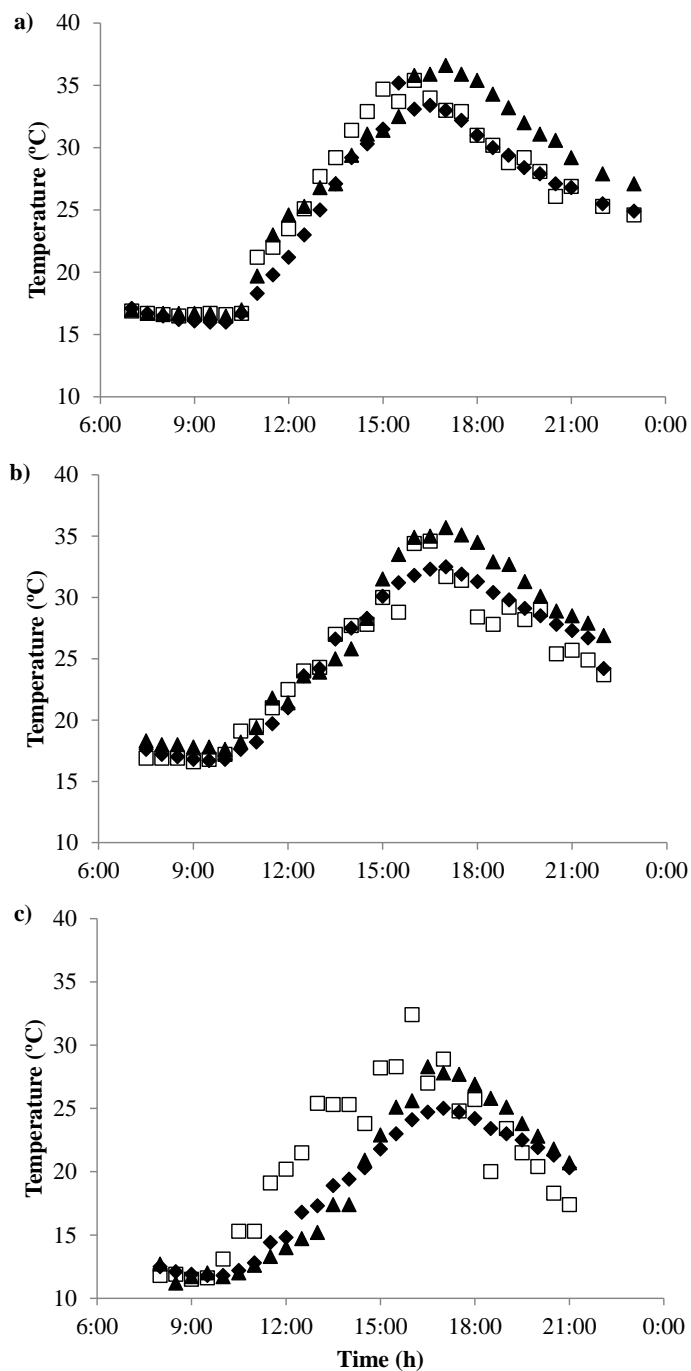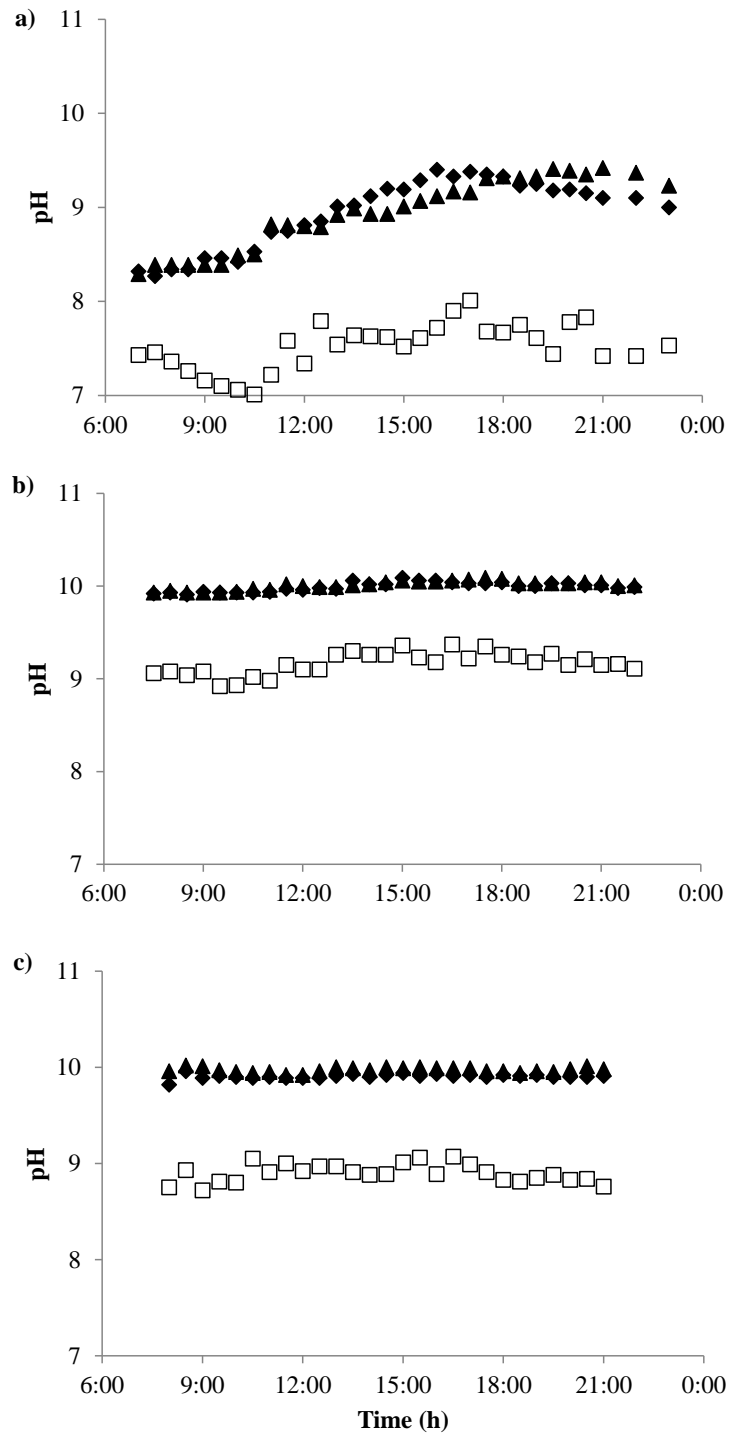**Figure A.4.** Time course of the pH in the cultivation broth of the HRAP (♦), AC (□) and settler (▲) during stages (a) I, (b) II and (c) III under steady state.

3. Evolution of the inorganic carbon concentration

Figure A.5. Time course of the inorganic carbon concentration in the cultivation broth of the HRAP (♦), AC (□) and settler (▲) during stages (a) I, (b) II and (c) III under steady state.

4. Evolution of the evaporation rate
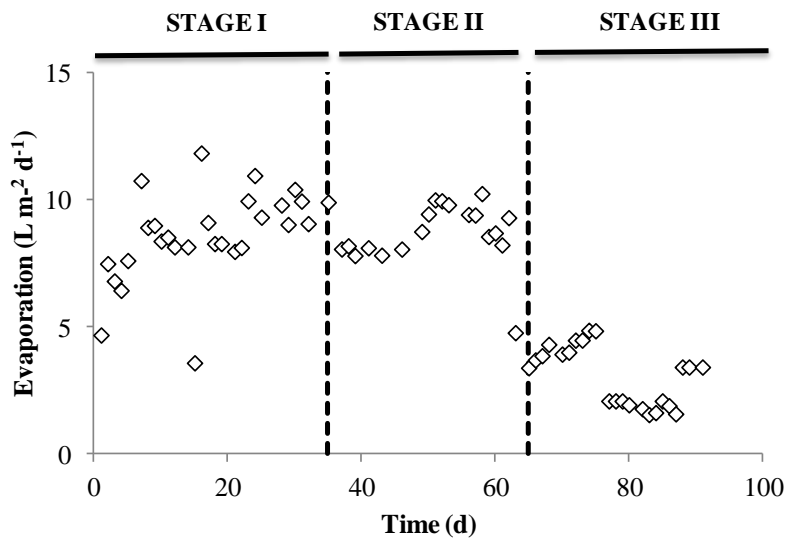
Figure A.6. Time course of the evaporation rate throughout the experimental period.

5. Influence of the L/G ratio on the quality of the upgraded biogas
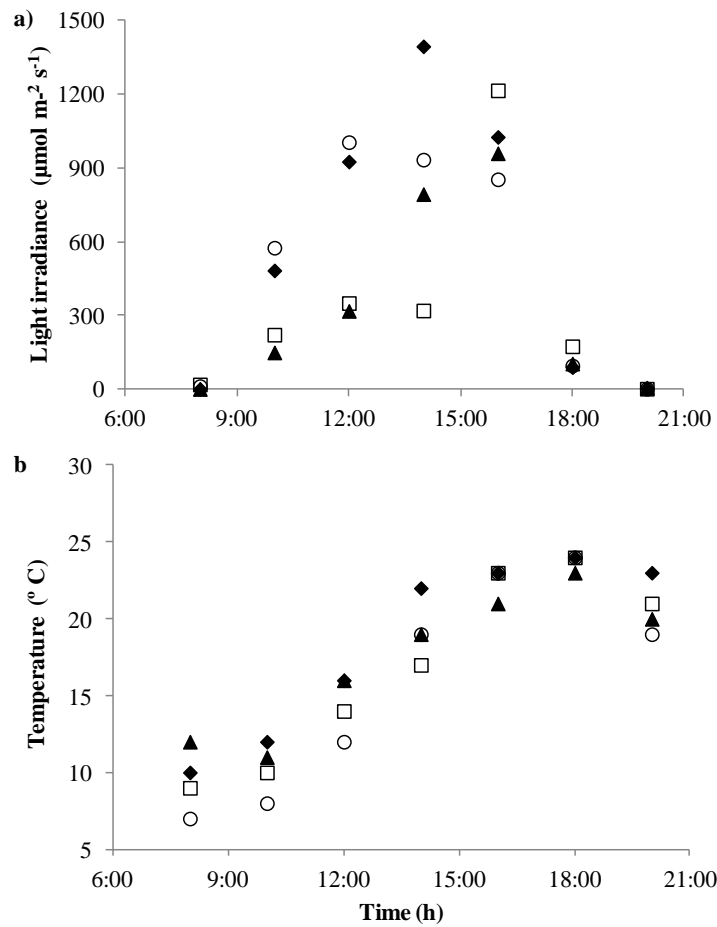
Figure A.7. Time course of (a) light radiance and (b) ambient temperature during the day at the different L/G ratios tested: 0.5 (♦), 1 (□), 2 (▲) and 5 (○).
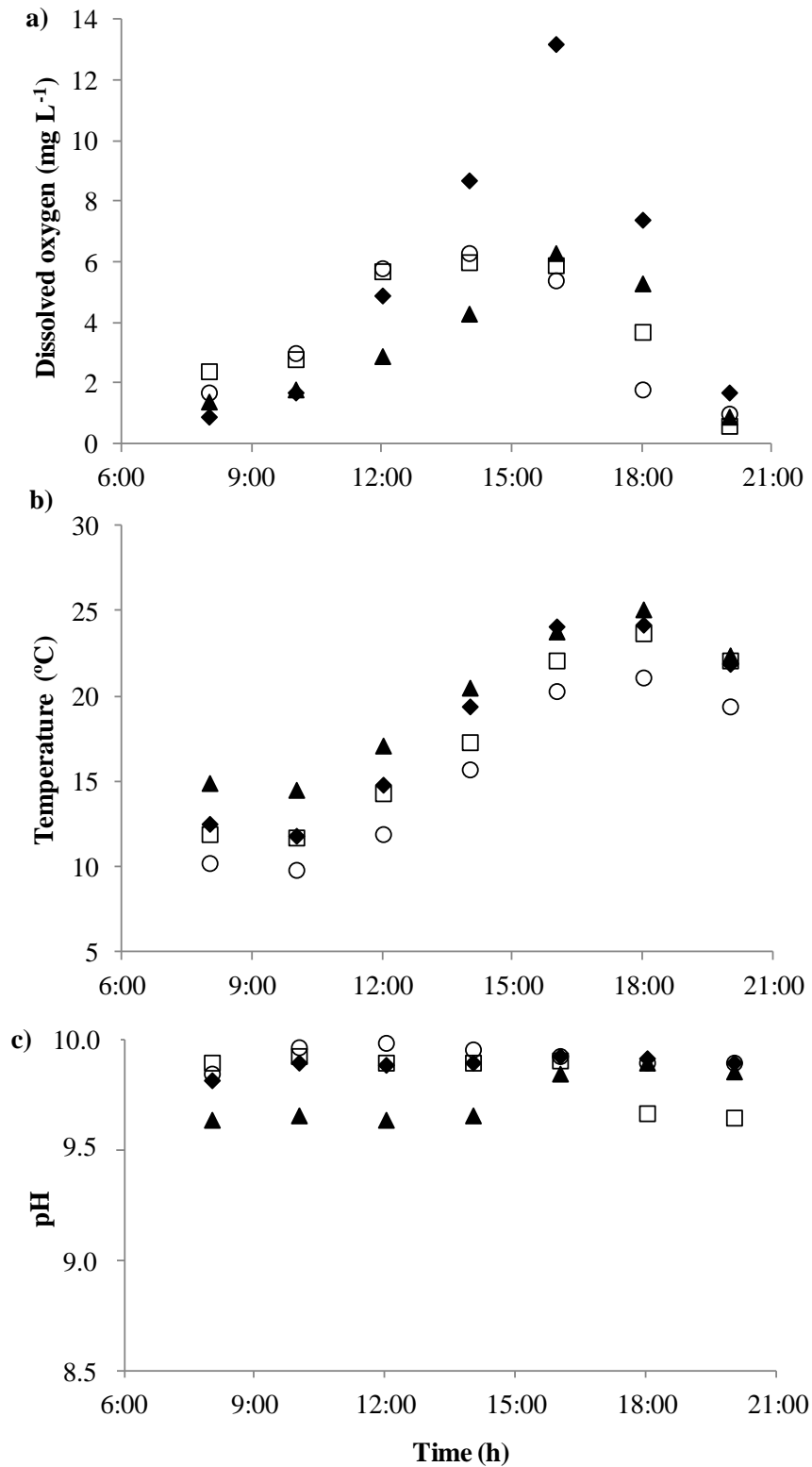
Figure A.8. Time course of the (a) DO concentration, (b) temperature and (c) pH during the day in the cultivation broth of the HRAP at the different L/G ratios tested: 0.5 (♦), 1 (□), 2 (▲) and 5 (○).
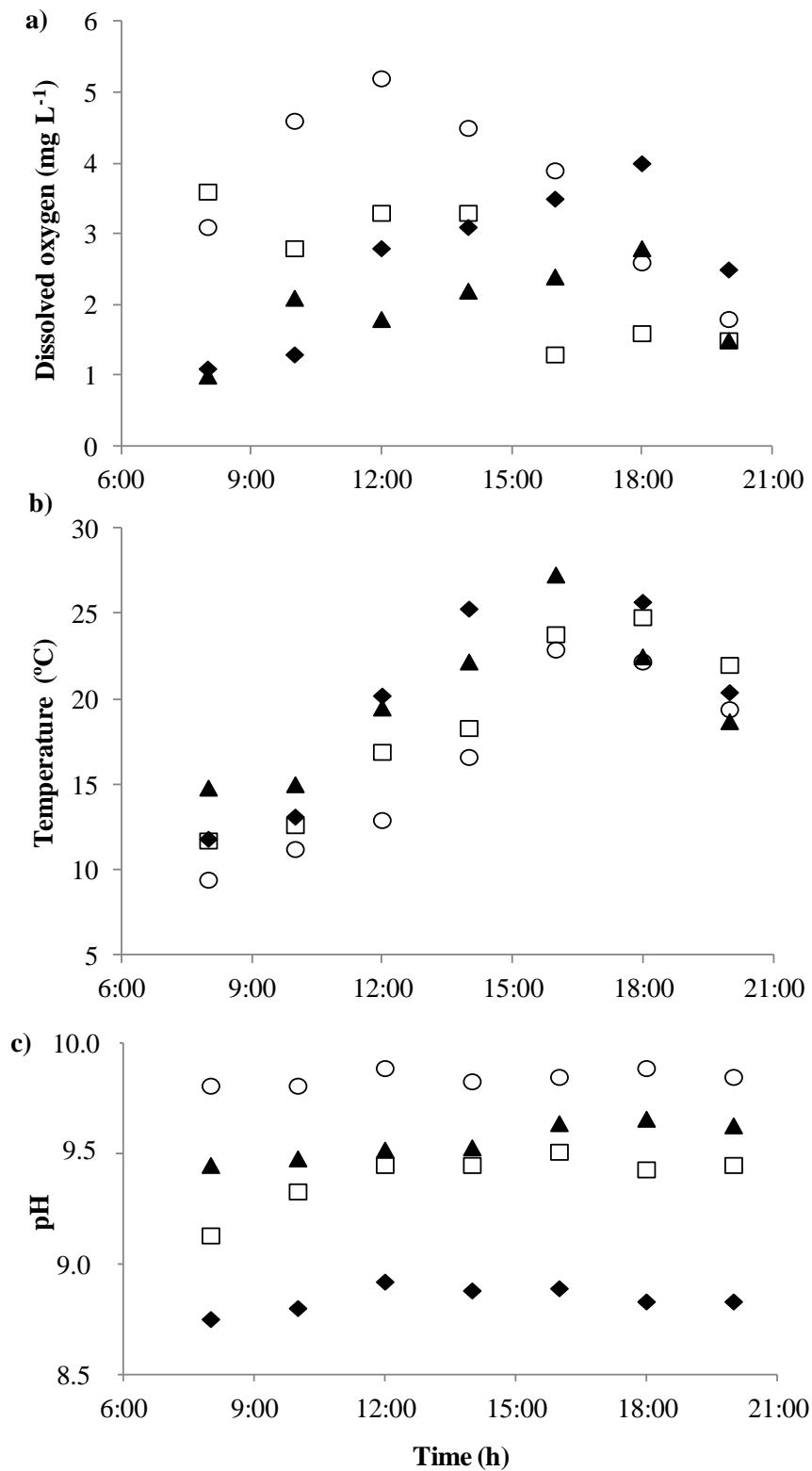
Figure A.9. Time course of the (a) DO concentration, (b) temperature and (c) pH during the day in the cultivation broth of the AC at the different L/G ratios tested: 0.5 (♦), 1 (□), 2 (▲) and 5 (○).
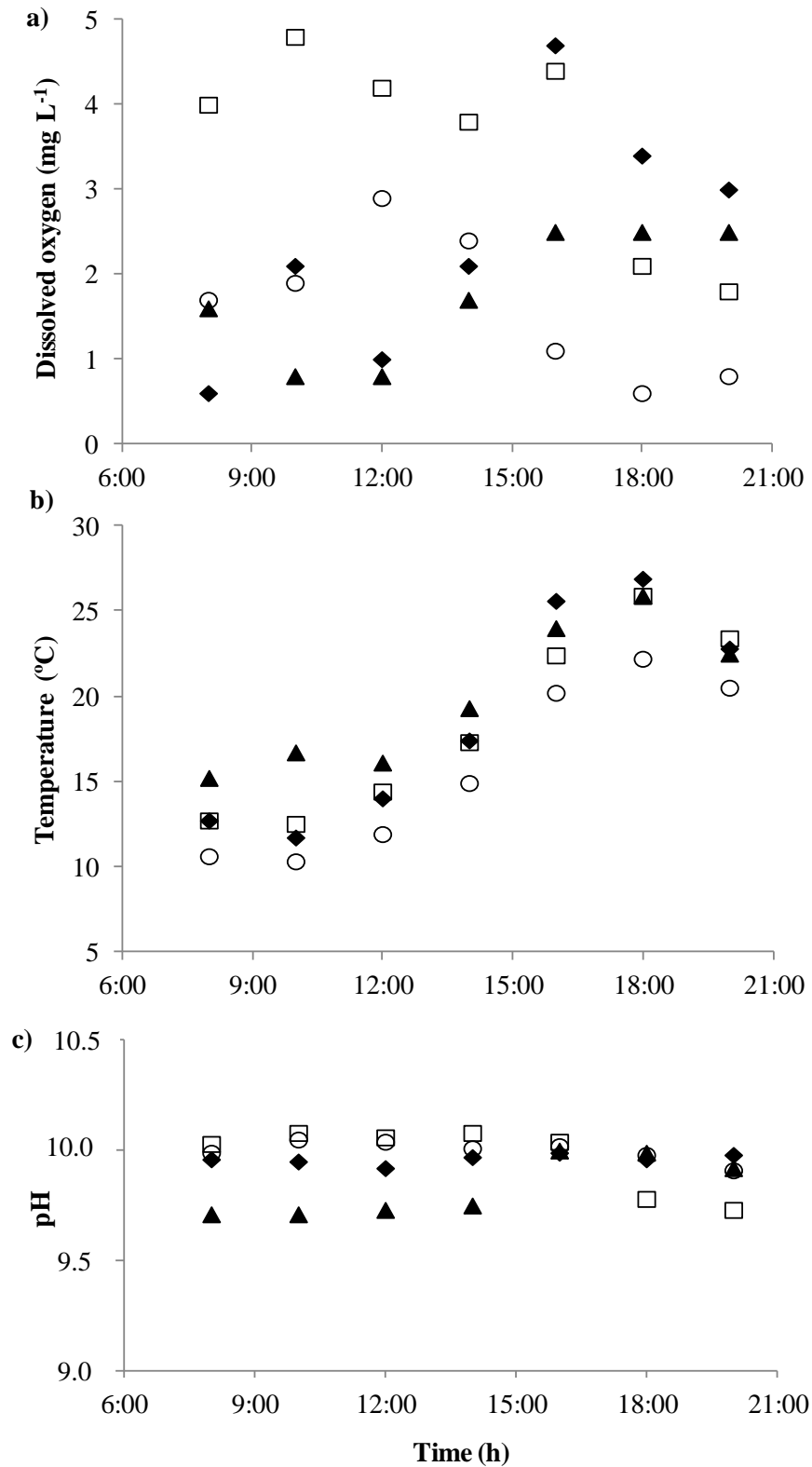
Figure A.10. Time course of the (a) DO concentration, (b) temperature and (c) pH during the day in the cultivation broth of the settler at the different L/G ratios tested: 0.5 (♦), 1 (□), 2 (▲) and 5 (○).

6. Evolution of the total organic carbon and total nitrogen concentration in the HRAP, AC and settler.
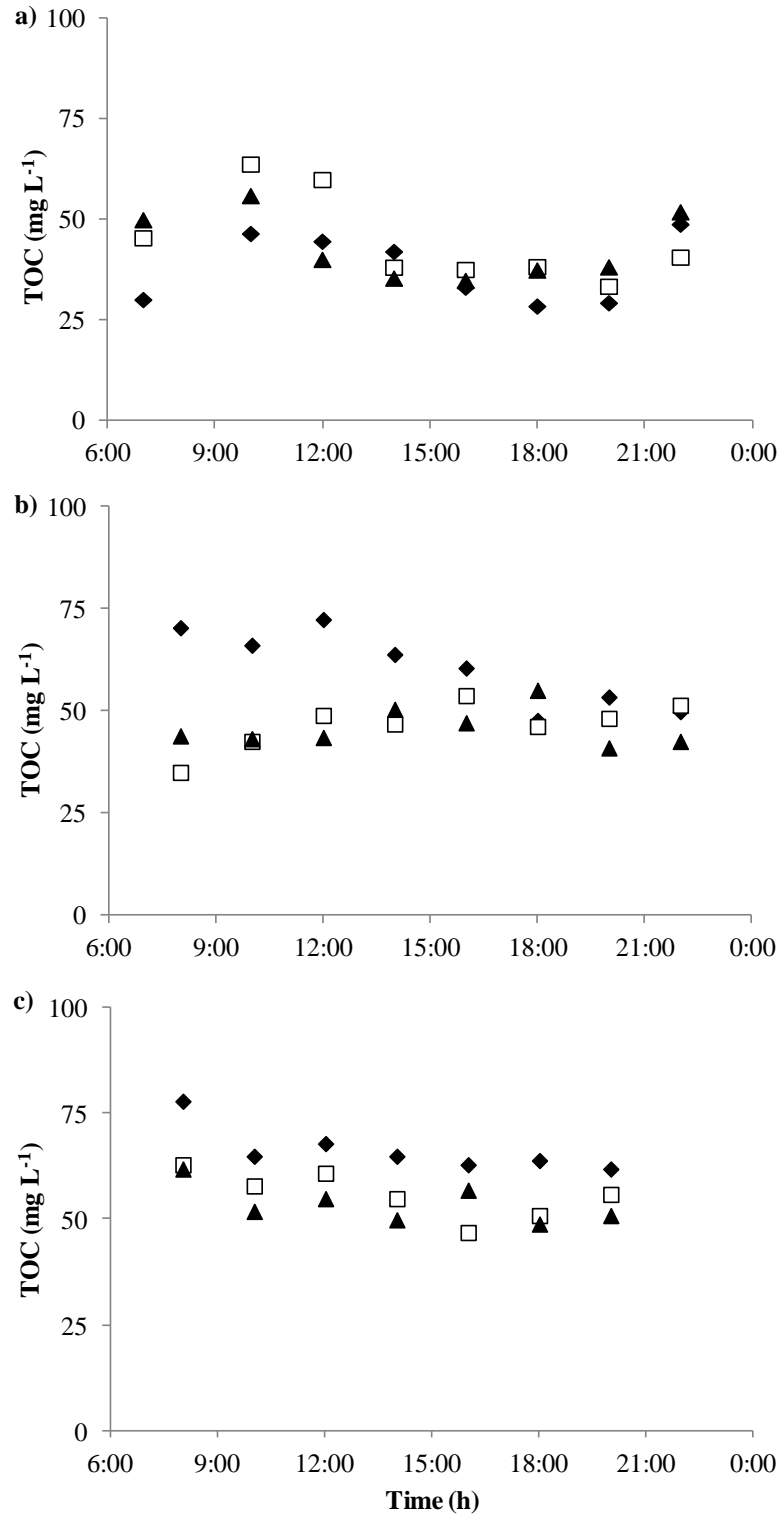
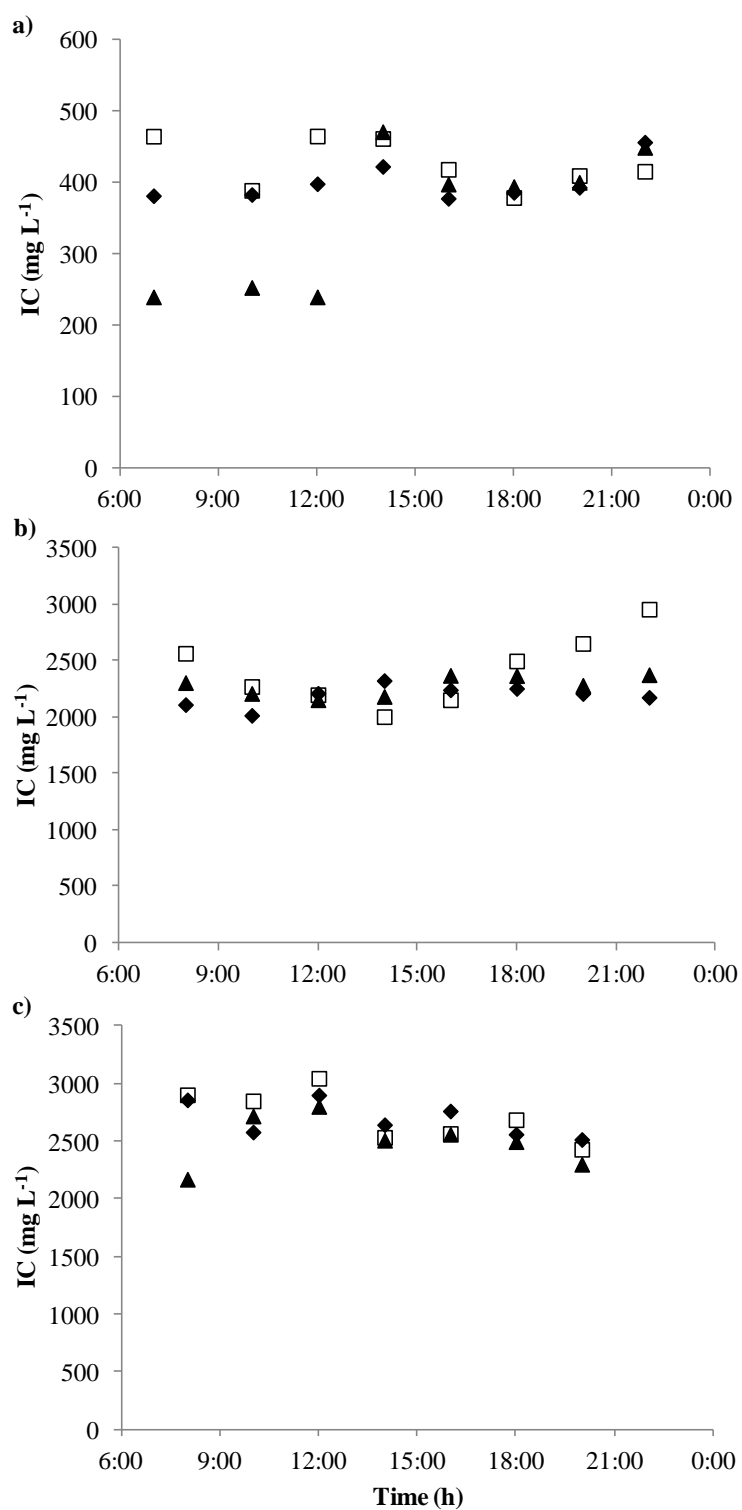**Figure A.11.** Time course of the total organic carbon concentration in the HRAP (♦), AC (□) and settler (▲) during stages (a) I, (b) II and (c) III under steady state.
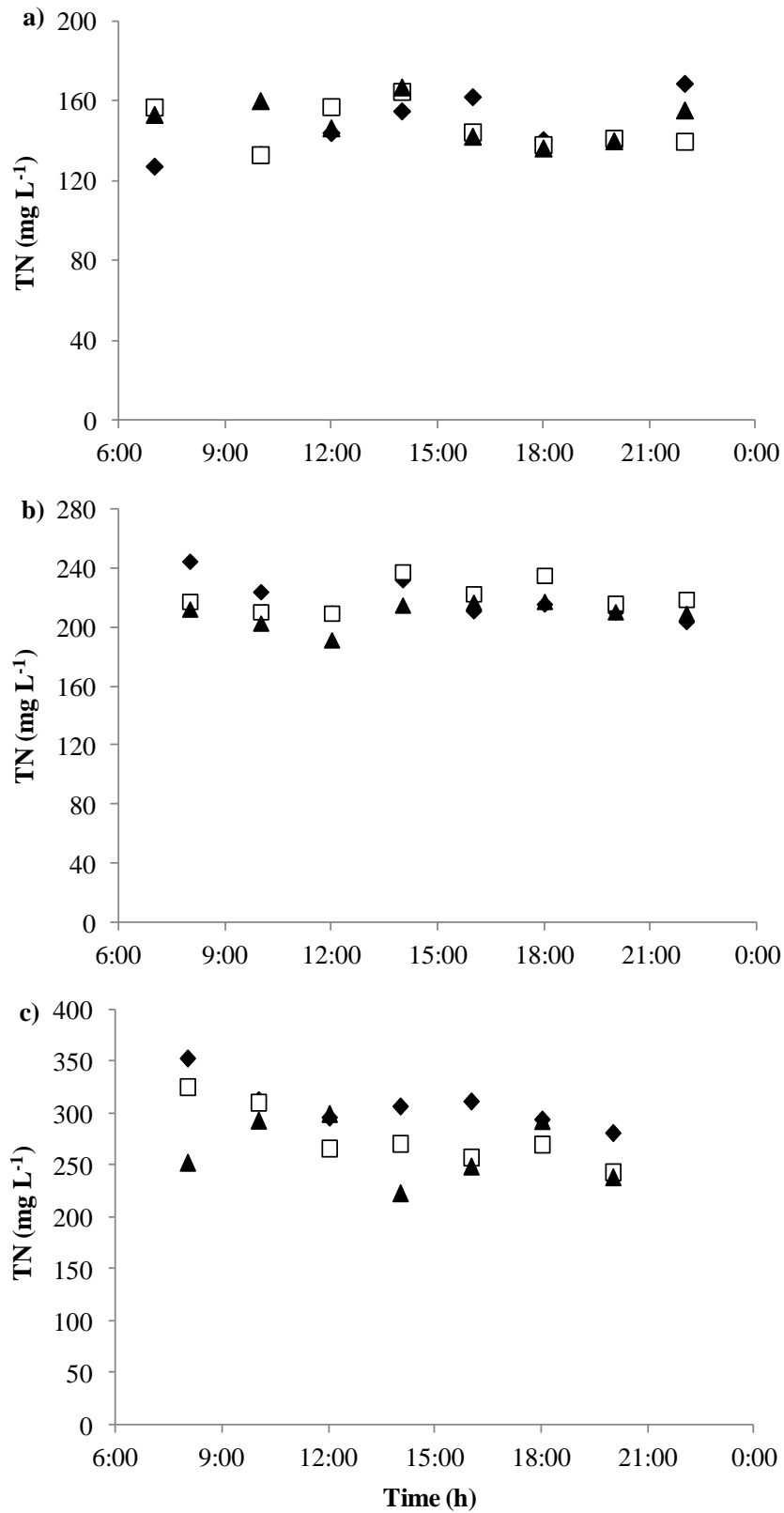
Figure A.12. Time course of the total nitrogen concentration in the HRAP (♦), AC (□) and settler (▲) during stages (a) I, (b) II and (c) III under steady state.

7. Evolution of the TSS concentration in the HRAP and microalgae population.
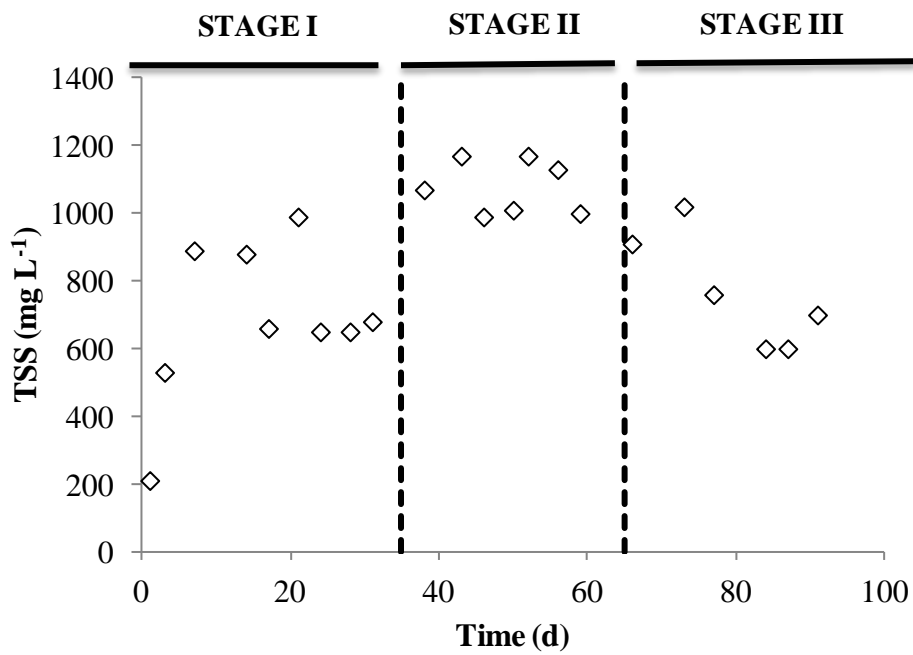
Figure A. 13. Evolution of TSS concentration in the broth of the HRAP during the experimental period.
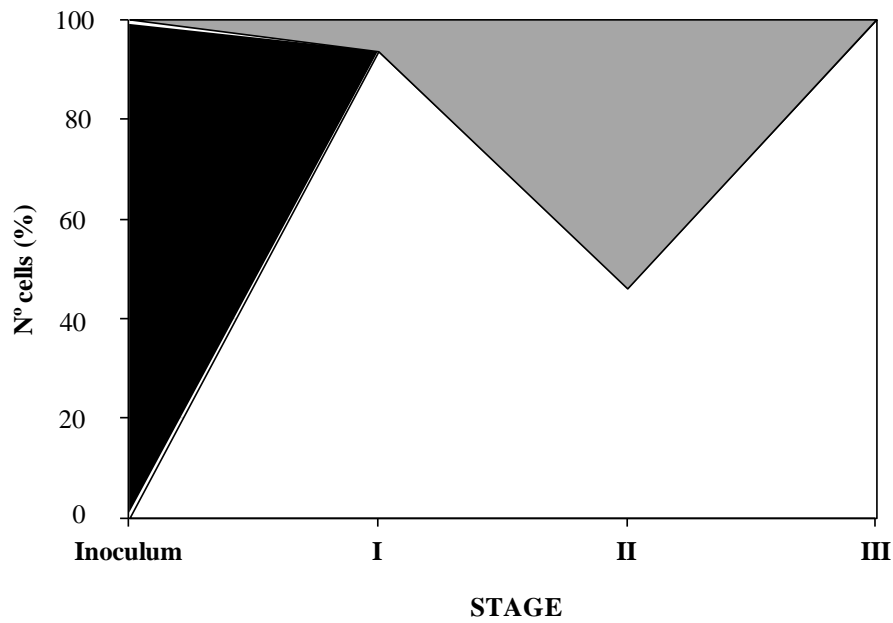
Figure A. 14. Time course of the structure of microalgae population in the HRAP: (■) Chlorella sp., (▨) Pseudanabaena sp. and (□) Chloroidium saccharophilum.

8. Sulfur precipitation in the diffuser of the absorption column

Photograph 1. Sulfur precipitation in the diffuser of the absorption column during stage I.

References

1. Murphy T. E., Berberog H., 2012. Temperature fluctuation and evaporative loss rate in an algae biofilm photobioreactor. J. Sol. Energy Eng. 134: 011002.

Chapter 2

Influence of the diffuser type and liquid-to-biogas ratio on biogas upgrading performance in an outdoor pilot scale high rate algal pond

David Marín[1, 2, 3], Alessandro A. Carmona-Martínez[1, 2], Raquel Lebrero[1, 2], Raúl Muñoz[1, 2, *]

[1] Department of Chemical Engineering and Environmental Technology, School of Industrial Engineering, Valladolid University, Dr. Mergelina, s/n, 47011, Valladolid, Spain.

[2] Institute of Sustainable Processes, Dr. Mergelina, s/n, 47011, Valladolid, Spain.

[3] Universidad Pedagógica Nacional Francisco Morazán, Boulevard Centroamérica, Tegucigalpa, Honduras.

[*] Corresponding author: mutora@iq.uva.es

Abstract

Four different types of biogas diffusers (metallic of 2 μm, porous stone, and two ceramic membranes of 0.2 and 0.4 μm) were evaluated to improve the quality of biomethane in an outdoor pilot scale photobioreactor interconnected to an external biogas absorption unit. Each type of diffuser was tested independently using three different liquid to biogas (L/G) ratios (0.5, 1 and 2). No significant difference was recorded in the CH_4 concentrations of biomethane (i.e. > 93.0%) working with the different types of diffusers at L/G ratios > 1. Only the metallic biogas diffuser supported CH_4 concentrations higher than 94.0% at a L/G ratio of 0.5. The increase in L/G ratio induced the stripping of the dissolved N_2 and O_2 into the biogas, which compensated the decrease in CO_2 concentration mediated by the higher pH value of the scrubbing solution. The ANOVA of the results here obtained confirmed that both the type of biogas diffuser and the L/G ratio significantly determined the quality of the upgraded biogas.

Keywords: Algal-bacterial photobioreactor; Biogas upgrading; Diffusers; Liquid/gas ratio; Outdoor cultivation.

1. Introduction

Nowadays, the biogas generated as a byproduct from the anaerobic treatment of organic waste and wastewater might represent an environmental problem if it is not energetically valorized. Biogas must be partially purified prior use as a renewable energy vector capable of reducing the dependence on fossil fuels in order to produce electricity and heat for industrial and domestic applications (Muñoz et al., 2015; Scarlat et al., 2018). A

stricter biogas purification must be implemented in order to fulfil with international regulations for its injection into natural gas grids or use as vehicle fuel. Typical compositions in biomethane standards are: $CH_4 \geq$ 90-95%, $CO_2 \leq$ 2-4%, $O_2 \leq$ 1 % and negligible amounts of H_2S (Muñoz et al., 2015; Ryckebosch et al., 2011).

Algal-bacterial processes have emerged as an environmentally friendly and cost-competitive alternative to conventional physicochemical processes capable of simultaneously removing CO_2 and H_2S in a single stage process (Angelidaki et al., 2018; Bose et al., 2019; Muñoz et al., 2015; Nagarajan et al., 2019). In algal-bacterial cultures, sulfur oxidizing bacteria oxidize the H_2S contained in biogas into SO_4^{2-} using the high dissolved oxygen (DO) concentrations present in the cultivation broth as a result of photosynthetic activity, while CO_2 is photosynthetically fixed by microalgae using solar energy (Posadas et al., 2015; Toledo-Cervantes et al., 2016). Microalgae-based biogas upgrading processes have been optimized under indoor conditions in photobioreactors interconnected to external biogas scrubbing units under artificial illumination and using metallic diffusers to sparge the biogas into the absorption column (Posadas et al., 2016; Rodero et al., 2018; Toledo-Cervantes et al., 2017, 2016). Similarly, photosynthetic biogas upgrading has been validated under outdoor conditions in different photobioreactor configurations. Posadas et al. (2017) evaluated the simultaneous upgrading of biogas and wastewater treatment in a 180 L algal pond using a metallic diffuser and liquid to biogas (L/G) ratios of 0.5, 1.0, 2.0 and 5.0. Marín et al. (2018a, 2018b) evaluated the influence of the seasonal variations of environmental conditions on biogas upgrading performance in a 180 L photobioreactor fed with carbonate supplemented centrate, using a metallic diffuser and L/G ratio of 1.0. Similarly, Rodero et al. (2019) investigated the influence of biogas flow rate and L/G ratios on biomethane quality in a 9.6 m^3 algal pond using a polymeric membrane diffuser. In addition, Marín et al. (2019) assessed the influence of the L/G ratio and alkalinity in the cultivation broth on the quality of the upgraded biogas in a 11.7 m^3 horizontal hybrid tubular photobioreactor using metallic diffusers. Table 1 summarizes the different types of photobioreactor configuration and biogas diffusers tested, along with the recorded CH_4 concentration in the upgraded biogas. Despite the promising results obtained so far, the effect of the type of diffuser used for biogas sparging in the absorption column on the biomethane quality has not been systematically assessed. The type of diffuser will directly

impact on the mass transfer, and therefore on the removal of the target pollutants in the biogas scrubbing unit, thus constituting a key element of process optimization.

In this sense, the influence of four different types of biogas diffusers with different pore sizes (namely metallic of 2 µm, porous stone, ceramic membrane of 0.2 and 0.4 µm) at three L/G ratios on biogas upgrading performance was herein investigated in an outdoor pilot scale photobioreactor interconnected to an external biogas absorption unit.

Table 1. CH_4 concentration in the upgraded biogas using different photobioreactor configurations with different types of diffuser.

Reference	Photobioreactor configuration	L/G ratios tested	Type of Diffuser	CH_4 concentration (%)
Toledo-Cervantes et al. (2016)	Indoor 180 L HRAP	1; 5; 10 and 20	Metallic 2 μm	95; 88; 68 and 68
Toledo-Cervantes et al. (2017)	Indoor 180 L HRAP	0.3; 0.5; 0.8 and 1	Metallic 2 μm	95; 98; 98 and 96
Rodero et al. (2018)	Indoor 180 L HRAP	1	Metallic 2 μm	98
Posadas et al. (2017)	Outdoor 180 L HRAP	0.5; 1; 2 and 5	Metallic 2 μm	86; 90; 92 and 80
Marín et al. (2018a)	Outdoor 180 L HRAP	1	Metallic 2 μm	85 – 98
Rodero et al. (2019b)	Outdoor 9.6 m^3 HRAP	1.2; 2.1 and 3.5	Polymeric membrane	85; 89 and 90
Marin et al (2019)	Outdoor 11.7 m^3 horizontal hybrid tubular photobioreactor	0.5; 1; 2; 3; 4 and 5	Metallic 2 μm	87; 90; 88; 89; 88 and 87

2. Materials and methods

2.1 Biogas and synthetic digestate

A synthetic biogas mixture composed of CO_2 (29.5%), H_2S (0.5%) and CH_4 (70%) was used as a raw biogas in the present study (Abello Linde; Spain). The synthetic digestate (SWW) used consisted of (per liter of distilled water): 6.00 g $NaHCO_3$, 3.00 g Na_2CO_3, 0.94 g K_2HPO_4, 1.91 g NH_4Cl, 0.02 g $CaCl_2·2H_2O$, 0.005 g $FeSO_2·7H_2O$, 0.10 g $MgSO_4·7H_2O$ and 5 ml of a micronutrient solution (composed of 0.10 g $ZnSO_4·7H_2O$, 0.10 g $MnCl_2·4H_2O$, 0.20 g H_3BO_3, 0.02 g $Co(NO_3)_2·6H_2O$, 0.02 g $Na_2MoO_4·2H_2O$, 0.0005 g $CuSO_4·5H_2O$, 0.70 g $FeSO_4·7H_2O$ and 1.02 g $EDTA·2Na·2H_2O$ per liter of distilled water). The resulting composition of the SWW was: total organic carbon 51 ± 8 mg L^{-1}, inorganic carbon 1211 ± 51 mg L^{-1} and total nitrogen 528 ± 33 mg L^{-1}. The composition of the SWW, characterized by a high nutrient concentration and high alkalinity, was selected according to Toledo-Cervantes et al., (2016) and Wilkie et al., (2000).

2.2. Experimental set-up

The experimental plant used for this experimentation was located outdoor at the Institute of Sustainable Processes of Valladolid University (Spain). The experimental set-up was integrated by a 180-L open photobioreactor divided in two water channels and with one baffle at each side of the photobioreactor. The open photobioreactor has an illuminated surface of 1.20 m^2 (length of 170 cm; depth of 15 cm; width of 82 cm). The cultivation broth inside the photobioreactor was recirculated with a velocity of 20 cm s^{-1} by a 6-blade paddlewheel. A biogas scrubbing column of 2.5 L (height: 165 cm; internal diameter: 4.4 cm) operating at atmospheric pressure was interconnected to the photobioreactor through a conical settler of 8 L. (Fig. 1). The implementation of a biogas scrubbing bubble column, and consequently the need for diffusers to sparge biogas, was selected due to the fact that the high concentrations of biomass present in the recirculating liquid will entail a severe clogging and malfunctioning in other types of biogas scrubbing technologies such as spray towers or packed absorption columns.
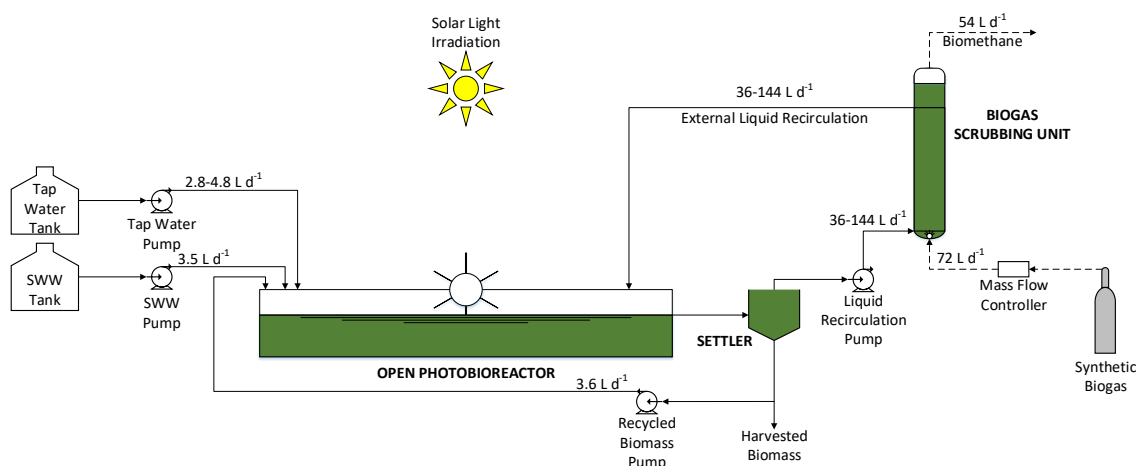
Figure 1. Schematic diagram of the outdoor experimental pilot plant used for the photosynthetic purification of biogas.

2.3. Operational conditions and sampling procedures

Process operation was carried out from September the 4th to October the 8th 2019. The photobioreactor was inoculated with a culture previously grown in an outdoors photobioreactor at an initial concentration of 450 mg total suspended solids L^{-1}. The microalgal inoculum was composed of *Mychonastes homosphaera, Pseudanabaena sp. and Scenedesmus sp.* with a share (based on the number of cells) of 82, 17 and 1%, respectively. The photobioreactor was fed with SWW as a nutrient source at a flow rate of 3.5 L d^{-1}. Four different types of biogas diffusers with different pore sizes were successively installed at the bottom of the scrubbing unit in order to analyze their influence on biogas upgrading performance: a cylindrical metallic diffuser with a pore size of 2 μm (height: 2.3 cm; diameter: 1.7 cm), a rectangular porous stone with a heterogeneous pore size distribution (length: 3.0 cm; height: 1.5 cm; width: 1.5 cm), a cylindrical ceramic membrane with a pore size of 0.2 μm (height: 20.0 cm; diameter: 1.0 cm) and a cylindrical ceramic membrane with a pore size of 0.4 μm (height: 20.0 cm; diameter: 1.0 cm). Three different L/G ratios were tested under process operation with each diffuser. In this sense, the biogas was sparged into the scrubbing unit, through the different types of diffusers at 72 L d^{-1}. The liquid recirculation from the settler to the absorption unit was operated under co-current flow at rates of 36, 72 and 144 L d^{-1} (corresponding to hydraulic retention times, HRT, in the column of 100, 50 and 25 min, respectively), resulting in L/G ratios of 0.5, 1.0 and 2.0, respectively. The different combinations of diffusers and L/G ratios were tested sequentially for each type of diffuser, starting with the lowest L/G ratio of 0.5 and ending with the highest L/G ratio

of 2.0. The pH in the photobioreactor remained constant during all experimentation period at an average value of 9.1 ± 0.1. Tap water was supplied in order to compensate water evaporation losses in the open photobioreactor and allow process operation without effluent. Gas samples of 100 µL of the upgraded biogas were drawn every two hours to monitor the gas concentrations of CO_2, H_2S, N_2, O_2 and CH_4. The pH in the photobioreactor and in the scrubbing unit was also monitored every two hours. The photosynthetic active radiation (PAR), DO concentration, and ambient and photobioreactor temperatures were daily monitored in each test (Table A1).

2.4. Analytical procedures

Gas concentrations of CO_2, H_2S, N_2, O_2 and CH_4 in the raw and upgraded biogas were determined using a Varian CP-3800 GC-TCD according to Posadas et al. (2015) (Palo Alto, USA). pH was determined with an Eutech Cyberscan pH 510 (Eutech instruments, The Netherlands). PAR, DO concentrations, and ambient and photobioreactor temperature were measured according to Marín et al., (2018a).

2.5. Statistical analysis

The results here presented were provided as the average values along with their standard deviation from five replicate measurements for each test run. An analysis of variance (ANOVA) was performed to determine the influence of the biogas diffusers on the quality of the upgraded biogas.

3. Results

3.1 Metallic diffuser

CO_2 concentration in the upgraded biogas reached values of 3.4, 3.4 and 1.3% and removal efficiencies (REs) of 88.9, 88.8 and 95.7% at L/G ratios of 0.5, 1.0 and 2.0, respectively (Fig. 2a). The pH in the scrubbing unit decreased by 4.5, 4.4 and 2.9%, at L/G ratios of 0.5, 1.0 and 2.0, respectively (Table 2). H_2S from raw biogas was completely removed regardless of the L/G ratio. On the other hand, N_2 concentrations reached values of 1.5, 1.9 and 3.0%, while O_2 concentrations in the upgraded biogas reached values of 0.2, 0.1 and 0.5% at L/G ratios of 0.5, 1.0 and 2.0, respectively (Fig. 2a). Finally, CH_4 concentrations in the upgraded biogas of 94.9, 94.6 and 95.2% were recorded at L/G ratios of 0.5, 1.0 and 2.0, respectively (Fig. 2a).
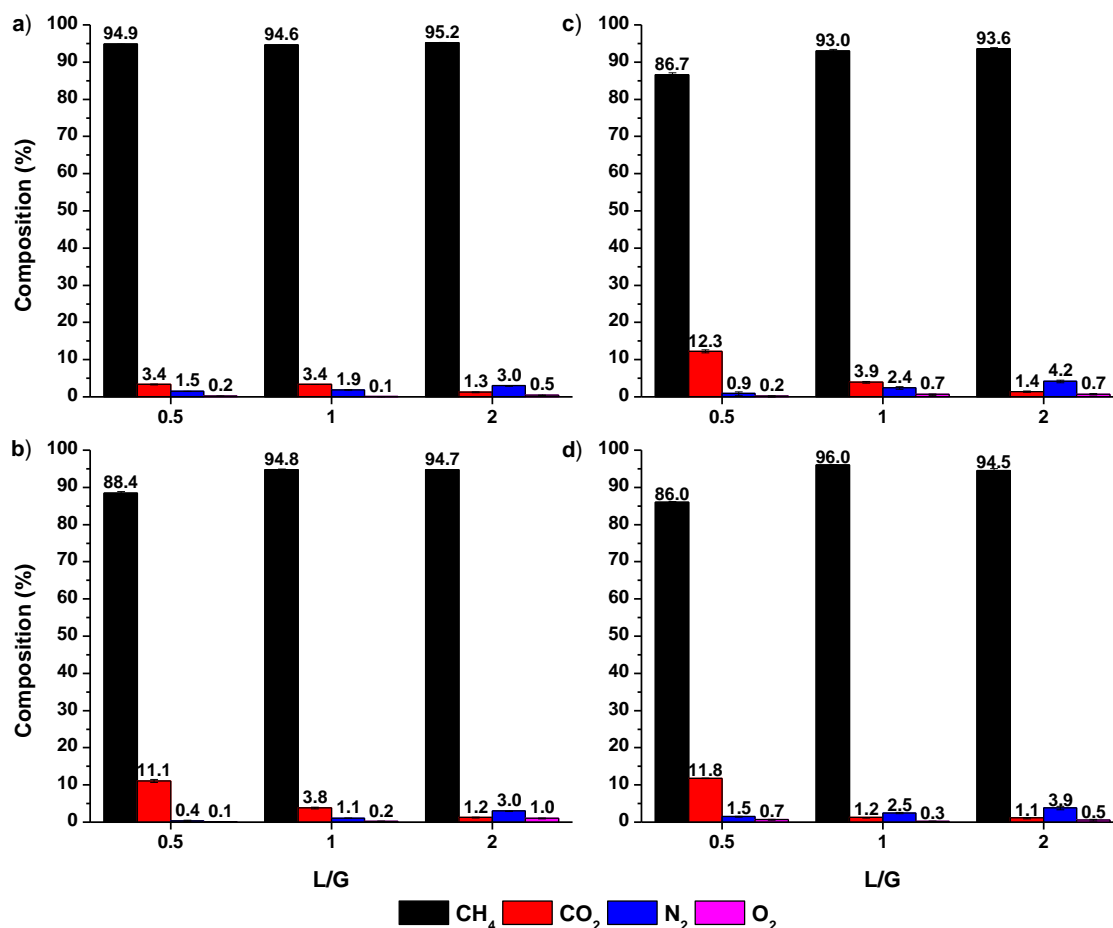
Figure 2. Concentration of CH_4, CO_2, N_2 and O_2 in the upgraded biogas using (a) metallic 2 μm, (b) porous stone, (c) ceramic membrane 0.2 μm and (d) ceramic membrane 0.4 μm diffusers.

3.2 Porous stone diffuser

CO_2 concentration in the biomethane accounted for 11.1, 3.8 and 1.2%, which corresponded to CO_2-REs of 63.4, 87.3 and 95.9% at L/G ratios of 0.5, 1.0 and 2.0, respectively (Fig. 2b). The reduction in the pH of the recirculating culture medium in the absorption unit at L/G ratios of 0.5, 1.0 and 2.0 were 10.0, 5.4 and 4.4%, respectively (Table 2). H_2S from the raw biogas was completely removed regardless of the L/G ratio. N_2 concentration reached values of 0.4, 1.1 and 3.0%, while O_2 concentrations accounted for 0.1, 0.2 and 1.0% at L/G ratios of 0.5, 1.0 and 2.0, respectively. Finally, the CH_4 concentrations observed at a L/G ratio of 0.5, 1 and 2 were 88.4, 94.8 and 94.7%, respectively (Fig. 2b).

3.3 Ceramic Membrane

The CO_2 concentrations achieved when using the ceramic membrane diffuser of 0.2 μm at L/G ratios of 0.5, 1.0 and 2.0 were 12.3, 3.9 and 1.4%, respectively, and 11.8, 1.2 and 1.1% when using the ceramic membrane of 0.4 μm, respectively. Therefore, the CO_2-REs corresponded to 59.5, 87.1 and 95.3% (ceramic membrane of 0.2 μm), and 61.0, 95.9 and 96.3% (ceramic membrane of 0.4 μm) (Fig. 2c; 2d). The decrease in pH in the cultivation medium in the experiment conducted with the ceramic membrane of 0.2 μm was higher than that with a pore size of 0.4 μm at L/G ratios of 0.5 and 1.0, and negligible in both membranes at a L/G ratio of 2 (Table 2). H_2S from raw biogas was completely removed in both ceramic membranes regardless of the L/G ratio. On the other hand, N_2 concentration in the experiments with the ceramic membrane of 0.2 μm reached values of 0.9, 2.4 and 4.2%, respectively, and 1.5, 2.5 and 3.9% in the ceramic membrane of 0.4 μm at L/G ratios of 0.5, 1.0 and 2.0. O_2 concentration in the upgraded biogas reached values of 0.2, 0.7 and 0.7% when using the ceramic membrane of 0.2 μm at L/G ratios of 0.5, 1 and 2, and 0.7, 0.3 and 0.5% with the ceramic membrane of 0.4 μm, respectively, (Fig. 2c; 2d). Finally, CH_4 concentrations in the upgraded biogas using the ceramic membrane of 0.2 μm were 86.7, 93.0 and 93.6%, respectively, and 86.0, 96.0 and 94.5% with ceramic membrane of 0.4 at L/G of 0.5, 1 and 2, respectively (Fig. 2c; 2d).

Table 2. pH values and decrease (as percentage) in the of the cultivation broth in the biogas scrubbing unit using the different types of diffusers.

	L/G								
	0.5			**1**			**2**		
Type of diffuser	**Bottom**	**Top**	**Decrease (%)**	**Bottom**	**Top**	**Decrease (%)**	**Bottom**	**Top**	**Decrease (%)**
Metallic	8.95	8.55	4.5 %	9.10	8.70	4.4 %	9.20	8.93	2.9 %
Porous Stone	9.09	8.18	10.0 %	9.13	8.64	5.4 %	9.14	8.74	4.4 %
Ceramic Membrane 0.2 μm	9.08	8.03	11.6 %	9.11	8.29	9.0 %	9.03	8.66	4.1 %
Ceramic Membrane 0.4 μm	9.02	8.68	3.8 %	9.05	8.75	3.3 %	9.15	8.78	4.0 %

4. Discussion

The diffuser that provided the most efficient upgrading of biogas at a L/G of 0.5 was the 2 μm metallic diffuser, which was the only one that fulfilled with most international regulations required for biogas injection into natural gas grids or use as a vehicle fuel: $CH_4 \geq$ 90-95%, $CO_2 \leq$ 2-4%, $O_2 \leq$ 1 % and negligible amounts of H_2S (European Committee for Standardization, 2018, 2017; Muñoz et al., 2015). When a L/G ratio of 1.0 was used, the four diffusers exhibited a similar upgrading performance in terms of CH_4 concentration, reaching values up to 96.0%. This increase in CH_4 concentrations was promoted by the increase in pH in the absorption unit, which supported a higher CO_2-REs due to the enhanced gradient of CO_2 concentration between the biogas and liquid phase. Similarly, the four diffusers provided comparable CH_4 concentrations (up to 95.2%) at a L/G of 2. However, this increase in the cultivation medium pumped into the biogas scrubbing unit resulted in increased in N_2 and O_2 concentrations regardless of the type of diffuser tested. This can be explained by the superior dissolved gas stripping at higher liquid flowrates, which negatively impacted on the final concentration of CH_4 in the upgraded biogas (Sovechles and Waters, 2015). The biogas quality at a L/G ratios of 1 and 2 fulfilled with the current European biomethane standard regardless of the diffuser configuration (European Committee for Standardization, 2018, 2017; Muñoz et al., 2015)

Overall, the results herein obtained confirmed that the metallic diffuser was the best system to purify biogas at the L/G ratios typically implemented in photosynthetic biogas upgrading processes in open photobioreactors. These results were in accordance to Marín et al. (2019), who reported higher CH_4 concentrations at decreasing L/G ratios. Indeed, the CH_4 content in biomethane decreased from 89% at L/G of 1 to 87% at L/G of 5 in an outdoor horizontal hybrid tubular photobioreactor constructed with metallic diffusers for biogas upgrading.

Finally, an ANOVA test was carried out to elucidate the influence of the type of diffusers and the L/G ratio on the quality of the upgraded biogas. The F critical value (value that will define if the means for each component are significantly different) was 3.2 for the three different L/G ratios tested in this work. The F values (ratio between the mean square of the component and the mean square of the error) for CH_4, CO_2, N_2 and O_2 were 206.7, 274.5, 28.9 and 36.3, respectively, at the L/G ratio of 0.5 (Table 3a). On the other hand,

the F values at L/G ratio of 1.0 were 18.5, 152.6, 53.3 and 21.4 for the above mentioned gases, respectively (Table 3b). Finally, the F values at L/G ratio of 2.0 were 16.7, 3.4, 19.2 and 4.0 for CH_4, CO_2, N_2 and O_2, respectively (Table 3c). The F values were greater than the F critical value of 3.2 regardless of the biomethane component, which confirmed that the quality of biomethane varied significantly with the type of diffuser and the L/G ratio implemented in the photosynthetic biogas upgrading process.

Unfortunately, the concentration of methane in the cultivation broth returned to the algal pond has not been measured in this particular study. However, no methane slippage into the photobioreactor was expected due to the low aqueous solubility of methane (according to its Henry´s Law constant, $H_{CH4} \approx 0.03$ at 25 ºC) compared to other contaminants (i.e. CO_2 and H_2S, $H_{CO2} \approx 0.83$ and $H_{H2S} \approx 2.45$ at 25 ºC). In addition, it was hypothesized that the inherent presence of bacteria (e.g. methanotrophs) would eventually oxidize any CH_4 transferred to the cultivation broth.

Table 3. Analysis of variance of biogas at L/G ratios of (a) 0.5, (b) 1 and (c) 2.

a)

	Sum of squares	Degrees of freedom	Mean square	F	F critical
CH_4	224.0	3.0	74.7	206.7	3.2
Error	5.8	16.0	0.4		
CO_2	242.9	3.0	81.0	274.5	3.2
Error	4.7	16.0	0.3		
N_2	4.9	3.0	1.6	28.9	3.2
Error	0.9	16.0	0.1		
O_2	1.0	3.0	0.3	36.3	3.2
Error	0.1	16.0	0.0		

Table 3. Continued.

b)

	Sum of squares	Degrees of freedom	Mean square	F	F critical
CH_4	10.8	3.0	3.6	18.5	3.2
Error	3.1	16.0	0.2		
CO_2	23.1	3.0	7.7	152.6	3.2
Error	0.8	16.0	0.1		
N_2	6.0	3.0	2.0	53.3	3.2
Error	0.6	16.0	0.0		
O_2	0.7	3.0	0.2	21.4	3.2
Error	0.2	16.0	0.0		

c)

	Sum of squares	Degrees of freedom	Mean square	F	F critical
CH_4	6.6	3.0	2.2	16.7	3.2
Error	2.1	16.0	0.1		
CO_2	0.3	3.0	0.1	3.4	3.2
Error	0.5	16.0	0.0		
N_2	5.7	3.0	1.9	19.2	3.2
Error	1.6	16.0	0.1		
O_2	0.4	3.0	0.1	4.0	3.2
Error	0.6	16.0	0.0		

5. Conclusions

This study demonstrated the statistically significant influence of the type of biogas diffuser and the L/G ratio in the scrubbing unit on the quality of biomethane in an outdoor pilot scale photobioreactor. L/G ratios > 1.0 supported a significant decrease in CO_2 concentration in the upgraded biogas along with a superior stripping of O_2 and N_2 from the scrubbing solution regardless of the type of diffuser used. The 2 μm metallic diffuser provided the highest CH_4 concentration in the upgraded biogas regardless of the L/G ratio (94.6-95.2%), which complied with most international regulations for biomethane injection into natural gas grids.

Acknowledgements

This work was supported by Fundación Domingo Martinez and the Regional Government of Castilla y León and the EU-FEDER programme (CLU 2017-09 and UIC 071). The financial support of the Regional Government of Castilla y León for the PhD grant of David Marín is also acknowledged.

References

1. Angelidaki, I., Treu, L., Tsapekos, P., Luo, G., Campanaro, S., Wenzel, H., Kougias, P.G., 2018. Biogas upgrading and utilization: Current status and perspectives. Biotechnol. Adv. 36, 452–466. https://doi.org/10.1016/j.biotechadv.2018.01.011

2. Bose, A., Lin, R., Rajendran, K., O'Shea, R., Xia, A., Murphy, J.D., 2019. How to optimise photosynthetic biogas upgrading: a perspective on system design and microalgae selection. Biotechnol. Adv. 107444. https://doi.org/10.1016/j.biotechadv.2019.107444

3. European Committee for Standardization, 2018. UNE EN 16723-2:2018 Natural gas and biomethane for use in transport and biomethane for injection in the natural gas network - Part 2: Automotive fuels specification [WWW Document]. URL https://www.en-standard.eu/une-en-16723-2-2018-natural-gas-and-biomethane-for-use-in-transport-and-biomethane-for-injection-in-the-natural-gas-network-part-2-automotive-fuels-specification/ (accessed 12.10.19).

4. European Committee for Standardization, 2017. UNE EN 16723-1:2017 Natural gas and biomethane for use in transport and biomethane for injection in the natural gas network - Part 1: Specifications for biomethane for injection in the natural gas network [WWW Document]. URL https://www.en-standard.eu/une-en-16723-1-2017-natural-gas-and-biomethane-for-use-in-transport-and-biomethane-for-injection-in-the-natural-gas-network-part-1-specifications-for-biomethane-for-injection-in-the-natural-gas-network/ (accessed 12.10.19).

5. Marín, D., Ortíz, A., Díez-Montero, R., Uggetti, E., García, J., Lebrero, R., Muñoz, R., 2019. Influence of liquid-to-biogas ratio and alkalinity on the biogas upgrading performance in a demo scale algal-bacterial photobioreactor. Bioresour. Technol. 280, 112–117. https://doi.org/10.1016/j.biortech.2019.02.029

6. Marín, D., Posadas, E., Cano, P., Pérez, V., Blanco, S., Lebrero, R., 2018a. Seasonal variation of biogas upgrading coupled with digestate treatment in an outdoors pilot scale algal-bacterial photobioreactor. Bioresour. Technol. 263, 58–66. https://doi.org/10.1016/j.biortech.2018.04.117

7. Marín, D., Posadas, E., Cano, P., Pérez, V., Lebrero, R., Muñoz, R., 2018b. Influence of the seasonal variation of environmental conditions on biogas upgrading in an outdoors pilot scale high rate algal pond. Bioresour. Technol. 255, 354–358. https://doi.org/10.1016/j.biortech.2018.01.136

8. Muñoz, R., Meier, L., Diaz, I., Jeison, D., 2015. A review on the state-of-the-art of physical/chemical and biological technologies for biogas upgrading. Rev. Environ. Sci. Bio/Technology 14, 727–759. https://doi.org/10.1007/s11157-015-9379-1

9. Nagarajan, D., Lee, D.-J., Chang, J.-S., 2019. Integration of anaerobic digestion and microalgal cultivation for digestate bioremediation and biogas upgrading. Bioresour. Technol. 290, 121804. https://doi.org/10.1016/j.biortech.2019.121804

10. Posadas, E., Marín, D., Blanco, S., Lebrero, R., Muñoz, R., 2017. Simultaneous biogas upgrading and centrate treatment in an outdoors pilot scale high rate algal pond. Bioresour. Technol. 232, 133–141. https://doi.org/10.1016/j.biortech.2017.01.071

11. Posadas, E., Serejo, M.L., Blanco, S., Pérez, R., García-Encina, P.A., Muñoz, R., 2015. Minimization of biomethane oxygen concentration during biogas upgrading in algal-bacterial photobioreactors. Algal Res. 12, 221–229. https://doi.org/10.1016/j.algal.2015.09.002

12. Posadas, E., Szpak, D., Lombó, F., Domínguez, A., Díaz, I., Blanco, S., García-Encina, P.A., Muñoz, R., 2016. Feasibility study of biogas upgrading coupled with nutrient removal from anaerobic effluents using microalgae-based processes. J. Appl. Phycol. 28, 2147–2157. https://doi.org/10.1007/s10811-015-0758-3

13. Rodero, R., Lebrero, R., Serrano, E., Lara, E., Arbib, Z., García-Encina, P.A., Muñoz, R., 2019. Technology validation of photosynthetic biogas upgrading in a semi-industrial scale algal-bacterial photobioreactor. Bioresour. Technol. 279, 43–49. https://doi.org/10.1016/j.biortech.2019.01.110

14. Rodero, R., Posadas, E., Toledo-Cervantes, A., Lebrero, R., Muñoz, R., 2018. Influence of alkalinity and temperature on photosynthetic biogas upgrading efficiency in high rate algal ponds. Algal Res. 33, 284–290. https://doi.org/10.1016/j.algal.2018.06.001

15. Ryckebosch, E., Drouillon, M., Vervaeren, H., 2011. Techniques for transformation of biogas to biomethane. Biomass and Bioenergy 35, 1633–1645. https://doi.org/10.1016/j.biombioe.2011.02.033

16. Scarlat, N., Dallemand, J.F., Fahl, F., 2018. Biogas: Developments and perspectives in Europe. Renew. Energy 129, 457–472. https://doi.org/10.1016/j.renene.2018.03.006

17. Sovechles, J.M., Waters, K.E., 2015. Effect of ionic strength on bubble coalescence in inorganic salt and seawater solutions. AICHE 61, 2489–2496. https://doi.org/doi.org/10.1002/aic.14851

18. Toledo-Cervantes, A., Madrid-Chirinos, C., Cantera, S., Lebrero, R., Muñoz, R., 2017. Influence of the gas-liquid flow configuration in the absorption column on photosynthetic biogas upgrading in algal-bacterial photobioreactors. Bioresour. Technol. 225, 336–342. https://doi.org/10.1016/j.biortech.2016.11.087

19. Toledo-Cervantes, A., Serejo, M.L., Blanco, S., Pérez, R., Lebrero, R., Muñoz, R., 2016. Photosynthetic biogas upgrading to bio-methane: Boosting nutrient recovery via biomass productivity control. Algal Res. 17, 46–52. https://doi.org/10.1016/j.algal.2016.04.017

20. Wilkie, A.C., Riedesel, K.J., Owens, J.M., 2000. Stillage characterization and anaerobic treatment of ethanol stillage from conventional and cellulosic feedstocks. Biomass and Bioenergy 19, 63–102. https://doi.org/10.1016/S0961-9534(00)00017-9

Supplementary material

Influence of the diffuser type and liquid-to-biogas ratio on biogas upgrading performance in an outdoor pilot scale high rate algal pond

David Marín[1, 2, 3], Alessandro A. Carmona-Martínez[1, 2], Raquel Lebrero[1, 2], Raúl Muñoz[1, 2, *]

[1] Department of Chemical Engineering and Environmental Technology, School of Industrial Engineering, Valladolid University, Dr. Mergelina, s/n, 47011, Valladolid, Spain.

[2] Institute of Sustainable Processes, Dr. Mergelina, s/n, 47011, Valladolid, Spain.

[3] Universidad Pedagógica Nacional Francisco Morazán, Boulevard Centroamérica, Tegucigalpa, Honduras.

[*] Corresponding author: mutora@iq.uva.es

Table A1. Environmental parameters during each test.

	Metallic			Porous Stone			Ceramic Membrane 0.2 μm			Ceramic Membrane 0.4 μm		
Diffuser and L/G												
Parameter	0.5	1	2	0.5	1	2	0.5	1	2	0.5	1	2
Ambient Temperature (°C)	10.0	13.0	13.0	14.0	15.0	11.0	13.0	13.0	12.0	14.0	11.0	10.0
Photobioreactor Temperature (°C)	11.2	12.1	11.6	14.9	15.1	10.7	12.3	11.4	14.1	13.7	11.1	12.3
PAR ($\mu mol\ m^{-2}\ s^{-1}$)	69	54	58	84	88	126	73	67	27	65	396	83
DO ($mg\ O_2\ L^{-1}$)	3.1	4.2	3.9	6.4	6.8	6.8	7.3	6.4	3.7	6.6	7.2	4.9

Chapter 3

Seasonal variation of biogas upgrading coupled with digestate treatment in an outdoors pilot scale algal-bacterial photobioreactor

David Marín, Esther Posadas, Patricia Cano, Victor Pérez, Saúl Blanco, Raquel Lebrero, Raúl Muñoz.

Seasonal variation of biogas upgrading coupled with digestate treatment in an outdoors pilot scale algal-bacterial photobioreactor

David Marín[1, 3], Esther Posadas[1], Patricia Cano[1], Victor Pérez[1], Saúl Blanco[2], Raquel Lebrero[1], Raúl Muñoz[1,*]

[1] Department of Chemical Engineering and Environmental Technology, School of Industrial Engineering, Valladolid University, Dr. Mergelina, s/n, 47011, Valladolid, Spain.

[2] Department of Biodiversity and Environmental Management, University of León, 24071 León, Spain.

[3] Universidad Pedagógica Nacional Francisco Morazán, Boulevard Centroamérica, Tegucigalpa, Honduras.

[*] Corresponding author: mutora@iq.uva.es

Abstract

The yearly variations of the quality of the upgraded biogas and the efficiency of digestate treatment were evaluated in an outdoors pilot scale high rate algal pond (HRAP) interconnected to an external absorption column (AC) via a conical settler. CO_2 concentrations in the upgraded biogas ranged from 0.7% in August to 11.9% in December, while a complete H_2S removal was achieved regardless of the operational month. CH_4 concentrations ranged from 85.2% in December to 97.9% in June, with a limited O_2 and N_2 stripping in the upgraded biogas mediated by the low recycling liquid/biogas ratio in the AC. Biomass productivity ranged from 0.0 g m^{-2} d^{-1} in winter to 22.5 g m^{-2} d^{-1} in summer. Finally, microalgae diversity was severely reduced throughout the year likely due to the increasing salinity in the cultivation broth of the HRAP induced by process operation in the absence of effluent.

Keywords: Algal-bacterial photobioreactor; Biogas upgrading; Digestate treatment; Outdoors conditions; Yearly evaluation.

1. Introduction

Biogas from the anaerobic digestion (AD) of organic waste and wastewater constitutes a renewable energy vector able to reduce the consumption of fossil fuels. Biogas is typically composed of CH_4 (40-75%), CO_2 (15-60%) and minor components such as H_2S (0.005-2%), N_2 (0-2%), O_2 (0-1%), NH_3 (<1%), CO (<0.6%), siloxanes (0-0.2%) and halogenated hydrocarbons (VOC <0.6%) (Ryckebosch et al., 2011). The increasing relevance of biogas in the EU-28 energy sector has increased by a factor of 3 the number

of plants from 6227 in 2009 to 17662 by the end of 2016 (European Biogas Association, 2017). This green energy vector can be used to produce either electricity and heat in industry or domestic heat, as a feedstock in fuel cells or as substitute of natural gas (Andriani et al., 2014; Muñoz et al., 2015). In this regard, the upgrading of biogas prior injection into natural gas grids or use as a vehicle fuel is mandatory according to most international regulations, which require a biomethane composition of: $CH_4 \geq 95\%$, $CO_2 \leq 2\text{-}4\%$, $O_2 \leq 1\%$ and negligible amounts of H_2S (Muñoz et al., 2015). The removal of the major biogas contaminant, CO_2, decreases the transportation costs of biomethane and increases its specific calorific value, while the removal of H_2S effectively limits the corrosion in pipelines, engines and biogas storage structures (Posadas et al., 2015).

Multiple physical-chemical technologies are nowadays commercially available to remove CO_2 and H_2S from biogas. Pressure swing adsorption, membrane separation, cryogenic separation or chemical/water/organic scrubbing provide the required levels of CO_2 removal for biomethane injection. On the other hand, adsorption on activated carbon or metal ions, in-situ chemical precipitation, membrane separation and absorption in conventional gas-liquid contactors are typically applied to desulphurise biogas (Toledo-cervantes et al., 2017). Nevertheless, these commercial processes must be implemented sequentially to abate H_2S prior CO_2 separation, which increases both CAPEX and OPEX (Muñoz et al., 2015; Toledo Cervantes et al., 2017b). Likewise, several biological technologies are nowadays available to remove CO_2 and H_2S from biogas, although most of them have been only validated at pilot scale. Thus, chemoautotrophic biogas upgrading (using a power to gas strategy) can provide the required levels of CO_2 removal, while *in-situ* micro-aerobic AD or biofiltration are typically applied to remove H_2S from biogas (Farooq et al., 2018; Muñoz et al., 2015). Similarly to their physical-chemical counterparts, these biological processes can only support the individual removal of CO_2 or H_2S, which also entails the need for a two-stage upgrading (with the subsequent increase in investment and operational costs). In this context, algal-bacterial processes have recently emerged as a cost-effective and environmentally friendly alternative to conventional biogas upgrading techniques due to their ability to simultaneous remove CO_2 and H_2S in a single stage process (Bahr et al., 2014).

Biogas upgrading in algal-bacterial photobioreactors is based on the photosynthetic fixation of CO_2 by microalgae and the concomitant oxidation of H_2S to SO_4^{2-} by sulfur oxidizing bacteria mediated by the high dissolved oxygen (DO) concentrations present in the cultivation broth as a result of photosynthetic activity (Toledo-Cervantes et al., 2016). The environmental sustainability and cost-competitiveness of this technology can be improved via digestate supplementation as the nutrient source to support microbial growth (Toledo-Cervantes et al., 2016). In this regard, the optimization of photosynthetic biogas upgrading coupled to digestate treatment has been recently carried out indoors under artificial illumination in high rate algal ponds (HRAPs) interconnected to biogas absorption columns (AC). Bahr et al. (2014) were the first to evaluate the potential of microalgal-bacterial consortium for the simultaneous removal of H_2S and CO_2 from biogas. Meier et al. (2015) focused their work on the development of a process for photosynthetic biogas upgrading using *Nannochloropsis gaditana* as model microalgae in a batch test. Serejo et al. (2015) evaluated the influence of biogas flow rate and the liquid/biogas ratio in the composition of the upgraded biogas, while Posadas et al. (2016) optimized the biogas upgrading process in a HRAP using centrate with multiple nutrient composition. This process optimization provided promising results in terms of wastewater treatment (total nitrogen (TN)-removal efficiencies (REs) of 98.0 ± 1.0 % and P-PO_4^{-3}- REs of 100 ± 0.5 %) and biomethane quality (CH_4 concentration of 96.2 ± 0.7 %) (Toledo-Cervantes et al., 2017). Likewise, comparable results were achieved by Posadas et al. (2017) in a similar photobioreactor configuration operated outdoors during summer, when both solar irradiation, the number of sun hours and temperatures were furthermost favorable to algal-bacterial activity. Therefore, a systematic evaluation for the influence of a year-round variations of environmental conditions on biogas purification and nutrient recovery from digestate is needed to validate this technology under outdoor conditions.

This study investigated for the first time the simultaneous upgrading of biogas and treatment of digestate in an pilot HRAP interconnected to an external AC via a conical settler over one year of outdoors operation to determine the influence of environmental conditions on process performance. The process was operated using a novel strategy to decouple biomass productivity from the hydraulic retention time via control of the biomass wastage rate from the settler in order to maximize the recovery of carbon and

nutrients in the form of algal-bacterial biomass. Finally, the dynamics of microalgae population structure were also investigated.

2. Materials and methods

2.1 Biogas and digestate

The synthetic gas mixture used as a model biogas was composed of CO_2 (29.5%), H_2S (0.5%) and CH_4 (70%) (Abello Linde; Spain). The digestate here used was monthly obtained from the centrifuges dehydrating the anaerobically digested sludge of the wastewater treatment plant (WWTP) of Valladolid and stored at 4 ºC. Digestate composition was subjected to variations along the experimental period due to the seasonal operational variations of the WWTP: total organic carbon (TOC) concentrations of 16-523 mg L^{-1}, inorganic carbon (IC) concentrations of 450-600 mg L^{-1}, TN concentrations of 374-718 mg L^{-1}, P-PO_4^{3-} concentrations of 26-135 mg L^{-1} and SO_4^{2-} concentrations of 0-38 mg L^{-1}. IC concentration was increased to 1999±26 mg L^{-1} via addition of $NaHCO_3$ and Na_2CO_3 to maintain the high buffer capacity and pHs (≥9) required in the cultivation broth to support an effective biogas upgrading (Posadas et al., 2017).

2.2 Experimental set-up

The photobioreactor set-up was built outdoors at Valladolid University (41.39º N, 4.44º W) according to Posadas et al. (2017). The pilot experimental plant consisted of a 180 L HRAP with an illuminated area of 1.20 m^2 (width = 82 cm; length = 170 cm; depth = 15 cm) and two water channels divided by a central wall and baffles in each side of the curvature. The cultivation broth in the HRAP was continuously agitated by a 6-blade paddlewheel at an internal liquid velocity of ≈ 20 cm s^{-1}. The HRAP was interconnected to a separate 2.5 L bubble absorption column (internal diameter = 4.4 cm; height = 165 cm) provided with a metallic biogas diffuser of 2 μm pore size situated at the bottom of the column. The HRAP and the AC were interconnected via an external liquid recirculation of the supernatant of the algal-bacterial cultivation broth from an 8 L settler (Fig. 1; Table A.1).

2.3 Operational conditions and sampling procedures

Process operation was carried out from November the 1st 2016 to October the 30st 2017. The HRAP was inoculated at an initial concentration of 210 mg total suspended solids

(TSS) L^{-1} with a microalgal inoculum composed of (percentage expressed in number of cells) *Leptolyngbya lagerheimii (54%), Chlorella vulgaris (28%), Parachlorella kessleri (9%), Tetradesmus obliquus (5%) and Mychonastes homosphaera (2%)* from a previous culture grown in an indoor HRAP located at the Department of Chemical Engineering and Environmental Technology of Valladolid University (Spain). Five operational stages (namely I, II, III, IV and V) were defined as a function of the environmental conditions, which ultimately determined the biomass productivity set in our experimental system (Table 1). The HRAP was fed with digestate as a nutrient source at a flow rate of 3.5 L d^{-1}. The synthetic biogas was sparged into the AC under co-current flow operation at 74.9 L d^{-1} and a recycling liquid to biogas ratio (L/G) of 1.0 according to Posadas et al. (2017). Tap water was supplied in order to compensate water evaporation losses and allow process operation without effluent. Biomass harvesting was performed by daily removing the required settled biomass volume to maintain the target biomass productivity during each stage as a function of the environmental conditions (Table 1). The remaining biomass accumulated in the settler was continuously recirculated to the HRAP at a flow rate of 7.2 L d^{-1}.

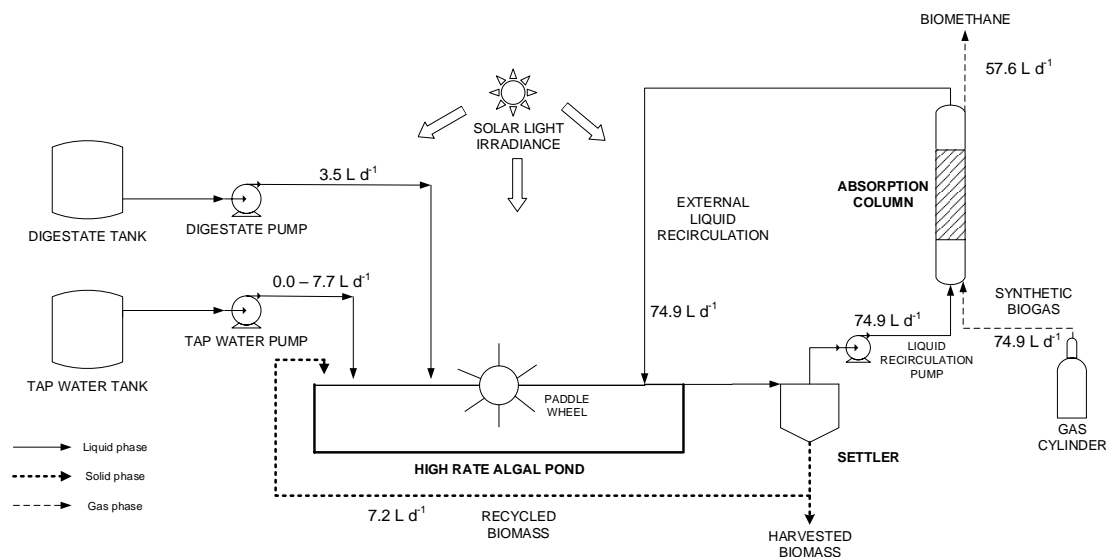**Figure 1.** Schematic diagram of the outdoors experimental set-up used for the continuous photosynthetic upgrading of biogas and treatment of digestate.

The photosynthetic active radiation (PAR), pH, temperature and DO concentration in the cultivation broth, the influent flow rate and the ambient temperature were daily monitored throughout the experimental period. Gas samples of 100 µL from the raw and upgraded

biogas were drawn twice a week to monitor the concentrations of CH_4, CO_2, H_2S, O_2 and N_2. The inlet and outlet biogas flow rates in the AC were also measured to accurately determine both CO_2 and H_2S removals. Liquid samples of 100 mL from the centrate and cultivation broth were drawn twice a week to monitor the pH, concentrations of dissolved TOC, IC, TN, $N-NH_4^+$, $N-NO_2^-$, $N-NO_3^-$, $P-PO_4^{3-}$ and SO_4^{2-} and the concentration of TSS. Process monitoring and biomass harvesting were always conducted at 9:00 a.m. along the entire experimental period. The algal-bacterial biomass harvested from the settler under steady state was washed three times with distilled water and dried for 24 hours at 105 ºC to determine its elemental composition (C, N, P and S) in order to carry out the elemental mass balances. The structure of the microalgae population in the HRAP was assessed at the end of each month from biomass samples preserved with lugol acid at 5% and formaldehyde at 10%, and stored at 4 ºC prior to analysis.

2.4 Analytical procedures

The concentrations of CH_4, CO_2, H_2S, O_2 and N_2 in biogas and biomethane were determined using a Varian CP-3800 GC-TCD (Palo Alto, USA) according to Posadas et al. (2015). Temperature and DO concentration were measured using an OXI 330i oximeter (WTW, Germany). PAR was measured with a LI-250A light meter (LI-COR Biosciences, Germany), while pH was determined with an Eutech Cyberscan pH 510 (Eutech instruments, The Netherlands). Dissolved TOC, IC and TN concentrations were analyzed using a Shimadzu TOC-VCSH analyzer (Japan) equipped with a TNM-1 chemiluminescence unit. $N-NO_3^-$, $N-NO_2^-$, $P-PO_4^{3-}$ and SO_4^{2-} concentrations were quantified by HPLC-IC according to Serejo et al. (2015), while $N-NH_4^+$ concentration was analyzed with an ammonium specific electrode Orion Dual Star (Thermo Scientific, The Netherlands). The determination of TSS concentration was performed according to Standard Methods (APHA, 2005). The determination of the algal-bacterial biomass C, N and S content was conducted in a LECO CHNS-932 analyzer, while P content was determined spectrophotometrically after acid digestion in a microwave based on the internal procedure of the Instrumental Techniques Laboratory of Valladolid University. The quantification, identification and biometry measurements of microalgae population structure were carried out by microscopic examination (OLYMPUS IX70, USA).

Table 1. Environmental and operational parameters during the five operational stages.

Parameter	Stage				
	I	**II**	**III**	**IV**	**V**
Date	01/11/16 - 28/02/17	01/03/17 - 31/05/17	01/06/17 - 31/07/17	01/08/17 - 30/09/17	01/10/17 - 31/10/17
Average Temperature (ºC)	9.1 ± 4.1	15.3 ± 7.3	24.4 ± 5.8	23.4 ± 3.8	18.4 ± 7.0
Maximum PAR (μmol m^{-2} s^{-1})	679 ± 420	1587 ± 150	1626 ± 60	1326 ± 71	820 ± 0
Average daylight hours (h)	10 ± 1	14 ± 1	15 ± 1	12 ± 1	10 ± 1
L/G ratio	1.0	1.0	1.0	1.0	1.0
Digestate flow rate (L d^{-1})	3.5	3.5	3.5	3.5	3.5
Synthetic biogas flow rate (L d^{-1})	74.9	74.9	74.9	74.9	74.9
Supplemented tap water (L d^{-1})	0.0 ± 0.0	3.9 ± 3.2	7.7 ± 2.0	5.9 ± 2.4	2.0 ± 1.8
Biomass productivity (g m^{-2} d^{-1})	0.0	7.5	15.0	22.5	15.0

3. Results and discussion

3.1 Environmental parameters

Large variations in the PAR, number of sun hours and ambient temperature were recorded along the year as a result of the inherent seasonal variability of the continental climate prevailing in Valladolid (Table 1). Thus, the average of the maximum PARs recorded in stage I, II, III, IV and V was 679 ± 420, 1587 ± 150, 1626 ± 60, 1326 ± 71 and 820 ± 0 µmol m^{-2} s^{-1}, respectively. The evolution of the number of sun hours was correlated with the variation of the PAR levels, with values ranging from 10 ± 1 h in stages I and V to 15 ± 1 h in stage III (Table 1). The average values of ambient temperature recorded in stage I, II, III, IV and V were 9.1 ± 4.1, 15.3 ± 7.3, 24.4 ± 5.8, 23.4 ± 3.8 and 18.4 ± 7.0 ºC, respectively (Table 1; Fig. A.1). Overall, environmental conditions governed process performance. For instance, the combination of low PAR, number of sun hours and ambient temperature during winter resulted in a negligible biomass productivity, while the high values of these parameters during spring and summer supported biomass productivities of 15-22.5 g m^{-2} d^{-1}. The latter biomass productivities were in accordance to those reported by Park et al. (2011) in conventional HRAPs.

The average evaporation rates ranged from -0.3 ± 1.8 L m^{-2} d^{-1} (December) to 0.9 ± 2.4 L m^{-2} d^{-1} (January) in stage I, and from 2.0 ± 1.1 L m^{-2} d^{-1} (March) to 6.2 ± 0.9 L m^{-2} d^{-1} (April) in stage II. Water losses remained constant at $\approx 6.7 \pm 4.9$ L m^{-2} d^{-1} in stage III and $\approx 5.9 \pm 3.4$ L m^{-2} d^{-1} during stage IV. Finally, the average evaporation rate in stage V accounted for 3.2 ± 2.1 L m^{-2} d^{-1} (Table 2; Fig. A.2). The negative values recorded in stage I were caused by the rain and agreed with those reported by Posadas et al. (2014), who recorded evaporation rates of up to -5 L m^{-2} d^{-1} during fish farm and domestic wastewater treatment in an outdoors 180 L HRAP located at Valladolid.

The seasonal variations of the environmental conditions and microbial activity directly impacted on the evolution of the DO concentration in the HRAP. In this context, the DO concentrations ranged from 6.0 ± 1.7 mg L^{-1} (November) to 10.9 ± 1.8 mg L^{-1} (January) in stage I, from 7.5 ± 2.1 mg L^{-1} (May) to 10.6 ± 2.9 mg L^{-1} (March) in stage II, from 6.8 ± 1.4 mg L^{-1} (June) to 7.9 ± 3.3 mg L^{-1} (July) in stage III; from 5.3 ± 2.0 mg L^{-1} (August) to 6.4 ± 1.6 mg L^{-1} (September) in stage IV and averaged 6.0 ± 1.6 mg L^{-1} in stage V (Table 2; Fig. A.4). The high DO concentrations observed in stage I in absence of biomass

productivity were caused by the increased aqueous solubility of oxygen at low temperatures. From stage II onwards, the decreased oxygen solubility at high temperatures and the higher endogenous oxygen consumption at the higher biomass concentrations prevailing in the HRAP were counterbalanced by a superior photosynthetic activity, which resulted in DO concentrations ranging from ≈5 to 10 mg L^{-1} at the monitoring time (Table 2).

Finally, the pH remained fairly constant throughout the year regardless of the operational stage as a result of the high buffer capacity of the cultivation broth (Table 2; Fig. A.5.). Thus, the pHs of the cultivation broth ranged from 9.2 ± 0.2 (February) to 9.4 ± 0.2 (November) during stage I, and from 9.3 ± 0.2 (May) to 9.6 ± 0.3 (April) in stage II. The pH in stage III and V remained constant at ≈9.4 ± 0.1 and 9.6 ± 0.1, respectively, and varied from 9.6 ± 0.1 (August) to 9.8 ± 0.1 (September) in stage IV. The slight increase in the pH of the cultivation broth during stages IV and V was due to both an enhanced photosynthetic activity and the higher IC concentrations in the HRAP caused by the high evaporation rates, which increased from 1714±103 mg L^{-1} in stage I to 4421±91 mg L^{-1} in stage V. This high operational pHs supported an effective microbial activity as described in sections 3.2 and 3.3 (Posadas et al., 2017).

Table 2. Environmental parameters in the cultivation broth of the HRAP during the five operational stages.

Stage	Month	Average Temperature (ºC)	Average pH	Average DO (mg L^{-1})	Average Evaporation Rate (L m^{-2} d^{-1})	Dissolved CO$_2$ (mg L^{-1})
I	November 2016	6.2 ± 3.0	9.4 ± 0.2	6.0 ± 1.7	-0.3 ± 3.4	1.55
	December 2016	3.8 ± 2.4	9.3 ± 0.1	8.8 ± 1.7	-0.3 ± 1.8	1.79
	January 2017	2.3 ± 3.1	9.4 ± 0.1	10.9 ± 1.8	0.9 ± 2.4	1.95
	February 2017	4.8 ± 2.1	9.2 ± 0.2	9.9 ± 0.6	0.4 ± 2.2	2.66
II	March 2017	6.0 ± 2.6	9.4 ± 0.2	10.6 ± 2.9	2.0 ± 1.1	1.34
	April 2017	8.8 ± 3.3	9.6 ± 0.3	7.7 ± 1.4	6.2 ± 0.9	0.57
	May 2017	12.9 ± 3.4	9.3 ± 0.2	7.5 ± 2.1	3.6 ± 5.2	1.25
III	June 2017	17.8 ± 4.0	9.5 ± 0.2	6.8 ± 1.4	6.8 ± 2.2	0.73
	July 2017	17.9 ± 3.1	9.4 ± 0.1	7.9 ± 3.3	6.6 ± 7.9	1.03
IV	August 2017	16.2 ± 2.4	9.6 ± 0.1	5.3 ± 2.0	6.2 ± 4.7	0.60
	September 2017	13.7 ± 2.8	9.8 ± 0.1	6.4 ± 1.6	5.7 ± 0.8	0.31
V	October 2017	11.0 ± 2.8	9.6 ± 0.1	6.0 ± 1.6	3.2 ± 2.1	0.96

3.2 Biogas upgrading

The biomethane produced in this innovative algal-bacterial photobioreactor exhibited a rather constant composition along the year, despite the high variations recorded during stage I (Fig. 2). In this context, the CO_2 concentration in stage I ranged from 2.6% (January) to 11.9% (December), with removal efficiencies (REs) ranging from 63.6% (December) to 85.9% (February). During stage II, CO_2 concentration varied from 0.8% (May) to 7.1% (March), with REs increasing from 85.5% (March) to 95.4% (May), while CO_2 concentrations remained at 0.9%-1.9% in stage III with constants REs of ≈96.0%. Similarly, CO_2 concentrations in stage IV ranged from 0.7% (August) to 1.8% (September), with REs of ≈ 96.0%. Finally, the CO_2 REs of 95.6% recorded in stage V supported CO_2 concentrations ranging from 1.1% to 2.1% (Fig. 2a). The high CO_2 REs here achieved were promoted by the previous optimization of the L/G ratio by Posadas et al. (2017), and the high pH and alkalinity on the cultivation broth during stages II-V (Lebrero et al., 2016; Posadas et al., 2015; Toledo-Cervantes et al., 2016). Therefore, the influence of the seasonal variations of environmental conditions on CO_2 RE was low. These results were in accordance to Posadas et al. (2017), who reported CO_2 concentrations in the upgraded biomethane ranging from 1.8% to 3.7% in a similar outdoors photobioreactor configuration during summer. The CO_2 concentrations here obtained fulfilled during most of the year the upcoming European regulation for biomethane, which will require concentrations ≤2.5-4% prior injection into natural gas grids (Muñoz et al., 2015).

H_2S was completely removed in the absorption column regardless of the operational stage and environmental conditions. This higher elimination compared to the removal of CO_2 was attributed to the higher H_2S aqueous solubility (Henry´s law constant = C_L/C_G ranging from $H_{H2S}≈5.16$ at -6.0 ℃ to $H_{H2S}≈2.30$ at 28.0 ℃ versus $H_{CO2}≈1.90$ at -6.0 ℃ to $H_{CO2}≈0.78$ at 28.0 ℃) (Sander, 2015). The high pHs of the recirculating cultivation broth also favored the H_2S REs observed (Serejo et al., 2015). These values were in accordance to Toledo-Cervantes et al. (2016), who reported a complete removal of H_2S during the optimization of photosynthetic biogas upgrading under laboratory conditions in a similar experimental set-up. These results confirmed the technical viability of photosynthetic upgrading, which yields H_2S levels ≤ 5 mg m^{-3} as per requested by

European regulations for the injection of biomethane into natural gas networks (Muñoz et al., 2015).

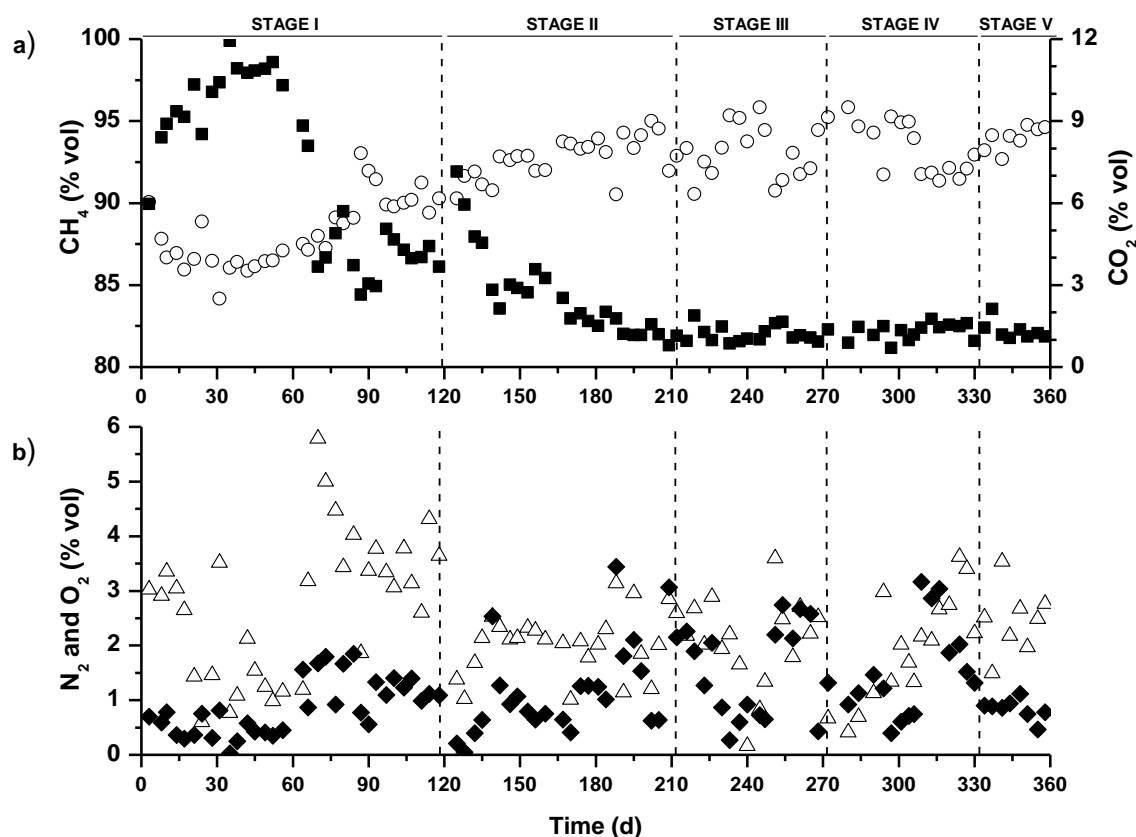**Figure 2.** Time course of the concentration of (a) CH_4 (○) and CO_2 (■), and (b) N_2 (△) and O_2 (◆) in the upgraded biogas

The N_2 and O_2 concentrations in the upgraded biogas did not show a seasonal correlation with the environmental parameters (Fig. 2b). The concentrations of N_2 and O_2 during stage I ranged from 0.6% (November) and 0.0% (December) to 5.8% and 1.8% (January), respectively. During stage II, N_2 and O_2 concentrations varied from 1.0% (April) and 0.1% (March) to 3.1% and 3.4% (May), respectively. On the other hand, these concentrations ranged from 0.2% and 0.3% (June) to 3.6% and 2.7% (July), respectively, in stage III. During stage IV, N_2 and O_2 concentrations fluctuated from 0.4% (August) to 3.6% and 3.2% (September), respectively. Finally, N_2 and O_2 concentrations during stage V ranged from 1.5% and 0.5% to 3.5% and 1.1%, respectively (Fig. 2b). The preliminary optimization of the L/G ratio conducted by Posadas et al. (2017) resulted into the low desorptions of N_2 and O_2 observed in this study. The highest N_2 concentration in stage I was correlated to the lowest ambient temperature, which increased N_2 solubility in the

cultivation broth and its further desorption. The O_2 concentrations here recorded were in accordance to Serejo et al. (2015), who reported values ranging from 0% to 4% in a similar experimental set-up under indoor conditions at an L/G ratio of 0.5. The O_2 concentration in the upgraded biogas did not comply during most of the study with international regulations ($\leq$1%), which requires further optimization.

CH_4 concentration in the upgraded biogas exhibited large variations during stage I compared to the values recorded in the further stages. Hence, the concentrations of CH_4 ranged from 85.2% (December) to 94.7% (January) in stage I, from 91.3% (March) to 97.7% (April) in stage II, from 92.6% (July) to 97.9% (June) in stage III, from 92.9% (September) to 97.8% (August) in stage IV and from 94.4% to 96.2% in stage V (Fig. 2a). The higher CH_4 concentrations obtained in the biomethane from stage II onwards were mediated by the higher CO_2 REs and the lower N_2 and O_2 desorptions above described. These concentrations were in accordance to Posadas et al. (2017) and Toledo-Cervantes et al. (2017), who reported CH_4 concentrations of 92.0% and 96.2%, respectively, in the upgraded biogas in a similar experimental set-up. Overall, the CH_4 concentration in the biomethane generated in this study complied during most of the year with most international regulations, which require concentrations $\geq$95% prior injection into natural gas grids (Muñoz et al., 2015).

Finally, an analysis of variance (ANOVA) was carried out to elucidate how changes in environmental parameters throughout the year influence the quality of the upgraded biogas (Table A.2). Since the F values for CH_4 and CO_2 (35.2 and 87.2, respectively) were greater than the F critical value of 1.9, it can be concluded that the stated hypothesis was correct and therefore the quality of the upgraded biogas throughout the year varied significantly with the environmental parameters.

3.3 Digestate treatment

IC concentration in the cultivation broth of the HRAP gradually increased from 1663 mg L^{-1} to 2238 mg L^{-1} during stages I and II (Fig. 3a). A rapid and steady increase in the IC concentration was then observed from the beginning of stage III until the end of the operation. Indeed, IC increased up to 2779 mg L^{-1} during stage III and up to 4138 mg L^{-1} during stage V, likely due to the operation of the process without effluent (Fig. 3a).

TOC concentrations in the cultivation broth of the HRAP and in the digestate fluctuated throughout the year, with concentrations ranging from 32 ± 10 mg L^{-1} to 288 ± 60 mg L^{-1}. The higher TOC concentrations in the cultivation broth of the HRAP compared to the digestate were mediated by the low biodegradability of digestate and the operation of the process without effluent (the latter concentrating all components of the cultivation broth) (Fig A.6). The share of C recovered in the harvested biomass in stage I was negligible due to the absence of algal biomass production, which entailed a C removal driven by CO_2 stripping. In stage II, the fraction of C recovered in the harvested biomass accounted for $47 \pm 2\%$, while in stage III this recovery increased to $94 \pm 0\%$. During stages IV and V, the share of C recovered as biomass amounted to $100 \pm 0\%$ and $99 \pm 2\%$, respectively (Table A.3). The increase in biomass productivities throughout the experimental period prevented carbon removal by stripping and increased the sustainability of the process based on the enhanced microbial fixation of the CO_2 from biogas. In this context, despite CO_2 removal from biogas was significant during the winter period, this carbon was not fixed in the form of microalgae biomass but desorb to the open atmosphere.

TN concentration in the cultivation of the HRAP remained relatively constant during stages I-III, with values ranging from 336 mg L^{-1} to 415 mg L^{-1}. Nevertheless, an increase in the TN concentration up to 652 mg L^{-1} was observed during stage IV and V (Fig. 3b). There was a progressive decrease in $N-NO_3^-$ concentration in the cultivation broth of the HRAP from 298 mg L^{-1} to 32 mg L^{-1} by the end of the study. On the contrary, $N-NO_2^-$ concentration increased from 24 mg L^{-1} to 228 mg L^{-1} by the end of stage V (Fig. 3c). These results revealed a partial $N-NH_4^+$ oxidation to nitrite despite the occurrence of high DO and IC concentrations and moderate temperatures, which suggested that the increasing salinity of the cultivation broth might exert a detrimental effect on the activity of NO_2^- oxidizers (Metcalf and Eddy, 2003). The mechanisms underlying $N-NO_3^-$ fate should be further investigated since no microbial uptake was likely to occur based on the negligible biomass productivities recorded in stage I and denitrification was inhibited by the high DO concentrations prevailing during this period in the HRAP (Alcántara et al., 2015; Norvill et al., 2017). $N-NH_4^+$ concentrations fluctuated from 6.8 mg L^{-1} to 110.5 mg L^{-1} during stage I, and remained at negligible values from stage II onwards (Fig. 3c). The N mass balance conducted in this study showed N recoveries in the harvested biomass in stage I, II, III, IV and V of 0%, $58 \pm 7\%$, $97 \pm 7\%$, $99 \pm 1\%$ and $69 \pm 3\%$,

respectively (Table A.3). These recoveries were higher than those reported by Posadas et al. (2015) and Toledo-Cervantes et al. (2017) ($19 \pm 13\%$ and $36 \pm 18\%$, respectively) in a similar indoors experimental set-up during the simultaneous treatment of biogas and centrate. In this context, the moderate-high biomass productivities set in the HRAP from stage II onwards prevented $N\text{-}NH_4^+$ stripping and increased N recovery in the form of biomass.

Despite the high variations in the concentration of $P\text{-}PO_4^{3-}$ in the digestate (from 25.3 mg L^{-1} to 134.9 mg L^{-1}), $P\text{-}PO_4^{3-}$ concentrations in the cultivation broth of the HRAP remained fairly constant along the five operational stages (average value of 14.5 ± 6.4 mg L^{-1}) (Fig A.7). P recoveries in the harvested biomass of 0%, $23 \pm 1\%$, $83 \pm 16\%$, $99 \pm 1\%$ and $100 \pm 0\%$, were achieved in stages I, II, III, IV and V, respectively (Table A.3). The high $P\text{-}PO_4^{3-}$ REs along with the poor P recoveries recorded during stages I, II and III suggested that pH-mediated P precipitation played a key role during process operation at low biomass productivities (Table A.3) (Cai et al., 2013). Indeed, most of the $P\text{-}PO_4^{3-}$ supplied to the HRAP was recovered in the harvested biomass when biomass productivity was increased to 15-22.5 g m^{-2} d^{-1}.
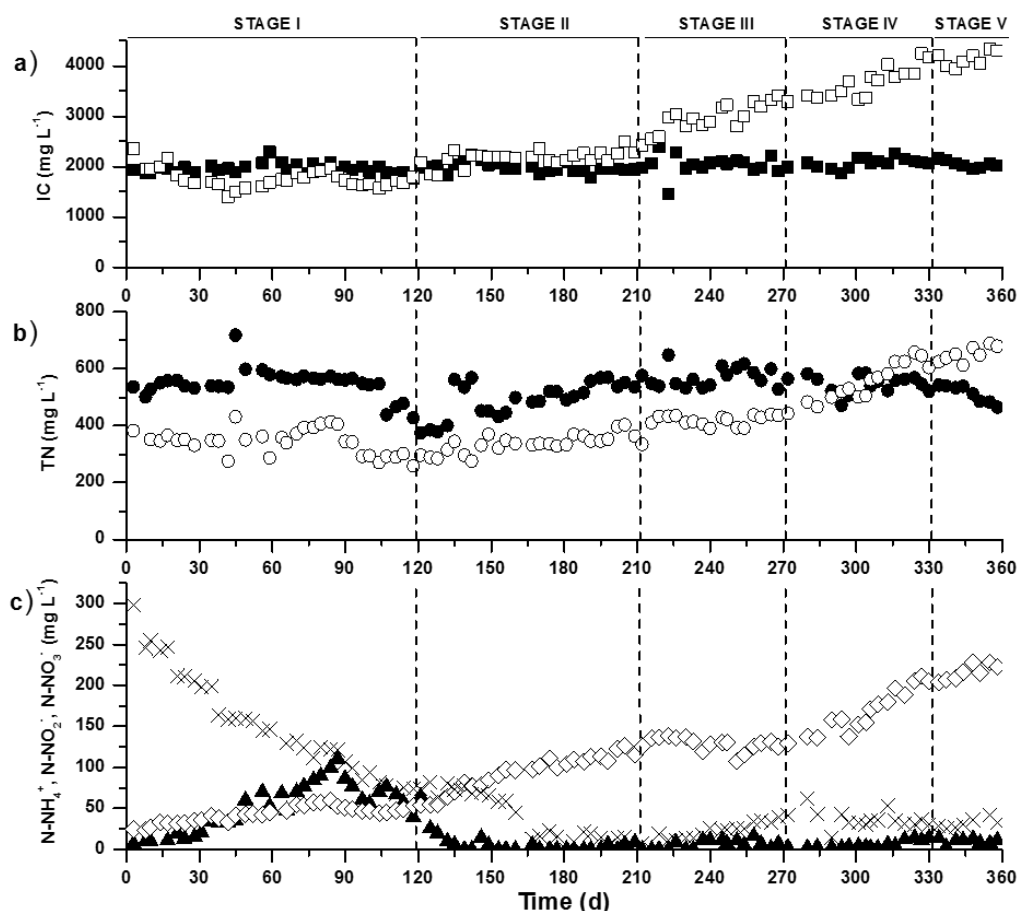
Figure 3. Time course of the concentration of (a) inorganic carbon in the digestate (■) and in the HRAP (□), (b) total nitrogen in the digestate (●) and in the HRAP (○), and (c) N-NH$_4^+$ (▲), N-NO$_2^-$ (◊) and N-NO$_3^-$ (×) in the HRAP.

Finally, an increase in SO$_4^{2-}$ concentration in the cultivation broth from 460 ± 20 mg L^{-1} (November 2016) to 1350 ± 80 mg L^{-1} (October 2017) was recorded. This SO$_4^{2-}$ built-up was caused by the aerobic oxidation of H$_2$S and process operation without effluent (Fig. A.8). The share of S recovered as biomass in stage I was negligible due to the absence of algal biomass production. However, the S assimilated by the algal-bacterial biomass increased up to $58 \pm 30\%$, $38 \pm 3\%$, $58 \pm 8\%$ and $91 \pm 13\%$ in stages II, III, IV and V, respectively, which confirmed the effectiveness of algal-bacterial symbiosis to recover nutrients from digestates (Table A.3).

3.4 Concentration and composition of the algal-bacterial biomass

The average TSS concentration in the cultivation broth of the HRAP decreased from 314 mg L^{-1} (November) to 55 mg L^{-1} (February) during stage I. Then, this concentration increased up to average values of 581 mg L^{-1} by the end of stage II, and fluctuated from

519 mg L^{-1} (June) to 571 mg L^{-1} (July). The average TSS concentrations ranged from 514 mg L^{-1} (September) to 625 mg L^{-1} (August) in stage IV, and decreased to 424 mg L^{-1} in stage V (Fig. 4). These concentrations were mainly determined by the prevailing environmental conditions and the biomass productivity imposed, which also influenced microalgae diversity (Fig. A.8).
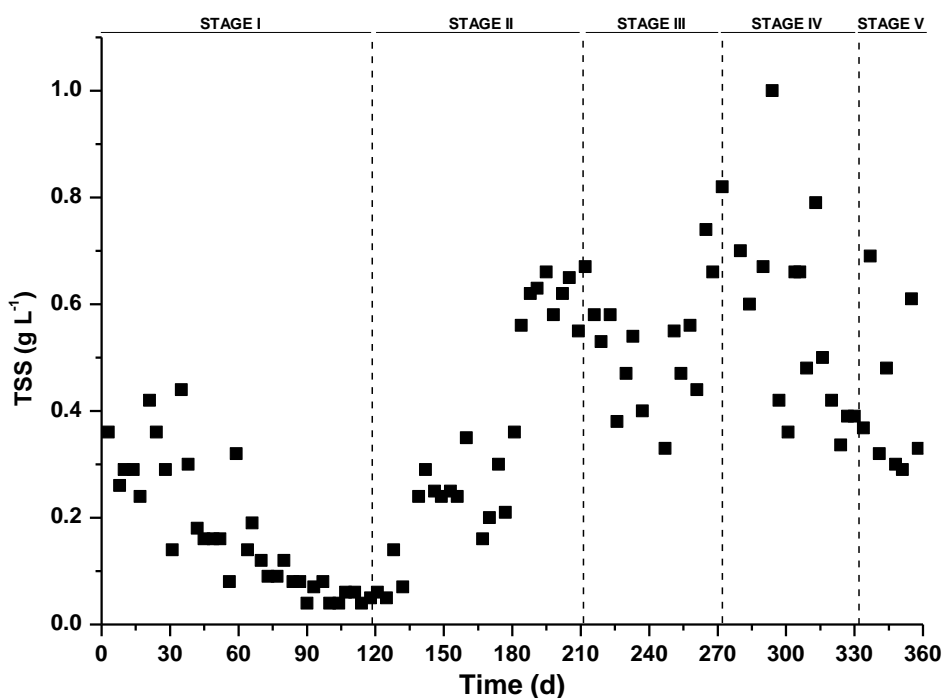

Figure 4. Time course of the concentration of total suspended solids in the HRAP.

Average C, N, P and S contents of 43.1 ± 1.9%, 8.0 ± 0.5%, 0.9 ± 0.1% and 0.5 ± 0.1%, respectively, were recorded in the harvested biomass regardless of the season (Table A.3). This elemental composition remained within the typical range of values reported in previous works. Bi and He (2013) reported C, N and S contents of 58.0%, 6.8% and 0.5%, respectively; Toledo-Cervantes et al. (2016) recorded values of C, P and N of 46.5%, 0.8% and 7.2%, respectively, while Posadas et al. (2017) found contents of C, N, P and S of 41.1%, 6.7%, 1.1% and 0.4%, respectively, in a biogas upgrading process in an outdoors pilot scale HRAP.

3.5 Microalgae population

Leptolyngbya lagerheimii was the dominant species in the HRAP during stage I (Fig. 5). Nevertheless, this species was gradually replaced by *Chlorella vulgaris*, which was the dominant microalga from stages II to IV. During stage V, a microalgae assemblage

composed of *Chlorella vulgaris (59%), Pseudanabaena sp. (15%), Chlorella kessieri (14%) and Leptolyngbya lagerheimii (11%)* was identified (Fig. 5; Fig. A.9). The gradual decrease in the number of microalgae species during stage I was likely mediated by the unfavorable environmental conditions during winter, while the dominance of a monoalgal culture in the HRAP during spring and summer could be attributed to the harsh environment induced by salinity built-up (Fig. 5; Fig. A.9) (Park et al., 2011; Posadas et al., 2015; Serejo et al., 2015; Toledo-Cervantes et al., 2016). In this context, microalgae from the genus *Chlorella* are highly resistant to high salinity and moderately polluted environments such as that prevailing in the HRAP as a result of process operation without effluent. Finally, it should be stressed that the gradual decrease in the total number of microalgae cells during stage I and the sudden increase at the beginning of stage II were correlated with the TSS concentrations recorded in the cultivation broth of the HRAP (Fig. 4; Fig. 5; Fig. A.9).
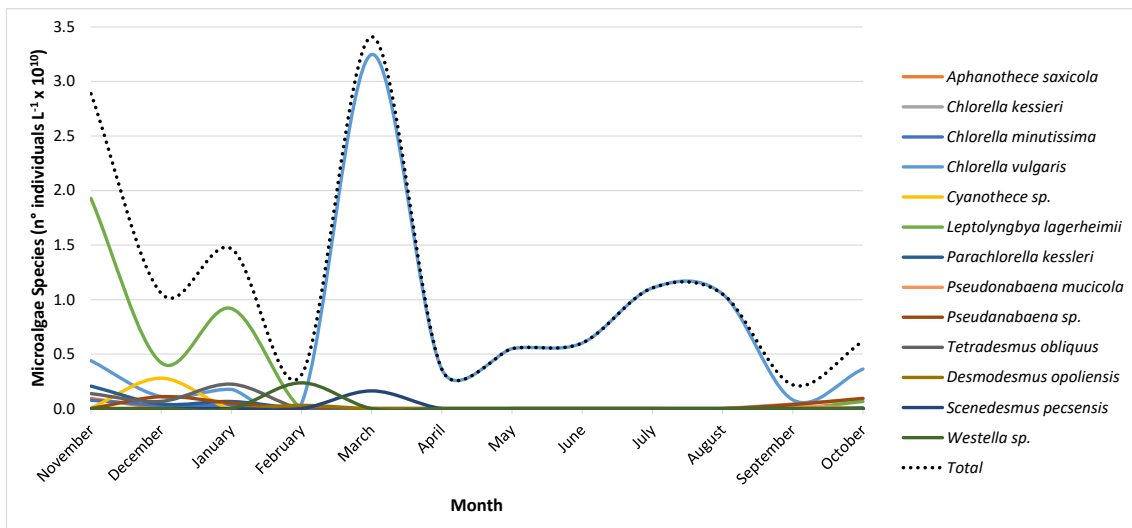
Figure 5. Time course of the structure of microalgae population in the HRAP.

3.6 Energy study

The power consumption E (kW-h) in the experimental set-up was calculated according to Toledo-cervantes et al. (2017) and Mendoza et al (2013) . Power consumption for biogas sparging in the AC was calculated according to Eq. (1), the power required for the liquid recirculation between the settler and the AC was calculated according to Eq. (2), the power requirements for pumping centrate to the HRAP and part of the settled biomass from the settler to the HRAP were both calculated according to Eq. (3) and the power requirement to circulate liquid in the HRAP was calculated according to Eq. (4).

$$E_{gas} = \frac{Q_{gas} \times \Delta P}{0.7} \tag{1}$$

$$E_{liq} = \frac{Q_{liq} \times \rho \times g \times H}{0.7} \tag{2}$$

$$E_{dig} = Q_{dig} \times \rho \times g \times H_f \tag{3}$$

$$E_{HRAP} = \frac{Q \times \rho \times g \times n^2 \times v^2 \times L}{R^{4/3}} \tag{4}$$

where Q_{gas} is the flowrate of biogas, ΔP is the pressure drop, Q_{liq} is the flowrate of liquid from settler to AC, H is water column height, Q_{dig} is the flowrate of centrate, Q is the volumetric flow rate of the HRAP, ρ is the water density, g is the Earth gravity constant, n in the Manning friction factor, v is internal liquid velocity in HRAP, L is the total length of the HRAP, R is the hydraulic radius and H_f is the pressure drop that is calculated according to the Darcy-Weisbach equation.

The energy demand in the system represented 0.14 kW-h m^{-3} of biogas treated. This lower value constitutes one of the key advantages of the biogas upgrading process in an outdoors photobioreactor.

4. Conclusions

This work constitutes, to the best of our knowledge, the first year round evaluation of biogas upgrading coupled with digestate treatment in an outdoors pilot scale HRAP integrated with an AC. The CO_2, H_2S and CH_4 concentrations in the biomethane complied with most international regulations for biogas injection into natural gas grids during most of the year. An effective carbon and nutrient recovery from biogas and digestate in the form of algal-bacterial biomass was achieved at the highest biomass productivity. Finally, the high alkalinity in the cultivation broth resulted in the dominance of a monoalgal *Chlorella* culture from February onwards.

References

1. Alcántara, C., García-encina, P.A., Muñoz, R., 2015. Evaluation of the simultaneous biogas upgrading and treatment of centrates in a high-rate algal pond through C , N and P mass balances 150–157. https://doi.org/10.2166/wst.2015.198

2. Andriani, D., Wresta, A., Atmaja, T.D., Saepudin, A., 2014. A Review on Optimization Production and Upgrading Biogas Through CO2 Removal Using Various Techniques. Appl. Biochem. Biotechnol. 172, 1909–1928. https://doi.org/10.1007/s12010-013-0652-x

3. Bahr, M., Díaz, I., Dominguez, A., González Sánchez, A., Muñoz, R., 2014. Microalgal-biotechnology as a platform for an integral biogas upgrading and nutrient removal from anaerobic effluents. Environ. Sci. Technol. 48, 573–581. https://doi.org/10.1021/es403596m

4. Bi, Z., He, B.B., 2013. Characterization of microalgae for the purpose of biofuel production. Trans. ASABE 56, 1529–1539.

5. Cai, T., Park, S.Y., Li, Y., 2013. Nutrient recovery from wastewater streams by microalgae : Status and prospects. Renew. Sustain. Energy Rev. 19, 360–369. https://doi.org/10.1016/j.rser.2012.11.030

6. European Biogas Association, 2016. 6th edition of the Statistical Report [WWW Document]. URL http://european-biogas.eu/2016/12/21/eba-launches-6th-edition-of-the-statistical-report-of-the-european-biogas-association/ (accessed 7.18.17).

7. Farooq, M., Almustapha, M.N., Imran, M., Saeed, M.A., Andresen, J.M., 2018. In-situ regeneration of activated carbon with electric potential swing desorption (EPSD) for the H2S removal from biogas. Bioresour. Technol. 249, 125–131. https://doi.org/10.1016/j.biortech.2017.09.198

8. Lebrero, R., Toledo-Cervantes, A., Muñoz, R., del Nery, V., Foresti, E., 2016. Biogas upgrading from vinasse digesters: a comparison between an anoxic biotrickling filter and an algal-bacterial photobioreactor. J. Chem. Technol. Biotechnol. 91, 2488–2495. https://doi.org/10.1002/jctb.4843

9. Meier, L., Pérez, R., Azócar, L., Rivas, M., Jeison, D., 2015. Photosynthetic CO2 uptake by microalgae: An attractive tool for biogas upgrading. Biomass and Bioenergy 73, 102–109. https://doi.org/10.1016/j.biombioe.2014.10.032

10. Mendoza, J. L., Granados, M. R., De Godos, I., Acién, F.G., Molina, E., Banks, C., Heaven, S., 2013. Fluid-dynamic characterization of real-scale raceway reactors for microalgae production. Biomass and Bioenergy 54, 267-275. http://dx.doi.org/10.1016/j.biombioe.2013.03.017

11. Metcalf, Eddy, 2003. Wastewater Engineeering and Reuse. Mc GrawHill.

12. Muñoz, R., Meier, L., Diaz, I., Jeison, D., 2015. A review on the state-of-the-art of physical/chemical and biological technologies for biogas upgrading. Rev. Environ. Sci. Biotechnol. 14, 727–759. https://doi.org/10.1007/s11157-015-9379-1

13. Norvill, Z.N., Toledo-Cervantes, A., Blanco, S., Shilton, A., Guieysse, B., Muñoz, R., 2017. Photodegradation and sorption govern tetracycline removal during wastewater treatment in algal ponds. Bioresour. Technol. 232, 35–43. https://doi.org/10.1016/j.biortech.2017.02.011

14. Park, J.B.K., Craggs, R.J., Shilton, A.N., 2011. Bioresource Technology Wastewater treatment high rate algal ponds for biofuel production. Bioresour. Technol. 102, 35–42. https://doi.org/10.1016/j.biortech.2010.06.158

15. Posadas, E., Alcántara, C., García-Encina, P.A., Gouveia, L., Guieysse, B., Norvill, Z., Acién, F.., Markou, G., Congestri, R., Koreiviene, J., Muñoz, R., 2017. Microalgae cultivation in wastewater, in: Microalgae-Bases Biofuels and Bioproducts. pp. 67–91. https://doi.org/10.1016/B978-0-08-101023-5.00003-0

16. Posadas, E., Marín, D., Blanco, S., Lebrero, R., Muñoz, R., 2017. Simultaneous biogas upgrading and centrate treatment in an outdoors pilot scale high rate algal pond. Bioresour. Technol. 232, 133–141. https://doi.org/10.1016/j.biortech.2017.01.071

17. Posadas, E., Muñoz, A., García-gonzález, M., García-encina, P.A., 2014. A case study of a pilot high rate algal pond for the treatment of fish farm and domestic wastewaters 1094–1101. https://doi.org/10.1002/jctb.4417

18. Posadas, E., Serejo, M.L., Blanco, S., Pérez, R., García-Encina, P.A., Muñoz, R., 2015. Minimization of biomethane oxygen concentration during biogas upgrading in algal-bacterial photobioreactors. Algal Res. 12, 221–229. https://doi.org/10.1016/j.algal.2015.09.002

19. Posadas, E., Szpak, D., Lombó, F., Domínguez, A., Díaz, I., Blanco, S., García-Encina, P.A., Muñoz, R., 2016. Feasibility study of biogas upgrading coupled with nutrient removal from anaerobic effluents using microalgae-based processes. J. Appl. Phycol. 28, 2147–2157. https://doi.org/10.1007/s10811-015-0758-3

20. Ryckebosch, E., Drouillon, M., Vervaeren, H., 2011. Techniques for transformation of biogas to biomethane. Biomass and Bioenergy 35, 1633–1645. https://doi.org/10.1016/j.biombioe.2011.02.033

21. Sander, R., 2015. Compilation of Henry 's law constants (version 4.0) for water as solvent 4399–4981. https://doi.org/10.5194/acp-15-4399-2015

22. Serejo, M.L., Posadas, E., Boncz, M.A., Blanco, S., García-Encina, P., Muñoz, R., 2015. Influence of biogas flow rate on biomass composition during the optimization of biogas upgrading in microalgal-bacterial processes. Environ. Sci. Technol. 49, 3228–3236. https://doi.org/10.1021/es5056116

23. Toledo-cervantes, A., Estrada, J.M., Lebrero, R., Muñoz, R., 2017. A comparative analysis of biogas upgrading technologies : Photosynthetic vs physical / chemical processes. Algal Res. 25, 237–243. https://doi.org/10.1016/j.algal.2017.05.006

24. Toledo-Cervantes, A., Madrid-Chirinos, C., Cantera, S., Lebrero, R., Muñoz, R., 2017. Influence of the gas-liquid flow configuration in the absorption column on photosynthetic biogas upgrading in algal-bacterial photobioreactors. Bioresour. Technol. 225, 336–342. https://doi.org/10.1016/j.biortech.2016.11.087

25. Toledo-Cervantes, A., Serejo, M.L., Blanco, S., Pérez, R., Lebrero, R., Muñoz, R., 2016. Photosynthetic biogas upgrading to bio-methane: Boosting nutrient recovery via biomass productivity control. Algal Res. 17, 46–52. https://doi.org/10.1016/j.algal.2016.04.017

26. Torzillo, G., Pushparahj, B., Masojidek, J., Vonshak, A., 2003. Biological constraints in algal Biotechnology. Biotechnol. Bioprocess Eng. 8, 338–348.

Supplementary material

Seasonal variation of biogas upgrading coupled with digestate treatment in an outdoors pilot scale algal-bacterial photobioreactor

David Marín[1, 3], Esther Posadas[1], Patricia Cano[1], Victor Pérez[1], Saúl Blanco[2], Raquel Lebrero[1], Raúl Muñoz[1,*]

[1] Department of Chemical Engineering and Environmental Technology, School of Industrial Engineering, Valladolid University, Dr. Mergelina, s/n, 47011, Valladolid, Spain.

[2] Department of Biodiversity and Environmental Management, University of León, 24071 León, Spain.

[3] Universidad Pedagógica Nacional Francisco Morazán, Boulevard Centroamérica, Tegucigalpa, Honduras.

* Corresponding author: mutora@iq.uva.es

Figure A.1. Time course of the ambient temperature throughout the 1-year monitoring period.
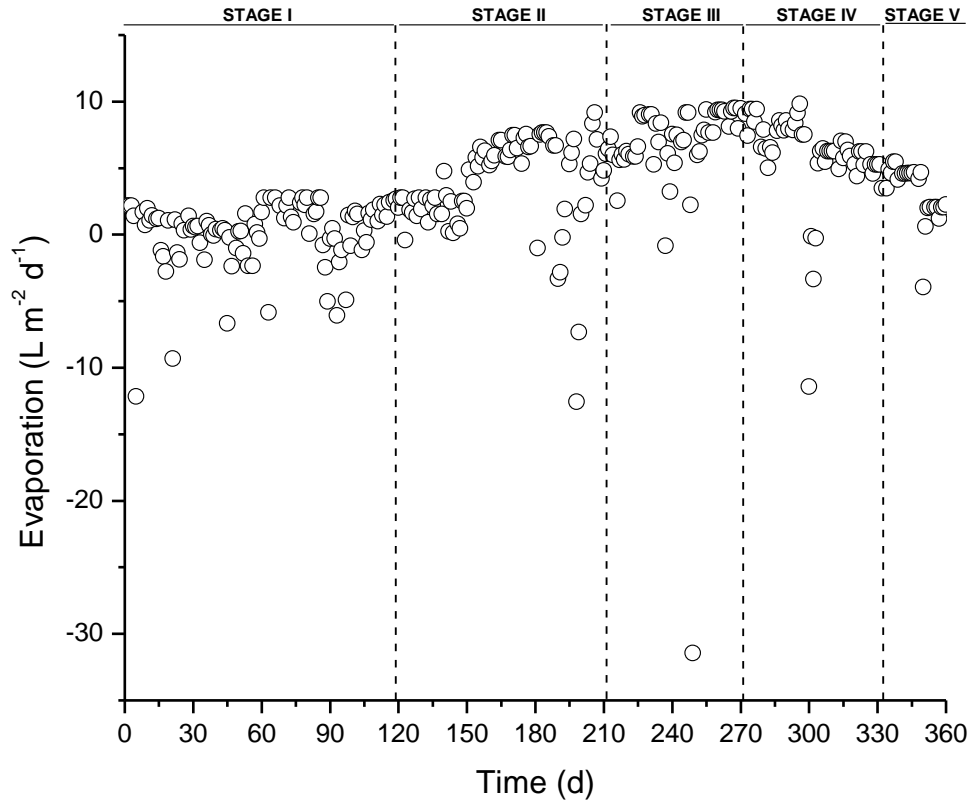
Figure A.2. Time course of the evaporation rate in the HRAP throughout the 1-year monitoring period.
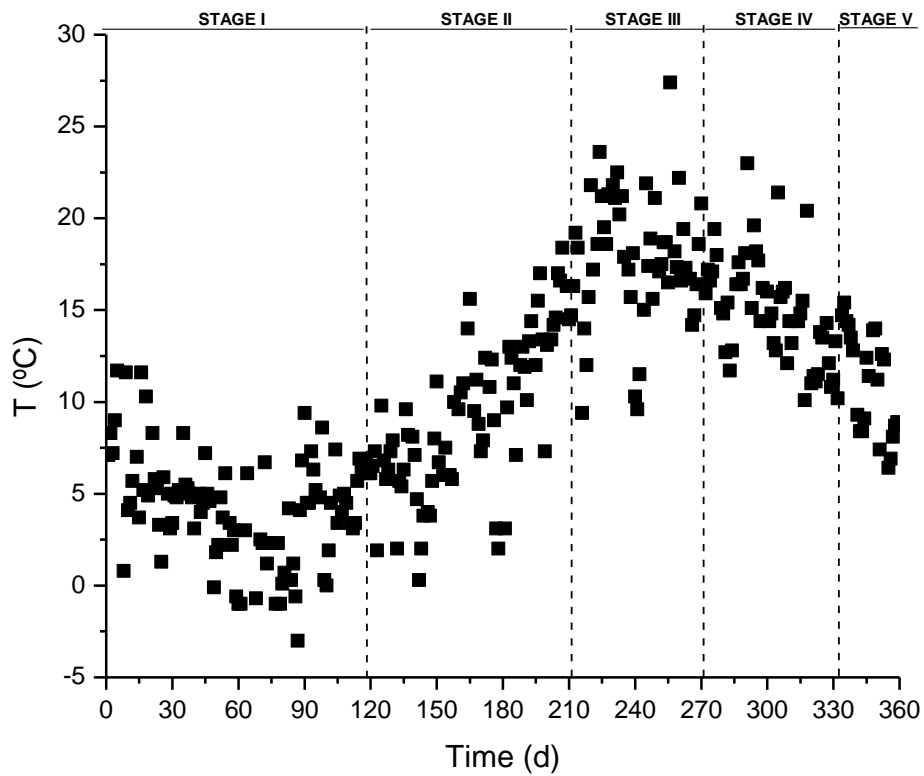
Figure A.3. Time course of the temperature (■) in the cultivation broth of the HRAP throughout the 1-year monitoring period
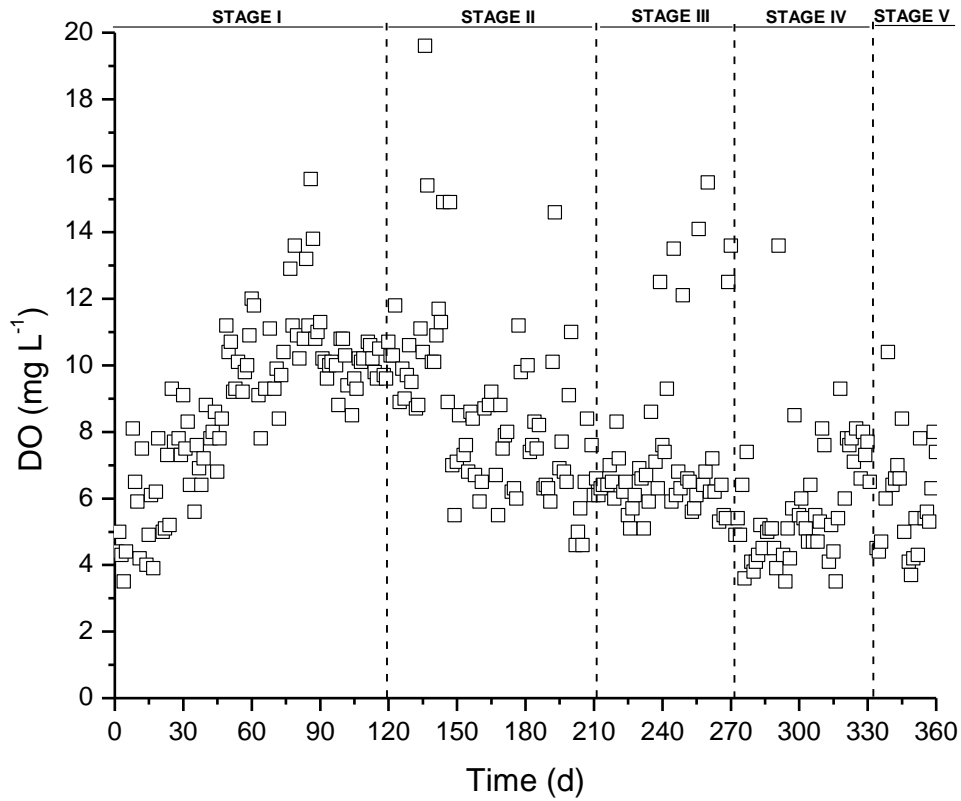
Figure A.4. Time course of the concentration of the dissolved oxygen in the cultivation broth of the HRAP throughout the 1-year monitoring period.
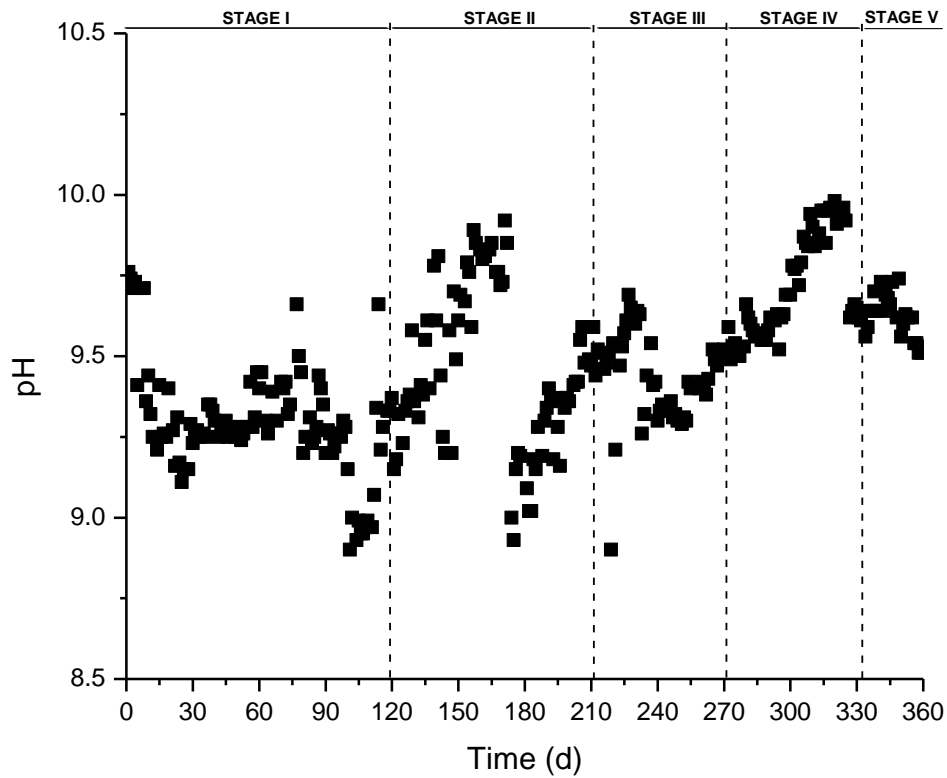
Figure A.5. Time course of the pH in the cultivation broth of the HRAP throughout the 1-year monitoring period.

Yearly variation of the digestate treatment performance
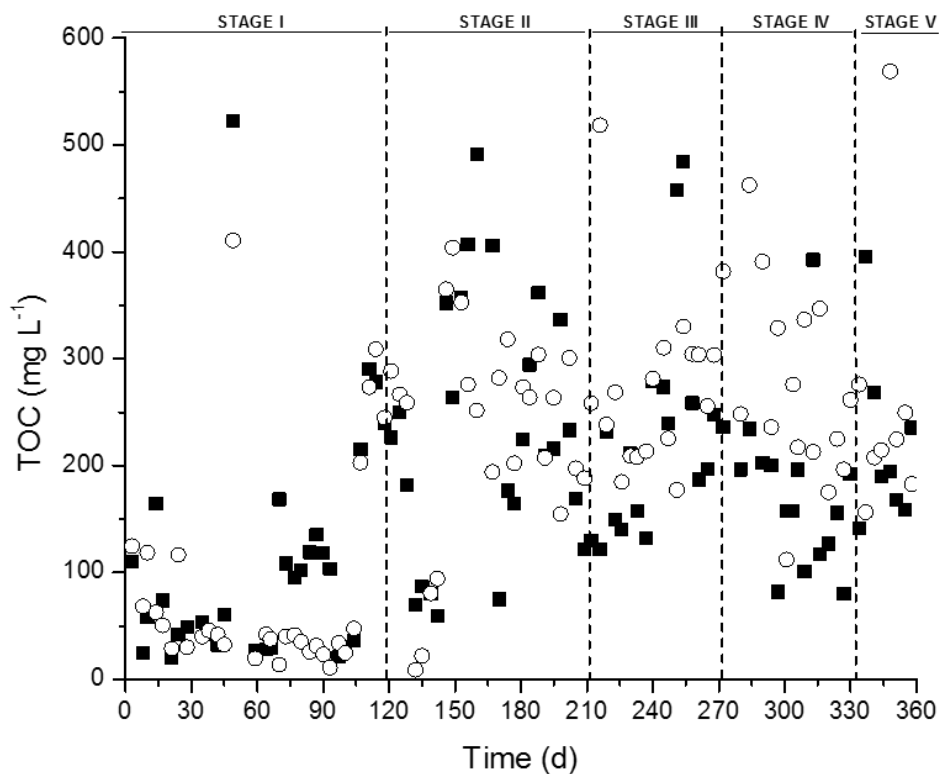
Figure A.6. Time course of the influent (■) and effluent (○) concentrations of TOC in the cultivation broth of the HRAP throughout the 1-year monitoring period.
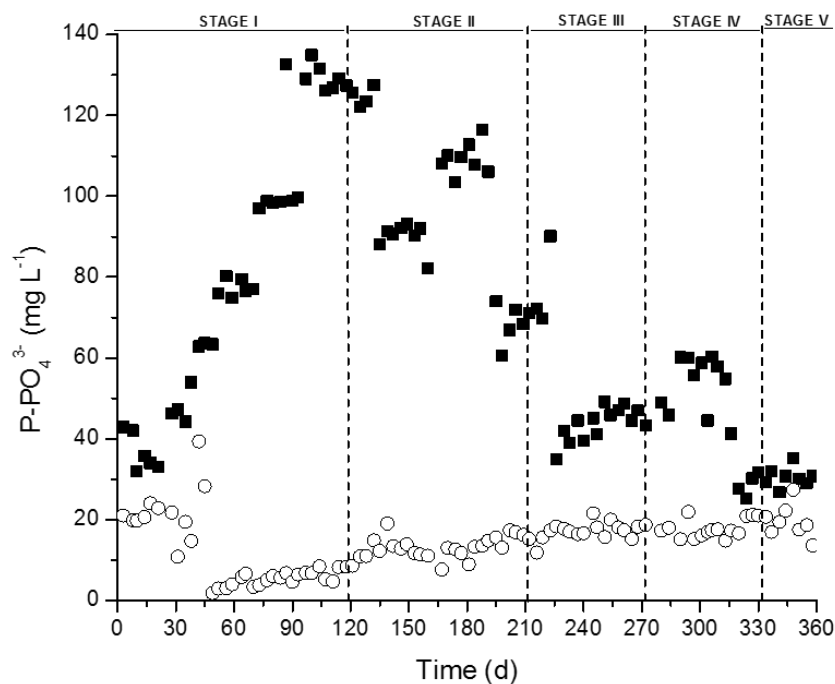
Figure A.7. Time course of the influent (■) and effluent (○) concentrations of P-PO$_4^{3-}$ in the cultivation broth of the HRAP throughout the 1-year monitoring period.
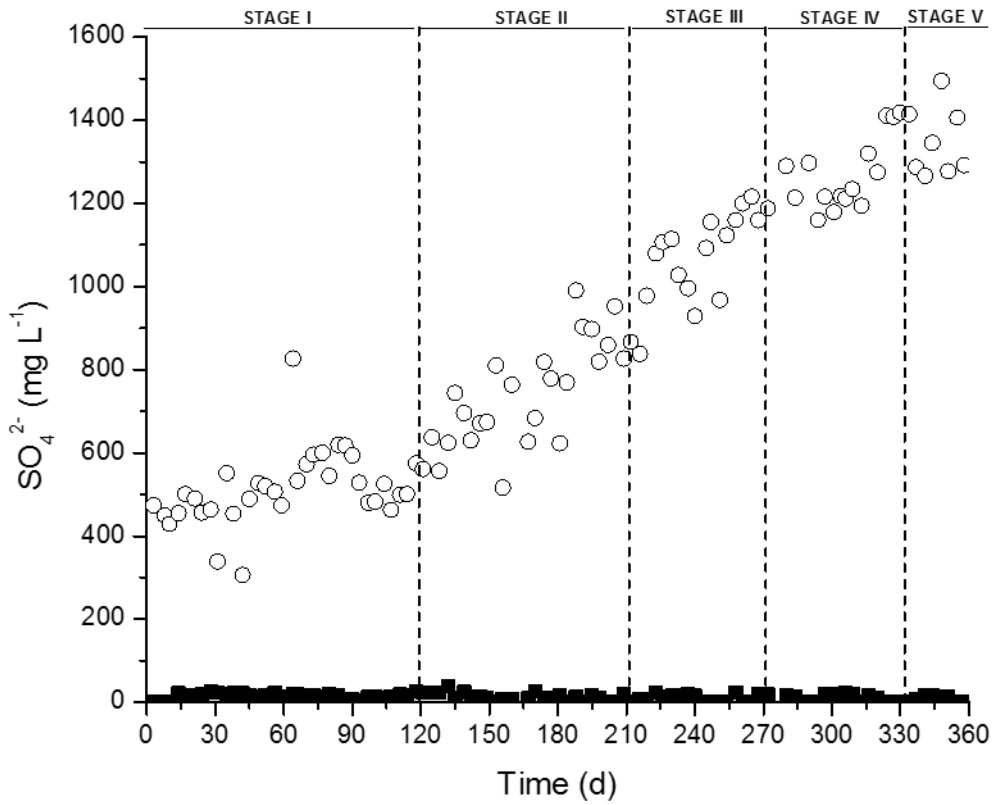
Figure A.8. Time course of the influent (■) and effluent (○) concentrations of SO_4^{2-} in the cultivation broth of the HRAP throughout the 1-year monitoring period.
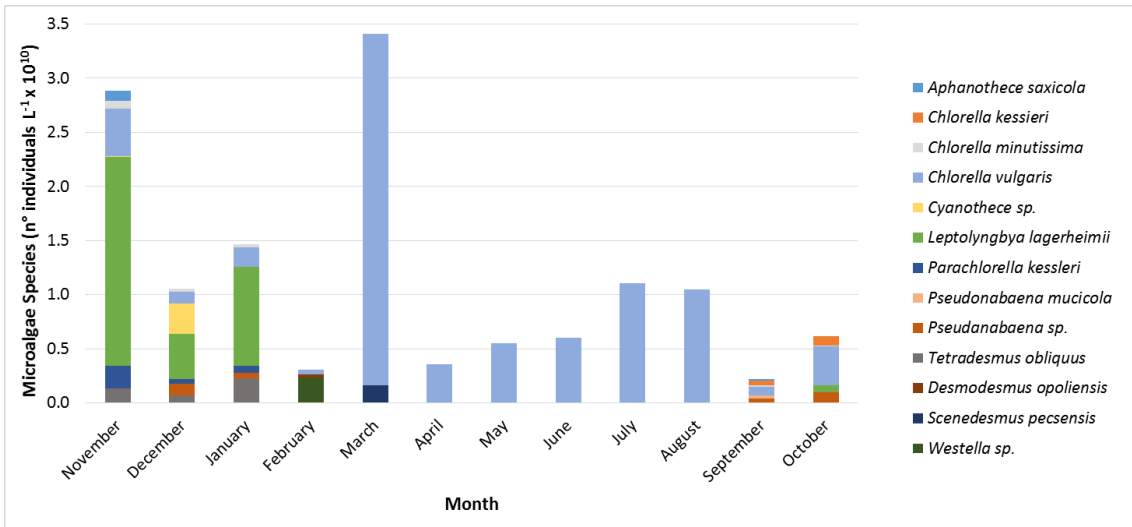
Figure A.9. Time course of the structure of microalgae population in the HRAP.

Table A.1. Main design parameters of the experimental plant

Volume of the HRAP (L)	180.0
Volume of the absorption column (L)	2.5
Volume of the settler (L)	8.0
HRAP illumination area (m^2)	1.2
Height of the absorption column (m)	1.65
Internal liquid velocity in HRAP (cm s^{-1})	20.0
Liquid flow rate in absorption column (L d^{-1})	74.9
Gas flow rate in the absorption column (L d^{-1})	74.9

Table A.2. Analysis of variance

	Sum of squares	Degrees of freedom	Mean square	F value	F critical
CH_4	761.5	11	69.2	35.2	1.9
Error	168.9	86	2.0		
CO_2	945.0	11	85.9	87.2	1.9
Error	84.7	86	1.0		
N_2	38.7	11	3.5	4.8	1.9
Error	62.4	86	0.7		
O_2	21.5	11	2.0	4.7	1.9
Error	35.4	86	0.4		

Table A.3. Carbon and nutrient recovery via biomass assimilation estimated from the carbon and nutrients removal, and the biomass elemental composition of the harvested biomass during all the stages.

Stage	Month	Carbon and nutrient recovery as biomass (%)				Biomass elemental composition (%)			
		C	N	P	S	C	N	P	S
I	November 2016	0 ± 0	0 ± 0	0 ± 0	0 ± 0	42.6	7.0	0.8	0.4
	December 2016	0 ± 0	0 ± 0	0 ± 0	0 ± 0	40.8	7.6	0.9	0.3
	January 2017	0 ± 0	0 ± 0	0 ± 0	0 ± 0	41.2	7.7	1.0	0.5
	February 2017	0 ± 0	0 ± 0	0 ± 0	0 ± 0	42.4	7.9	0.9	0.5
II	March 2017	48 ± 3	64 ± 6	22 ± 4	89 ± 11	42.6	7.9	0.9	0.7
	April 2017	48 ± 6	59 ± 2	23 ± 2	56 ± 8	42.1	7.8	0.9	0.6
	May 2017	44 ± 2	50 ± 6	24 ± 5	29 ± 8	41.6	7.7	0.9	0.5
III	June 2017	94 ± 5	96 ± 4	72 ± 21	41 ± 6	42.6	8.0	0.8	0.5
	July 2017	94 ± 6	97 ± 2	71 ± 5	36 ± 1	44.7	8.4	0.8	0.5
IV	August 2017	100 ± 0	100 ± 0	99 ± 2	64 ± 18	44.4	8.3	0.9	0.4
	September 2017	100 ± 0	98 ± 2	100 ± 0	53 ± 11	44.1	8.2	0.9	0.3
V	October 2017	99 ± 2	69 ± 3	100 ± 0	91 ± 13	47.9	9.0	1.1	0.5

Chapter 4

Influence of the seasonal variation of environmental conditions on biogas upgrading in an outdoors pilot scale high rate algal pond

David Marín, Esther Posadas, Patricia Cano, Víctor Pérez, Raquel Lebrero, Raúl Muñoz. Bioresource Technology 255 (2018) 354-358

Influence of the seasonal variation of environmental conditions on biogas upgrading in an outdoors pilot scale high rate algal pond

David Marín[1, 2], Esther Posadas[1], Patricia Cano[1], Víctor Pérez[1], Raquel Lebrero[1], Raúl Muñoz[1, *]

[1] Department of Chemical Engineering and Environmental Technology, School of Industrial Engineerings, Valladolid University, Dr. Mergelina, s/n, 47011, Valladolid, Spain.

[2] Universidad Pedagógica Nacional Francisco Morazán, Boulevard Centroamérica, Tegucigalpa, Honduras.

[*] Corresponding author: mutora@iq.uva.es

Abstract

The influence of the daily and seasonal variations of environmental conditions on the quality of the upgraded biogas was evaluated in an outdoors pilot scale high rate algal pond (HRAP) interconnected to an external absorption column (AC) via a conical settler. The high alkalinity in the cultivation broth resulted in a constant biomethane composition during the day regardless of the monitored month, while the high algal-bacterial activity during spring and summer boosted a superior biomethane quality. CO_2 concentrations in the upgraded biogas ranged from 0.1% in May to 11.6% in December, while a complete H_2S removal was always achieved regardless of the month. A limited N_2 and O_2 stripping from the scrubbing cultivation broth was recorded in the upgraded biogas at a recycling liquid/biogas ratio in the AC of 1. Finally, CH_4 concentration in the upgraded biogas ranged from 85.6% in December to 99.6% in August.

Keywords: Algal-bacterial photobioreactor; Biogas upgrading; Biomethane; Outdoors operation; Yearly evaluation.

1. Introduction

Biogas from the anaerobic digestion of wastewaters and organic waste constitutes a renewable source of energy to generate electricity or heat (Muñoz et al., 2015). However, the use of biogas as a substitute of natural gas or fuel in transportation requires an effective purification to levels set by national regulations. For instance, biogas injection into natural gas grids typically requires concentrations of $CH_4 \geq 95\%$, $CO_2 \leq 2\%$, $O_2 \leq 0.3\%$ and trace levels of H_2S (Muñoz et al., 2015; Toledo-Cervantes et al., 2017).

Algal-bacterial processes have emerged as a platform technology capable of simultaneously removing CO_2 and H_2S in a single stage, and constitute a cost-effective and environmentally friendly alternative to conventional biogas upgrading technologies (Bahr et al., 2014; Muñoz et al., 2015). Biogas upgrading in algal-bacterial photobioreactors is based on the oxidation of H_2S to SO_4^{2-} by sulfur oxidizing bacteria promoted by the high dissolved oxygen (DO) concentrations in the scrubbing cultivation broth, and on the photosynthetic fixation of the absorbed CO_2 by microalgae. The economic and environmental sustainability of this biotechnology can be boosted via digestate supplementation as a nutrient and water source, which will support an effective recovery of nutrients in the form of algal-bacterial biomass (Posadas et al., 2017; Toledo-Cervantes et al., 2016).

Biogas upgrading coupled to digestate treatment has been typically evaluated indoors in high rate algal ponds (HRAPs) interconnected to biogas absorption columns (AC) under artificial illumination (Alcántara et al., 2015; Bahr et al., 2014; Meier et al., 2015; Posadas et al., 2016, 2015; Serejo et al., 2015; Toledo-cervantes et al., 2017; Toledo-Cervantes et al., 2017, 2016). The optimization of this process has reached promising results in terms of biomethane quality (CH_4 concentrations of 96.2±0.7 %), nutrient removal (total nitrogen (TN)-removal efficiencies (REs) of 98.0±1.0 % and $P-PO_4^{-3}$- REs of 100±0.5 %) and biomass productivities (15.0 g m^{-2} d^{-1}) (Toledo-Cervantes et al., 2017). Comparable results were also obtained by Posadas et al. (2017) in a similar biogas upgrading photobioreactor configuration operated outdoors during summer in Spain, when solar irradiation, temperature and the number of sun hours were most favorable to support algal-bacterial activity. In this context, a systematic year-round evaluation of the influence of the daily and seasonal variations of environmental conditions on biogas upgrading and nutrient recovery from digestate is needed to validate this technology under outdoor conditions.

This study investigated for the first time the year-round performance of biogas upgrading in an outdoors pilot HRAP interconnected to an external AC by monthly monitoring the daily variations of biogas quality and cultivation broth parameters under continental climate conditions.

2. Materials and methods

2.1. Biogas and centrate

A synthetic biogas mixture composed of CO_2 (29.5%), H_2S (0.5%) and CH_4 (70%) was used as a raw biogas in the present study (Abello Linde; Spain). Centrate was monthly obtained from the centrifuges dehydrating the anaerobically digested mixed sludge of Valladolid wastewater treatment plant (WWTP) and stored at 4 ºC. The composition of centrate varied along the experimental period as a result of the seasonal operational variations of the WWTP: total organic carbon (TOC) = 16-523 mg L^{-1}, inorganic carbon (IC) = 450-600 mg L^{-1}, TN = 374-718 mg L^{-1}, P-PO_4^{3-} = 26-135 mg L^{-1} and SO_4^{2-} = 0-38 mg L^{-1}. The IC concentration in the centrate was adjusted to 1999 ± 26 mg L^{-1} via addition of $NaHCO_3$ and Na_2CO_3 in order to maintain the required high alkalinity and pHs (≥9) in the cultivation broth to support an effective CO_2 and H_2S absorption in the AC (Posadas et al., 2017).

2.2. Experimental set-up

The experimental set-up, constructed according to Posadas et al. (2017), was located outdoors at the Department of Chemical Engineering and Environmental Technology of Valladolid University (41.39º N, 4.44º W). The pilot plant consisted of a 180 L HRAP with an illuminated area of 1.20 m^2 (width = 82 cm; length = 170 cm; depth = 15 cm) and two water channels divided by a central wall and baffles in each side of the curvature. The internal recirculation velocity of the cultivation broth in the HRAP was ≈ 20 cm s^{-1}, which was supported by the continuous rotation of a 6-blade paddlewheel. The HRAP was interconnected to an external 2.5 L bubble AC (height = 165 cm; internal diameter = 4.4 cm) provided with a metallic biogas diffuser of 2 μm pore size located at the bottom of the column. The HRAP and the AC were interconnected via an external liquid recirculation of the algal-bacterial cultivation broth from an 8 L conical settler (Fig. 1). The efficiency of the settler in terms of biomass removal was almost complete.
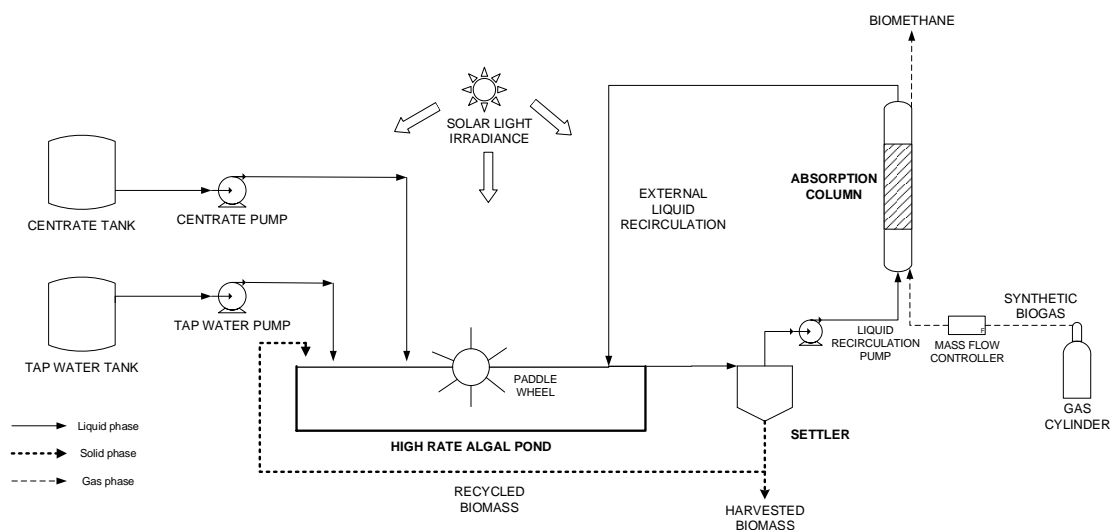
Figure 1. Schematic diagram of the outdoors experimental set-up used for the continuous photosynthetic upgrading of biogas.

2.3. Operational conditions and sampling procedures

Process operation was carried out from November the 1st 2016 to October the 30st 2017. The HRAP was inoculated to an initial concentration of 210 mg TSS L^{-1} with a microalgae inoculum composed of *Leptolyngbya lagerheimii (54%), Chlorella vulgaris (28%), Parachlorella kessleri (9%), Tetrademus obliquus (5%) and Chlorella minutissima (2%)* from an indoor HRAP treating biogas and centrate at the Department of Chemical Engineering and Environmental Technology of Valladolid University (Spain). Five different operational stages (namely I, II, III, IV and V) were defined as a function of the temperature, photosynthetic active radiation (PAR), number of sun hours and biomass productivity imposed (Table 1). The synthetic biogas was sparged into the AC under co-current flow operation at 74.9 L d^{-1} under a recycling liquid to biogas ratio (L/G) of 1.0 according to Posadas et al. (2017), which resulted in gas and liquid retention time of 48 min and. The liquid velocity accounted for 2 m h^{-1}. The HRAP was fed with IC-supplemented centrate as a nutrient source at a flow rate of 3.5 L d^{-1}, which entailed a hydraulic retention time of 50 d. Tap water was supplied in order to compensate water evaporation losses and allow process operation without effluent (Table 1).

The pH, temperature and DO concentration in the cultivation broth of the HRAP, AC and settler, along with PAR, were monitored every thirty minutes during the daytime of one day every month where the environmental conditions were representative of the conditions in the entire month. Gas samples of 100 μL from the upgraded biogas were

drawn every hour to monitor the gas concentrations of CH_4, CO_2, H_2S, O_2 and N_2. Liquid samples of 100 mL from the cultivation broth of the HRAP, AC and settler were drawn every two hours to monitor the concentrations of dissolved TOC, IC, TN.

2.4. Analytical procedures

PAR was measured using a LI-250A light meter (LI-COR Biosciences, Germany), while pH was determined with an Eutech Cyberscan pH 510 (Eutech instruments, The Netherlands). Temperature and DO were measured using an OXI 330i oximeter (WTW, Germany). Gas concentrations of CH_4, CO_2, H_2S, O_2 and N_2 were determined using a Varian CP-3800 GC-TCD according to Posadas et al. (2015) (Palo Alto, USA). Dissolved TOC, IC and TN concentrations were measured using a Shimadzu TOC-VCSH analyzer (Japan) coupled with a TNM-1 chemiluminescence module.

Table 1. Environmental and operational parameters during the five operational stages.

Stage	Month	Parameter			
		Average ambient temperature (ºC)	Average photosynthetic active radiation ($\mu mol\ m^{-2}\ s^{-1}$)	Nº of sun hours (h)	Biomass Productivity ($g\ m^{-2}\ d^{-1}$)
I	November 30, 2016	4.4 ± 1.6	170 ± 33	10 ± 1	0.0
	December 28, 2016	7.5 ± 4.9	349 ± 119	10 ± 1	
	January 31, 2017	10.2 ± 3.9	339 ± 174	10 ± 1	
	February 28, 2017	14.1 ± 6.6	921 ± 237	12 ± 1	
II	March 29, 2017	14.2 ± 6.2	1213 ± 191	13 ± 1	7.5
	April 26, 2017	8.6 ± 1.5	301 ± 138	14 ± 1	
	May 31, 2017	23.1 ± 5.8	1399 ± 183	15 ± 1	
III	June 28, 2017	20.3 ± 2.7	297 ± 105	15 ± 1	15.0
	July 27, 2017	28.5 ± 6.5	1411 ± 155	15 ± 1	
IV	August 25, 2017	26.0 ± 6.3	1070 ± 199	13 ± 1	22.5
	September 27, 2017	20.7 ± 7.2	1009 ± 237	12 ± 1	
V	October 26, 2017	18.4 ± 7.0	113 ± 83	10 ± 1	15.0

3. Results and discussion

3.1. Biogas Upgrading

3.1.1 CO_2 biomethane concentration

Negligible variations in CO_2 concentration in the biomethane were recorded throughout the daytime regardless of the operational month likely due to the high alkalinity of the cultivation broth (Fig. 2; Fig. S6). These results were in agreement with Posadas et al. (2017), who observed a constant CO_2 concentration in the upgraded biogas during the daytime in a similar set-up operated with a high ionic strength cultivation broth (IC concentration $\approx 2660 \pm 48$ mg L^{-1}). This study also suggested that the influence of the cultivation broth temperature on CO_2 absorption (Henry's law constant ranged from $H_{CO2} \approx 1.27$ at 8.3 ºC in November to $H_{CO2} \approx 0.59$ at 40.3 ºC in July) was lower than that of the IC concentration (Sander, 2015). Hence, the biomethane CO_2 concentration in stage I ranged from 1.4% in January to 11.6% in December. This concentration varied from 0.1% in March to 3.9% in May during stage II, and from 0.6% in June to 2.2% in July in stage III. CO_2 concentrations in stage IV and V ranged from 0.4% to 1.8% and from 0.8% to 1.2%, respectively (Fig. 2). Thus, the concentration of CO_2 in the biomethane produced in the algal-bacterial photobioreactor complied during most of the year with European regulations, which require CO_2 concentrations $\leq 2\%$ prior injection into natural gas grids or use as a vehicle fuel (Muñoz et al., 2015). The high CO_2 REs here obtained (estimated from $\approx 60.7\%$ in December to 99.7% in May) were promoted by the optimum L/G ratio reported by Posadas et al. (2017) and the high pHs/alkalinity of the cultivation broth in the AC, which enhanced CO_2 absorption (Lebrero et al., 2016; Posadas et al., 2015; Toledo-Cervantes et al., 2016). These results were in accordance with Rodero et al. (2017), who reported an increase in the CO_2-RE from 30.8% to 99.3% when alkalinity increased from 102 ± 7 mg IC L^{-1} to 1581 ± 135 mg IC L^{-1} at 35.0ºC in a similar photobioreactor configuration under indoor conditions.

This year-round evaluation of the performance of the algal-bacterial photobioreactor confirmed the key role of biotic mechanisms on this biogas upgrading technology (Fig. 2). Hence, despite the low temperatures of the cultivation broth during winter increased CO_2 aqueous solubility, the lower pHs of the cultivation broth supported by the low photosynthetic activity (from 8.1 to 9.0) resulted in higher CO_2 concentrations in the upgraded biogas. The higher photosynthetic activity mediated by the favorable

environmental conditions prevailing during spring and summer, along with the accumulation of IC in the cultivation broth from 1785 mg L^{-1} to 4599 mg L^{-1} from stage II to V, increased the pH from 8.8 to 9.8, which resulted in biomethane CO_2 concentrations complying with most international regulations. In this context, although a 60% decrease in CO_2 solubility is expected when the cultivation broth temperature increases from 10 to 40°C, the high CO_2 concentration gradient supported by the high alkalinity/pH of the cultivation broth during stages II - V compensated this decrease in CO_2 solubility.
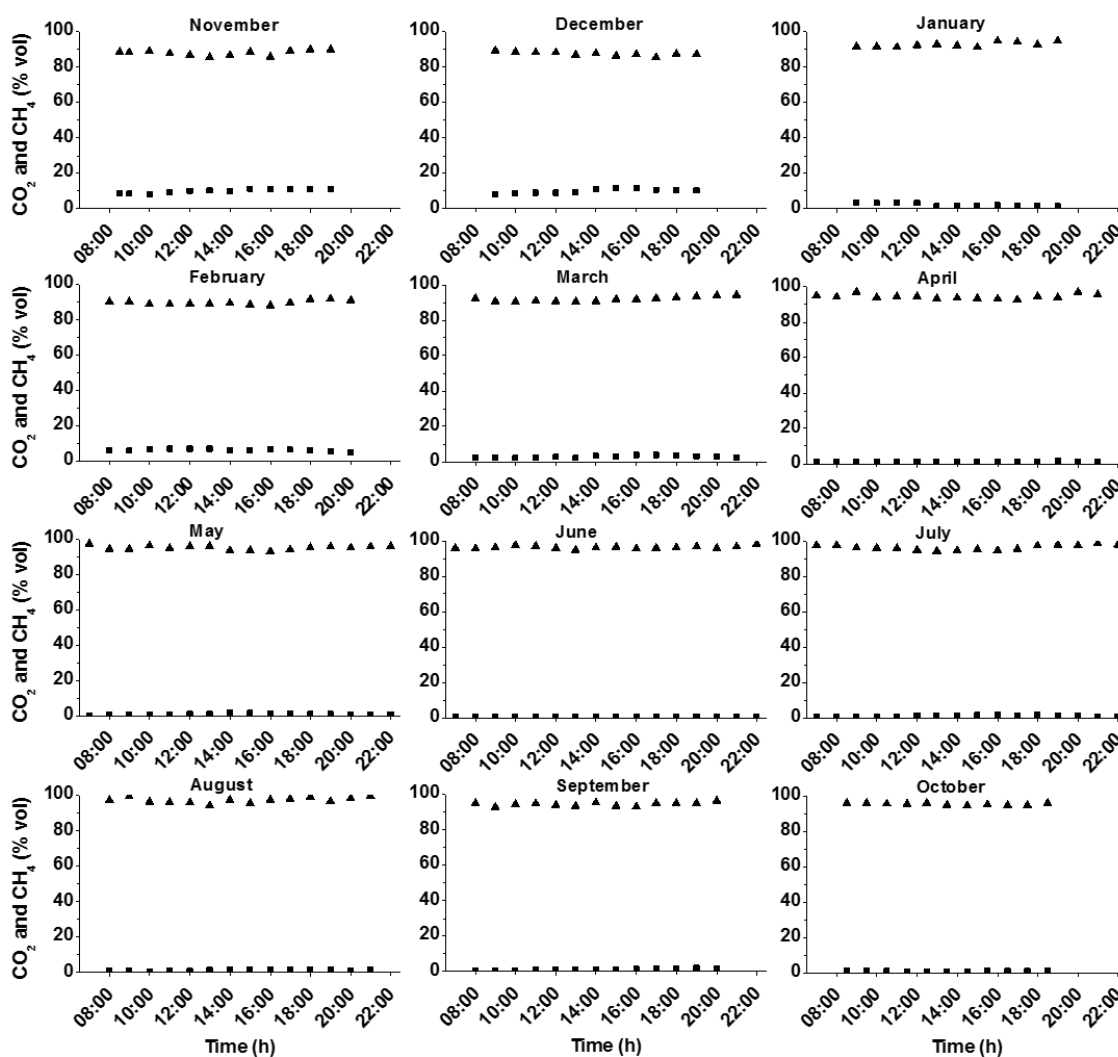

Figure 2. Time course of the concentration of CO_2 (■) and CH_4 (▲) in the upgraded biogas during one diurnal cycle under steady state as a function of the operational months.

3.1.2 H_2S biomethane concentration

H_2S was completely removed in the system regardless of the environmental parameters and alkalinity. This higher elimination compared to the removal of CO_2 was attributed to the higher H_2S aqueous solubility (Henry´s law constant ranging from $H_{H2S} \approx 3.58$ at 8.3 ºC to $H_{H2s} \approx 1.80$ at 40.3 ºC) (Sander, 2015). The high pHs also promoted the complete removal of this acidic gas in the AC (Bahr et al., 2014). These results were in accordance to Posadas et al. (2017), who reported a complete removal of H_2S during the simultaneous treatment of centrate and biogas in a similar outdoors experimental set-up, and to Toledo-Cervantes et al. (2016) who also observed a complete depletion of H_2S during the optimization of photosynthetic biogas upgrading under laboratory conditions. In brief, the H_2S concentration in the biomethane herein obtained complied with most European regulations for biomethane injection into natural gas grids or use as a vehicle fuel, which requires H_2S levels ≤ 5 mg m^{-3} (Muñoz et al., 2015).

3.1.3 N_2 and O_2 concentrations in the biomethane

Despite no clear trend in the evolution of biomethane N_2 concentration along the daytime was recorded, the highest O_2 concentrations in the upgraded biogas were recorded around midday, concomitantly with the highest DO concentrations in the cultivation broth (Fig. S3; Fig. S8). Biomethane N_2 and O_2 concentrations during stage I ranged from 0.0% in November to 5.5% and 1.8%, respectively, in January. During stage II, N_2 and O_2 concentrations varied from 1.2% (April) and 0.3% (March), respectively, to 5.9% (March) and 2.4% (May), respectively. In stage III, these concentrations ranged from 0.1% and 0.0% (July), respectively, to 3.3% (June) and 1.5% (July), respectively. During stage IV, N_2 and O_2 concentrations fluctuated from 0.0% (August) to 5.2% and 1.9% (September), respectively. Finally, N_2 and O_2 concentrations during stage V ranged from 1.9% and 0.4%, respectively, to 3.2% and 1.2%, respectively (Fig. S8). Overall, the highest N_2 and O_2 concentrations in the upgraded biogas were recorded during stages I and II (and during September in stage III) likely due to the lower ambient temperatures, which increased the solubility of these gases in the HRAP and their further desorption in the AC.

The previous optimization of the L/G ratio in the AC entailed a low N_2 and O_2 desorption (Posadas et al., 2017). Thus, the O_2 concentrations here recorded in the biomethane were

in accordance to Posadas et al. (2017) and Serejo et al. (2015), who reported values ranging from 0% to 2% and from 0% to 4%, respectively, in a similar experimental set-up (under outdoors and laboratory conditions, respectively) at a L/G of 0.5. The O_2 concentration in the upgraded biogas only complied with international regulations during the periods of low PAR ($\leq$1%), which requires a further optimization.

3.1.4 CH_4 biomethane concentration

Negligible variations in the CH_4 concentration of the upgraded biogas were recorded throughout the daytime regardless of the operational month (Fig. 2). Hence, CH_4 concentration in the biomethane in stage I ranged from 85.6% in December to 94.8% in January. During stage II, CH_4 concentration varied from 90.4% in March to 97.2% in May, and from 94.5% to 99.0% in stage III (July). Finally, the range of CH_4 concentrations in stage IV and V were 93.0%-99.6% and 94.5%-96.0%, respectively (Fig. 2). Therefore, the CH_4 concentration in the biomethane here produced during stages II-V complied with most European regulation for injection into natural gas grids or use as a vehicle fuel (Muñoz et al., 2015). The higher CH_4 concentrations from stage II onwards were mainly due to the higher CO_2 removals and lower N_2 and O_2 desorptions recorded (Fig. 2). These concentrations were in accordance to Posadas et al. (2017) and Toledo-Cervantes et al. (2017), who reported CH_4 concentrations of 92.0% and 96.2%, respectively, in the upgraded biogas using the same photobioreactor configuration. Finally, negligible CH_4 losses by absorption in the AC were measured regardless of the operational month as a result of the low CH_4 aqueous solubility (Henry´s law constant of CH_4 ranged from $H_{CH4} \approx 0.044$ at 8.3 ℃ to $H_{CH4} \approx 0.028$ at 40.3℃) (Sander, 2015). Finally, it should be noted that the CH_4 content in the upgraded biogas remained constant during the night period as a result of the high buffer capacity and pH of the cultivation broth.

4. Conclusions

This work constitutes the first year-round evaluation of biogas upgrading in a pilot scale outdoors HRAP. The high alkalinity and pHs in the cultivation broth were identified as key parameters to maintain a constant biomethane composition during the daytime. Environmental conditions significantly influenced the quality of biomethane. CO_2, H_2S and CH_4 concentrations in the upgraded biogas complied with most international regulations for biomethane injection into natural gas grids or use as a vehicle fuel. This

study confirmed the year-round feasibility of outdoors algal-bacterial processes for the simultaneous removal of CO_2 and H_2S from biogas coupled to nutrient removal from digestates.

Acknowledgements

References

1. Alcántara, C., García-encina, P.A., Muñoz, R., 2015. Evaluation of the simultaneous biogas upgrading and treatment of centrates in a high-rate algal pond through C , N and P mass balances 150–157. doi:10.2166/wst.2015.198

2. Bahr, M., Díaz, I., Dominguez, A., González Sánchez, A., Muñoz, R., 2014. Microalgal-biotechnology as a platform for an integral biogas upgrading and nutrient removal from anaerobic effluents. Environ. Sci. Technol. 48, 573–581. doi:10.1021/es403596m

3. Lebrero, R., Toledo-Cervantes, A., Muñoz, R., del Nery, V., Foresti, E., 2016. Biogas upgrading from vinasse digesters: a comparison between an anoxic biotrickling filter and an algal-bacterial photobioreactor. J. Chem. Technol. Biotechnol. 91, 2488–2495. doi:10.1002/jctb.4843

4. Meier, L., Pérez, R., Azócar, L., Rivas, M., Jeison, D., 2015. Photosynthetic CO2 uptake by microalgae: An attractive tool for biogas upgrading. Biomass and Bioenergy 73, 102–109. doi:10.1016/j.biombioe.2014.10.032

5. Muñoz, R., Meier, L., Diaz, I., Jeison, D., 2015. A review on the state-of-the-art of physical/chemical and biological technologies for biogas upgrading. Rev. Environ. Sci. Biotechnol. 14, 727–759. doi:10.1007/s11157-015-9379-1

6. Posadas, E., Marín, D., Blanco, S., Lebrero, R., Muñoz, R., 2017. Simultaneous biogas upgrading and centrate treatment in an outdoors pilot scale high rate algal pond. Bioresour. Technol. 232, 133–141. doi:10.1016/j.biortech.2017.01.071

7. Posadas, E., Serejo, M.L., Blanco, S., Pérez, R., García-Encina, P.A., Muñoz, R., 2015. Minimization of biomethane oxygen concentration during biogas upgrading in algal-bacterial photobioreactors. Algal Res. 12, 221–229. doi:10.1016/j.algal.2015.09.002

8. Posadas, E., Szpak, D., Lombó, F., Domínguez, A., Díaz, I., Blanco, S., García-Encina, P.A., Muñoz, R., 2016. Feasibility study of biogas upgrading coupled with nutrient removal from anaerobic effluents using microalgae-based processes. J. Appl. Phycol. 28, 2147–2157. doi:10.1007/s10811-015-0758-3

9. Rodero, M. del R., Posadas, E., Toledo-Cervantes, A., Lebrero, R., Muñoz, R., 2017. Influence of alkalinity and temperature on photosynthetic biogas upgrading efficiency in high rate algal ponds. Submitted for publication to Algal Research.

10. Sander, R., 2015. Compilation of Henry 's law constants (version 4.0) for water as solvent 4399–4981. doi:10.5194/acp-15-4399-2015

11. Serejo, M.L., Posadas, E., Boncz, M.A., Blanco, S., García-Encina, P., Muñoz, R., 2015. Influence of biogas flow rate on biomass composition during the optimization of biogas upgrading in microalgal-bacterial processes. Environ. Sci. Technol. 49, 3228–3236. doi:10.1021/es5056116

12. Toledo-cervantes, A., Estrada, J.M., Lebrero, R., Muñoz, R., 2017. A comparative analysis of biogas upgrading technologies : Photosynthetic vs physical / chemical processes. Algal Res. 25, 237–243. doi:10.1016/j.algal.2017.05.006

13. Toledo-Cervantes, A., Madrid-Chirinos, C., Cantera, S., Lebrero, R., Muñoz, R., 2017. Influence of the gas-liquid flow configuration in the absorption column on photosynthetic biogas upgrading in algal-bacterial photobioreactors. Bioresour. Technol. 225, 336–342. doi:10.1016/j.biortech.2016.11.087

14. Toledo-Cervantes, A., Serejo, M.L., Blanco, S., Pérez, R., Lebrero, R., Muñoz, R., 2016. Photosynthetic biogas upgrading to bio-methane: Boosting nutrient recovery via biomass productivity control. Algal Res. 17, 46–52. doi:10.1016/j.algal.2016.04.017

Supplementary material

Influence of the seasonal variation of environmental conditions on biogas upgrading in an outdoors pilot scale high rate algal pond

David Marín[1, 2], Esther Posadas[1], Patricia Cano[1], Victor Pérez[1], Raquel Lebrero[1], Raúl Muñoz[1,*]

[1] Department of Chemical Engineering and Environmental Technology, Valladolid University, Dr. Mergelina, s/n, 47011, Valladolid, Spain.

[2] Universidad Pedagógica Nacional Francisco Morazán, Boulevard Centroamérica, Tegucigalpa, Honduras.

* Corresponding author: mutora@iq.uva.es

Environmental parameters

Large daily and monthly variations of PAR and environmental temperature were recorded throughout this study (Fig. S1). Thus, light irradiance progressively increased during the first hours in the morning, reaching a maximum at midday (based on the total number of sun hours at the corresponding month) and decreasing by the end of the day. The unexpectedly low PAR recorded in April or June were caused by the presence of clouds (Fig. S1). Similarly, the minimum temperatures were always recorded during the first hour in the morning, although progressively increased throughout the day up to maximum values achieved during the last sunny hours, regardless of the month (Fig. S1).

Light irradiance and ambient temperature remained quite low during stage I. Thus, the maximum daily PAR ranged from 220 μmol m^{-2} s^{-1} in November to 1230 μmol m^{-2} s^{-1} in February, while the minimum temperature recorded was -1.0 ℃ in December and the maximum was 21.0 ℃ in February. PAR and ambient temperature gradually increased from March onwards along with an increase in the number of sun hours from 10 to 15 h from stage I to II, respectively (Fig. S1; Table 1). In this context, the maximum daily PAR during stage II ranged from 1419 μmol m^{-2} s^{-1} in March to 1710 μmol m^{-2} s^{-1} in April, while ambient temperature varied from 3 ℃ in March to 28 ℃ in May. Stage III was characterized by the highest number of sun hours (15±1 h) (Table 1), maximum PAR (ranging from 1583 μmol m^{-2} s^{-1} in July to 1669 μmol m^{-2} s^{-1} in June) and ambient temperatures oscillating from 15.0 ℃ in June to 34.0 ℃ in July. On the other hand, stage IV was also characterized by a high number of sun hours ($\approx$13±1 h), high maximum daily PARs (1270 μmol m^{-2} s^{-1} in August to 1376 μmol m^{-2} s^{-1} in September) and moderately

high ambient temperatures (from 8 ºC in September to 32.0 ºC in August) (Fig. S1; Table 1). Finally, the number of sun hours during stage V was similar to stage I (10±1 h), with a maximum daily PAR of 253 µmol m^{-2} s^{-1} and ambient temperatures ranging from 7.0 to 26.0 ºC (Fig. S1).

The high outdoors light irradiances here recorded during midday likely caused photo-inhibition in the HRAP at the low-moderate culture densities prevailing in the cultivation broth, since the photosynthetic apparatus of most microalgae species gets saturated at ≈ 200-250 µmol m^{-2} s^{-1} (Sousa et al., 2012; Torzillo et al., 2003). In addition, light limitation was likely to occur in the early morning and late evening, and probably during most of the daytime in stage I and stage V (Fig. S1).
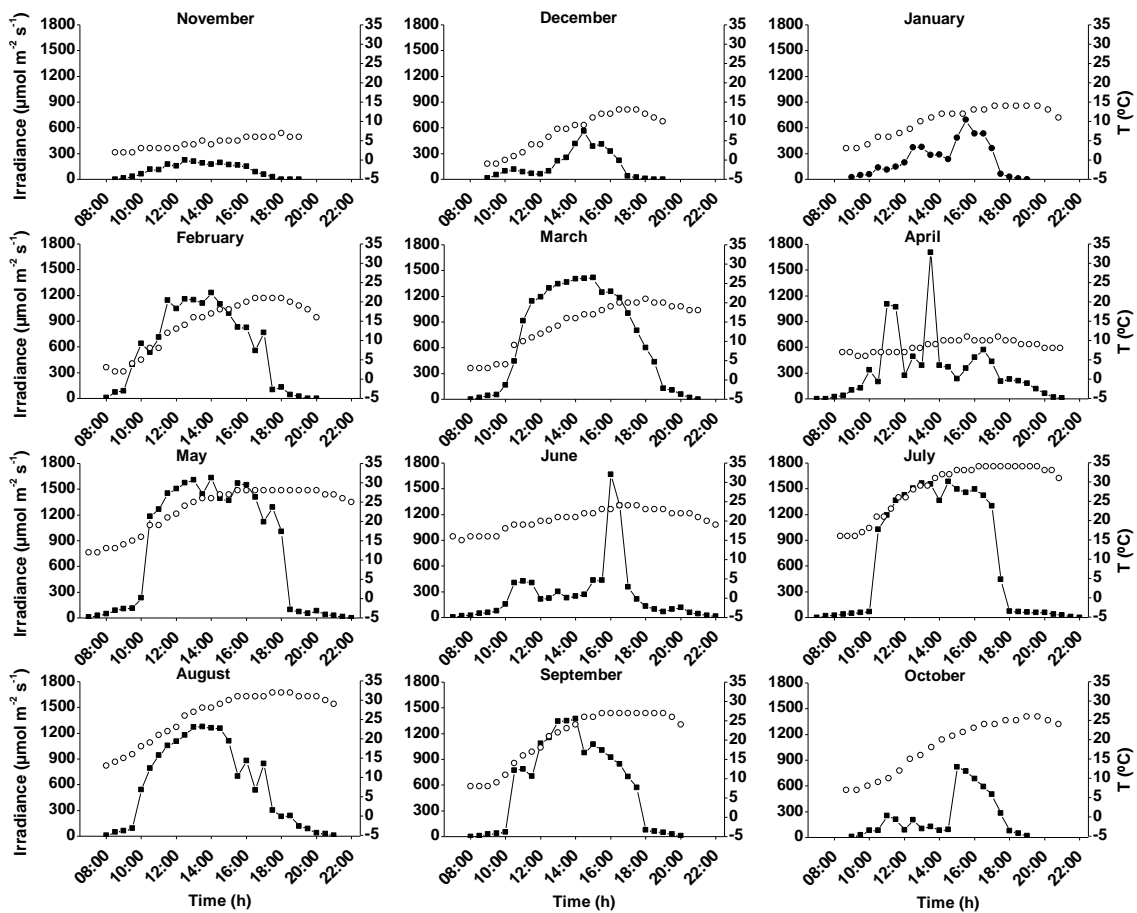

Figure S1. Time course of the light irradiance (■) and ambient temperature (○) during one diurnal cycle under steady state as a function of the month of operation.

Temperature, Dissolved Oxygen and pH

Temperature

Ambient temperature directly influenced the temperatures of the cultivation broth in the HRAP, AC and settler (Fig. S1; Fig. S2; Table 1). During stage I, the temperatures in the HRAP, AC and settler ranged from 2 °C, 2 °C and 2 °C, respectively, in December to 21 °C, 21 °C and 23 °C, respectively, in February (Fig. S2). In stage II, the temperatures in the HRAP, AC and settler varied from 6 °C, 4 °C and 6 °C, respectively, in March to 31 °C, 36 °C and 34 °C, respectively, in May. Stage III was characterized by temperatures in the HRAP, AC and settler fluctuating from 16 °C, 15 °C and 17 °C, respectively, in June to 32 °C, 41 °C and 38 °C, respectively, in July. On the other hand, the temperatures in stage IV in the HRAP, AC and settler ranged from 11 °C, 10 °C and 12 °C, respectively, in September to 29 °C, 36 °C and 34 °C, respectively, in August. Finally, the temperatures in stage V in the HRAP, AC and settler ranged from 8 to 19 °C, 8 to 27 °C and 9 to 21 °C, respectively (Fig. S2).

The typically lowest temperatures recorded in the HRAP were mediated by the heat exchange of the cultivation broth with the open atmosphere and temperature regulation through water evaporation (Boelee et al., 2014). The higher thermal inertia of the HRAP compared to the AC and settler due to its larger volume could also explain the phenomenon observed (Murphy and Berberoglu, 2017). Despite the concomitant variation in the temperature of the cultivation broth in the three units regardless of the operational month, the largest differences were recorded in July-September (≈5 °C), when the daily variations in ambient temperature were largest (Fig. S1; Fig. S3).

Figure S2. Time course of the temperature in the cultivation broth of the HRAP (●), AC (□) and settler (×) during one diurnal cycle under steady state as a function of the month of operation.

Dissolved Oxygen concentration

The daily variations of the DO concentration in the cultivation broth during stage I differed from that recorded during the other stages (Fig. S3). Hence, DO remained constant throughout the daytime regardless of the operational unit as a result of the lack of algal activity (which was only significant in November). The increase in the number of sun hours, PAR and ambient temperature from March onwards brought about a correlation of the DO concentration with the daily variation of the above environmental parameters in all operational units (Fig. S3). Thus, the DO concentration increased during the first hours in the morning mediated by the increase in photosynthetic activity to, peak 2 or 3 hours after the maximum irradiance. This variation was significant in the cultivation broth of the HRAP but less pronounced in the settler and AC due to the active endogenous

oxygen consumption and oxidation of H_2S to SO_4^{2-}, respectively (Bahr et al., 2014; Posadas et al., 2017). In this context, the DO concentration during stage I in the HRAP ranged from 6.1 mg L^{-1} in February to 15.0 mg L^{-1} in November, from 2.2 mg L^{-1} in February to 5.8 mg L^{-1} in January in the AC, and from 3.7 mg L^{-1} to 9.6 mg L^{-1} in the settler in November. In stage II, the DO concentration in the HRAP varied from 4.2 mg L^{-1} in April to 18.6 mg L^{-1} in March, from 2.0 mg L^{-1} to 8.3 mg L^{-1} in the AC in May and from 1.4 mg L^{-1} in May to 7.7 mg L^{-1} in March in the settler (Fig. S3). During stage III, the DO concentration in the HRAP ranged from 3.9 mg L^{-1} to 21.4 mg L^{-1} in July, from 2.0 mg L^{-1} in June to 14.0 mg L^{-1} in July in the AC, and from 1.0 mg L^{-1} in July to 8.7 mg L^{-1} in June in the settler (Fig. S3). Similarly, the concentration of DO in the HRAP during stage IV ranged from 3.4 mg L^{-1} to 25.0 mg L^{-1} in August, from 2.3 mg L^{-1} in September to 12.3 mg L^{-1} in August in the AC, and from 1.2 mg L^{-1} in August to 6.9 mg L^{-1} in September in the settler. Finally, the DO concentration in the HRAP, AC and settler ranged from 6.3 mg L^{-1}, 2.8 mg L^{-1} and 2.2 mg L^{-1}, respectively, to 18.6 mg L^{-1}, 7.3 mg L^{-1} and 7.5 mg L^{-1}, respectively, in stage V (Fig. S3).

The highest DO concentrations recorded during the first hours in the morning in stages I and II were likely mediated by the prevailing low temperatures, which induced higher oxygen aqueous solubilities and limited the endogenous oxygen consumption in the cultivation broth. On the other hand, the inhibition of microalgae activity could have eventually occurred during stage III since DO concentrations above 25 mg L^{-1} can inhibit algal growth (Molina et al., 2001). Overall, the DO concentrations recorded in the HRAP during the entire monitored period supported and effective organic matter and NH_4^+ oxidation regardless of the stage (Fig. S4).

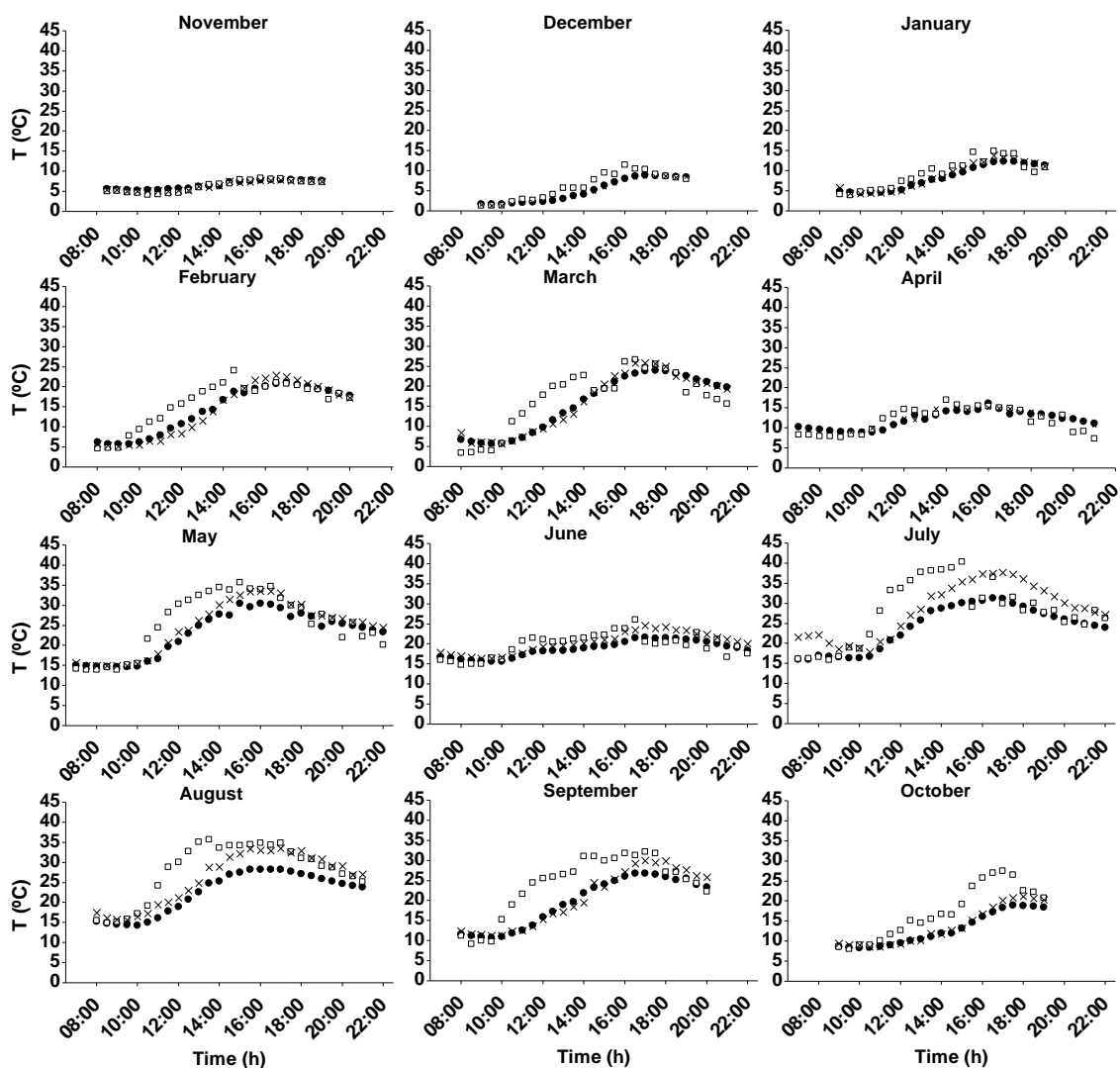**Figure S3.** Time course of the dissolved oxygen concentration in the cultivation broth of the HRAP (●), AC (□) and settler (×) during one diurnal cycle under steady state as a function of the operational month.

Figure S4. Time course of total organic carbon concentration in the cultivation broth of the HRAP (●), AC (□) and settler (x) during one diurnal cycle under steady state in one year.

pH

The pH in each unit of the experimental set-up remained constant throughout the daytime regardless of the operational stage due to the high buffer capacity of the cultivation broth (Fig. S5; Fig. S6). Indeed, microalgae activity at midday did not significantly increased the pH of the cultivation broth (Posadas et al., 2015). In stage I, the pH ranged from 9.2 in January to 9.6 in December in the HRAP, from 8.1 in November to 9.0 in January in the AC and from 9.2 in January to 9.6 in December in the settler. During stage II, the pH varied from 9.1 in April to 9.8 in March in the HRAP, from 8.8 in April to 9.5 in May in the AC, and from 9.1 in April to 9.8 in March in the settler (Fig. S5). In Stage III, the pH in the HRAP, AC and settler ranged from 9.4, 9.3 and 9.4, respectively, in June to 9.5, 9.4 and 9.6, respectively, in July (Fig. S5). During stage IV, the pH in the HRAP, AC and settler varied from 9.6 in all the units in September to 9.9, 9.8 and 10.1, respectively, in August (Fig. S5). Finally, the pH in the HRAP, AC and settler during stage V ranged

from $\approx$ 9.4 to 9.6 regardless of the unit (Fig. S5). Overall, the pH in the HRAP and settler were similar regardless of the operational stage and oscillated around 9.5 throughout the year. The results clearly showed a progressive increase in the pH of the AC from $\approx$8.3 in November to $\approx$9.5 in October due to the higher buffer capacity in the cultivation broth mediated by the gradual increase in the IC concentration in the HRAP from 1714$\pm$103 mg L^{-1} in stage I to 4421$\pm$91 mg L^{-1} in stage V (which itself was induced by process operation without effluent) (Fig. S5; Fig. S6). Indeed, the pH of the cultivation broth at the end of the experiment was constant during the daytime and similar in all units. These high pHs values likely triggered TN removal by volatilization (pKa N-NH$_4^+$ = 9.25) during stages IV and V, and explain the significant TN removal recorded during stages I and II in absence of biomass production (Posadas et al., 2017) (Fig. S7).

Evolution of the inorganic carbon concentration in the HRAP, AC and settler

A gradual increase in the IC concentration in the cultivation broth in the HRAP and consequently in the settler and AC, was observed due to the operation of the process without effluent (Fig. S6).
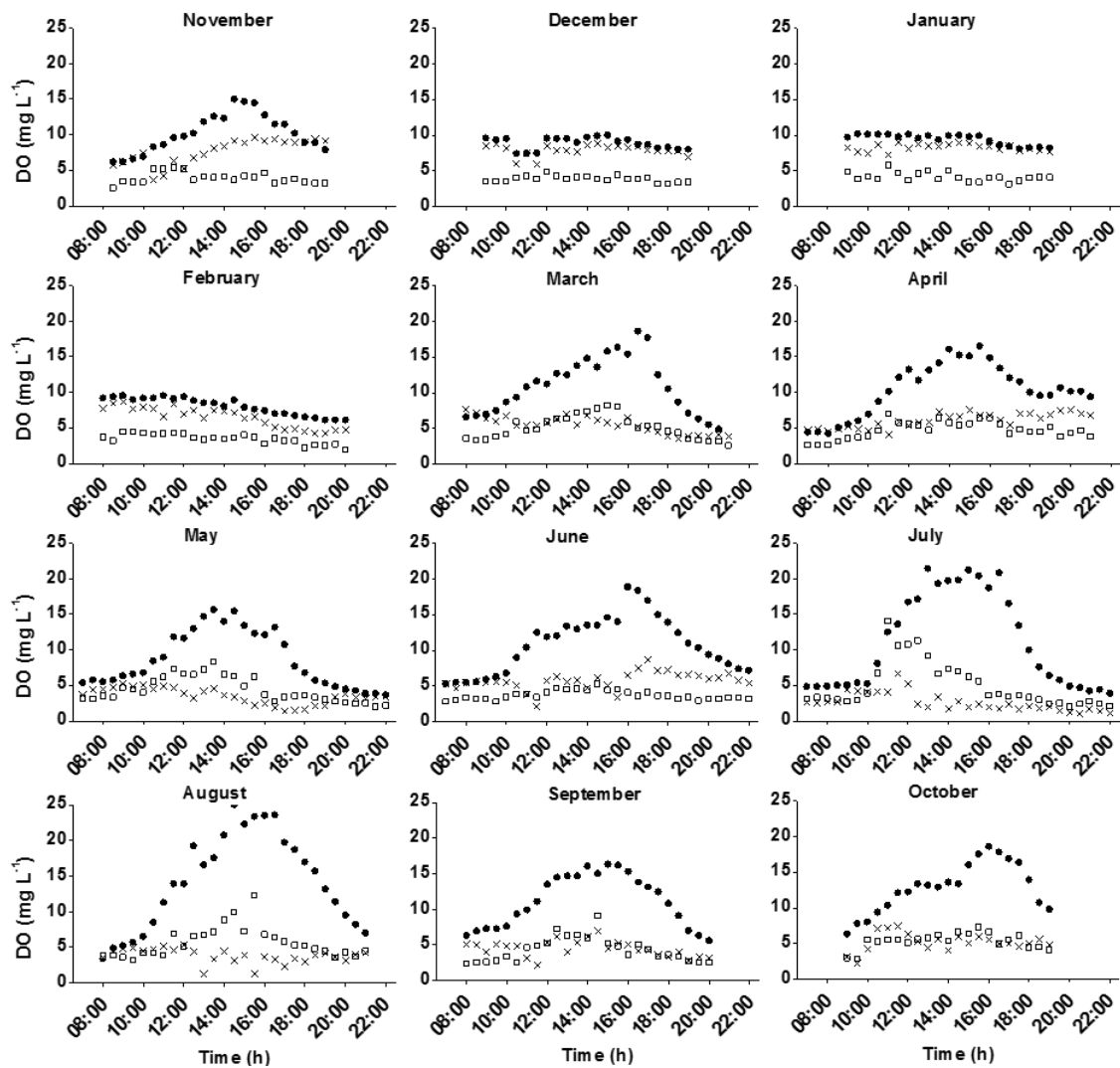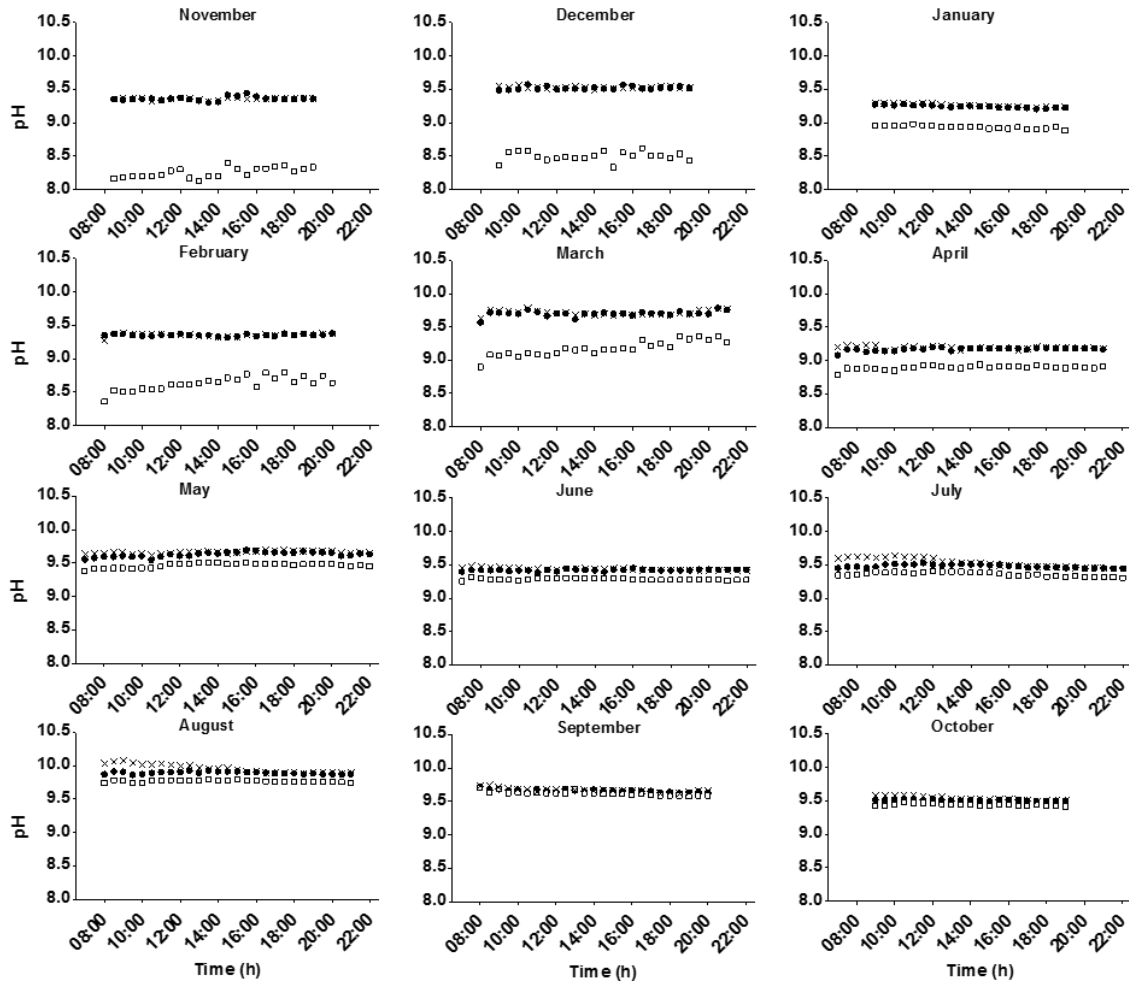
Figure S5. Time course of the pH in the cultivation broth of the HRAP (●), AC (□) and settler (×) during one diurnal cycle under steady state as a function of the operational month.
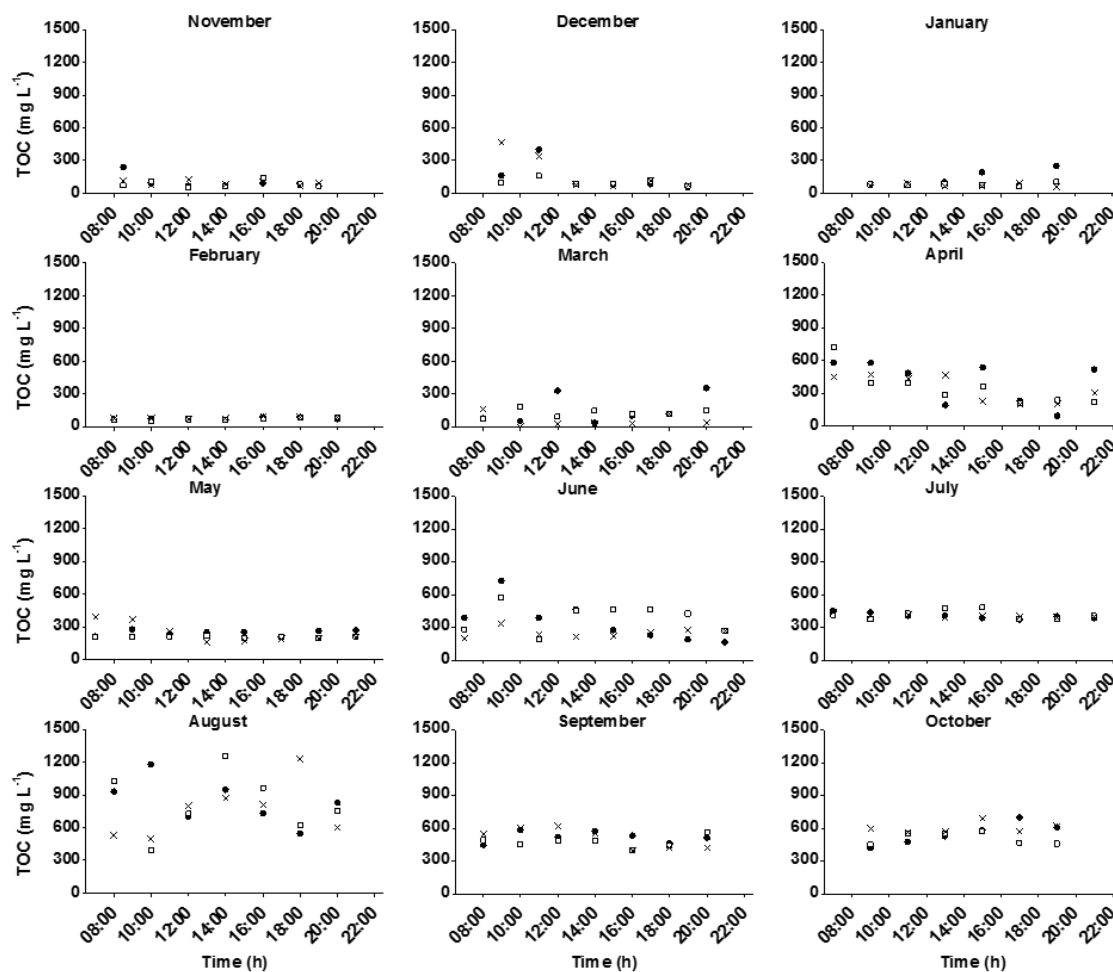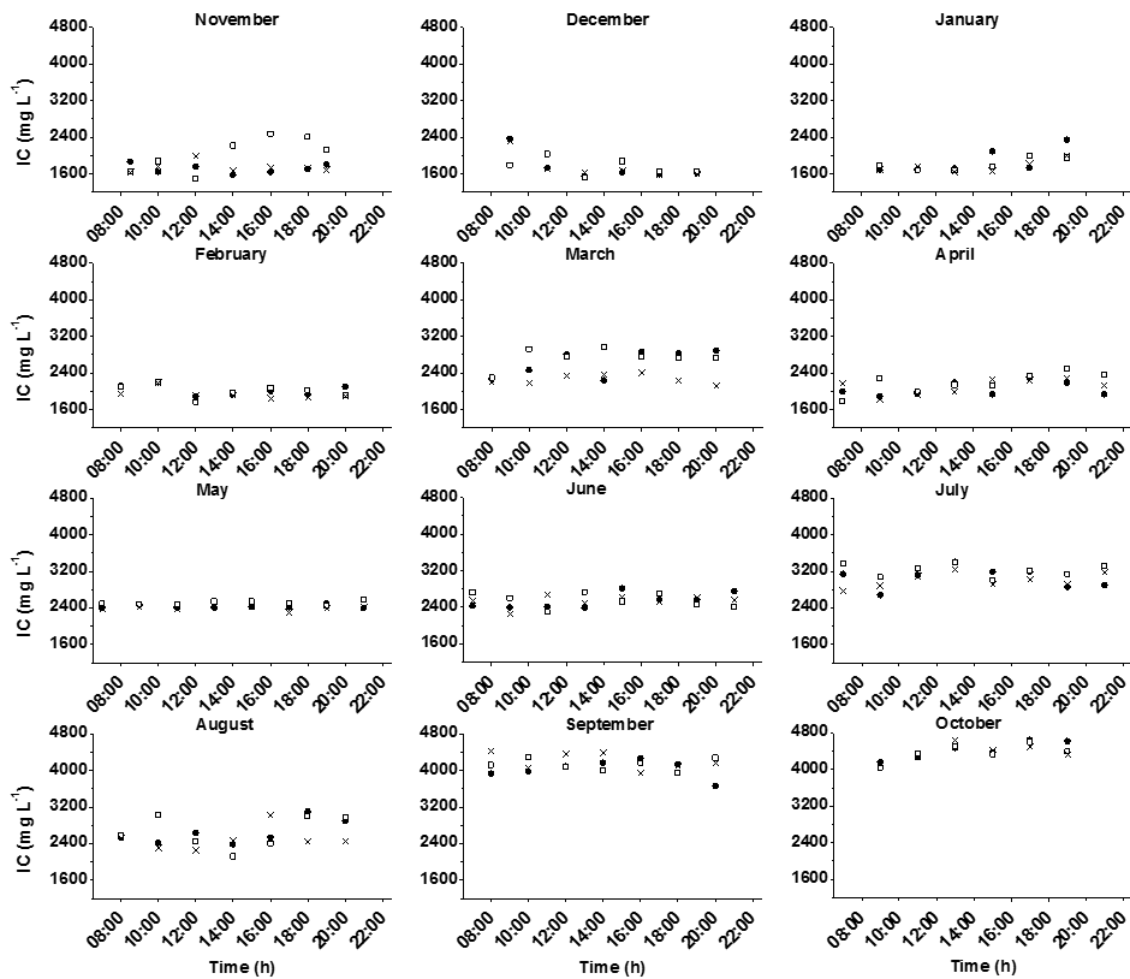
Figure S6. Time course of inorganic carbon concentration in the cultivation broth of the HRAP (●), AC (□) and settler (x) during one diurnal cycle under steady state in one year.
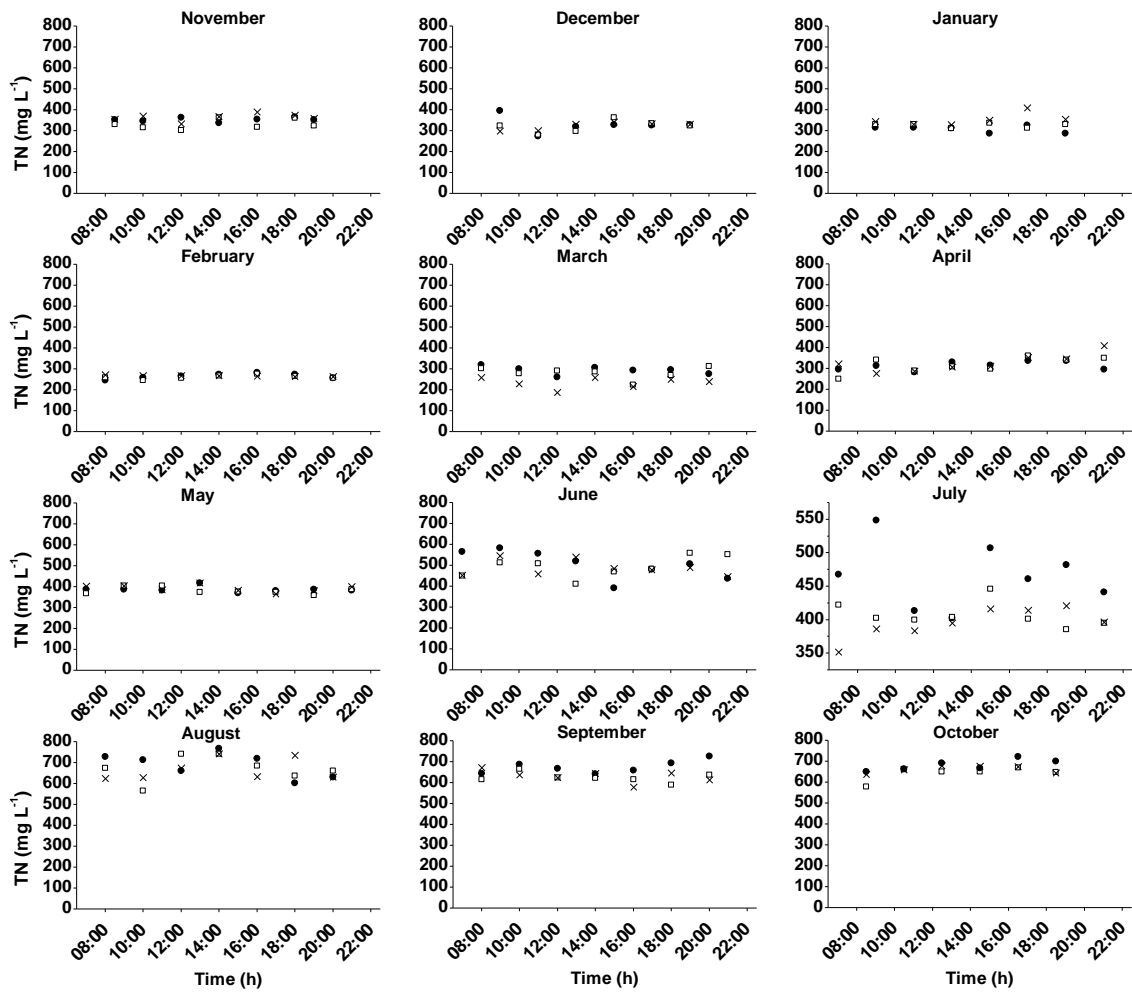
Figure S7. Time course of total nitrogen concentration in the cultivation broth of the HRAP (●), AC (□) and settler (x) during one diurnal cycle under steady state in one year.
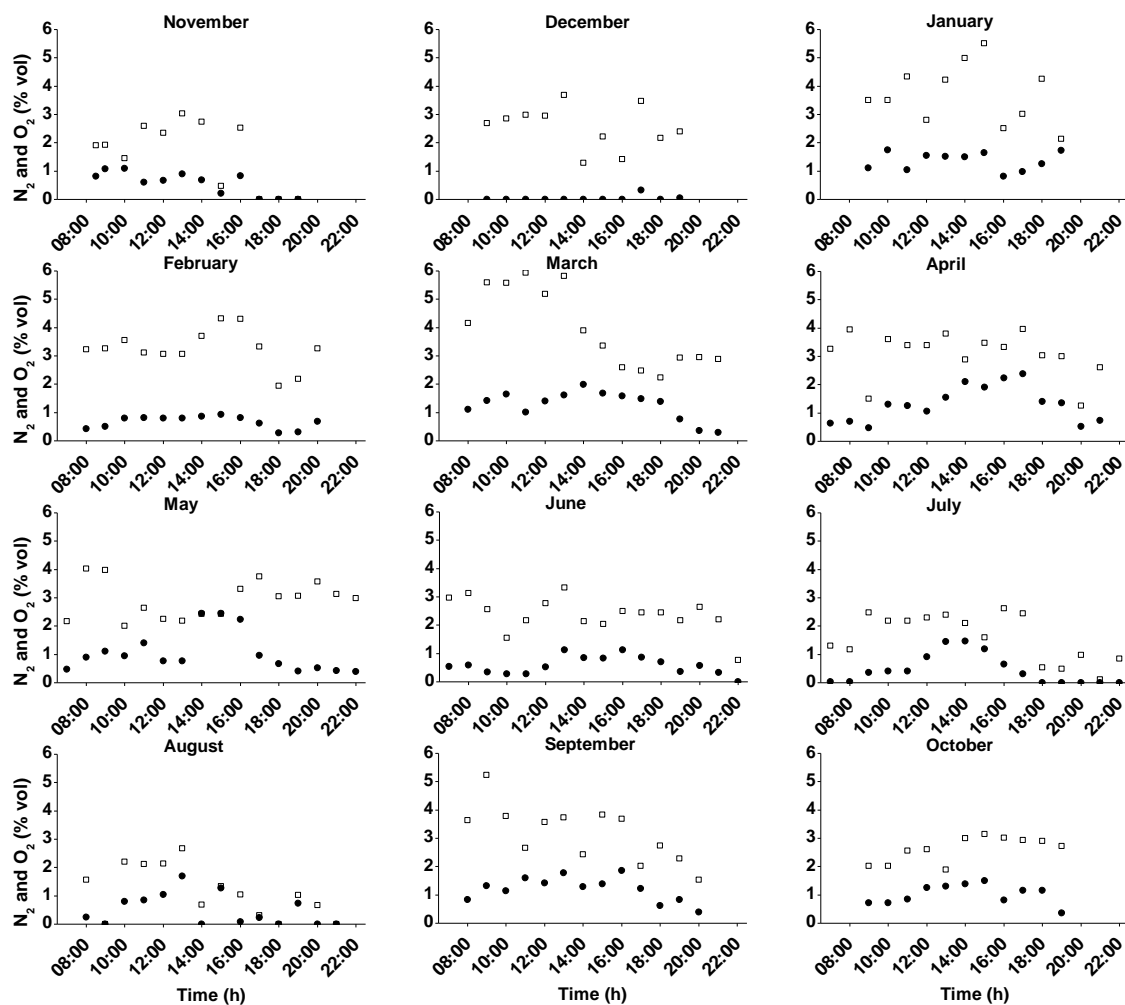
Figure S8. Time course of the concentration of the N_2 (□) and O_2 (●) in the upgraded biogas during one diurnal cycle under steady state in one year.

References

1. Bahr, M., Díaz, I., Dominguez, A., González Sánchez, A., Muñoz, R., 2014. Microalgal-biotechnology as a platform for an integral biogas upgrading and nutrient removal from anaerobic effluents. Environ. Sci. Technol. 48, 573–581. doi:10.1021/es403596m

2. Boelee, N.C., Janssen, M., Temmink, H., 2014. The effect of harvesting on biomass production and nutrient removal in phototrophic biofilm reactors for effluent polishing 1439–1452. doi:10.1007/s10811-013-0178-1

3. Molina, E., Ferna, J., Acie, F.G., Chisti, Y., 2001. Tubular photobioreactor design for algal cultures. J. Biotechnol. 92, 113–131.

4. Murphy, T.E., Berberoglu, H., 2017. Temperature Fluctuation and Evaporative Loss Rate in an Algae Biofilm Photobioreactor 134, 1–9. doi:10.1115/1.4005088

5. Posadas, E., Marín, D., Blanco, S., Lebrero, R., Muñoz, R., 2017. Simultaneous biogas upgrading and centrate treatment in an outdoors pilot scale high rate algal pond. Bioresour. Technol. 232, 133–141. doi:10.1016/j.biortech.2017.01.071

6. Posadas, E., Serejo, M.L., Blanco, S., Pérez, R., García-Encina, P.A., Muñoz, R., 2015. Minimization of biomethane oxygen concentration during biogas upgrading in algal-bacterial photobioreactors. Algal Res. 12, 221–229. doi:10.1016/j.algal.2015.09.002

7. Sousa, C., Winter, L. De, Janssen, M., Vermuë, M.H., Wijffels, R.H., 2012. Bioresource Technology Growth of the microalgae Neochloris oleoabundans at high partial oxygen pressures and sub-saturating light intensity 104, 565–570. doi:10.1016/j.biortech.2011.10.048

8. Torzillo, G., Pushparahj, B., Masojidek, J., Vonshak, A., 2003. Biological constraints in algal Biotechnology. Biotechnol. Bioprocess Eng. 8, 338–348.

Chapter 5

Innovative operational strategies in photosynthetic biogas upgrading in an outdoors pilot scale algal-bacterial photobioreactor

David Marín, Alessandro A. Carmona-Martínez, Saúl Blanco, Raquel Lebrero, Raúl Muñoz. Chemosphere 264 (2021) 128470

Innovative operational strategies in photosynthetic biogas upgrading in an outdoors pilot scale algal-bacterial photobioreactor

David Marín[1, 2, 3], Alessandro A. Carmona-Martínez[1, 2], Saúl Blanco[4], Raquel Lebrero[1, 2], Raúl Muñoz*[1, 2]

[1] Department of Chemical Engineering and Environmental Technology, School of Industrial Engineering, Valladolid University, Dr. Mergelina, s/n, 47011, Valladolid, Spain.

[2] Institute of Sustainable Processes, Dr. Mergelina, s/n, 47011, Valladolid, Spain.

[3] Universidad Pedagógica Nacional Francisco Morazán, Boulevard Centroamérica, Tegucigalpa, Honduras.

[4] Department of Biodiversity and Environmental Management, University of León, 24071 León, Spain.

[*] Corresponding author: mutora@iq.uva.es

Abstract

Three innovative operational strategies were successfully evaluated to improve the quality of biomethane in an outdoors pilot scale photobioreactor interconnected to an external absorption unit: i) the use of a greenhouse during winter conditions, ii) a direct CO_2 stripping in the photobioreactor via air stripping during winter conditions and iii) the use of digestate as make-up water during summer conditions. CO_2 concentrations in the biomethane ranged from 0.4% to 6.1% using the greenhouse, from 0.3% to 2.6% when air was injected in the photobioreactor and from 0.4% to 0.9% using digestate as make up water. H_2S was completely removed under all strategies tested. On the other hand, CH_4 concentrations in biomethane ranged from 89.5% to 98.2%, from 93.0% to 98.2% and from 96.3% to 97.9%, when implementing strategies i), ii) and iii), respectively. The greenhouse was capable of maintaining microalgae productivities of 7.5 g m^{-2} d^{-1} during continental weather conditions, while mechanical CO_2 stripping increased the pH in order to support an effective CO_2 and H_2S removal. Finally, the high evaporation rates during summer conditions allowed maintaining high inorganic carbon concentrations in the cultivation broth using centrate, which provided a cost-effective biogas upgrading.

Keywords:

Algal bacterial photobioreactor; Biogas upgrading; Greenhouse; Innovative operational strategies; Outdoors conditions

1. Introduction

Biogas originating at the anaerobic treatment of wastewater and organic waste represents a renewable energy vector capable of reducing the use of fossil fuels to satisfy the demand of electricity and heat for domestic and industrial applications (Muñoz et al., 2015). Biogas upgrading is required prior use as vehicle fuel or it is injection into gas network due to the high concentration of impurities present in raw biogas such as CO_2 (15-60%), CO (<0.6%), O_2 (0-1%), N_2 (0-2%), H_2S (0.005-2%), siloxanes (0-0.2%), NH_3 (<1%) and volatile organic compounds (<0.6%) (Ryckebosch et al., 2011). Typical compositions in biomethane varies depending on the national regulations or regional standards: $CH_4 \geq$ 90-95%, $CO_2 \leq$ 2-4%, $O_2 \leq$ 1% and insignificant amounts of H_2S (Muñoz et al., 2015). In this context, the relevance of biogas and biomethane in the EU energy sector has increased within the past years as result of the active policies for decarbonization of European economy. Indeed, the number of biogas plants has escalated from 6227 in 2009 to 17783 by the end of 2017, while biomethane production capacity has escalated from 752 GWh by 2011 to 19352 GWh by the end of 2017 (European Biogas Association, 2018).

Multiple physicochemical technologies existing at present are commercially available to remove CO_2 and H_2S from biogas in order to comply with biomethane standards. Pressure swing adsorption, water/chemical/organic scrubbing, membrane separation, or cryogenic separation provide the required levels of CO_2 removal at energy demands ranging from 0.3-0.8 kWh Nm^{-3}. *In-situ* chemical precipitation or adsorption onto activated carbon or metal ions provide the required levels of H_2S removal at operating costs in the range of 2-3 € cent Nm^{-3} (Angelidaki et al., 2018; Marín et al., 2019; Muñoz et al., 2015; Rodero et al., 2018). An integral upgrading of biogas to comply with biomethane standards requires the sequential combination of these H_2S and CO_2 removal technologies, which significantly increases the initial investment and operational fees of the process (nowadays accounting for ~30 % of the biomethane price (Stürmer et al., 2016)). The urgent need to decrease the cost and energy demand of conventional biogas upgrading has triggered research on biological methods for CO_2 and H_2S removal. Chemoautotrophic biogas upgrading can support the required levels of CO_2 bioconversion to CH_4 with renewable H_2, while *in-situ* micro-aerobic anaerobic digestion or biofiltration can provide a cost-effective H_2S removal (Farooq et al., 2018; Marín et al., 2018a; Muñoz et al., 2015; Rodero et al., 2018). However, algal-bacterial

photobioreactors constitute the only biological alternative to conventional physical-chemical processes capable of simultaneously removing CO_2 and H_2S in a single step process at low operating costs (Bahr et al., 2014; Bose et al., 2019; Muñoz et al., 2015; Nagarajan et al., 2019).

Photosynthetic biogas upgrading processes using algal-bacterial photobioreactors are based on the fixation of CO_2 by microalgae using solar energy and the aerobic oxidation of H_2S to SO_4^{2-} by sulfur oxidizing bacteria mediated by the elevated dissolved oxygen (DO) concentrations in the photobioreactor as a result of photosynthetic activity (Posadas et al., 2015; Toledo-Cervantes et al., 2016). Photosynthetic biogas upgrading processes have been previously optimized in commercially interconnected to external biogas absorption columns under indoors conditions and with artificial illumination (Bahr et al., 2014; Franco-Morgado et al., 2017; Posadas et al., 2016; Rodero et al., 2018; Serejo et al., 2015). In addition, these processes have been validated under outdoors conditions in multiple photobioreactor configurations. For instance, Posadas et al., (2017) evaluated for the first time the upgrading of biogas and centrate treatment in a 180 L commercially during summer time. Marín et al., (2018b, 2018a) assessed the impact of seasonal variations of environmental conditions on biogas upgrading performance in a 180 L commercially fed with HCO_3^-/CO_3^{2-} supplemented digestate. Similarly, Marín et al., (2019) investigated the impact of the liquid to biogas flowrate (L/G) ratio and alkalinity in the cultivation broth on the quality of biomethane in a 11.7 m^3 horizontal hybrid tubular photobioreactor. Despite the satisfactory results obtained to date, the photosynthetic biogas upgrading processes under outdoor conditions is limited by the low temperatures during winter conditions under continental climate and the need for external alkalinity sources. Therefore, innovative operating strategies are needed to provide a cost-effective photosynthetic biogas upgrading during unfavorable environmental conditions and without external alkalinity supplementation (Toledo-cervantes et al., 2017).

This study investigated, for the first time, the performance of three innovative operational strategies in order to improve the quality of biomethane and process sustainability in an outdoors pilot scale photobioreactor interconnected to an external absorption unit. These strategies aimed at overcoming previous limitations encountered during process validation under outdoors conditions (Marin et al. 2018). For this purpose, the outdoors

pilot photobioreactor interconnected to an external biogas scrubbing unit was located inside of a greenhouse during winter conditions. The potential of direct CO_2 stripping in the photobioreactor via air stripping during winter conditions and of the use of digestate as make-up water (to compensate water losses by evaporation) during summer conditions to improve the quality of biomethane were evaluated.

2. Materials and methods

2.1 Biogas and synthetic digestate

A synthetic gas mixture composed of CH_4 (70%), CO_2 (29.5%) and H_2S (0.5%) was used as a raw biogas in the present study (Abello Linde; Spain). The synthetic digestate (SWW) used during the first 225 days of experiment consisted of (per liter of distilled water): 7.40 g $NaHCO_3$, 3.70 g Na_2CO_3, 0.94 g K_2HPO_4, 1.91 g NH_4Cl, 0.02 g $CaCl_2·2H_2O$, 0.005 g $FeSO_2·7H_2O$, 0.10 g $MgSO_4·7H_2O$ and 5 ml of a micronutrient solution (composed of 0.10 g $ZnSO_4·7H_2O$, 0.10 g $MnCl_2·4H_2O$, 0.20 g H_3BO_3, 0.02 g $Co(NO_3)_2·6H_2O$, 0.02 g $Na_2MoO_4·2H_2O$, 0.0005 g $CuSO_4·5H_2O$, 0.70 g $FeSO_4·7H_2O$ and 1.02 g $EDTA·2Na·2H_2O$ per liter of distilled water). This resulted in an inorganic carbon (IC) concentration of 1500 ± 43 mg L^{-1}, total organic carbon (TOC) concentration of 54 ± 4 mg L^{-1}, total nitrogen (TN) concentration of 530 ± 19 mg L^{-1}, P-PO_4^{3-} concentration of 94 ± 8 mg L^{-1} and S-SO_4^{2-} concentration of 112 ± 7 mg L^{-1}. During the last 25 days of experiment, the IC concentration of the SWW was decreased to 532 ± 24 mg L^{-1} in order to mimic the typical composition of centrate from Valladolid wastewater treatment plant.

2.2 Experimental set-up

The photobioreactor set-up was located outdoors at the Institute of Sustainable Processes of Valladolid University. The experimental set-up was integrated by a 180 L photobioreactor divided in two water channels and with one baffle at each side of the photobioreactor. The photobioreactor has an illuminated surface of 1.20 m^2 (length = 170 cm; depth = 15 cm; width = 82 cm). The cultivation broth inside the photobioreactor was recirculated with a velocity of 20 cm s^{-1} by a 6-blade paddlewheel. An absorption unit of 2.5 L was interconnected to the photobioreactor through a conical settler of 8 L. A metallic diffuser of 2 μm pore size was installed at the bottom of the biogas scrubbing column. The photobioreactor was installed inside of a greenhouse in order to enhance the performance of the technology during winter conditions (Fig. 1). From day 99 until day

225 of experiment, air was injected directly into the photobioreactor via 3 porous stone diffusers evenly distributed along the photobioreactor.
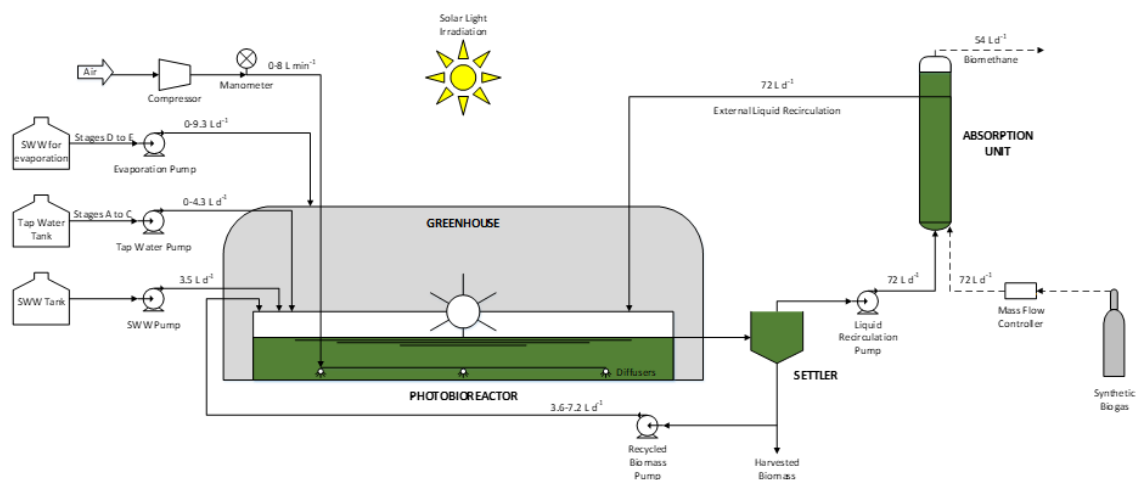
Figure 1. Schematic diagram of the outdoors experimental pilot plant used for the continuous photosynthetic upgrading of biogas.

2.3 Operational conditions and sampling procedures

The photobioreactor was inoculated with a microalgal inoculum composed of *Mychonastes homosphaera (82%), Pseudanabaena sp. (17%) and Scenedesmus sp. (1%)* (percentages are expressed in number of cells) to a concentration of 450 mg total suspended solids (TSS) L^{-1}. Five stages (namely A, B, C, D and E) were defined as a function of the operational conditions (Table 1). The SWW used as a source of nutrients was fed to the photobioreactor at a flow rate of 3.5 L d^{-1}. Meanwhile, biogas was injected at the bottom of the absorption unit at a flow rate of 72 L d^{-1} under co-current flow operation with a L/G ratio of 1.0 (Posadas et al., 2017). Tap water (days 99 – 198), highly carbonated SWW (days 199 – 225) and SWW (days 226 – 250) were supplied in order to compensate water evaporation losses but allowing process operation without effluent. Air was injected in the photobioreactor at a flow rate of 8.0 L min^{-1} from days 99 to 225 in order to evaluate the influence of mechanical CO_2 stripping in the photobioreactor on biomethane quality. Biomass productivity was fixed according to the environmental conditions present at each operational stage in order to provide a constant growth of microalgae during stages A (0.0 g m^{-2} d^{-1}), B and C (7.5 g m^{-2} d^{-1}) and D and E (15.0 g m^{-2} d^{-1}) (Table 1). Harvesting of algae-bacteria from the settler was carried out to maintain this productivity. The remaining biomass at the bottom of the settler was recirculated to the photobioreactor at a flow rate of 3.6 or 7.2 L d^{-1}.

Table 1. Environmental and operational parameters during the five operational stages.

Parameter	Stage				
	A	**B**	**C**	**D**	**E**
Date	15-Oct – 04-Nov	05-Nov – 20-Jan	21-Jan – 30-Apr	01-May – 27-May	28-May – 21-Jun
Stage period (approx. weeks)	3	11	14	3	4
Use of Greenhouse	Yes	Yes	Yes	No	No
Air Supply ($L\ min^{-1}$)	0.0	0.0	8.0	8.0	0.0
Make up water ($L\ d^{-1}$)	0.5 ± 0.2 (Tap water)	0.0 ± 0.0 (Tap water)	1.1 ± 1.2 (Tap water)	2.8 ± 1.4 (SWW)	5.2 ± 1.4 (SWW*)
Morning Average DO ($mg\ L^{-1}$)	8.2 ± 2.2	9.2 ± 1.7	10.6 ± 0.8	9.8 ± 0.7	7.7 ± 0.6
Afternoon Average DO ($mg\ L^{-1}$)	12.5 ± 5.5	12.8 ± 1.4	9.2 ± 1.1	8.2 ± 0.2	7.3 ± 0.3

Table 1. Continued.

Parameter	Stage				
	A	**B**	**C**	**D**	**E**
Average Evaporation Rate ($L\ m^{-2}\ d^{-1}$)	1.7 ± 1.2	1.1 ± 0.4	2.4 ± 1.0	5.2 ± 1.2	7.3 ± 1.1
Biomass productivity ($g\ m^{-2}\ d^{-1}$)	0.0	7.5	7.5	15.0	15.0

* - SWW with an inorganic carbon concentration of 532 ± 24 mg C L^{-1}.

The photosynthetic active radiation (PAR) outdoors and inside the greenhouse, the temperature outdoors, inside the greenhouse and in the photobioreactor and the DO concentration were daily monitored at 9:00 a.m and 4:00 p.m throughout the entire experimental period. The pH was daily measured only at 9:00 a.m since it remained constant throughout the daytime as a result of the high buffer capacity of the cultivation broth (Marín et al., 2018b). In order to measure IC, TOC, TN, $N-NO_3^-$, $N-NO_2^-$, $P-PO_4^{3-}$, $S-SO_4^{2-}$ and biomass concentrations, 100 mL of liquid samples from the photobioreactor and the SWW were drawn twice a week. In order to determine CH_4, CO_2, H_2S, N_2 and O_2 concentrations in raw biogas and biomethane, gas samples of 100 µL were taken in duplicate at 10:00 a.m twice a week. At each month, samples of the photobioreactor were taken in order to morphologically determine the structure of microalgae population.

2.4 Analytical procedures

PAR, pH, temperature and DO concentration were recorded according to Marín et al., (2018a). The concentrations of TOC, IC and TN were analyzed according to Posadas et al., (2017). $N-NO_3^-$, $N-NO_2^-$, $P-PO_4^{3-}$ and $S-SO_4^{2-}$ concentrations were quantified by HPLC-IC according to Posadas et al., (2013). The determination of TSS and VSS concentrations was carried out according to APHA (2005). Biogas and biomethane composition were determined according to Marín et al., (2018a). The determination of the N and P content of the algal bacterial biomass was determined according to Posadas et al., (2017). Finally, the identification, quantification and biometry measurements of microalgae were conducted by microscopic examination (OLYMPUS IX70, USA) of the algal–bacterial cultivation broths (fixed with lugol acid at 5% and stored at 4ºC prior to analysis) according to Sournia (1978). The microalgae growing on each unit were identified and quantified according to the European standard CEN TC 230/WG2/TG3/N83, which is based on Utermöhl´s (1958) method.

3. Results and discussion

3.1 Environmental parameters

Considerable variations in the ambient, greenhouse and photobioreactor temperatures were recorded in the course of the experimental time due to the seasonal climate variation. The ambient temperature recorded in stages A, B, C, D and E ranged from 4.0 to 23.0, -3.0 to 17.0, -3.0 to 23.0, 7.0 to 27.0 and 7.0 to 30.0 ºC, respectively (Fig. 2a). This ambient

temperature influenced directly the temperatures recorded inside the greenhouse, which ranged from 5.0 to 40.0, -4.0 to 26.0 and -2.0 to 43.0 °C in stages A, B and C, respectively (Fig. 2b). The greenhouse was responsible of the difference of temperatures due to its inherent ability to retain solar radiation. This increase in the temperature of the greenhouse exerted an important effect in the temperature of the photobioreactor. Hence, the photobioreactor temperature recorded in stages A, B, C, D and E ranged from 4.2 to 24.1, -0.2 to 18.7, 0.5 to 31.7, 6.1 to 27.6 and 8.1 to 32.2 °C, respectively (Fig. 2c). The temperature values here reported during winter time were significantly higher than those previously recorded by Marín et al., (2018a) in the same period (2.3 ± 3.1 °C), and prevent the freezing of the photobioreactor.
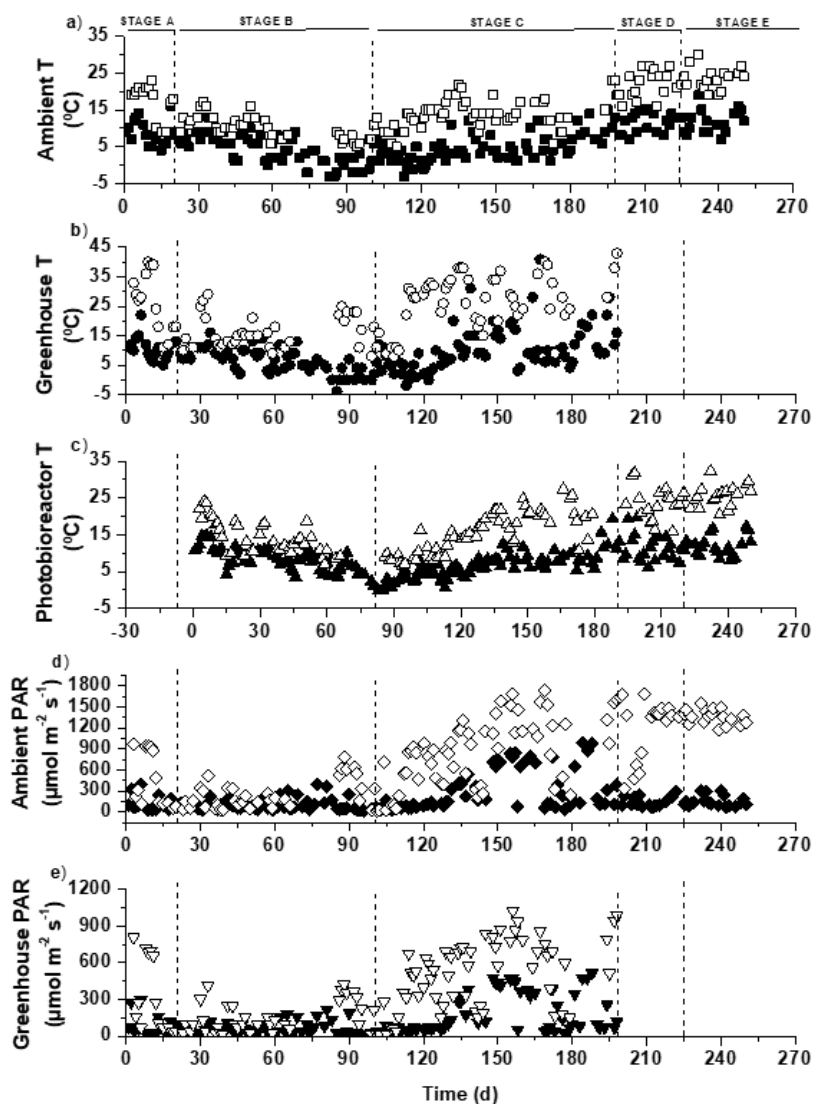

Figure 2. Time course of (a) ambient temperature, (b) temperature inside the greenhouse (c) photobioreactor temperature, (d) ambient PAR and (e) PAR inside the greenhouse during the morning (solid symbols) and afternoon (empty symbols).

The ambient PAR recorded in stages A, B, C, D and E ranged from 26 to 966, 24 to 790, 27 to 1738, 65 to 1684 and 76 to 1549 $\mu mol\ m^{-2}\ s^{-1}$, respectively (Fig. 2d). The plastic material of the greenhouse produced a significant decrease in the PAR recorded inside during stages A, B and C, which ranged from 17 to 807, 12 to 422 and 17 to 1024 $\mu mol\ m^{-2}\ s^{-1}$, respectively (Fig. 2e). Overall, the average decrease in PAR during the daytime was 36% along the three initial stages carried out inside the greenhouse. It is important to stress that these differences in PAR among the three initial stages were inherent to the seasonal variability of the environmental conditions throughout the experimental period. Environmental parameters such as temperature and PAR governed the biomass productivity set (and controlled via biomass wasting through the settler) at each stage, which was gradually increased from 0.0 to 15.0 $g\ m^{-2}\ d^{-1}$ (Table 1), in accordance with Marín et al., (2018a) and Posadas et al., (2017) in a similar photobioreactor under outdoor conditions.

The gradual increases in ambient temperature and ambient PAR during the experimentation time were correlated with the evaporation rate from the cultivation broth of the photobioreactor. The average evaporation rates recorded in stages A, B, C, D and E were 1.7 ± 1.2, 1.1 ± 0.4, 2.4 ± 1.0, 5.2 ± 1.2 and $7.3 \pm 1.1\ L\ m^{-2}\ d^{-1}$, respectively (Table 1; Fig. S1). The greenhouse prevented the external input of water from rain into the photobioreactor, which resulted in positive evaporation rates values throughout the entire experiment. In this context, Marín et al., (2018a) reported an evaporation rate value of $-0.3 \pm 1.8\ L\ m^{-2}\ d^{-1}$ in a 180 L outdoors photobioreactor during winter time in Valladolid, while Rodero et al., (2019) reported rain inputs of $4.4\ L\ m^{-2}\ d^{-1}$ in a 9.6 m^3 outdoors photobioreactor in Chiclana de la Frontera (Spain), which resulted in evaporation rates of $-0.1 \pm 0.6\ L\ m^{-2}\ d^{-1}$.

Finally, the mean DO concentrations recorded in stages A, B, C, D and E in the morning accounted for 8.2 ± 2.2, 9.2 ± 1.7, 10.6 ± 0.8, 9.8 ± 0.7 and $7.7 \pm 0.6\ mg\ L^{-1}$, respectively. In the afternoon, the average values were 12.5 ± 5.5, 12.8 ± 1.4, 9.2 ± 1.1, 8.2 ± 0.2 and $7.3 \pm 0.3\ mg\ L^{-1}$, respectively (Table 1; Fig. S2). The high DO values here reported as a result of the low oxygen demand of the synthetic digestate used did not inhibit the photosynthetic activity of microalgae. In this context, Molina et al., (2001) reported that outdoors *Spirulina* productivities increased when the DO concentration decreased from

35 to 20 mg O_2 L^{-1}. The lower DO concentrations recorded under favorable environmental conditions (stages D and E) were likely due to the higher endogenous respiration, which supported an active oxygen demand to oxidize the intracellular reserves of algae and bacteria for cell maintenance, mediated by the higher biomass concentrations prevailing in the cultivation broth (approx. 3 times higher than in stages A, B and C) and the higher ambient temperature that decreased DO in equilibrium with air and accelerated biological reactions.

3.2 Photobioreactor parameters

The pH in the photobioreactor remained fairly constant throughout stage A and B, with an average value of 9.1 ± 0.1, as consequence of the high buffer capacity of the cultivation broth (Fig. 3a). In stage C and D, the injection of air directly into the photobioreactor caused a gradual increase in the pH up to 9.9 as a result of a direct CO_2 stripping in the microalgae medium of the photobioreactor (Fig 3a). Finally, the pH remained constant at 9.8 ± 0.1 in stage E. This high pH in the absence of air stripping was likely due to the high photosynthetic activity of microalgae and the high IC concentration prevailing in the the photobioreactor mediated by the high evaporation rates.
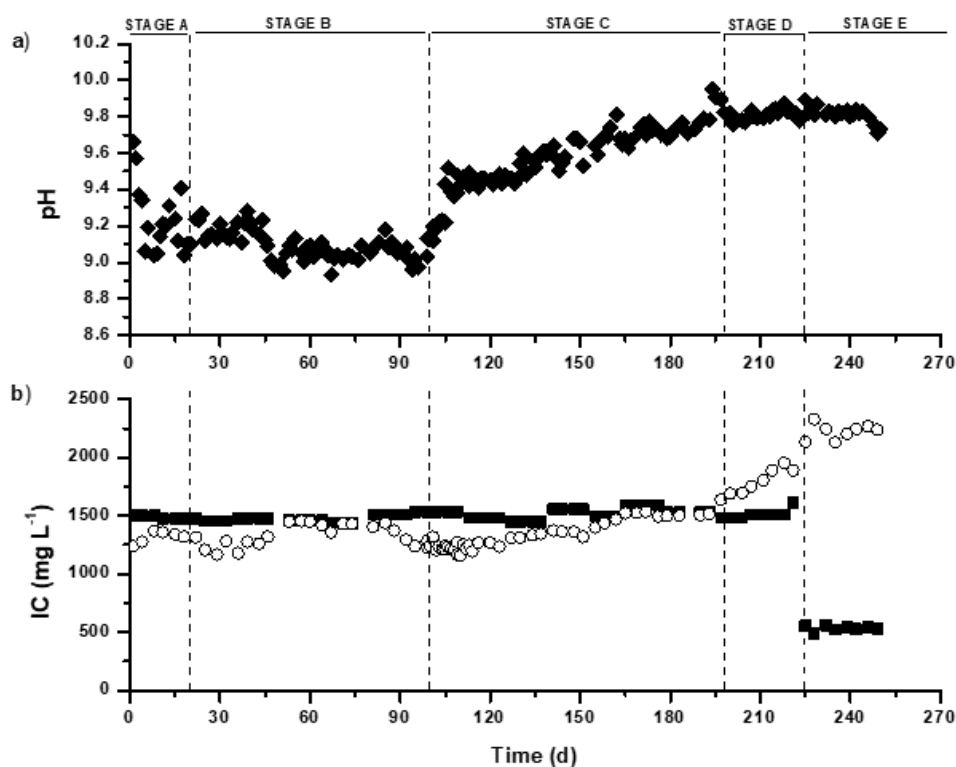

Figure 3. Time course of the (a) pH in the photobioreactor and (b) concentration of inorganic carbon in the SWW (■) and in the photobioreactor (○).

The IC concentration in the photobioreactor fluctuated during stages A and B, with an average value of 1332 ± 87 mg L^{-1} (Fig. 3b). A gradual increase in the IC concentration up to 1639 mg L^{-1} was observed in stage C likely due to the increase in pH induced by the injection of air directly into the photobioreactor. A rapid increase in the IC concentration up to 1952 mg L^{-1} was recorded during stage D mediated by the increase in water evaporation losses caused by the higher temperatures and removal of the greenhouse (Fig. 3b; Table 1). Interestingly, the external supply of air in the photobioreactor directly impacted on the pH and IC concentration of the cultivation broth, but it did not increase the evaporation rate. The increase in the evaporation rate was correlated to the gradual increase in ambient temperature and PAR during the experimental period. Despite the decrease in the IC concentration of the SWW from 1500 ± 43 mg L^{-1} to 532 ± 24 mg L^{-1} during stage E, the IC concentration in the photobioreactor remained constant at 2236 ± 61 mg L^{-1}, which confirmed that a high alkalinity can be maintained in the cultivation broth using centrate as consequence of the high evaporation losses in the photobioreactor under favorable environmental conditions (Fig. 3b).

TN concentration recorded in the photobioreactor steadily increased from 65 mg N L^{-1} at the beginning of the experiment up to 556 mg L^{-1} by day 250 (Fig. S3a). This increase suggests that the nitrogen loading rate exceeded the nitrogen fixation rate by microalgae and was also promoted by the gradual increase of the evaporation rates. Nitrifying bacteria were responsible of the oxidation of NH_4^+ from the SWW used as a source of nutrients, to $N-NO_2^-$ and $N-NO_3^-$. In this sense, $N-NO_2^-$ concentration progressively increased from stage A till the middle of stage C (day 144) up to 220 mg L^{-1} as consequence of the partial oxidation of NH_4^+ (Fig. S3b). However, a rapid decrease in the $N-NO_2^-$ concentration was observed from day 144 concomitantly with an increase in $N-NO_3^-$ concentration up to values of 440 mg L^{-1} by the end of stage E (Fig. S3c). The reasons underlying the partial nitrification of NH_4^+ at temperatures < 28 ºC in excess of DO during stages A and B, and the sudden increase in NO_2^- oxidation activity in stage C, remain unclear (Metcalf and Eddy, 2003).

On the contrary, $P-PO_4^{3-}$ concentrations recorded in the photobioreactor remained constant during stages A and B (109 mg L^{-1}), and gradually increased in stage C up to 263 mg L^{-1} concomitantly with the increase in water evaporation from the

photobioreactor. In stage D the $P-PO_4^{3-}$ concentration further increased up to 395 mg L^{-1} and remained constant in stage E at 400 ± 7 mg L^{-1} (Fig. S4). The increase in $P-PO_4^{3-}$ concentration in stages D and E was likely due to the operation without greenhouse, which along with the higher temperatures of the cultivation broth, boosted water evaporation and the concentration of all dissolved salts in the medium.

Finally, an increase in the $S-SO_4^{2-}$ concentration of the photobioreactor from 123 mg L^{-1} at the beginning of stage A to 1027 mg L^{-1} by the end of stage E was recorded as result of the aerobic microbial oxidation of the H_2S. $S-SO_4^{2-}$ accumulation was also triggered with the increase in evaporation losses during stages D and E (Fig. S5). These $S-SO_4^{2-}$ concentrations were below the typical inhibitory thresholds for microbial activity reported in literature (74 g L^{-1}) (Lee et al., 2006; Muñoz et al., 2015).

3.3 Biogas upgrading

Eukaryotic algae and prokaryotic cyanobacteria were responsible of the bioconversion of the CO_2 present in biogas into biomass using the electrons released during water photolysis, which entailed a concomitant release O_2. In this sense, the CO_2 concentration of biomethane in stage A ranged between 1.9% and 4.9%, with CO_2 removal efficiencies (REs) changing from 83.5% to 93.6% (Fig. 4a). During stage B, CO_2 concentration varied from 2.4% to 6.1%, with CO_2-REs between 79.7% and 92.0%. A decrease in CO_2 concentration from 2.6% to 0.3% was observed during stage C due to the pH increase mediated by the injection of air, which entailed CO_2-REs between 91.4% and 98.7%. Finally, CO_2 concentrations in stages D and E remained constant at 0.5%, which corresponded to CO_2-REs of 98.2% (Fig. 4a). The high CO_2 removal efficiencies observed in stages C to E were supported by the high pH and buffer capacity of the cultivation broth under the prevailing operational conditions. These values here achieved were higher than those reported by Rodero et al., (2020), who observed CO_2 concentrations between 1.5 and 4.4% in a similar indoors experimental set-up with a higher IC concentration in the cultivation broth (1203-3814 mg L^{-1}). It should be also stressed that the CO_2-REs observed in stages A to C were higher than those previously described during winter by Marín et al., (2018a), who recorded CO_2 REs between 63.6% and 85.9% in a similar outdoors photobioreactor configuration during winter without greenhouse. Therefore, these results validated the use of greenhouses and the injection of

air during winter conditions in order to enhance the CO_2-REs. The CO_2 concentrations achieved in stages C, D and E fulfilled with the current legislation on the use of biogas ($CO_2 \leq$ 2-4%) (European Committee for Standardization, 2018, 2017; Muñoz et al., 2015).

H_2S was completely removed from biogas regardless of the operational conditions tested. H_2S was transferred from biogas to the algal-bacterial cultivation broth in the scrubbing column, where it was oxidized into SO_4^{2-} by aerobic sulphur oxidizing bacteria using the dissolved oxygen contained in the recirculating broth. The main biological mechanism of H_2S oxidation into SO_4^{2-} can be described by the following equation:

$$H_2S + CO_2 + N,P + O_2 \rightarrow biomass + S/SO_4^{2-} + H_2O$$
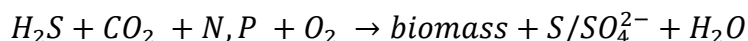
In addition, direct chemical oxidization into sulphate could also occur. This complete elimination was associated to the higher H_2S aqueous solubility (Henry´s law constant = C_L/C_G) compared to that of CO_2. Indeed, H_{H2S} is approximately three times higher than the H_{CO2} (Sander, 2015). These results were in accordance to Marín et al., (2018a), who reported a complete removal of H_2S in a similar outdoors photobioreactor configuration without greenhouse.

The N_2 concentration in biomethane in stages A and B remained constant at average values of 2.6 ± 0.5%. Interestingly, air stripping induced a reduce in the N_2 concentration from 2.5% to 1.0% during stage C, which remained constant at an average value of 1.7 ± 0.3% in stages D and E (Fig. 4b). This decrease in N_2 concentration at a constant L/G ratio might be explained by a decrease in the N_2 dissolved in the photobioreactor as consequence of the gradual increase in the salinity of the cultivation broth (ultimately induced by the increasing water evaporations). The N_2 concentrations here obtained were lower than those reported by Marín et al., (2018a), who recorded N_2 concentration values of up to 5.8% in a similar outdoors photobioreactor configuration during winter time at a L/G of 1.

The O_2 concentration recorded in biomethane exhibited a similar behavior than that observed for N_2. Thus, O_2 concentration remained constant at an average value of 1.0 ±

0.3% during stages A and B, and decreased to 0.4% during stage C. Similarly, the O_2 concentration remained constant in stages D and E at average values of $0.4 \pm 0.1\%$ (Fig. 4b). The decrease in biomethane O_2 concentrations from stage C to E was likely induced by the lower DO present in the cultivation broth used as scrubbing solution in the biogas absorption column. The biomethane O_2 concentration here reported fulfilled with the current legislation on the use of biogas which demands O_2 levels $\leq 1\%$ (European Committee for Standardization, 2018, 2017; Muñoz et al., 2015).

Finally, CH_4 concentration recorded in biomethane ranged from 91.5% to 94.4% in stage A, 89.5% to 94.6% in stage B, 93.0% to 98.2% in stage C, 96.3% to 97.6% in stage D and 97.0% to 97.9% in stage E (Fig. 4c). The high CH_4 concentration obtained during winter conditions compared to previous studies was due to the high capacity of the system to remove CO_2 while preventing an active desorption of N_2 and O_2. Negligible losses of CH_4, lower than 1% of the CH_4 input, were recorded as a result of the low aqueous solubity of methane ($H_{CH4} \approx 0.03$ at 25 ºC). In addition, the presence of aerobic conditions likely supported the growth of methanotrophs, which prevented CH_4 emission from the cultivation broth in the photobioreactor (Muñoz et al., 2015; Serejo et al., 2015). The biogas upgrading performance here achieved was superior to that reported by Marín et al., (2020), who observed CH_4 concentrations up to 94.6% in a similar outdoors experimental set-up without greenhouse during autumn at a L/G of 1. The CH_4 concentrations obtained in the upgraded biogas also fulfilled with the current legislation on the use of biogas (European Committee for Standardization, 2018, 2017; Muñoz et al., 2015).
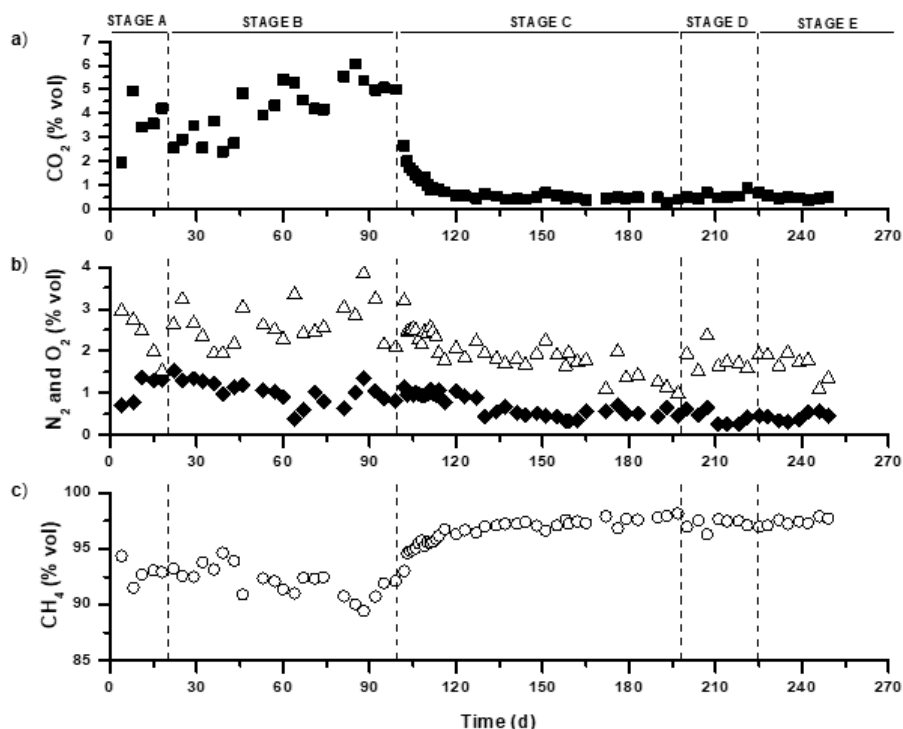
Figure 4. Time course of the concentration of (a) CO_2 (■), (b) N_2 (△) and O_2 (◆), and (c) CH_4 (○) in the upgraded biogas.

3.4 Microalgae biomass parameters

The VSS concentration in the photobioreactor increased from 0.14 g L^{-1} at day one to 0.53 g L^{-1} at the end of stage A. This increase was due to the fact that no biomass harvesting was conducted in order to reach a pre-determined biomass concentration in this stage (Fig. 5a; Table 1). In stage B, this concentration decreased to steady state values of 0.30 g L^{-1} as a result of the constant withdrawal of biomass to maintain a biomass productivity of 7.5 g m^{-2} d^{-1}. By the end of stage C, an increase in biomass concentration up 0.83 g L^{-1} was observed, which was supported by the more favorable environmental conditions. Similarly, an increased in biomass concentration up to 1.34 g L^{-1} was observed by the end of stage D regardless of the increase in biomass withdrawal to 15 g m^{-2} d^{-1}. Finally, an average VSS concentration of 1.25 g L^{-1} was recorded in stage E (Fig. 5a). At this point, it is important to highlight that the VSS concentration during each stage was determined by the predominanting environmental conditions and biomass productivity imposed in each stage (Table 1). The greenhouse provided the local environmental conditions in the photobioreactor to maintain higher VSS concentrations in the photobioreactor during the winter months than those reported by Marín et al., (2018a) in a similar photobioreactor.

Figure 5. Time course of the (a) concentration of volatile suspended solids in the photobioreactor and (b) structure of microalgae population in the photobioreactor.

The structure of the microalgal inoculum was gradually replaced by a microalgae assemblage composed of *Mychonastes homosphaera* (78%) and *Navicula sp.* (22%) during stage A (October) (Fig. 5b). In stage B, *Mychonastes homosphaera* was the dominant microalga in the consortium, accounting for a share of 95% in November, 61% in December and 100% in January. The dominant microalgae by the end of stage C was *Pseudanabaena sp.* (66%) and *Mychonastes homosphaer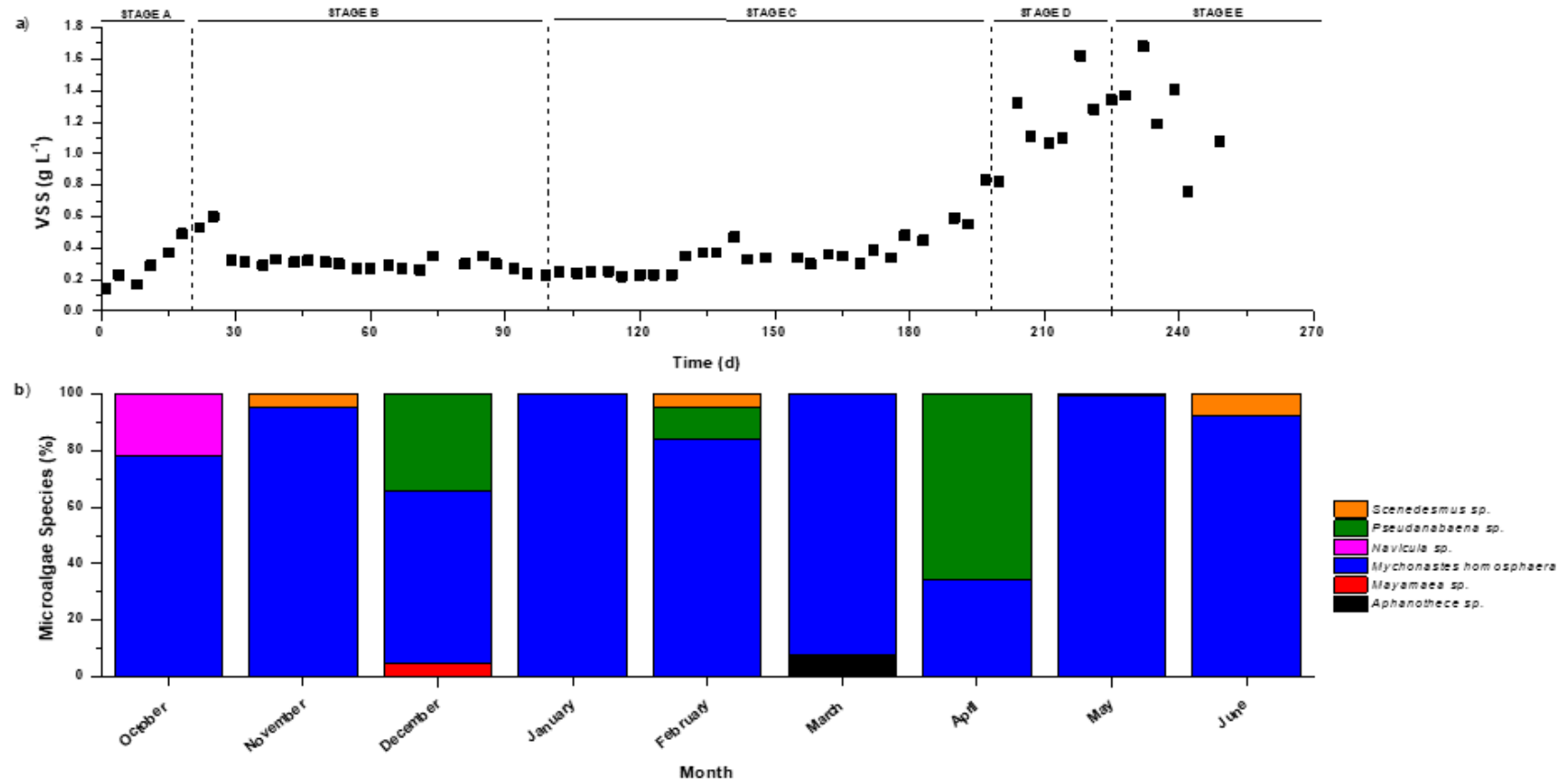a* (34%) (April). Interestingly, *Mychonastes homosphaera* represented 99% of the microalgae population and *Pseudanabaena sp.* accounted only for 1% (May) in stage D. Finally, the microalgae assemblage in stage E was composed of *Mychonastes homosphaera* (92%) and *Scenedesmus sp.* (8%) (June) (Fig. 5b). It's important to highlight the fact that ambient temperature and PAR were the most important environmental parameters determining the microalgae population structure prevailing in the photobioreactor, which were directly impacted by the use of a greenhouse during stages A to C. Temperature induce an exponential influence on the bioreactions occurring in microalgae, which ultimately determine the specific microalgae growth rate and the dominance of a microalga species under continuous cultivation. Variations in temperature can also affect the magnitude of algal nutrients uptake and therefore the phytoplankton growth processes can be indirectly affected (Beardall and Stojkovic, 2006). The PAR controls microalgae growth rate, inducing the inhibition of photosynthesis at high light intensities in some species, which would result in changes in the dominant species in the system (Beardall and Stojkovic, 2006). The use of tap water or $Na_2CO_3/NaHCO_3$ supplemented SWW in order to compensate water evaporation also modified the characteristics of the cultivation broth (in terms of salinity), which likely impacted microalgae growth. Finally, process operation under different biomass productivities (set by controlling the biomass wastage rate from the settler) likely influenced the microalgae population structure. However, the changes in microalgae population structure along the experiment were not correlated to biogas upgrading efficiency, since photosynthetic activity was actively maintained regardless of the dominant microalgae species. Indeed, different CO_2 removal efficiencies and CH_4 contents were recorded in November and June or January and May under similar microalgae population structures.

An analysis of the N and P fixed and oxidized by the algal-bacterial biomass was conducted and summarized in Table 2. A share of 34 ± 5, 83 ± 5, 88 ± 3, 50 ± 8 and 39

$\pm$ 5% of the nitrogen supplied with the SWW was fixed into biomass at stages A to E, respectively. Similarly, the share of the input nitrogen oxidized into NO_2^- and NO_3^- accounted for 66 ± 6, 12 ± 3, 29 ± 4, 16 ± 3 and $3 \pm 1\%$ in stages A, B, C, D and E, respectively. Similarly, a share of 32 ± 3, 62 ± 6, 53 ± 13, 30 ± 4 and $25 \pm 4\%$ of the phosphate input was assimilated into biomass.

Table 2. Nutrient recovery via biomass assimilation.

Stage	N		P
	Fixed (%)	**Oxidized (%)**	**Fixed (%)**
A	34 ± 5	66 ± 6	32 ± 3
B	83 ± 5	12 ± 3	62 ± 6
C	88 ± 3	29 ± 4	53 ± 13
D	50 ± 8	16 ± 3	30 ± 4
E	39 ± 5	3 ± 1	25 ± 4

4. Conclusions

This study proved for the first time the effectiveness of three innovative operational strategies in an outdoors pilot photobioreactor interconnected to a biogas absorption unit to overcome the main technical limitations of photosynthetic biogas upgrading. The use of a greenhouse and direct CO_2 stripping in the photobioreactor via air stripping during winter conditions, and the use of digestate as a make-up water during summer conditions can provide a biomethane that fulfilled with the current legislation on the use of biogas.

Acknowledgements

References

1. Angelidaki, I., Treu, L., Tsapekos, P., Luo, G., Campanaro, S., Wenzel, H., Kougias, P.G., 2018. Biogas upgrading and utilization: Current status and perspectives. Biotechnol. Adv. 36, 452–466. https://doi.org/10.1016/j.biotechadv.2018.01.011

2. APHA, 2005. Standard Methods for the Examination of Water and Wastewater, 21st ed. Public Health Association, Washington DC.

3. Bahr, M., Díaz, I., Dominguez, A., González Sánchez, A., Muñoz, R., 2014. Microalgal-biotechnology as a platform for an integral biogas upgrading and nutrient removal from anaerobic effluents. Environ. Sci. Technol. 48, 573–581. https://doi.org/10.1021/es403596m

4. Beardall, J., Stojkovic, S., 2006. Microalgae under Global Environmental Change : Implications for Growth and Productivity , Populations and Trophic Flow. Scienceasia 1, 1–10. https://doi.org/10.2306/scienceasia1513-1874.2006.32(s1).001

5. Bose, A., Lin, R., Rajendran, K., O'Shea, R., Xia, A., Murphy, J.D., 2019. How to optimise photosynthetic biogas upgrading: a perspective on system design and microalgae selection. Biotechnol. Adv. 107444. https://doi.org/10.1016/j.biotechadv.2019.107444

6. European Biogas Association, 2018. EBA Statistical Report 2018 [WWW Document]. URL https://www.europeanbiogas.eu/eba-statistical-report-2018/ (accessed 12.2.19).

7. European Committee for Standardization, 2018. UNE EN 16723-2:2018 Natural gas and biomethane for use in transport and biomethane for injection in the natural gas network - Part 2: Automotive fuels specification [WWW Document]. URL https://www.en-standard.eu/une-en-16723-2-2018-natural-gas-and-biomethane-for-use-in-transport-and-biomethane-for-injection-in-the-natural-gas-network-part-2-automotive-fuels-specification/ (accessed 12.10.19).

8. European Committee for Standardization, 2017. UNE EN 16723-1:2017 Natural gas and biomethane for use in transport and biomethane for injection in the natural gas network - Part 1: Specifications for biomethane for injection in the natural gas network [WWW Document]. URL https://www.en-standard.eu/une-en-16723-1-2017-natural-gas-and-biomethane-for-use-in-transport-and-biomethane-for-injection-in-the-natural-gas-network-part-1-specifications-for-biomethane-for-injection-in-the-natural-gas-network/ (accessed 12.10.19).

9. Farooq, M., Almustapha, M.N., Imran, M., Saeed, M.A., Andresen, J.M., 2018. In-situ regeneration of activated carbon with electric potential swing desorption (EPSD) for the H2S removal from biogas. Bioresour. Technol. 249, 125–131. https://doi.org/10.1016/j.biortech.2017.09.198

10. Franco-Morgado, M., Alcántara, C., Noyola, A., Muñoz, R., González-Sánchez, A., 2017. A study of photosynthetic biogas upgrading based on a high rate algal pond under alkaline conditions: Influence of the illumination regime. Sci. Total Environ. 592, 419–425. https://doi.org/10.1016/j.scitotenv.2017.03.077

11. Lee, E.Y., Lee, N.Y., Cho, K.S., Ryu, H.W., 2006. Removal of hydrogen sulfide by sulfate-resistant Acidithiobacillus thiooxidans AZ11. J. Biosci. Bioeng. 101, 309–314. https://doi.org/10.1263/jbb.101.309

12. Marín, D., Carmona-Martínez, A.A., Lebrero, R., Muñoz, R., 2020. Influence of the diffuser type and liquid-to-biogas ratio on biogas upgrading performance in an outdoor pilot scale high rate algal pond. Fuel 275, 117999. https://doi.org/10.1016/j.fuel.2020.117999

13. Marín, D., Ortíz, A., Díez-Montero, R., Uggetti, E., García, J., Lebrero, R., Muñoz, R., 2019. Influence of liquid-to-biogas ratio and alkalinity on the biogas upgrading performance in a demo scale algal-bacterial photobioreactor. Bioresour. Technol. 280, 112–117. https://doi.org/10.1016/j.biortech.2019.02.029

14. Marín, D., Posadas, E., Cano, P., Pérez, V., Blanco, S., Lebrero, R., 2018a. Seasonal variation of biogas upgrading coupled with digestate treatment in an outdoors pilot scale algal-bacterial photobioreactor. Bioresour. Technol. 263, 58–66. https://doi.org/10.1016/j.biortech.2018.04.117

15. Marín, D., Posadas, E., Cano, P., Pérez, V., Lebrero, R., Muñoz, R., 2018b. Influence of the seasonal variation of environmental conditions on biogas upgrading in an outdoors pilot scale high rate algal pond. Bioresour. Technol. 255, 354–358. https://doi.org/10.1016/j.biortech.2018.01.136

16. Metcalf, Eddy, 2003. Wastewater Engineeering and Reuse. Mc GrawHill.

17. Molina, E., Ferna, J., Acie, F.G., Chisti, Y., 2001. Tubular photobioreactor design for algal cultures. J. Biotechnol. 92, 113–131.

18. Muñoz, R., Meier, L., Diaz, I., Jeison, D., 2015. A review on the state-of-the-art of physical/chemical and

biological technologies for biogas upgrading. Rev. Environ. Sci. Bio/Technology 14, 727–759. https://doi.org/10.1007/s11157-015-9379-1

19. Nagarajan, D., Lee, D.-J., Chang, J.-S., 2019. Integration of anaerobic digestion and microalgal cultivation for digestate bioremediation and biogas upgrading. Bioresour. Technol. 290, 121804. https://doi.org/10.1016/j.biortech.2019.121804

20. Posadas, E., García-Encina, P.A., Soltau, A., Domínguez, A., Díaz, I., Muñoz, R., 2013. Carbon and nutrient removal from centrates and domestic wastewater using algal-bacterial biofilm bioreactors. Bioresour. Technol. 139, 50–58. https://doi.org/10.1016/j.biortech.2013.04.008

21. Posadas, E., Marín, D., Blanco, S., Lebrero, R., Muñoz, R., 2017. Simultaneous biogas upgrading and centrate treatment in an outdoors pilot scale high rate algal pond. Bioresour. Technol. 232, 133–141. https://doi.org/10.1016/j.biortech.2017.01.071

22. Posadas, E., Serejo, M.L., Blanco, S., Pérez, R., García-Encina, P.A., Muñoz, R., 2015. Minimization of biomethane oxygen concentration during biogas upgrading in algal-bacterial photobioreactors. Algal Res. 12, 221–229. https://doi.org/10.1016/j.algal.2015.09.002

23. Posadas, E., Szpak, D., Lombó, F., Domínguez, A., Díaz, I., Blanco, S., García-Encina, P.A., Muñoz, R., 2016. Feasibility study of biogas upgrading coupled with nutrient removal from anaerobic effluents using microalgae-based processes. J. Appl. Phycol. 28, 2147–2157. https://doi.org/10.1007/s10811-015-0758-3

24. Rodero, M. del R., Severi, C.A., Rocher-Rivas, R., Quijano, G., Muñoz, R., 2020. Long-term influence of high alkalinity on the performance of photosynthetic biogas upgrading. Fuel 281, 118804. https://doi.org/10.1016/j.fuel.2020.118804

25. Rodero, R., Ángeles, R., Marín, D., Díaz, I., Colzi, A., Posadas, E., Lebrero, R., Muñoz, R., 2018a. Biogas Purification and Upgrading Technologies, in: Tabatabaei, M., Ghanavati, H. (Eds.), Biogas: Fundamentals, Process, and Operation. Springer International Publishing, pp. 239–276. https://doi.org/10.1007/978-3-319-77335-3

26. Rodero, R., Lebrero, R., Serrano, E., Lara, E., Arbib, Z., García-Encina, P.A., Muñoz, R., 2019. Technology validation of photosynthetic biogas upgrading in a semi-industrial scale algal-bacterial photobioreactor. Bioresour. Technol. 279, 43–49. https://doi.org/10.1016/j.biortech.2019.01.110

27. Rodero, R., Posadas, E., Toledo-Cervantes, A., Lebrero, R., Muñoz, R., 2018b. Influence of alkalinity and temperature on photosynthetic biogas upgrading efficiency in high rate algal ponds. Algal Res. 33, 284–290. https://doi.org/10.1016/j.algal.2018.06.001

28. Ryckebosch, E., Drouillon, M., Vervaeren, H., 2011. Techniques for transformation of biogas to biomethane. Biomass and Bioenergy 35, 1633–1645. https://doi.org/10.1016/j.biombioe.2011.02.033

29. Sander, R., 2015. Compilation of Henry 's law constants (version 4.0) for water as solvent 4399–4981. https://doi.org/10.5194/acp-15-4399-2015

30. Serejo, M.L., Posadas, E., Boncz, M.A., Blanco, S., García-Encina, P., Muñoz, R., 2015. Influence of biogas flow rate on biomass composition during the optimization of biogas upgrading in microalgal-bacterial processes. Environ. Sci. Technol. 49, 3228–3236. https://doi.org/10.1021/es5056116

31. Sournia, A., 1978. Phytoplankton manual.

32. Stürmer, B., Kirchmeyr, F., Kovacs, K., Gba, F.H., Rea, D.C., Atee, I., Eba, J.S., Proietti, S., 2016. Technical-economic analysis for determining the feasibility threshold for tradable biomethane certificates [WWW Document]. URL http://www.ergar.org/wp-content/uploads/2018/07/BIOSURF-D3.4.pdf (accessed 6.1.20).

33. Toledo-cervantes, A., Estrada, J.M., Lebrero, R., Muñoz, R., 2017. A comparative analysis of biogas upgrading technologies : Photosynthetic vs physical / chemical processes. Algal Res. 25, 237–243. https://doi.org/10.1016/j.algal.2017.05.006

34. Toledo-Cervantes, A., Serejo, M.L., Blanco, S., Pérez, R., Lebrero, R., Muñoz, R., 2016. Photosynthetic biogas

upgrading to bio-methane: Boosting nutrient recovery via biomass productivity control. Algal Res. 17, 46–52. https://doi.org/10.1016/j.algal.2016.04.017

35. Utermöhl, H., 1958. Zur vervollkommnung der quantitativen phytoplankton-methodik: mit 1 Tabelle und 15 abbildungen im Text und auf 1 Tafel, in: Internationale Vereinigung Für Theoretische Und Angewandte Limnologie: Mitteilungen. pp. 1–38.

Supplementary material

Innovative operational strategies in photosynthetic biogas upgrading in an outdoors pilot scale algal-bacterial photobioreactor

David Marín[1, 2, 3], Alessandro A. Carmona-Martínez[1, 2], Saúl Blanco[4], Raquel Lebrero[1, 2], Raúl Muñoz*[1, 2]

[1] Department of Chemical Engineering and Environmental Technology, School of Industrial Engineering, Valladolid University, Dr. Mergelina, s/n, 47011, Valladolid, Spain.

[2] Institute of Sustainable Processes, Dr. Mergelina, s/n, 47011, Valladolid, Spain.

[3] Universidad Pedagógica Nacional Francisco Morazán, Boulevard Centroamérica, Tegucigalpa, Honduras.

[4] Department of Biodiversity and Environmental Management, University of León, 24071 León, Spain.

* Corresponding author: mutora@iq.uva.es

Environmental parameters

Figure S1. Time course of the evaporation rate in the photobioreactor.
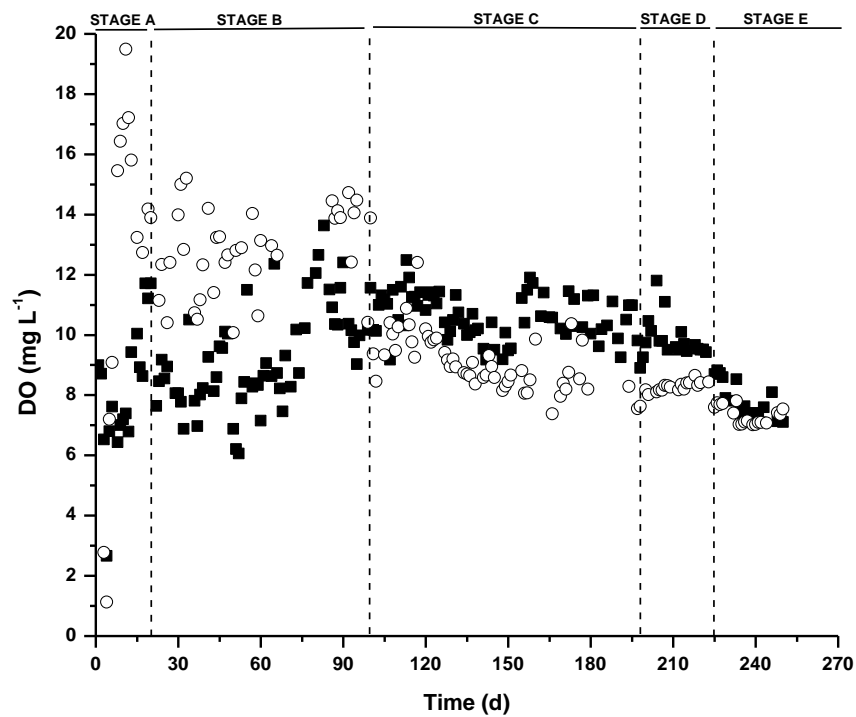
Figure S2. Time course of the dissolved oxygen concentration in the photobioreactor in the morning (solid symbols) and afternoon (empty symbols).

Cultivation broth parameters
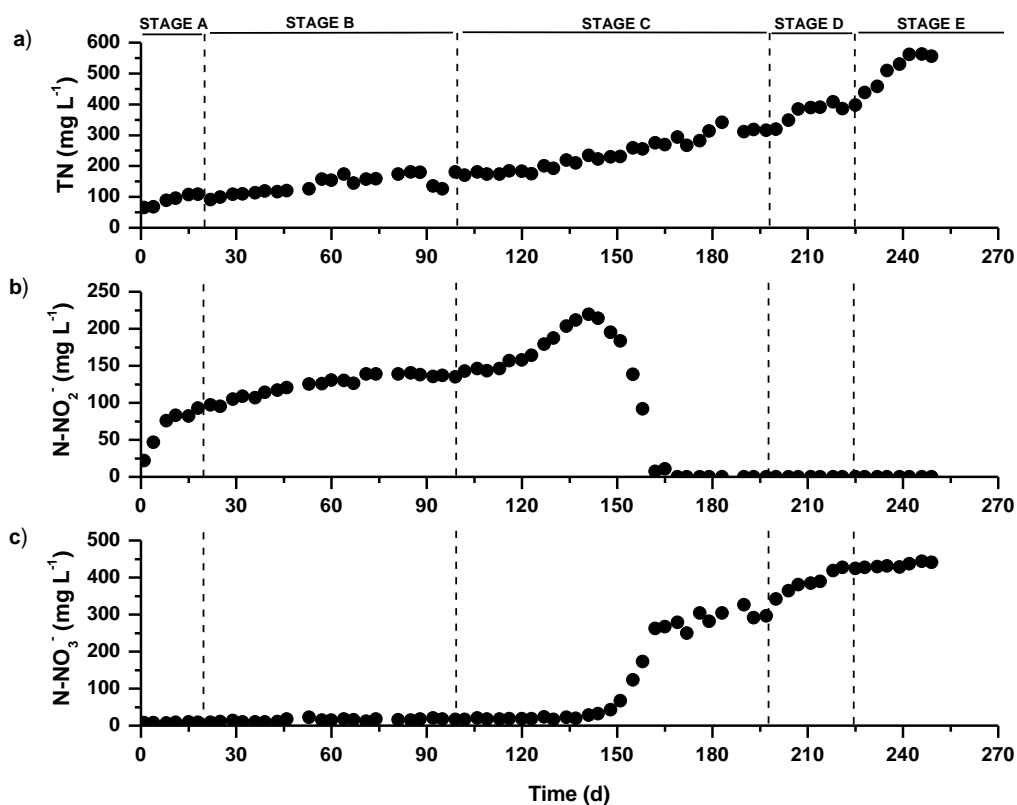
Figure S3. Time course of the concentration of (a) total nitrogen, (b) N-NO$_2^-$ and (c) N-NO$_3^-$ in the photobioreactor.
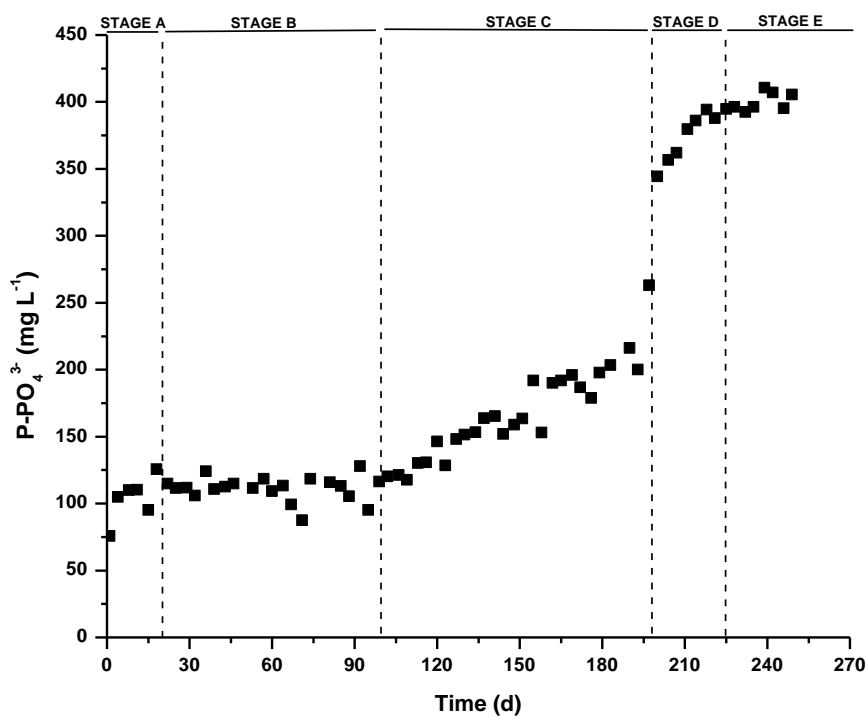
Figure S4. Time course of the concentration of P-PO$_4^{3-}$ in the photobioreactor.
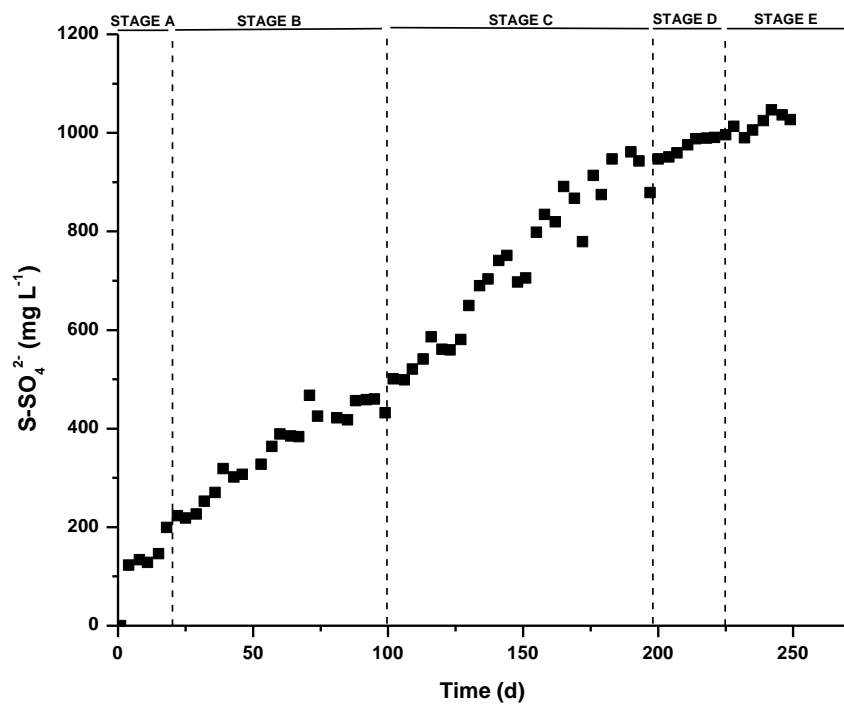
Figure S5. Time course of the concentration of S-SO$_4^{2-}$ in the photobioreactor.

Chapter 6

Influence of liquid-to-biogas ratio and alkalinity on the biogas upgrading performance in a demo scale algal-bacterial photobioreactor

David Marín[1, 2, 3], Antonio Ortíz[4], Rubén Díez-Montero[4], Enrica Uggetti[4], Joan García[4], Raquel Lebrero[1, 2], Raúl Muñoz[1, 2, *]

[1] Department of Chemical Engineering and Environmental Technology, School of Industrial Engineering, University of Valladolid, Dr. Mergelina, s/n, 47011, Valladolid, Spain.

[2] Institute of Sustainable Processes, University of Valladolid, Dr. Mergelina, s/n, 47011, Valladolid, Spain.

[3] Universidad Pedagógica Nacional Francisco Morazán, Boulevard Centroamérica, Tegucigalpa, Honduras.

[4] GEMMA – Group of Environmental Engineering and Microbiology, Department of Civil and Environmental Engineering, Universitat Politècnica de Catalunya – BarcelonaTech, c/ Jordi Girona 1-3, Barcelona E-08034, Spain.

[*] Corresponding author: mutora@iq.uva.es

Abstract

The influence of the liquid-to-biogas ratio (L/G) and alkalinity on methane quality was evaluated in a 11.7 m^3 outdoors horizontal semi-closed tubular photobioreactor interconnected to a 45-L absorption column (AC). CO_2 concentrations in the upgraded methane ranged from <0.1 to 9.6% at L/G of 2.0 and 0.5, respectively, with maximum CH_4 concentrations of 89.7% at a L/G of 1.0. Moreover, an enhanced CO_2 removal (mediating a decrease in CO_2 concentration from 9.6 to 1.2%) and therefore higher CH_4 contents (increasing from 88.0 to 93.2%) were observed when increasing the alkalinity of the AC cultivation broth from 42±1 mg L^{-1} to 996±42 mg L^{-1}. H_2S was completely removed regardless of the L/G or the alkalinity in AC. The continuous operation of the photobioreactor with optimized operating parameters resulted in contents of CO_2 (<0.1%-1.4%), H_2S (<0.7 mg m^{-3}) and CH_4 (94.1%-98.8%) complying with international regulations for methane injection into natural gas grids.

Keywords: Algal-bacterial photobioreactor, Alkalinity, Biogas upgrading, Liquid/Gas ratio, Outdoors conditions.

1. Introduction

The anaerobic digestion (AD) of organic solid waste and sludge from wastewater treatment generates a biogas that represents a potential renewable energy source capable of generating electricity and reduce the dependence on fossil fuels (Muñoz et al., 2015). Biogas can be purified and injected into natural gas grids or used as a vehicle fuel, or desulphurised and used for the generation of domestic heat or steam and electricity in industry (Andriani et al., 2014; Muñoz et al., 2015). In this regard, a growing contribution of biogas to the EU energy sector has been observed within the past years, with an increase in the numbers of biogas producing plants by a factor of 3 (from 6,772 in 2009 to 17,439 by the end of 2016) (European Biogas Association, 2017). The upgrading of biogas prior injection into natural gas grids or use as a vehicle fuel is required due to the large number and high concentrations of impurities in raw biogas: CO_2 (15-60%), H_2S (0.005-2%), O_2 (0-1%), N_2 (0-2%), CO (<0.6%), NH_3 (<1%), siloxanes (0-0.2%) and volatile organic compounds (<0.6%) (Ryckebosch et al., 2011). In this context, most international regulations establish that a methane composition of $CH_4 \geq 95\%$, $CO_2 \leq 2$-4%, $O_2 \leq 1\%$ and negligible amounts of H_2S is mandatory for its injection into natural gas grids, while a lower CH_4 content is required when methane is used as a vehicle fuel (Muñoz et al., 2015). The removal of biogas contaminants like H_2S reduces the corrosion in pipelines, engines and biogas storage structures, while the reduction in CO_2 contributes to increase the calorific value of methane and reduces its transportation costs (Posadas et al., 2015).

Nowadays, several biological technologies are available to remove CO_2 and H_2S from biogas. For instance, chemoautotrophic biogas upgrading is used for the removal of CO_2, while biofiltration or in situ micro-aerobic AD are applied for H_2S removal (Farooq et al., 2018; Marín et al., 2018a; Muñoz et al., 2015). The removal of only one biogas contaminant at a time represents the main disadvantage associated to these biological technologies, resulting in the need of implementing two-stage biological upgrading processes. Likewise, several physical-chemical technologies are commercially available to remove CO_2 and H_2S from biogas. Membrane separation, pressure swing adsorption or chemical/water/organic scrubbing are applied for CO_2 removal, while *in-situ* chemical precipitation or adsorption onto activated carbon or metal ions provide satisfactory levels of H_2S removal (Marín et al., 2018a; Muñoz et al., 2015; Toledo-cervantes et al., 2017).

Two sequential stages are also necessary for a complete biogas upgrading, which entails an increase in investment and operational costs. In this context, algal-bacterial photobioreactors can be engineered as an environmentally friendly and cost-effective technology due to their capacity to simultaneously remove CO_2 and H_2S in a single stage process (Bahr et al., 2014).

Algal-bacterial processes have emerged as a cost-competitive technology capable of removing CO_2 and H_2S from biogas in a single stage at low environmental impacts (Bahr et al., 2014; Muñoz et al., 2015). Biogas upgrading in algal-bacterial photobioreactors is based on the simultaneous photosynthetic fixation of CO_2 by microalgae and the oxidation of H_2S to SO_4^{2-} by sulfur oxidizing bacteria promoted by the high dissolved oxygen (DO) concentration present in the cultivation broth as a result of photosynthesis (Posadas et al., 2017, 2015; Toledo-Cervantes et al., 2016). Photosynthetic biogas upgrading has been recently evaluated indoors in high rate algal ponds (HRAPs) interconnected to a biogas absorption column (AC) under artificial illumination. Bahr et al. (2014) demonstrated for the first time the capability of microalgal-bacterial processes for the simultaneous removal of CO_2 and H_2S from biogas. Serejo et al. (2015) studied the influence of the liquid/biogas (L/G) ratio on the composition of the upgraded biogas. Posadas et al. (2016) optimized the biogas upgrading process in a HRAP using centrate as a source of nutrients under laboratory conditions, while Rodero et al. (2018) evaluated the influence of alkalinity and temperature on the photosynthetic biogas upgrading efficiency in an indoor HRAP. In addition, Posadas et al. (2017) evaluated the simultaneous biogas upgrading and centrate treatment in a HRAP operated under outdoors conditions during summer, while Marín et al. (2018a,b) investigated the influence of the yearly variations of environmental conditions on the biogas upgrading performance. Nevertheless, and despite the satisfactory results obtained so far, new photobioreactor configurations should be tested in order to overcome design constraints associated to algal ponds such as their high footprint. In this sense, semi-closed or closed tubular photobioreactors have been proposed as a promising alternative to reduce land requirement, while offering higher photosynthetic efficiencies, enhanced biomass productivities and a superior CO_2 mass transfer (Toledo-Cervantes et al., 2018).

This study investigated for the first time the biogas upgrading potential of an outdoors pilot-scale hybrid (semi-closed) horizontal tubular photobioreactor (PBR) interconnected to an external AC. The influence of the L/G ratio and the alkalinity of the cultivation medium in the AC on the quality of the upgraded biogas was assessed and optimized. In addition, the PBR-AC was operated continuously under optimized process parameters.

2. Materials and methods

2.1 Biogas

The biogas used in this experiment was obtained from the anaerobic digestion of microalgal biomass in a pilot anaerobic digester located at the Agròpolis experimental campus of the Universitat Politécnica de Catalunya-BarcelonaTech (Catalunya, Spain) (García et al., 2018; Uggetti et al., 2018). The average biogas composition was CO_2 (13.7 ± 1.0%), H_2S (0.1 ± 0.05%) and CH_4 (86.2 ± 1.0%).

2.2 Experimental set-up

The experimental set-up was built outdoors at the Agròpolis experimental campus of the Universitat Politécnica de Catalunya-BarcelonaTech (41.29ºN, 2.04ºE). The horizontal hybrid (semi-closed) tubular photobioreactor (PBR) consisted of 2 lateral open tanks made of polypropylene (width=1 m; length=5 m; depth=0.6 m) interconnected by 16 low density transparent polyethylene tubes (length=47 m; diameter=125 mm). The total working volume of the PBR was 11.7 m^3. The cultivation broth was continuously circulated in each tank by a 6-blade paddlewheel with a rotational speed of 9-12 rpm, which resulted in a velocity of the cultivation broth inside the tubes of 0.20-0.25 m s^{-1}. This recirculation rate ensured a homogeneous distribution and mixing of the cultivation broth and a turbulent flow inside the tubes, avoiding biomass settling. The different height level between the two open tanks caused a gravity flow through 8 tubes from the deep side of one tank to the shallow side of the opposite one (Uggetti et al., 2018). The open tanks supported the release of the DO accumulated along the closed tubes and also provided a cooling effect via water evaporation, thus preventing the occurrence of the extremely high temperatures that would be reached in completely closed tubular PBRs. The PBR was interconnected to a separate 45 L bubble AC (internal diameter=12 cm; height=4 m) made of PVC and provided with a ring of seven metallic biogas diffusers of 2 µm pore size located at the bottom of the column. (Fig. 1).
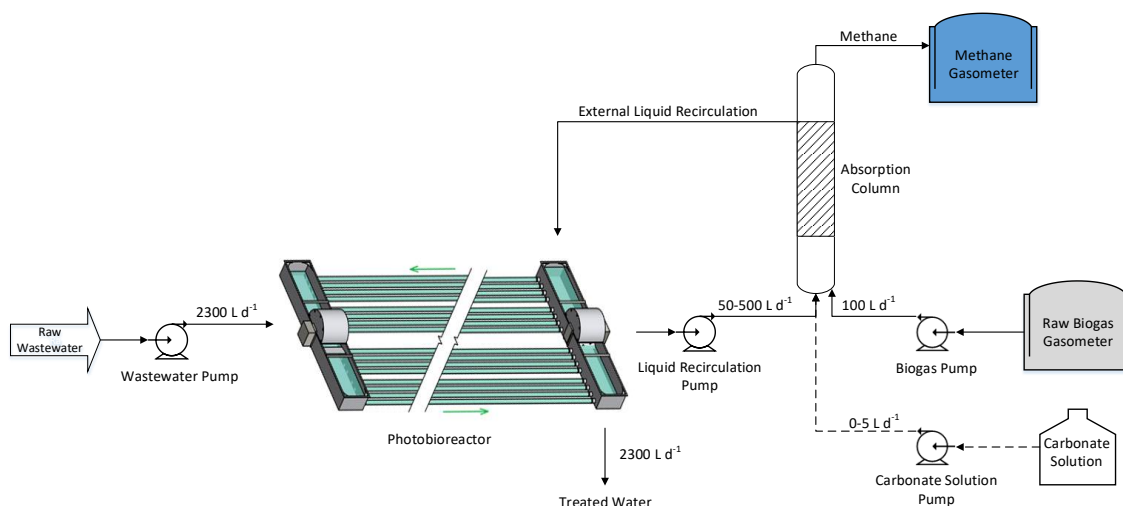
Figure 1. Schematic diagram of the experimental set-up used for the continuous photosynthetic upgrading of biogas.

2.3 Operational conditions and experimental procedure

The PBR was inoculated at an initial concentration of 220 mg volatile suspended solids (VSS) L^{-1} with a microalgal consortium composed of *Chlorella vulgaris, Stigeoclonium tenue, Nitzschia closterium and Navicula amphora,* obtained from an outdoors HRAP located at the facilities of the Environmental Engineering and Microbiology Research Group (GEMMA) the Universitat Politécnica de Catalunya-BarcelonaTech (Gutiérrez et al., 2016). The PBR was operated as the third of a set of 3 identical PBRs interconnected in series and treating 2.3 m^3 d^{-1} of agricultural wastewater with the following composition: total organic carbon (TOC) = 131 ± 80 mg L^{-1}, inorganic carbon (IC) = 36 ± 10 mg L^{-1}, total nitrogen (TN) = 15 ± 7 mg L^{-1} and total phosphorus (TP) = 0.9 ± 1.0 mg L^{-1}. Three experimental series were conducted as described below:

2.3.1 Influence of the liquid-to-biogas ratio in the absorption column on the quality of the upgraded biogas

L/G ratios ranging from 0.5 to 5.0 were tested in order to optimize the quality of the upgraded biogas. Biogas was sparged into the AC at 100 L d^{-1}, while the cultivation broth from the PBR was supplied in co-current mode at different flow rates in order to provide L/G ratios of 0.5, 1.0, 2.0, 3.0, 4.0 and 5.0. The duration of each L/G ratio condition was at least four times the hydraulic retention time (HRT) of the liquid in the AC (Table 1). The ambient and cultivation broth temperatures, the pH, dissolved TOC, IC, TN, N-NH$_4^+$

and TP concentrations in the cultivation broth of the PBR, and the composition of the raw and upgraded biogas were analyzed in triplicate at the end of each operational condition.

Table 1. Operational parameters during the evaluation of the influence of the L/G ratio in the AC.

L/G ratio	Liquid flowrate (L d^{-1})	Biogas flowrate (L d^{-1})	Biogas HRT (h)
0.5	50	100	10.8
1.0	100	100	5.4
2.0	200	100	2.7
3.0	300	100	1.8
4.0	400	100	1.4
5.0	500	100	1.1

2.3.2 Influence of the alkalinity in the cultivation broth on the quality of the upgraded biogas

In order to assess the impact of different alkalinities of the cultivation broth in the AC on the upgrading efficiency, a carbonate solution ($NaHCO_3$ and Na_2CO_3) with a concentration of 16,000 mg L^{-1} of IC was injected at the bottom of the AC in co-current mode (Fig. 1, dashed line). Biogas flowrate and L/G ratio were fixed at 100 L d^{-1} and 0.5, respectively. Carbonate solution flowrates of 0, 1, 2, 3 and 5 L d^{-1} (corresponding to an IC concentration in the cultivation broth of the AC of 42 ± 1; 311 ± 6; 634 ± 48; 996 ± 42 and $1,557 \pm 26$ mg L^{-1}, respectively) were tested in order to optimize the quality of the upgraded biogas. Each carbonate solution flowrate was maintained for at least four times the HRT of the liquid in the AC. The ambient and PBR cultivation broth temperatures, the pH, dissolved TOC, IC, TN, N-NH$_4^+$ and TP concentrations in the cultivation broth of the PBR, and the composition of the raw and the upgraded biogas were analyzed in triplicate at the end of each operational condition.

2.3.3 Continuous photosynthetic biogas upgrading operation

Biogas upgrading performance of the demo scale PBR was evaluated throughout 42 days under continuous operation. The optimum operating parameters previously identified

were selected: biogas flowrate of 100 L d^{-1}, L/G ratio of 0.5 and the supplementation of 2.0 L d^{-1} of carbonate solution to the AC. The ambient and cultivation broth temperatures, the pH, dissolved TOC, IC, TN, N-NH$_4^+$ and TP concentrations in the cultivation broth of the PBR, and the composition of the raw and the upgraded biogas were analyzed in duplicate once per week.

2.4 Analytical procedures

The concentration of CH$_4$, CO$_2$, N$_2$ and O$_2$ in biogas and methane were determined using a gas chromatograph (GC) equipped with a thermal conductivity detector (Trace GC Thermo Finnigan with Hayesep packed column). Injector, detector and oven temperatures were maintained at 150, 250 and 35 ºC, respectively, with helium as a carrier gas. The concentration of H$_2$S in the raw biogas was determined using Gastec colorimetric tubes, while its concentration in the upgraded methane was analyzed by a Dräger X-am 5000 electrochemical sensor (lower detection limit of 0.5 ppm$_v$). Temperature and pH were measured *in-situ* by a pH-meter with temperature sensor (Mettler Toledo, USA). Dissolved TOC, IC and TN concentrations were determined using a C/N analyzer (21005, Analytikjena, Germany). The analysis of TP concentration was performed according to the Ascorbic Acid Method of Standard Methods (APHA, 2005), while N-NH$_4^+$ concentration was measured by a colorimetric method according to Solorzano (1969). The determination of the concentration of total suspended solids (TSS) and VSS in the PBR was performed according to Standard Methods (APHA, 2005), and the temperature of the cultivation broth was periodically monitored with a temperature sensor (Campbell Scientific Inc., USA).

3. Results and discussion

3.1 Influence of the liquid-to-biogas ratio in the absorption column on the quality of the upgraded biogas

The composition of the methane produced in the PBR-AC varied depending on the L/G ratio tested (Fig. 2). At a L/G ratio of 2.0, CO$_2$ was not detected in the upgraded methane, thus achieving minimum concentrations < 0.1% according to the GC detection limit. On the contrary, a maximum concentration of 9.6 ± 0.1% was recorded at a L/G ratio of 0.5 (Fig. 2). These results were in accordance with Posadas et al. (2017), who recorded the highest concentration of CO$_2$ in methane at the lowest L/G ratio (≈12.0% at a L/G ratio

of 0.5). L/G ratios > 2.0 supported a significant decrease in the CO_2 concentration of the upgraded biogas, which ranged from <0.1 to 1.4% (corresponding to removal efficiencies (REs) between 90.4 and >99.9%). On the other hand, H_2S was not detected in the upgraded methane regardless of the tested L/G ratio, its complete removal being attributed to the high aqueous solubility of this biogas contaminant. An efficient removal of H_2S from raw biogas in algal-bacterial PBRs with a negligible impact of the L/G ratio has been consistently reported both in outdoors (Posadas et al. 2017) and indoors HRAPs (Serejo et al. 2015).

Unfortunately, the concentrations of N_2 and O_2 recorded in the upgraded biogas increased from 3.4% at a L/G ratio of 0.5 to 11.9% at a L/G ratio of 5.0 (Fig. 2), which clearly indicated that the stripping of these gases from the recirculating cultivation broth was promoted at higher liquid flowrates (Sovechles and Waters, 2015). These results were in accordance with Toledo-Cervantes et al. (2016), who reported N_2/O_2 concentrations between 2.5 and 37.0% at L/G ratios ranging from 0 to 40 in a closed tubular photobioreactor. Likewise, Posadas et al. (2017) also reported an increase in N_2 and O_2 concentration in the upgraded biogas from 1.4 to 18.3% when the L/G ratio increased from 0.5 to 5, respectively. Similarly, Rodero et al., 2019 found N_2/O_2 concentrations ranging from 6.6 and 11.4% at L/G ratios ranging from 1.2 to 3.5 in an outdoors HRAP.

Finally, a maximum concentration of CH_4 of 89.7% in the upgraded biogas was recorded at a L/G ratio = 1 (Fig. 2). Interestingly, although further increases in the L/G ratio resulted in lower CO_2 concentrations, they also mediated a higher desorption of N_2 and O_2, which negatively impacted the final concentration of CH_4 in the upgraded biogas.
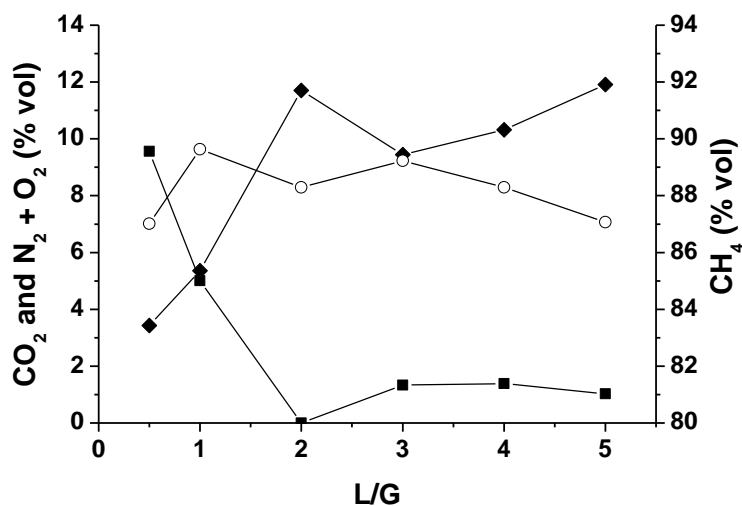
Figure 2. Concentration of CO_2 (■), $N_2 + O2$ (◆) and CH_4 (○) in the upgraded biogas at different L/G ratios.

3.2 Influence of the alkalinity in the cultivation broth on the quality of the upgraded biogas

The supplementation of a carbonate solution to the absorption column resulted in an improved quality of the final methane. In this context, average concentrations of CO_2 of 9.6 ± 0.2; 2.6 ± 0.2; 1.3 ± 0.0; 1.2 ± 0.0 and $1.1 \pm 0.2\%$ were recorded at IC concentrations in the AC cultivation broth of 42 ± 1; 311 ± 6; 634 ± 48; 996 ± 42 and $1,557 \pm 26$ mg L^{-1}, respectively (Fig. 3). The increase in CO_2-REs resulting from the addition of alkalinity (from $24.0 \pm 0.2\%$ at 42 ± 1 mg IC L^{-1} to $91.9 \pm 0.2\%$ at $1,557 \pm 26$ mg IC L^{-1}) was associated to the concomitant increase of pH in the cultivation broth of the AC (from 6.5 ± 0.1 at 42 ± 1 mg IC L^{-1} up to 9.3 ± 0.0 at $1,557 \pm 26$ mg IC L^{-1}). The beneficial effect of alkalinity on CO_2 removal performance has been previously reported in literature. For instance, Rodero et al. (2018) reported CO_2-REs of 97.8 ± 0.8, 50.6 ± 3.0 and $41.5 \pm 2.0\%$ during the operation of an indoors HRAP interconnected to an AC using a feeding nutrient solution with an average IC concentration of $1,500$ mg L^{-1}, 500 mg L^{-1} and 100 mg L^{-1}, respectively. On the other hand, the higher solubility of H_2S compared to that of CO_2 also mediated complete removals of this biogas contaminant regardless of the alkalinity of the AC cultivation broth. These results were in accordance with Franco-Morgado et al. (2017), who reported values of H_2S-REs of $99.5 \pm 0.5\%$ throughout the operation of an indoors HRAP interconnected to an AC using a highly carbonated medium at a pH of 9.5. Likewise, Rodero et al. (2018) observed H_2S-REs of 100.0 ± 0.0, 94.7 ± 1.9 and $80.3 \pm$

3.9% using a feeding nutrient solution with an average IC concentration of 1,500 mg L^{-1}, 500 mg L^{-1} and 100 mg L^{-1}, respectively.

The N_2 and O_2 concentration in the upgraded biogas increased from 2.4% at an IC concentration of 42 ± 1 mg L^{-1} to 6.1% at $1,557 \pm 26$ mg IC L^{-1} (Fig. 3). This increase was attributed to the enhanced N_2 and O_2 stripped out from the recycling cultivation broth mediated by the increase in medium salinity (which ultimately decreased the solubility of these gases).

Finally, the lowest concentration of CH_4 in the upgraded biogas (88.0%) was recorded at an IC concentration of 42 ± 1 mg L^{-1}, increasing up to a maximum concentration of 93.2% at 634 ± 48 mg L^{-1} (Fig. 3). Interestingly, higher carbonate supplementation rates did not result in an additional increase in the CH_4 content. The increased CH_4 concentration at higher alkalinity loads was attributed to the limited desorption of N_2 and O_2 when operating at the optimum L/G ratio and the high absorption efficiency of CO_2 and H_2S due to the acidic nature of these gases. Similar results were obtained by Rodero et al. (2018), who reported CH_4 contents of 98.9 ± 0.2, 80.9 ± 0.8 and $75.9 \pm 0.7\%$ at average IC feed concentrations of 1,500, 500 and 100 mg L^{-1}, respectively. Therefore, the results herein obtained confirmed the key role of alkalinity on the methane quality.
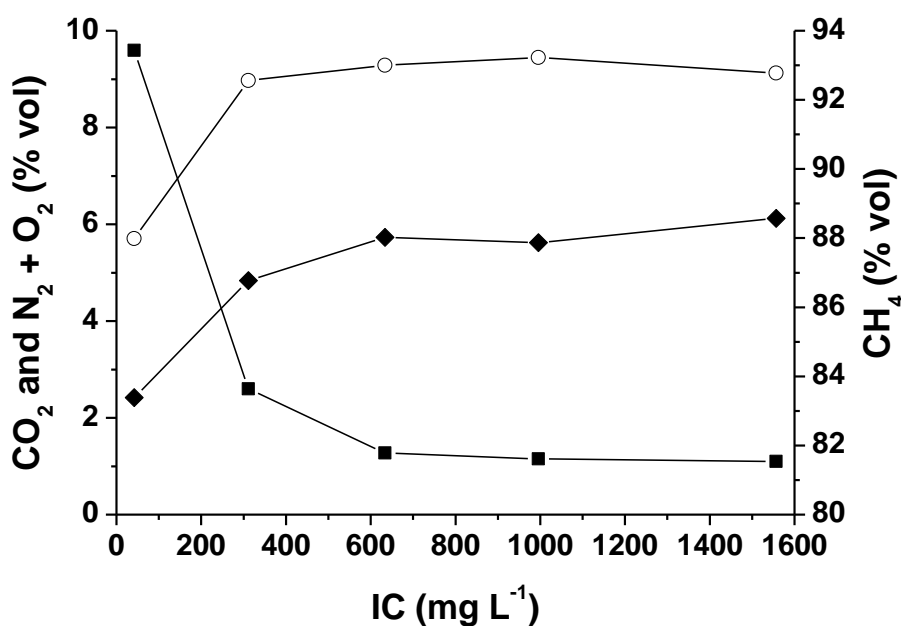
Figure 3. Concentration of CO_2 (■), $N_2 + O_2$ (◆) and CH_4 (○) in the upgraded biogas at different IC concentration in the cultivation broth of the AC.

3.3 Continuous photosynthetic biogas upgrading operation

The optimum operating parameters (i.e. L/G ratio of 0.5 and supplementation of a 16,000 mg IC L^{-1} solution to the AC at a flowrate of 2.0 L d^{-1}) identified in sections 3.1 and 3.2 were selected to test the performance of the PBR during the continuous upgrading of raw biogas coupled with the treatment of the mixed wastewater.

3.3.1 Biogas upgrading

The composition of the methane obtained exhibited a rather constant value along the 42 days of operation (Fig. 4). CO_2 concentrations ranged between <0.1% and 1.4%, corresponding to REs >91.0% (Fig. 4). The previous optimization of key operating parameters such as the L/G ratio and the alkalinity in the cultivation broth of the AC supported these consistent CO_2 removals. Similarly, Marín et al. (2018a) reported values of CO_2 concentration in the upgraded biogas ranging from 0.7 to 1.9% throughout the operation of an outdoors HRAP interconnected to an external AC. It is important to highlight that the CO_2 concentrations here obtained fulfilled most international regulations for methane, which require CO_2 concentrations ≤ 2-4% to be acceptable for injection into natural gas grids (Muñoz et al., 2015). Moreover, no H_2S was detected in the methane during the whole experimental period regardless of the environmental conditions, which agreed with the results previously observed during the optimization assays. Therefore, the resulting methane also complied with the maximum H_2S levels enforced by international regulations for methane injection into natural gas grids (< 5 mg m^{-3}) (Muñoz et al., 2015).
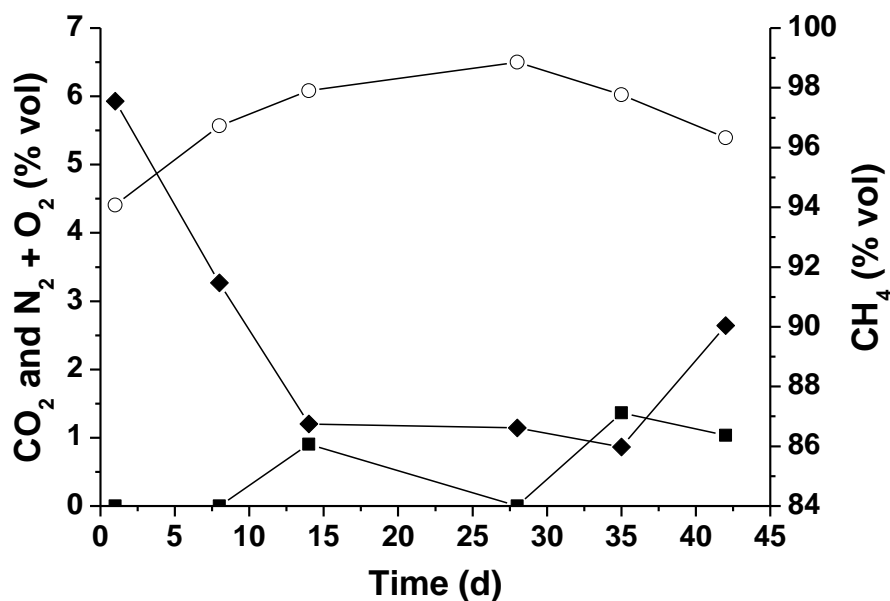
Figure 4. Time course of the concentration of CO_2 (■), $N_2 + O_2$ (◆) and CH_4 (○) in the upgraded biogas during continuous process operation.

The N_2 and O_2 concentration in the upgraded biogas ranged from 0.9 to 5.9% throughout the entire operating period (Fig. 4), similar concentrations to those recorded by Marín et al. (2018a), who reported N_2 and O_2 contents in the upgraded biogas between 0.5 and 6.3% during the operation of an outdoors HRAP interconnected to an AC. Likewise, Posadas et al. (2017) also recorded similar N_2 and O_2 concentrations of 1.4-6.1% in the upgraded biogas. Unfortunately, these concentrations exceeded most of the time the maximum quality requirements demanded for methane injection into natural gas grids of ≤ 1% (please note that the GC-TCD method did not allow to quantify separately O_2 and N_2). O_2 is a hazardous biomethane contaminant based on its associated explosion risks, while the presence of N_2 typically lowers the content of the biomethane. Therefore, a further optimization of the technology in order to avoid an active stripping of N_2 and O_2 from the cultivation broth into the upgraded methane is still necessary.

Finally, high CH_4 concentrations in the upgraded biogas ranging from 94.1 to 98.9% were recorded during this continuous assay (Fig. 4), likely due to the high CO_2-REs, the complete elimination of H_2S and the limited N_2 and O_2 desorption obtained under these operating conditions. In this regard, the quality of the upgraded methane was similar or even higher in terms of CH_4 content than that reported in previous studies. Indeed, Posadas et al. (2017) obtained CH_4 concentrations in the upgraded biogas of 87.0 - 93.0%,

while Marín et al. (2018a) achieved values up to 97.8% in a similar outdoors experimental set-up (HRAP-AC) with a L/G ratio of 1.0 and IC concentrations in the cultivation broth of ~ 2,600 mg IC L^{-1}. Finally, it should be highlighted that process performance here recorded in this demo-scale PBR was superior to that recently recorded by Rodero et al. (2019) in an outdoors 10 m^3 HRAP interconnected to an AC, where CH_4 concentrations did not exceed 91% in the upgraded biogas. In this context, a minimum CH_4 concentrations of $\geq$ 95% must be typically ensured prior injection of the methane into natural gas grids in most international methane regulations (Muñoz et al., 2015).

3.3.2 Wastewater Treatment

Wastewater treatment performance in the PBR during biogas upgrading was evaluated in terms of dissolved TOC, IC and TN removal (Fig. 5). Dissolved TOC concentrations in the influent and effluent varied throughout the process with values ranging from 69.9 to 277.3 mg L^{-1} in the influent and from 90.4 to 217.0 mg L^{-1} in the effluent (Fig. 5). The low TOC-REs recorded were attributed to the low biodegradability of the mixture of agricultural and domestic wastewater used as influent to the PBR. Moreover, the significant water evaporation rates from the cultivation broth in the open tanks and the lysis of the microalgae generated during photosynthetic CO_2 fixation likely contributed to increase the TOC concentration in the effluent in comparison to that of the influent, thus resulting in the negative TOC-REs observed. On the other hand, the dissolved IC concentration in the influent varied from 21.6 to 46.3 3 mg L^{-1} and from 29.8 to 91.8 mg L^{-1} in the effluent (Fig. 5). Although no correlation between the IC concentration in the effluent of the PBR and the addition of the carbonate solution in the AC was found due to the high dilution effect associated to the large volume and short hydraulic retention time of the PBR, the high values of pH in the PBR ranging between 7.9 and 8.9 might have promoted the increase in the IC concentration of the effluent supported by biogas absorption. Finally, no effective TN removal was observed during the entire experimental period, with dissolved TN concentrations in the influent (ranging from 9.1 to 25.0 mg L^{-1}) comparable to those recorded in the effluent (ranging from 11.1 to 25.9 mg L^{-1}) (Fig. 5).
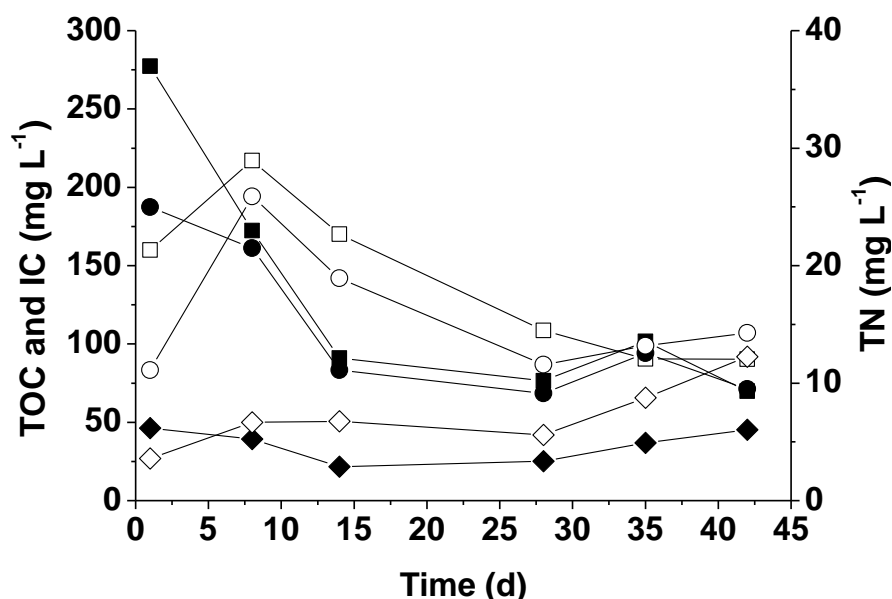
Figure 5. Time course of the influent (solid symbols) and effluent (empty symbols) concentration of total organic carbon (squares), inorganic carbon (diamonds) and total nitrogen (circles) throughout the continuous operation of the PBR.

4. Conclusions

This work constitutes, to the best of our knowledge, the first validation of photosynthetic biogas upgrading in a pilot-scale semi-closed PBR interconnected to an AC under outdoors conditions. Both the L/G ratio and the alkalinity in the AC were identified as key parameters influencing the quality of the final methane, with optimum values of 0.5 and 634 ± 48 mg L^{-1}, respectively. The implementation of the optimum operating parameters during continuous operation resulted in a methane with CO_2 concentrations of <0.1%-1.4%, H_2S<0.5ppm$_v$ and CH_4 contents of 94.1-98.9%, which complied with most international regulations for methane injection into natural gas grids.

References

1. Andriani, D., Wresta, A., Atmaja, T.D., Saepudin, A., 2014. A Review on Optimization Production and Upgrading Biogas Through CO2 Removal Using Various Techniques. Appl. Biochem. Biotechnol. 172, 1909–1928. doi:10.1007/s12010-013-0652-x

2. APHA, 2005. Standard Methods for the Examination of Water and Wastewater, 21st ed. Public Health Association, Washington DC.

3. Bahr, M., Díaz, I., Dominguez, A., González Sánchez, A., Muñoz, R., 2014. Microalgal-biotechnology as a platform for an integral biogas upgrading and nutrient removal from anaerobic effluents. Environ. Sci. Technol. 48, 573–581. doi:10.1021/es403596m

4. European Biogas Association, 2017. EBA Statistical Report 2017 [WWW Document]. URL http://european-biogas.eu/2017/12/14/eba-statistical-report-2017-published-soon/ (accessed 11.13.18).

5. Farooq, M., Almustapha, M.N., Imran, M., Saeed, M.A., Andresen, J.M., 2018. In-situ regeneration of activated carbon with electric potential swing desorption (EPSD) for the H2S removal from biogas. Bioresour. Technol. 249, 125–131. doi:10.1016/j.biortech.2017.09.198

6. Franco-Morgado, M., Alcántara, C., Noyola, A., Muñoz, R., González-Sánchez, A., 2017. A study of photosynthetic biogas upgrading based on a high rate algal pond under alkaline conditions: Influence of the illumination regime. Sci. Total Environ. 592, 419–425. doi:10.1016/j.scitotenv.2017.03.077

7. García, J., Ortiz, A., Álvarez, E., Belohlav, V., García-Galán, M.J., Díez-Montero, R., Álvarez, J.A., Uggetti, E., 2018. Nutrient removal from agricultural run-off in demonstrative full scale tubular photobioreactors for microalgae growth. Ecol. Eng. 120, 513–521. doi:10.1016/j.ecoleng.2018.07.002

8. Gutiérrez, R., Ferrer, I., González-Molina, A., Salvadó, H., García, J., Uggetti, E., 2016. Microalgae recycling improves biomass recovery from wastewater treatment high rate algal ponds. Water Res. 106, 539–549. doi:10.1016/j.watres.2016.10.039

9. Marín, D., Posadas, E., Cano, P., Pérez, V., Blanco, S., Lebrero, R., 2018a. Seasonal variation of biogas upgrading coupled with digestate treatment in an outdoors pilot scale algal-bacterial photobioreactor. Bioresour. Technol. 263, 58–66. doi:10.1016/j.biortech.2018.04.117

10. Marín, D., Posadas, E., Cano, P., Pérez, V., Lebrero, R., Muñoz, R., 2018b. Influence of the seasonal variation of environmental conditions on biogas upgrading in an outdoors pilot scale high rate algal pond. Bioresour. Technol. 255, 354–358. doi:10.1016/j.biortech.2018.01.136

11. Muñoz, R., Meier, L., Diaz, I., Jeison, D., 2015. A review on the state-of-the-art of physical/chemical and biological technologies for biogas upgrading. Rev. Environ. Sci. Biotechnol. 14, 727–759. doi:10.1007/s11157-015-9379-1

12. Posadas, E., Marín, D., Blanco, S., Lebrero, R., Muñoz, R., 2017. Simultaneous biogas upgrading and centrate treatment in an outdoors pilot scale high rate algal pond. Bioresour. Technol. 232, 133–141. doi:10.1016/j.biortech.2017.01.071

13. Posadas, E., Serejo, M.L., Blanco, S., Pérez, R., García-Encina, P.A., Muñoz, R., 2015. Minimization of biomethane oxygen concentration during biogas upgrading in algal-bacterial photobioreactors. Algal Res. 12, 221–229. doi:10.1016/j.algal.2015.09.002

14. Posadas, E., Szpak, D., Lombó, F., Domínguez, A., Díaz, I., Blanco, S., García-Encina, P.A., Muñoz, R., 2016. Feasibility study of biogas upgrading coupled with nutrient removal from anaerobic effluents using microalgae-based processes. J. Appl. Phycol. 28, 2147–2157. doi:10.1007/s10811-015-0758-3

15. Rodero, M. del R., Lebrero, R., Serrano, E., Lara, E., Arbib, Z., García-Encina, P.A., Muñoz, R., 2019. Technology validation of photosynthetic biogas upgrading in a semi-industrial scale algal-bacterial photobioreactor. Bioresour. Technol. 279, 43–49. doi:10.1016/j.biortech.2019.01.110

16. Rodero, M. del R., Posadas, E., Toledo-Cervantes, A., Lebrero, R., Muñoz, R., 2018. Influence of alkalinity and temperature on photosynthetic biogas upgrading efficiency in high rate algal ponds. Algal Res. 33, 284–290. doi:10.1016/j.algal.2018.06.001

17. Ryckebosch, E., Drouillon, M., Vervaeren, H., 2011. Techniques for transformation of biogas to biomethane. Biomass and Bioenergy 35, 1633–1645. doi:10.1016/j.biombioe.2011.02.033

18. Serejo, M.L., Posadas, E., Boncz, M.A., Blanco, S., García-Encina, P., Muñoz, R., 2015. Influence of biogas flow rate on biomass composition during the optimization of biogas upgrading in microalgal-bacterial processes. Environ. Sci. Technol. 49, 3228–3236. doi:10.1021/es5056116

19. Solorzano, L., 1969. Determination of ammonia in natural waters by the phenolhypochlorite method. Limnol. Oceanogr. 799–801. doi:10.4319/lo.1969.14.5.0799

20. Sovechles, J.M., Waters, K.E., 2015. Effect of ionic strength on bubble coalescence in inorganic salt and seawater solutions. AICHE 61, 2489–2496. doi:doi.org/10.1002/aic.14851

21. Toledo-cervantes, A., Estrada, J.M., Lebrero, R., Muñoz, R., 2017. A comparative analysis of biogas upgrading technologies : Photosynthetic vs physical / chemical processes. Algal Res. 25, 237–243. doi:10.1016/j.algal.2017.05.006

22. Toledo-Cervantes, A., Morales, T., González, Á., Muñoz, R., Lebrero, R., 2018. Long-term photosynthetic CO_2 removal from biogas and flue-gas: Exploring the potential of closed photobioreactors for high-value biomass production. Sci. Total Environ. 640–641, 1272–1278. doi:10.1016/j.scitotenv.2018.05.270

23. Toledo-Cervantes, A., Serejo, M.L., Blanco, S., Pérez, R., Lebrero, R., Muñoz, R., 2016. Photosynthetic biogas upgrading to bio-methane: Boosting nutrient recovery via biomass productivity control. Algal Res. 17, 46–52. doi:10.1016/j.algal.2016.04.017

24. Uggetti, E., García, J., Álvarez, J.A., García-Galán, M.J., 2018. Start-up of a microalgae-based treatment system within the biorefinery concept: From wastewater to bioproducts. Water Sci. Technol. 78, 114–124. doi:10.2166/wst.2018.195

Supplementary material

Influence of liquid-to-biogas ratio and alkalinity on the biogas upgrading performance in a demo scale algal-bacterial photobioreactor

David Marín[1, 2, 3], Antonio Ortíz[4], Rubén Díez-Montero[4], Enrica Uggetti[4], Joan García[4], Raquel Lebrero[1, 2], Raúl Muñoz[1, 2, *]

[1] Department of Chemical Engineering and Environmental Technology, School of Industrial Engineering, University of Valladolid, Dr. Mergelina, s/n, 47011, Valladolid, Spain.

[2] Institute of Sustainable Processes, University of Valladolid, Dr. Mergelina, s/n, 47011, Valladolid, Spain.

[3] Universidad Pedagógica Nacional Francisco Morazán, Boulevard Centroamérica, Tegucigalpa, Honduras.

[4] GEMMA – Group of Environmental Engineering and Microbiology, Department of Civil and Environmental Engineering, Universitat Politècnica de Catalunya – BarcelonaTech, c/ Jordi Girona 1-3, Barcelona E-08034, Spain.

* Corresponding author: mutora@iq.uva.es

1. Influence of alkalinity on the quality of the upgraded biogas
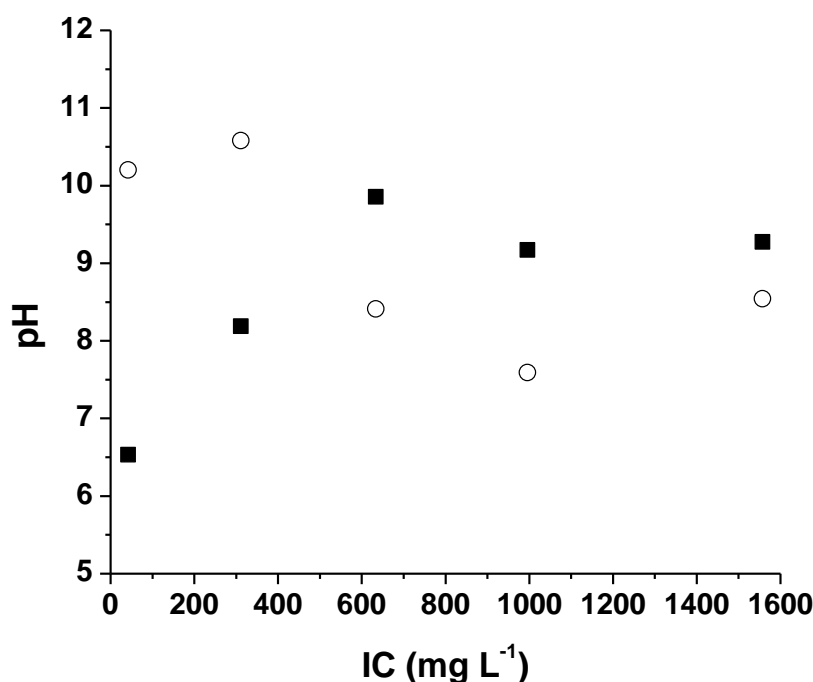
Figure S1. Influence of the IC concentration in the cultivation broth of the AC on the pH of the cultivation broth in the (○) PBR and (■) AC.
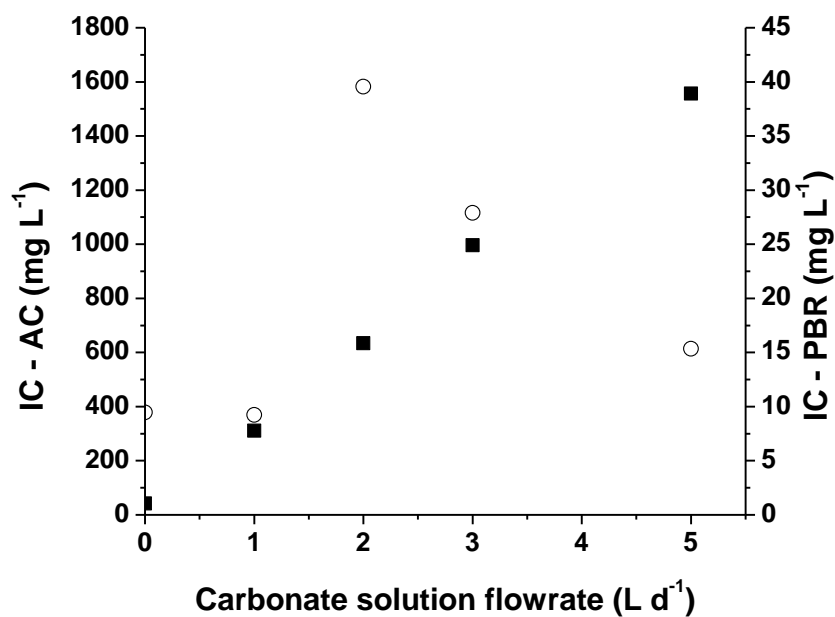
Figure S2. Influence of the carbonate solution flowrate on the IC concentration in the cultivation broth of the (○) PBR and (■) AC.

2. Continuous Operation
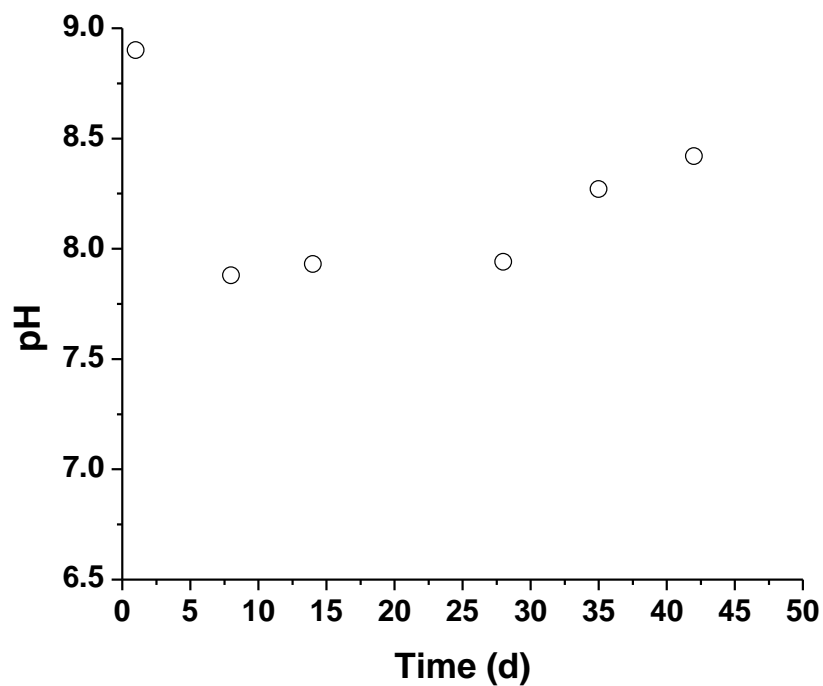
Figure S3. Time course of the pH in the cultivation broth of the PBR during the continuous biogas upgrading assay.

3. Temperature and biomass concentration

Table S1. Temperature and biomass concentration in the PBR during the evaluation of the influence of the L/G ratio on the quality of the upgraded biogas.

L/G ratio	Temperature in the AC (ºC)	Temperature in the PBR (ºC)	TSS (g L^{-1})
0.5	29.9	27.4	0.11
1.0	30.3	28.0	0.15
2.0	33.4	37.2	0.20
3.0	33.5	36.9	0.45
4.0	32.3	35.0	0.37
5.0	32.4	22.1	0.27

Table S2. Temperature and biomass concentration in the PBR during the evaluation of the influence of the alkalinity of the cultivation broth in AC on the quality of the upgraded biogas.

IC Concentration (mg L^{-1})	Temperature in the AC (ºC)	Temperature in the PBR (ºC)	TSS (g L^{-1})
42	31.7	28.4	0.40
311	32.5	27.4	0.43
634	31.3	29.4	0.49
996	35.0	32.8	0.19
1557	31.3	30.1	0.25

Table S3. Temperature and biomass concentration in the PBR during the continuous photosynthetic biogas upgrading experiment.

Day	Temperature in the AC (ºC)	Temperature in the PBR (ºC)	TSS (g L-1)
1	32.4	26.1	0.98
8	31.6	21.2	1.27
14	33.4	21.0	0.77
28	31.3	19.2	0.68
35	30.5	16.1	1.27
42	31.2	18.2	0.98

Chapter 7

Assessing the potential of purple phototrophic bacteria for the simultaneous treatment of piggery wastewater and upgrading of biogas

David Marín, Esther Posadas, Dimas García, Daniel Puyol, Raquel Lebrero, Raúl Muñoz.

Assessing the potential of purple phototrophic bacteria for the simultaneous treatment of piggery wastewater and upgrading of biogas

David Marín[1, 2, 3], Esther Posadas[1], Dimas García[1, 2, 5], Daniel Puyol[4], Raquel Lebrero[1, 2], Raúl Muñoz[1, 2, *]

[1] Department of Chemical Engineering and Environmental Technology, School of Industrial Engineering, Valladolid University, Dr. Mergelina, s/n, 47011, Valladolid, Spain.

[2] Institute of Sustainable Processes, University of Valladolid, Dr. Mergelina, s/n, 47011, Valladolid, Spain.

[3] Universidad Pedagógica Nacional Francisco Morazán, Boulevard Centroamérica, Tegucigalpa, Honduras.

[4] Group of Chemical and Environmental Engineering (GIQA), University Rey Juan Carlos, Madrid, Spain.

[5] Centro para la Investigación en Recursos Acuáticos de Nicaragua, CIRA/UNAN-Managua, Apdo. Postal 4598, Nicaragua.

*Corresponding author: mutora@iq.uva.es

Abstract

The potential of purple phototrophic bacteria (PPB) for the simultaneous treatment of piggery wastewater (PWW) and biogas upgrading was evaluated batchwise in gas-tight photobioreactors. PWW dilution was identified as a key parameter determining the efficiency of wastewater treatment and biomethane quality in PPB photobioreactors. Four times diluted PWW supported the most efficient total organic carbon (TOC) and total nitrogen removals (78% and 13%, respectively), with CH_4 concentrations of 90.8%. The influence of phosphorous concentration (supplementation of 50 mg L^{-1} of $P-PO_4^{3-}$) on PPB-based PWW treatment coupled to biogas upgrading was investigated. TOC removals of ≈60% and CH_4 concentrations of ≈90.0% were obtained regardless of phosphorus supplementation. Finally, the use of PPB and algal-bacterial consortia supported CH_4 concentrations in the upgraded biogas of 93.3% and 73.6%, respectively, which confirmed the potential PPB for biogas upgrading coupled to PWW treatment.

Keywords: Biogas upgrading, Biomethane, Piggery wastewater treatment, Purple phototrophic bacteria

1. Introduction

The annual production of pig meat in the European Union (EU) accounted for 24.1 million tons in 2017, which ranked the EU as the second largest pig producer in the world. In this

context, a total of 150.1 million pig heads were produced in the EU in 2017 (Statista, 2018). Unfortunately, this key economic sector annually generates in the EU between 217 and 434 million m^3 of piggery wastewater (PWW) containing high concentrations of organic matter, nitrogen and phosphorus (De Godos et al., 2009; García et al., 2017). The management of such high volumes of PWW represents nowadays an economic, environmental and technical challenge for the EU livestock industry. Anaerobic digestion and activated sludge processes are typically implemented on-site or in centralized facilities in order to fulfill with European wastewater discharge regulations (Andreoli and Von, 2007). In addition, alternative technologies based on the intensification of algal-bacterial symbiosis have been also tested both at lab and pilot scale in order to reduce the operating costs and enhance nutrient recovery during PWW treatment compared to conventional technologies (De Godos et al., 2009; García et al., 2018, 2017). Nevertheless, PWW treatment based on algal-bacterial symbiosis is limited by the high NH$_4^+$ concentrations of this type of wastewater and its poor performance at low temperatures, which requires the development of more resilient biotechnologies capable of cost-competitively recovering the carbon and nutrients from PWW.

In this context, purple phototrophic bacteria (PPB) have emerged as a promising technology platform for wastewater treatment based on their ability to assimilate a higher fraction of the carbon, nitrogen and phosphorous present in wastewater compared to their aerobic and anaerobic counterparts (Hiraishi et al., 1991; Khatipov et al., 1998; Takabatake et al., 2004). Compared to microalgae, PPB utilize infrared radiation (IR) as source of energy, which reduces the power required by photon emission and allows a deeper light penetration into the cultivation broth (thus reducing the footprint of the process) (Hülsen et al., 2014). In addition, the influence of temperature on the growth of PPB is low, which makes them ideal microorganisms to support wastewater treatment under multiple weather conditions. Literature studies have shown the promising potential of these microorganisms for municipal and PWW treatment. For instance, Kim et al. (2004) reported chemical oxygen demand (COD) and orthophosphate removals of 50% and 58%, respectively, under anaerobic conditions in a PPB photobioreactor. PPB have been also successfully applied for industrial wastewater treatment in membrane photobioreactors and sequencing batch stirred tank photobioreactors with COD removal efficiencies of 73-75% (Chitapornpan et al., 2012; Kaewsuk et al., 2010). The ability of

PPB to simultaneously remove COD, nitrogen and phosphorus from domestic wastewater has been recently evaluated in photo-anaerobic batch tests and in a continuous membrane photobioreactor (Hülsen et al., 2016, 2014). A recent comparison between the use of PPB and microalgae for the recovery of carbon, nitrogen and phosphorous from pork, poultry, sugar, dairy and red meat wastewater was carried out by Hülsen et al. (2018), who confirmed that PPB are more efficient for organic and nutrient removal than microalgae.

On the other hand, biogas from the anaerobic digestion of wastewater or organic solid waste represents a renewable energy vector with potential to partially reduce the current world's dependence on fossil fuels (Andriani et al., 2014; Muñoz et al., 2015). In the EU, the contribution of biogas to the energy sector has increased by a factor of 3 concomitantly with an increase in the number of biogas plants from 6227 in 2009 to 17662 by the end of 2016 (European Biogas Association, 2017). Biogas upgrading to biomethane is required prior injection into gas grids or use as a vehicle fuel due to the large number and high concentrations of impurities: CO_2 (15-60%), H_2S (0.005-2%), O_2 (0-1%), N_2 (0-2%), CO (<0.6%), NH_3 (<1%), volatile organic compounds (<0.6%) and siloxanes (0-02%) (Ryckebosch et al., 2011); while most international regulations require concentrations of $CH_4 \geq 95\%$, $CO_2 \leq 2\text{-}4\%$, $O_2 \leq 1\%$ and negligible amounts of H_2S (Muñoz et al., 2015). Algal-bacterial systems have been consistently investigated as a low cost and environmentally sustainable technology to simultaneously remove CO_2 and H_2S from biogas. However, O_2 stripping from the cultivation broth to the biomethane as a result of the oxygenic nature of algal photosynthesis represents the main limitation of algal-bacterial systems in biogas upgrading (Marín et al., 2018; Posadas et al., 2017, 2015). In this sense, the versatile metabolism of PPB, capable of using H_2S in biogas or the organic matter present in wastewater as electron donor to reduce CO_2 from biogas without O_2 generation, could eventually support a cost-effective biogas upgrading. Overall, there is a lack of comparative studies assessing the potential of PPB and algal-bacterial systems in order to determine the most cost-effective and environmentally friendly biotechnology for biogas upgrading.

This study aimed at evaluating, for the first time, the potential and limitations of using PPB for the simultaneous treatment of PWW and upgrading of biogas under IR in batch photobioreactors. The influence of PWW dilution and phosphorous concentration on

PPB-based PWW treatment coupled to biogas upgrading were also investigated batchwise. The mechanisms and limiting factors underlying wastewater treatment and CO_2/H_2S removal by PPB were investigated. A comparative evaluation of PPB-based biogas upgrading vs. algae-based photobioreactors was finally conducted batchwise. The use of batch photobioreactors allowed to systematically test multiple environmental conditions. This work constitutes, to the best of our knowledge, the first proof of concept of the biogas upgrading using PPB under IR.

2. Materials and methods

2.1 Cultivation media

Fresh centrifuged PWW was collected from a nearby farm at Segovia (Spain) and stored at 4°C prior to use. The composition of the PWW was: total organic carbon (TOC) concentration of 10350 mg L^{-1}, inorganic carbon (IC) concentration of 215 mg L^{-1}, total nitrogen (TN) concentration of 2685 mg L^{-1}, P-PO$_4^{3-}$ concentration of 15 mg L^{-1}, total suspended solids (TSS) concentration of 5.9 g L^{-1}. Prior to each test, PWW was centrifuged at 10000 rpm for 20 min in order to separate the soluble from the solid phase. A mineral salt medium (MSM) consisting of distilled water with 1.00 g $(NH_4)_2SO_4$, 0.05 g K_2HPO_4, 0.02 g $MgSO_4$ and 2.00 g NaCl per liter was used in the control tests. A synthetic biogas mixture composed of CO_2 (29.5%), H_2S (0.5%) and CH_4 (70%) was used as a raw biogas in the present study (Abello Linde; Spain).

2.2 Inocula

A set of duplicate glass bottles of 1.2 L was initially filled with 450 ml of centrifuged PWW under a helium headspace, while another set was filled with 440 ml of centrifuged PWW and 10 ml of activated sludge (Valladolid wastewater treatment plant) under a helium headspace. The pH of the cultivation broth was 7.3. The systems were incubated batchwise under magnetic agitation at 200 rpm, 30 °C and continuous IR of 50 W m^{-2} (Oslon black series model SFH4780S with centroid wavelength of 850 nm, OSRAM GmbH, Germany) for 24 days in order to enrich PPB to a final concentration of 0.88 g TSS L^{-1}. A mixture of the enrichments from both sets of bottles was used as inoculum to conduct test series 1-3.

2.3 Piggery wastewater treatment coupled to biogas upgrading in purple phototrophic bacteria photobioreactors

2.3.1. Test series 1: Influence of piggery wastewater dilution on purple phototrophic bacteria-based piggery wastewater treatment coupled to biogas upgrading

The influence of PWW dilution on PPB-based treatment performance was evaluated in 1.2 L bottles under a biogas headspace. The bottles were filled with 360 ml of PWW (undiluted, 2 times diluted and 4 times diluted) and 40 ml of PPB inoculum, and incubated under magnetic agitation at 200 rpm, 30 °C and 50 W m^{-2} of continuous IR for 25 days. A test with 2 times diluted PWW, prepared as above described and incubated in the darkness, was used as control to assess the influence of IR. An additional set of duplicate glass bottles was filled with 360 ml of MSM and 40 ml of inoculum under a biogas headspace to serve as biotic control. Finally, a set of glass bottles was prepared with 360 ml of MSM and 40 ml of inoculum under a biogas headspace and its pH adjusted to 2.0 (thus preventing biological activity) to serve as abiotic control. The assays were conducted in duplicate.

2.3.2 Test Series 2: Influence of phosphorous concentration on purple phototrophic bacteria-based piggery wastewater treatment coupled to biogas upgrading

A set of duplicate glass bottles of 1.2 L was filled with 360 ml of 4 times diluted PWW and 40 ml of inoculum under a biogas headspace. A second set of duplicate glass bottles was filled with 360 ml of 4 times diluted PWW, 40 ml of inoculum and supplemented with a P-PO$_4^{3-}$ concentration of 50 mg L^{-1} under a biogas headspace. The systems were incubated under magnetic agitation at 200 rpm, 30 °C and IR at 50 W m^{-2} for 22 days. The assays were conducted in duplicate.

2.3.3 Test Series 3: Comparative evaluation of the potential of purple phototrophic bacteria and algal-bacterial consortia for biogas upgrading

A set of duplicate glass bottles of 1.2 L was filled with 360 ml of 4 times diluted PWW and 40 ml of inoculum under a biogas headspace. A second set of bottles was prepared with 400 ml of MSM under a biogas headspace to serve as abiotic control. The systems were incubated under magnetic agitation at 200 rpm, 30 °C and an IR of 50 W m^{-2} for 23 days.

At the same time, a set of duplicate glass bottles of 1.2 L was filled with 360 ml of MSM and 40 ml of algal-bacterial inoculum (obtained from an outdoor high rate algal pond treating biogas and centrate at the Valladolid University (Spain)) under a biogas headspace. The pH of the cultivation medium was adjusted to 7.0. A second set of duplicate bottles was prepared with 400 ml of MSM under a biogas headspace to serve as abiotic control. The bottles were incubated under magnetic agitation at 200 rpm, 30 °C and 200 $\mu mol\ m^{-2}\ s^{-1}$ of photosynthetic active radiation provided by high intensity LED PCBs (Phillips SA, Spain) for 23 days. The assays were conducted in duplicate.

In all test series, the pH, headspace gas composition (CH_4, CO_2, H_2S, O_2, and N_2) and concentrations of dissolved TOC, IC, TN, $N-NO_3^-$, $N-NO_2^-$, $P-PO_4^{3-}$, SO_4^{2-} and volatile fatty acids (VFAs) were periodically monitored. The initial and final biomass concentrations (measured as TSS) were also determined.

2.4 Analytical Procedures

Dissolved TOC, IC and TN concentrations were analyzed using a Shimadzu TOC-VCSH analyzer (Japan) equipped with a TNM-1 chemiluminescence unit. $N-NO_3^-$, $N-NO_2^-$, $P-PO_4^{3-}$ and SO_4^{2-} concentrations were quantified by HPLC-IC according to Serejo et al. (2015). VFAs were analyzed in an Agilent 7820A GC-FID (Agilent Technologies, Santa Clara, USA) according to López et al. (2018). The pH was determined with an Eutech Cyberscan pH 510 (Eutech instruments, The Netherlands), while the determination of TSS concentration was performed according to Standard Methods (APHA, 2005). The concentration of CH_4, CO_2, H_2S, O_2, and N_2 in the headspace of the bottles was determined using a Varian CP-3800 GC-TCD (Palo Alto, USA) according to Posadas et al., (2015).

2.5 Statistical analysis

The results here presented were provided as the average values along with their standard deviation from replicate measurements. An analysis of variance (ANOVA) was performed to determine how changes in PWW dilution influenced the quality of the upgraded biogas.

3. Results and discussion

3.1 Influence of piggery wastewater dilution on purple phototrophic bacteria-based piggery wastewater treatment coupled to biogas upgrading

TOC concentration in biotic and abiotic control tests conducted with MSM remained constant at 134 ± 16 mg L^{-1} and 69 ± 9 mg L^{-1}, respectively (Fig. 1a). On the other hand, TOC concentration in undiluted PWW and non-irradiated biotic control tests remained constant at 10318 ± 957 mg L^{-1} and 3535 ± 236 mg L^{-1}, respectively (Fig. 1a). A significant TOC removal from 3977 ± 336 mg L^{-1} to 1453 ± 134 mg L^{-1} (TOC-removal efficiencies (REs) of 63%) in 2 times diluted PWW tests, and from 1989 ± 12 mg L^{-1} to 436 ± 14 mg L^{-1} (TOC-REs of 78%) in 4 times diluted PWW tests (Fig. 1a) was observed. The TOC-REs herein recorded were higher than those obtained by Hülsen et al. (2018), who reported removal efficiencies of COD of approximately 10% for the treatment of PWW in batch tests. At this point it should be highlighted that the TOC instrumental methodology exhibited an error lower than 2 %, while the error of the COD analytical methodology was < 10 %. These results confirmed the potential of PPB to anaerobically degrade organic matter at high concentrations in the presence of IR as energy source, although the high TN concentrations in undiluted PWW seems to inhibit PWW treatment. The pH in the undiluted, biotic control and non-irradiated biotic control tests initially decreased as a result of the CO_2/H_2S acidification mediated by biogas, but remained stable at 6.9 ± 0.1, 6.7 ± 0.1 and 6.6 ± 0.1, respectively, from day 4 onwards. Meanwhile, the pH in the abiotic control remained constant at 2.1 ± 0.1. However, an increase from 6.6 ± 0.1 and 6.8 ± 0.1 (day 4) to 7.8 ± 0.1 and 8.0 ± 0.0 was observed by day 25 in 2 and 4 times diluted PWW tests likely mediated by the release of basic TOC biodegradation metabolites. The high TN concentration in PWW (mainly composed by 80-90% of NH_4^+ (Godos et al., 2010)) and relatively high pH represents a perfect combination for microbial toxicity by free ammonia (FA). Indeed, the main inhibitory mechanism of ammonium in anaerobic organisms is specifically the concentration of FA as a result of a high pH in anaerobic systems (Hansen et al., 1998). FA is a potent uncoupler of membrane transport in any microorganism, as is capable of destabilizing the proton gradient, thus preventing phosphorylation (Gallert et al., 1998; Rajagopal et al., 2013). In this context, only the presence of valinomycin, a potent antibiotic and a K^{2+} transporter in membranes, can activate a similar effect over photophosphorylation in PPB (Fleischman and Clayton, 1968). PWW may contain other organic Na^+-K^{2+} transporters that could

boost the toxicity of FA upon proton motive force in PPB. Indeed, PWW usually contains a wide variety of emerging pollutants like antibiotics or animal health-care products that may act as FA transporters in membranes (Milić et al., 2013).

Similarly, in the assays conducted with undiluted PWW, the IC concentration remained approximately constant at 179 ± 21 mg L^{-1}. In 2 and 4 times diluted tests, IC concentrations increased from 105 ± 9 by day 7 to 336 ± 46 and 397 ± 15 mg L^{-1}, respectively, by day 20 (Fig 1b). This increase in IC concentration was mediated by the absorption of a fraction of the CO_2 present in the biogas. IC concentrations in the non-irradiated biotic control tests remained constant at 119 ± 19 mg L^{-1}, which confirm the absence of biological activity of PPB without IR radiation.

Finally, while TN concentration remained constant in the tests without biological activity (undiluted, abiotic, biotic and non-irradiated biotic control), TN concentration decreased from 1083 ± 75 to 811 ± 15 mg L^{-1} and from 563 ± 5 to 488 ± 18 mg L^{-1} in 2 and 4 times diluted PWW assays, respectively (Fig. 1c). This removal was likely due to nitrogen assimilation into PPB biomass, which amounted 1.5 ± 0.3 and 2.2 ± 0.2 g TSS L^{-1} by the end of the tests conducted in 2 and 4 times diluted PWW, respectively. Neither NO_2^- nor NO_3^- were detected regardless of the TN concentration, which ruled out the occurrence of NH_4^+ nitrification (as expected from the reductive conditions prevailing in the tests).

PWW dilution and the presence of IR significantly impacted on the biogas upgrading performance. Thus, a decrease in CO_2 headspace concentrations from $28.7 \pm 0.4\%$ to $26.2 \pm 0.2\%$, $23.1 \pm 2.0\%$ and $25.7 \pm 0.9\%$ mediated by CO_2 absorption in the cultivation broth was recorded in the assays containing undiluted, biotic and non-irradiated 2 times diluted PWW control tests, while in the abiotic test no significant variation in CO_2 concentration was observed (Fig. 1d). The largest reductions in CO_2 headspace concentrations, down to $9.6 \pm 1.4\%$ and $7.5 \pm 0.1\%$, were recorded in 2 and 4 times diluted PWW tests (Fig. 1d). This removal of CO_2 from biogas was mediated by both an absorption into the cultivation broth (promoted by the above reported increase in pH) and a PPB-based CO_2 fixation using H_2S from biogas and the biodegradable TOC as electron donor. Indeed, H_2S in the headspace decreased from 0.40 to 0.24% and 0.04% in 2 and 4 times diluted PWW tests under reductive conditions, which suggests its biological utilization as electron donor

(Fig. 1e). The unexpected increase in H_2S concentration to 1.0% in undiluted PWW tests and 0.7% in the non-irradiated biotic control tests was likely induced by the use of dissolved sulphate as electron acceptor by sulfate-reducers in the mixed culture during the biodegradation of a minor fraction of biodegradable TOC. Finally, H_2S concentration in the headspace initially decreased to 0.19% and 0.15% in the biotic and abiotic tests, respectively, as a result of H_2S absorption in the MSM. On the other hand, CH_4 headspace concentrations of 88.7% and 90.8% were recorded at the end of the tests containing 2 and 4 times diluted PWW under IR radiation, which confirmed the technical feasibility of combining PWW treatment and biogas upgrading in PPB photobioreactors (Fig. 1f). In addition, a similar variation in CH_4 concentration in the headspace was recorded in the biotic and abiotic tests, increasing from 70 % up to 74.7% and 74.2%, respectively. The biomethane herein obtained in the test conducted with 2 and 4 times diluted PWW and irradiated PPB could be used as a vehicle fuel (a CH_4 content > 80% is required in some countries of the European Union) (Muñoz et al., 2015).
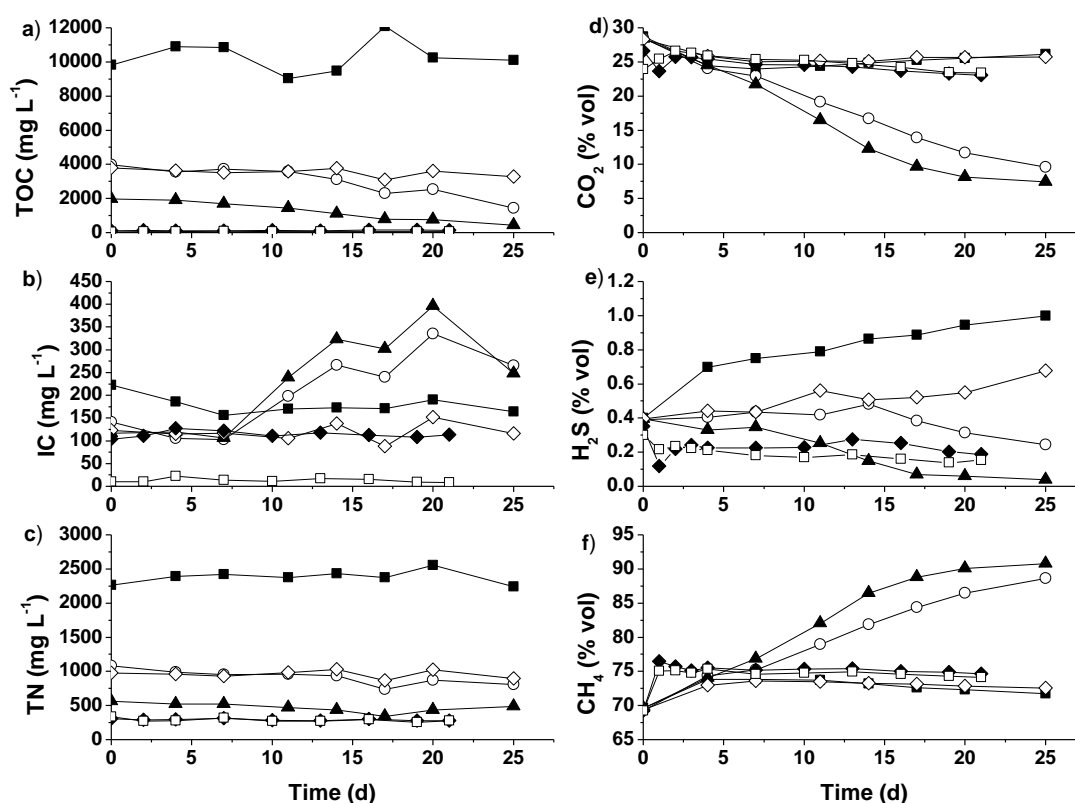
Figure 1. Time course of (a) total organic carbon, (b) inorganic carbon, (c) total nitrogen, (d) CO_2, (e) H_2S and (f) CH_4 concentrations during the biodegradation of undiluted (■), 2 times diluted (○), and 4 times diluted (▲) PWW coupled to biogas upgrading. Inoculated IR-deprived control test with 2 times diluted PWW (◊). Biotic control test with MSM (◆) and abiotic control test with MSM at pH 2.0 (□).

Finally, an ANOVA was carried out to elucidate how changes in PWW dilution influenced the quality of the upgraded biogas. Since the F values for CH_4 and CO_2 (5.6 and 5.2, respectively) were greater than the F critical value of 3.5, it can be concluded that the stated hypothesis was correct and therefore the quality of the upgraded biogas varied significantly with PWW dilution.

CO_2 capture in the Calvin cycle by PPB is possible only when the organic substrates present in the cultivation medium are in a reduced form, since PPB need CO_2 for maintaining the redox homeostasis (McKinlay and Harwood, 2010). This is crucial to achieve a net CO_2 capture, thus allowing biogas upgrading by using the biodegradable organic matter present in wastewater as electron donor. In order to confirm this hypothesis, the time course of VFAs in the experiments conducted with diluted PWW was recorded (Fig. 2). The initial characterization of the wastewater revealed that PWW contained highly reduced organics in the form of VFAs. The main VFAs detected were acetate (963 mg L^{-1}), propionate (230 mg L^{-1}), isobutyrate (126 mg L^{-1}), butyrate (109 mg L^{-1}), isovalerate (72 mg L^{-1}) and valerate (27 mg L^{-1}). The average oxidation state of the VFAs in the PWW herein used was calculated as -0.63 following (McKinlay and Harwood, 2010). These environmental conditions require PPB to use CO_2 to support microbial growth. Indeed, PPB consumed the VFAs concomitantly with biomass growth and CO_2 assimilation in the 2 and 4 times diluted tests (Fig. 2b and 2c, respectively), which confirmed the hypothesis proposed. Meanwhile VFAs remained constant in the undiluted and non-irradiated biotic control tests (Fig. 2a and 2d, respectively). Therefore, PPB use the excess of electrons from the VFAs to assimilate CO_2 in the Calvin cycle. The other major mechanism to achieve redox homeostasis is H_2 production, which was strongly inhibited by the high nitrogen concentration in these particular assays (Sweet and Burris, 1981).

Since 4 times diluted PWW (with a TN concentration of 600 mg L^{-1}) supported the most efficient TOC, TN, CO_2 and H_2S removal, test series 2 and 3 were conducted under these experimental conditions.
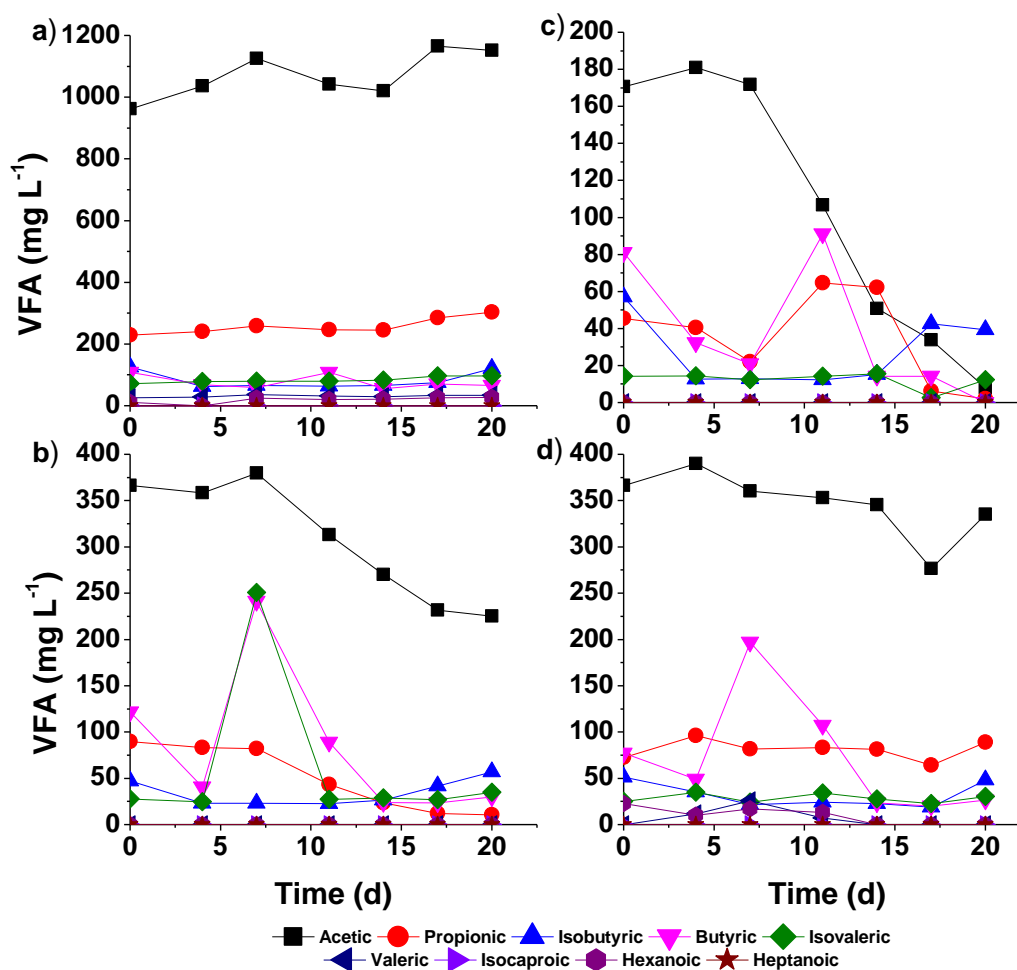
Figure 2. Time course of VFA concentration during the biodegradation of (a) undiluted, (b) 2 times diluted and (c) 4 times diluted PWW coupled to biogas upgrading. (d) Inoculated IR-deprived control test with 2 times diluted PWW.

3.2 Influence of phosphorous concentration on purple phototrophic bacteria-based piggery wastewater treatment coupled to biogas upgrading

A significant TOC removal from 1712 ± 143 to 803 ± 123 mg L^{-1} (TOC-REs of 53%) was recorded in 4 times diluted PWW, while phosphorus supplementation supported a decrease in TOC concentration from 1625 ± 86 to 646 ± 110 mg L^{-1} (TOC-REs of 60%) (Fig. 3a). The high TOC-REs recorded in test series 2 were mediated by the assimilation as biomass instead of by TOC oxidation to CO_2, and confirmed the potential of PPB to anaerobically degrade organic matter assisted by IR regardless of phosphorus supplementation. A pH increase from 6.7 ± 0.1 and 6.8 ± 0.0 (day 4) to 7.5 ± 0.1 and 7.7 ± 0.0 was observed by the end of day 22 in tests conducted without and with phosphorus supplementation to 4 times diluted PWW, respectively, due to PPB-based TOC biodegradation. IC concentration increased as a result of pollutant mineralization and CO_2

capture/fixation from 56 ± 3 to 369 ± 21 and 364 ± 9 mg L^{-1} (day 19) without and with phosphorus addition, respectively (Fig 3b). TN concentration decreased from 620 ± 20 to 308 ± 39 mg L^{-1} without phosphorous addition and from 611 ± 10 to 285 ± 33 mg L^{-1} when phosphorus was supplemented (Fig. 3c). This removal was likely due nitrogen assimilation into PPB biomass, which averaged 1.8 ± 0.8 and 1.9 ± 0.1 g TSS L^{-1} by the end of the tests without and with phosphorus supplementation, respectively. The TN-REs herein recorded were higher those reported by Hülsen et al. (2018), who achieved values of approximately 10% during the batch treatment of PWW by PPB. Neither NO_2^- nor NO_3^- were detected in these tests series. The results here recorded for TOC, IC and TN concentrations confirmed that phosphorous supplementation did not enhance significantly PPB-based PWW treatment under photo-anaerobic conditions. Finally, P-PO_4^{3-} in the test supplemented with phosphorus was completely removed by day 13 mainly due to P assimilation into biomass, while P-PO_4^{3-} in the non-supplemented test remained below the detection limit of the HPLC-IC (3 mg P L^{-1}).

The impact of phosphorus supplementation was more noticeable in the upgrading of biogas. A reduction in CO_2 concentration from 29.4% to 8.2% and from 29.0% to 5.2% was recorded with and without phosphorus supplementation, respectively (Fig. 3d). H_2S concentration in the headspace decreased from 0.36% to 0.07% without phosphorus supplementation, while phosphorus supplementation supported a complete removal of H_2S. This suggested its biological utilization as electron donor to support CO_2 assimilation (Fig. 3e). Finally, an increase in CH_4 concentration from 70 % to 89.2% and 91.9% without and with phosphorus supplementation was recorded (Fig. 3f). The quality of the biomethane produced in P-supplemented tests complied with biomethane requirements for use as a vehicle fuel (Muñoz et al., 2015).
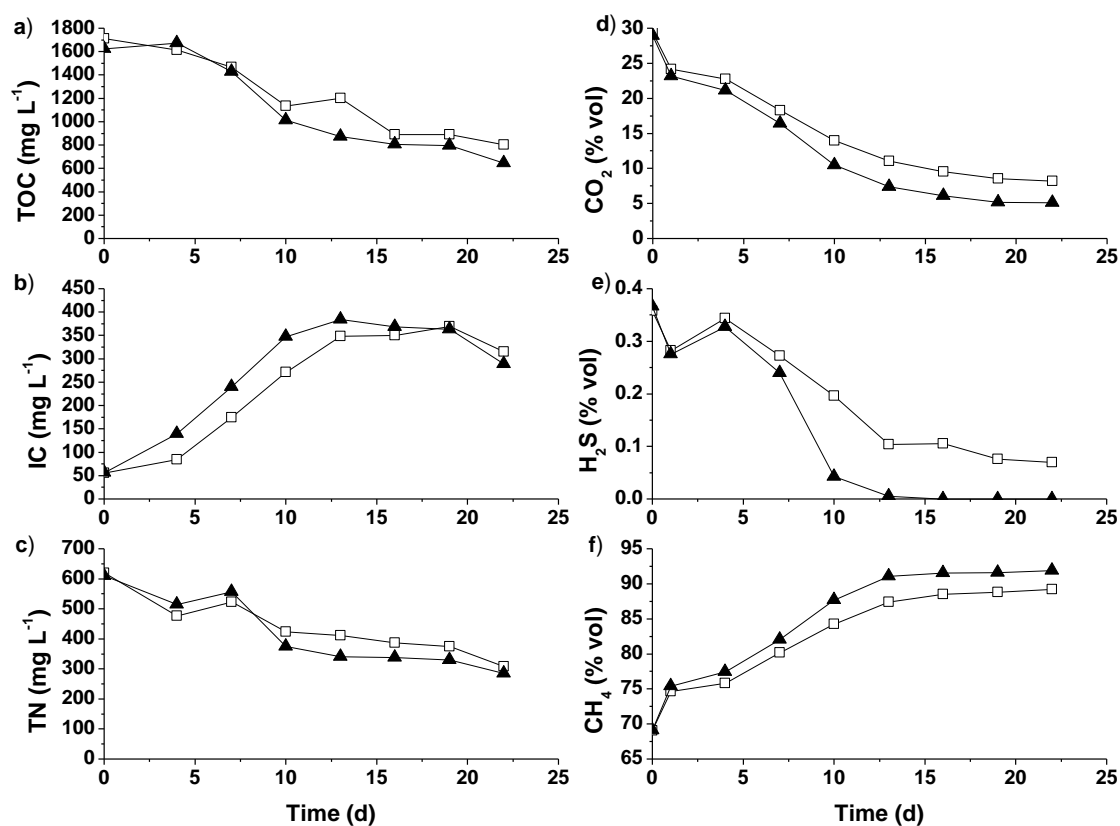
Figure 3. Time course of (a) total organic carbon, (b) inorganic carbon, (c) total nitrogen, (d) CO_2, (e) H_2S and (f) CH_4 concentrations during the treatment of 4 times diluted PWW (□) and 4 times diluted PWW supplemented with 50 mg P-PO_4^{3-} L^{-1} (▲).

3.3 Comparative evaluation of the potential of purple phototrophic bacteria and algal-bacterial consortia for biogas upgrading

The ability of PPB and an algal-bacterial consortium to simultaneously treat PWW and upgrade biogas was comparatively assessed. A limited decrease in CO_2 headspace concentrations from 28.6% to 24.1% was recorded in the test inoculated with the algal-bacterial consortium, while CO_2 concentrations of 3.3% were obtained at the end of the experiment inoculated with PPB (Fig. 4a). The low pH in the cultivation broth of the algal-bacterial system (5.4 ± 0.7) imposed by the biogas headspace likely inhibited photosynthetic activity of microalgae. H_2S concentration in the headspace of the PPB tests decreased from 0.35% to 0.10%, while in the algal-bacterial systems a H_2S concentration of 0.47% was recorded by day 23 (Fig. 4b). CH_4 headspace concentration reached values of 93.3% and 73.6% in the tests with PPB and algal-bacterial consortium, respectively (Fig. 4c). Therefore, an enhanced biogas upgrading capacity was observed for PPB compared with the algal-bacterial consortium.
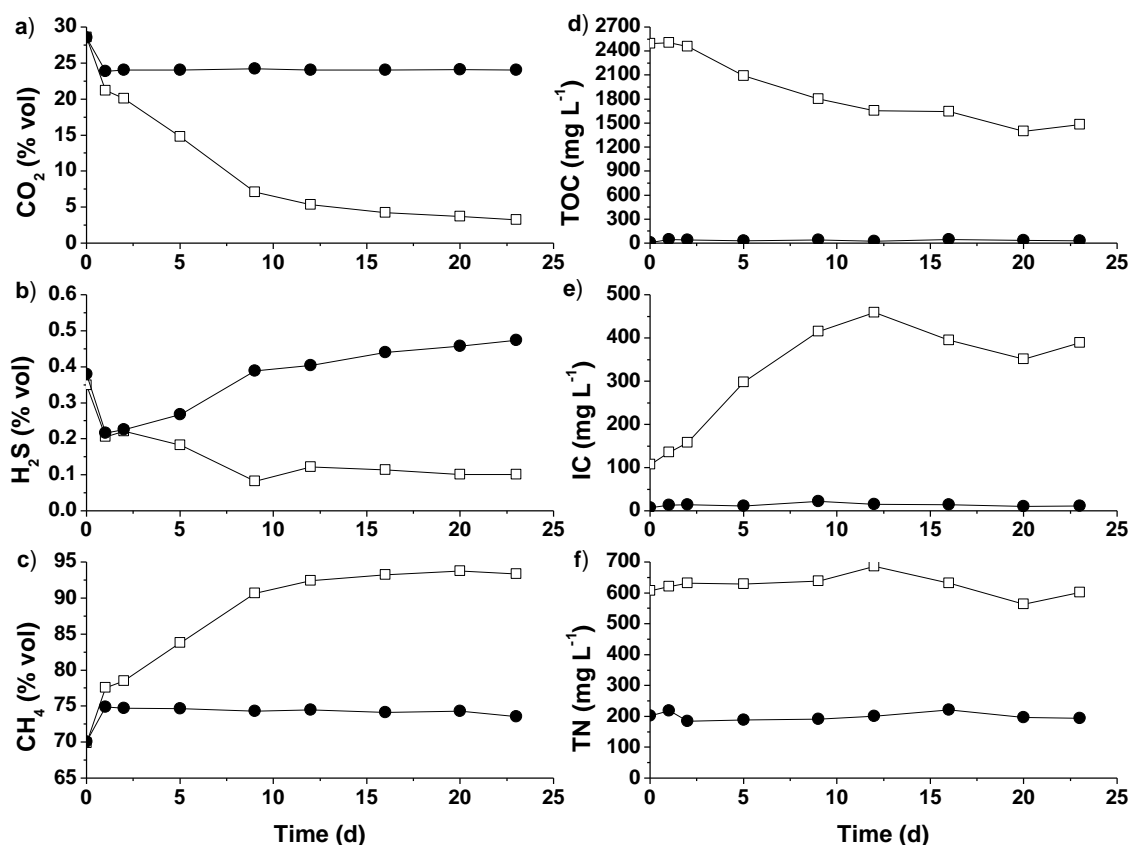
Figure 4. Time course of (a) CO_2, (b) H_2S, (c) CH_4, (d) total organic carbon, (e) inorganic carbon and (f) total nitrogen concentration during biogas upgrading with a PPB consortium treating PWW (□) and an algal-bacterial consortium (●).

Finally, the TOC concentration in the algal-bacterial tests remained constant at 38 ± 7 mg L^{-1}, and gradually decreased from 2498 ± 0 to 1483 ± 7 mg L^{-1} (TOC-RE of 41%) in PPB tests (Fig. 4d). On the other hand, the IC concentration in the algal-bacterial tests remained constant at 14 ± 4 mg L^{-1} and increased in the PPB tests from 108 ± 0 to 459 ± 40 mg L^{-1} by day 12 (Fig. 4e). Finally, no significant variation in the TN concentration was observed regardless of the consortia (624 ± 33 mg L^{-1} in PPB tests and 200 ± 13 mg L^{-1} in algal-bacterial tests) (Fig. 4f).

4. Conclusions

PPB represent an innovative biological platform for the simultaneous treatment of PWW and upgrading of biogas under photo-anaerobic conditions. PWW with TN concentrations of 600 mg L^{-1} provided the best conditions for wastewater treatment and biogas upgrading. The presence of VFA in PWW supported CO_2 fixation in the Calvin cycle, thus allowing biogas upgrading. The low phosphorous concentrations inherent to PWW

did not significantly impact on wastewater treatment performance but slightly improved biomethane quality. CH_4 concentrations of 93.3% can be achieved using PPB, which complied with most international regulations for biogas use as a vehicle fuel.

Acknowledgements

References

1. Andreoli, C.V., Von, M., 2007. Sludge Treatment and Disposal, Environmental Protection. doi:10.1016/B978-1-85617-705-4.00021-6

2. Andriani, D., Wresta, A., Atmaja, T.D., Saepudin, A., 2014. A Review on Optimization Production and Upgrading Biogas Through CO_2 Removal Using Various Techniques. Appl. Biochem. Biotechnol. 172, 1909–1928. doi:10.1007/s12010-013-0652-x

3. APHA, 2005. Standard Methods for the Examination of Water and Wastewater, 21st ed. Public Health Association, Washington DC.

4. Chitapornpan, S., Chiemchaisri, C., Chiemchaisri, W., Honda, R., Yamamoto, K., 2012. Photosynthetic bacteria production from food processing wastewater in sequencing batch and membrane photo-bioreactors. Water Sci. Technol. 65, 504–512. doi:10.2166/wst.2012.740

5. De Godos, I., Blanco, S., García-encina, P.A., Becares, E., Muñoz, R., 2009. Bioresource Technology Long-term operation of high rate algal ponds for the bioremediation of piggery wastewaters at high loading rates. Bioresour. Technol. 100, 4332–4339. doi:10.1016/j.biortech.2009.04.016

6. European Biogas Association, 2017. EBA Statistical Report 2017 [WWW Document]. URL http://european-biogas.eu/2017/12/14/eba-statistical-report-2017-published-soon/ (accessed 11.13.18).

7. Fleischman, D.E., Clayton, R.K., 1968. The effect of phosphorylation uncouplers and electron transport inhibitors upon spectral shifts and delayed light emission of photosynthetic bacteria. Photochem. Photobiol. 8, 287–298. doi:10.1111/j.1751-1097.1968.tb05872.x

8. Gallert, C., Bauer, S., Winter, J., 1998. Effect of ammonia on the anaerobic degradation of protein by a mesophilic and thermophilic biowaste population. Appl. Microbiol. Biotechnol. 50, 495–501. doi:10.1007/s002530051326

9. García, D., Posadas, E., Blanco, S., Acién, G., García-Encina, P., Bolado, S., Muñoz, R., 2018. Evaluation of the dynamics of microalgae population structure and process performance during piggery wastewater treatment in algal-bacterial photobioreactors. Bioresour. Technol. 248, 120–126. doi:10.1016/j.biortech.2017.06.079

10. García, D., Posadas, E., Grajeda, C., Blanco, S., Martínez-Páramo, S., Acién, G., García-Encina, P., Bolado, S., Muñoz, R., 2017. Comparative evaluation of piggery wastewater treatment in algal-bacterial photobioreactors under indoor and outdoor conditions. Bioresour. Technol. 245, 483–490. doi:10.1016/j.biortech.2017.08.135

11. Godos, I. de, Vargas, V.A., Blanco, S., González, M.C.G., Soto, R., García-Encina, P.A., Becares, E., Muñoz, R., 2010. A comparative evaluation of microalgae for the degradation of piggery wastewater under photosynthetic oxygenation. Bioresour. Technol. 101, 5150–5158. doi:10.1016/j.biortech.2010.02.010

12. Hansen, K.H., Angelidaki, I., Ahring, B.K., 1998. Anaerobic digestion of swine manure: inhibition by ammonia. Water Res. 32, 5–12. doi:10.1016/S0043-1354(97)00201-7

13. Hiraishi, A., Yanase, A., Kitamura, H., 1991. Polyphosphate Grown Accumulation under Different by Rhodobacter Environmental on the sphaeroides Conditions with Special Emphasis Phosphate Effect of External Concentrations. Bull. Japanese Soc. Microb. Ecol. 6, 25–32.

14. Hülsen, T., Barry, E.M., Lu, Y., Puyol, D., Keller, J., Batstone, D.J., 2016. Domestic wastewater treatment with purple phototrophic bacteria using a novel continuous photo anaerobic membrane bioreactor. Water Res. 100, 486–495. doi:10.1016/j.watres.2016.04.061

15. Hülsen, T., Batstone, D.J., Keller, J., 2014. Phototrophic bacteria for nutrient recovery from domestic wastewater. Water Res. 50, 18–26. doi:10.1016/j.watres.2013.10.051

16. Hülsen, T., Hsieh, K., Lu, Y., Tait, S., Batstone, D.J., 2018. Simultaneous treatment and single cell protein production from agri-industrial wastewaters using purple phototrophic bacteria or microalgae – A comparison. Bioresour. Technol. 254, 214–223. doi:10.1016/j.biortech.2018.01.032

17. Kaewsuk, J., Thorasampan, W., Thanuttamavong, M., Seo, G.T., 2010. Kinetic development and evaluation of membrane sequencing batch reactor (MSBR) with mixed cultures photosynthetic bacteria for dairy wastewater treatment. J. Environ. Manage. 91, 1161–1168. doi:10.1016/j.jenvman.2010.01.012

18. Khatipov, E., Miyakea, M., Miyakec, J., Asadaa, Y., 1998. Accumulation of poly- L -hydroxybutyrate by Rhodobacter sphaeroides on various carbon and nitrogen substrates. FEMS Microbiol. Lett. 162, 39–45.

19. Kim, M.K., Choi, K., Yin, C., Lee, K., Im, W., Lim, H., Lee, S., 2004. Odorous swine wastewater treatment by purple non-sulfur bacteria , Rhodopseudomonas palustris , isolated from eutrophicated ponds. Biotechnol. Lett. 26, 819–822.

20. López, J.C., Arnáiz, E., Merchán, L., Lebrero, R., Muñoz, R., 2018. Biogas-based polyhydroxyalkanoates production by Methylocystis hirsuta: A step further in anaerobic digestion biorefineries. Chem. Eng. J. 333, 529–536. doi:10.1016/j.cej.2017.09.185

21. Marín, D., Posadas, E., Cano, P., Pérez, V., Blanco, S., Lebrero, R., 2018. Seasonal variation of biogas upgrading coupled with digestate treatment in an outdoors pilot scale algal-bacterial photobioreactor. Bioresour. Technol. 263, 58–66. doi:10.1016/j.biortech.2018.04.117

22. McKinlay, J.B., Harwood, C.S., 2010. Carbon dioxide fixation as a central redox cofactor recycling mechanism in bacteria. Proc. Natl. Acad. Sci. 107, 11669–11675. doi:10.1073/pnas.1006175107

23. Milić, N., Milanović, M., Letić, N.G., Sekulić, M.T., Radonić, J., Mihajlović, I., Miloradov, M.V., 2013. Occurrence of antibiotics as emerging contaminant substances in aquatic environment. Int. J. Environ. Health Res. 23, 296–310. doi:10.1080/09603123.2012.733934

24. Muñoz, R., Meier, L., Diaz, I., Jeison, D., 2015. A review on the state-of-the-art of physical/chemical and biological technologies for biogas upgrading. Rev. Environ. Sci. Biotechnol. 14, 727–759. doi:10.1007/s11157-015-9379-1

25. Posadas, E., Marín, D., Blanco, S., Lebrero, R., Muñoz, R., 2017. Simultaneous biogas upgrading and centrate treatment in an outdoors pilot scale high rate algal pond. Bioresour. Technol. 232, 133–141. doi:10.1016/j.biortech.2017.01.071

26. Posadas, E., Serejo, M.L., Blanco, S., Pérez, R., García-Encina, P.A., Muñoz, R., 2015. Minimization of biomethane oxygen concentration during biogas upgrading in algal-bacterial photobioreactors. Algal Res. 12, 221–229. doi:10.1016/j.algal.2015.09.002

27. Rajagopal, R., Massé, D.I., Singh, G., 2013. A critical review on inhibition of anaerobic digestion process by excess ammonia. Bioresour. Technol. 143, 632–641. doi:10.1016/j.biortech.2013.06.030

28. Ryckebosch, E., Drouillon, M., Vervaeren, H., 2011. Techniques for transformation of biogas to biomethane. Biomass and Bioenergy 35, 1633–1645. doi:10.1016/j.biombioe.2011.02.033

29. Serejo, M.L., Posadas, E., Boncz, M.A., Blanco, S., García-Encina, P., Muñoz, R., 2015. Influence of biogas flow rate on biomass composition during the optimization of biogas upgrading in microalgal-bacterial processes. Environ. Sci. Technol. 49, 3228–3236. doi:10.1021/es5056116

30. Statista, 2018. Global pork production in 2018, by country [WWW Document]. URL https://www.statista.com/ (accessed 1.8.19).

31. Sweet, W.J., Burris, R.H., 1981. Inhibition of nitrogenase activity by NH+4 in Rhodospirillum rubrum. J. Bacteriol. 145, 824–831.

32. Takabatake, H., Suzuki, K., Ko, I.-B., Noike, T., 2004. Characteristics of anaerobic ammonia removal by a mixed culture of hydrogen producing photosynthetic bacteria. Bioresour. Technol. 95, 151–158. doi:10.1016/j.biortech.2003.12.019

Supplementary material

Assessing the potential of purple phototrophic bacteria for the simultaneous treatment of piggery wastewater and upgrading of biogas

David Marín[1, 2, 3], Esther Posadas[1], Dimas García[1, 2, 5], Daniel Puyol[4], Raquel Lebrero[1, 2], Raúl Muñoz[1, 2, *]

[1] Department of Chemical Engineering and Environmental Technology, School of Industrial Engineering, Valladolid University, Dr. Mergelina, s/n, 47011, Valladolid, Spain.

[2] Institute of Sustainable Processes, University of Valladolid, Dr. Mergelina, s/n, 47011, Valladolid, Spain.

[3] Universidad Pedagógica Nacional Francisco Morazán, Boulevard Centroamérica, Tegucigalpa, Honduras.

[4] Group of Chemical and Environmental Engineering (GIQA), University Rey Juan Carlos, Madrid, Spain.

[5] Centro para la Investigación en Recursos Acuáticos de Nicaragua, CIRA/UNAN-Managua, Apdo. Postal 4598, Nicaragua.

*Corresponding author: mutora@iq.uva.es

Figure S1. Inoculum enrichment set-up

pH values
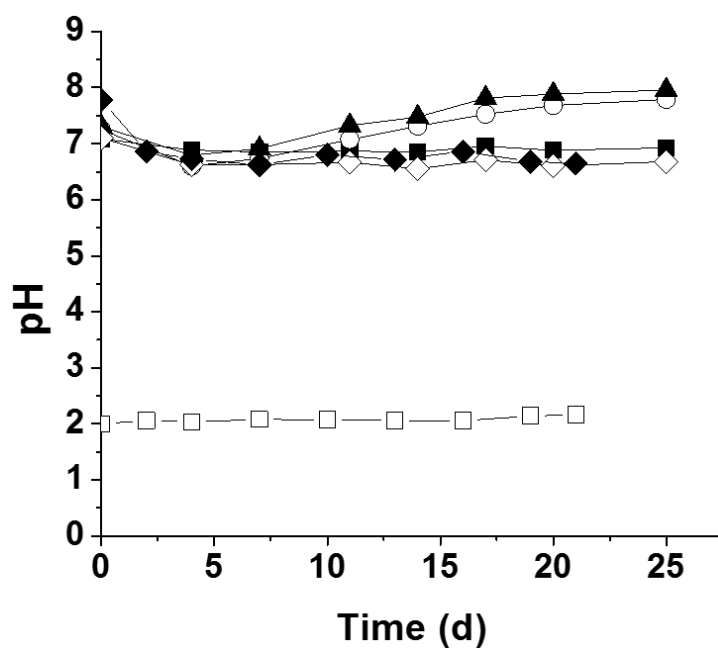
Figure S2. Time course of pH during the biodegradation of undiluted (■), 2 times diluted (○), and 4 times diluted (▲) PWW coupled to biogas upgrading. Inoculated IR-deprived control test with 2 times diluted PWW (◊), biotic control test with MSM (◆), abiotic control test with MSM at pH 2.0 (□).
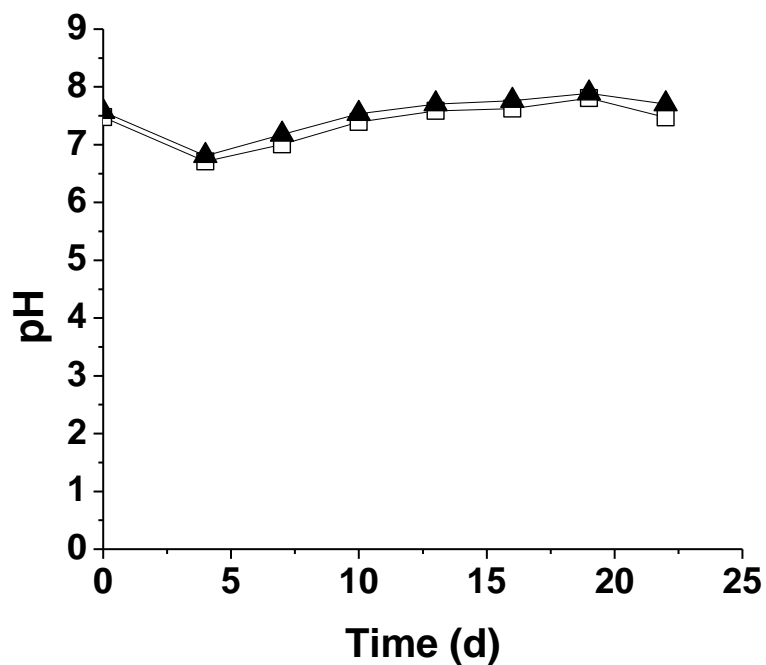
Figure S3. Time course of pH in test series 2. Four times diluted PWW without (□) and with $P-PO_4^{3-}$ supplementation (▲).
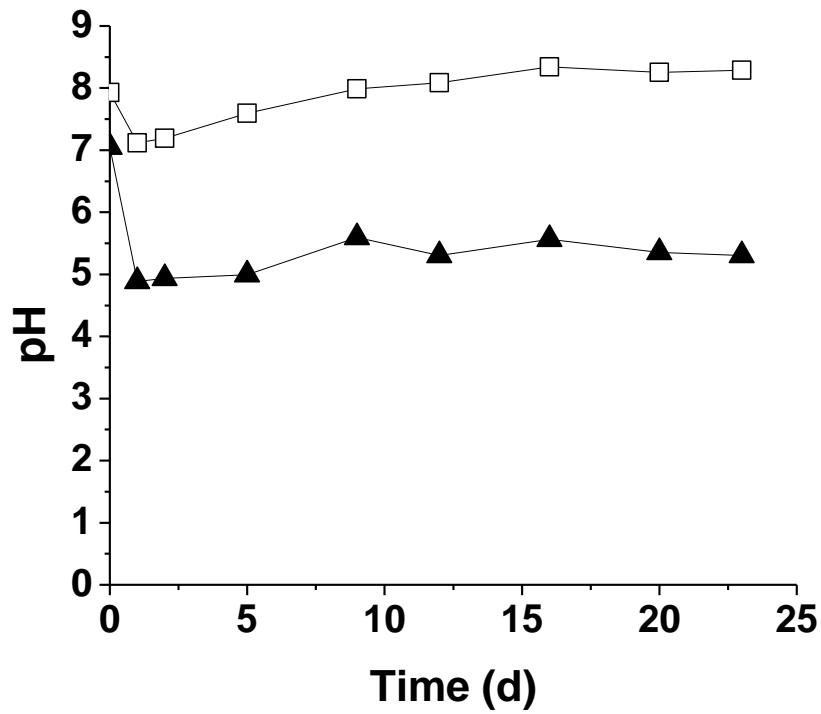
Figure S4. Time course of pH in test series 3. Purple phototrophic bacteria treating 4 times diluted PWW under a biogas atmosphere (□), algal-bacterial consortium in MSM under a biogas atmosphere (▲).

P-PO$_4^{3-}$ concentration in test series 3
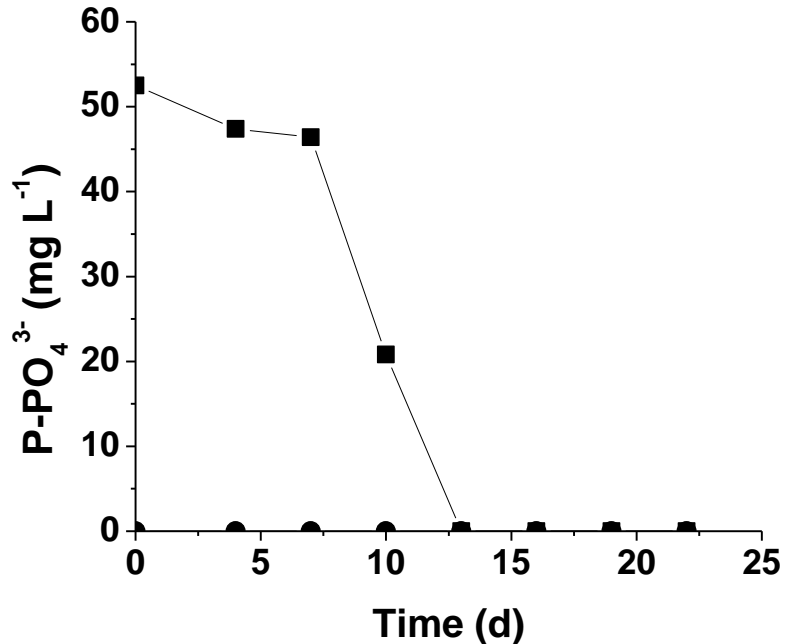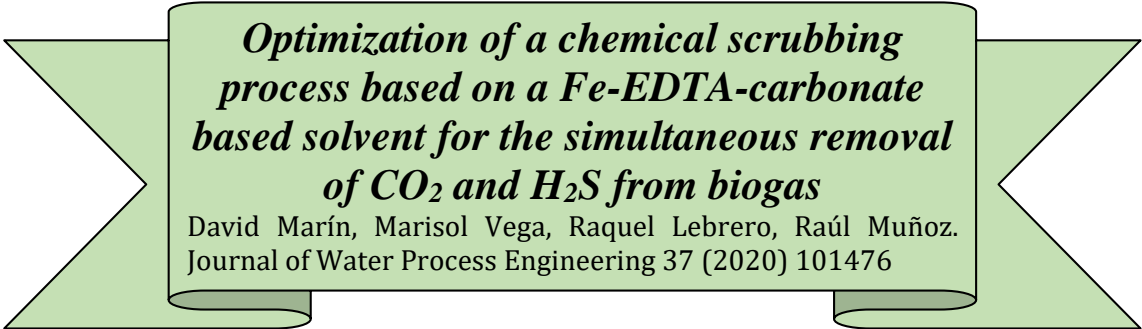
Figure S5. Time course of P-PO$_4^{3-}$ concentration in the cultivation broth of the assays conducted with 4 times diluted PWW (●) and 4 times diluted PWW supplemented with PO$_4^{3-}$ (■) in test series 3.

Table S.1. Analysis of variance

	Sum of squares	Degrees of freedom	Mean square	F value	F critical
CH_4	410.8	2	205.4	5.6	3.5
Error	775.1	21	36.9		
CO_2	380.6	2	190.3	5.2	3.5
Error	763.9	21	36.4		
H_2S	1.4	2	0.7	35.4	3.5
Error	0.4	21	0.1		

Chapter 8

Optimization of a chemical scrubbing process based on a Fe-EDTA-carbonate based solvent for the simultaneous removal of CO_2 and H_2S from biogas

David Marín, Marisol Vega, Raquel Lebrero, Raúl Muñoz.

Optimization of a chemical scrubbing process based on a Fe-EDTA-carbonate based solvent for the simultaneous removal of CO_2 and H_2S from biogas

David Marín[1, 2, 3], Marisol Vega[2, 4], Raquel Lebrero[1, 2], Raúl Muñoz*[1, 2]

[1] Department of Chemical Engineering and Environmental Technology, School of Industrial Engineering, Valladolid University, Dr. Mergelina, s/n, 47011, Valladolid, Spain.

[2] Institute of Sustainable Processes, Dr. Mergelina, s/n, 47011, Valladolid, Spain.

[3] Universidad Pedagógica Nacional Francisco Morazán, Boulevard Centroamérica, Tegucigalpa, Honduras.

[4] Department of Analytical Chemistry, University of Valladolid, Campus Miguel Delibes, Paseo Belén 7, 47011 Valladolid, Spain.

[*] Corresponding author: mutora@iq.uva.es

Abstract

The potential of a novel Fe/EDTA/carbonate-based scrubbing process for the simultaneous removal of H_2S and CO_2 from biogas was studied by evaluating the influence of Fe/EDTA molarity (M), carbonate concentration (IC), biogas (B), air (A) and liquid (L) flow rates on biogas upgrading performance using a Taguchi $L_{16}(4^5)$ experimental design. The ANOVA demonstrated that molarity of the Fe/EDTA solution was a significant factor influencing H_2S concentration (0.035% at 0.00M to 0.000% at 0.05M). IC impacted on the concentrations of CO_2 (13.1 and 4.5% at 4000 and 10000mg IC L^{-1}, respectively), N_2 and CH_4 (85.9 and 94.5% at 4000 and 10000mgIC L^{-1}, respectively). The biogas flow rate affected the concentrations of CO_2 (2.5 to 13.8% at 10 and 40mL min^{-1}, respectively), O_2, N_2 and CH_4 (95.9 to 85.4% at 10 and 40mL min^{-1}, respectively). Likewise, the recycling liquid flow rate affected CO_2 (8.3 and 5.9% at 5 and 30mL min^{-1}, respectively), O_2, N_2 and CH_4 (90.5 and 93.3% at 5 and 40mL min^{-1}, respectively) concentrations. Finally, the air flow rate impacted on CO_2 (10.8 and 6.7% at 800 and 1000mL min^{-1}, respectively), H_2S, N_2 and CH_4 (87.9 and 92.2% at 800 and 1000mL min^{-1}, respectively) concentrations. Process optimization provided the optimal conditions for each control factor. Continuous biogas upgrading operation at M_2-IC_1-B_2-A_4-L_4 (0.05M, 10000mgIC L^{-1}, 10mL min^{-1}, 1000mL min^{-1} and 30mL min^{-1}, respectively) provided CH_4, CO_2, O_2, N_2 and H_2S concentration in the upgrading biogas of 97.4, 1.4, 0.29, 0.97 and 0%, respectively, which complied with biomethane regulations.

Keywords: Absorption-stripping process; Biogas upgrading; Biomethane; Chemical scrubbing; Taguchi's design.

1. Introduction

Biogas from anaerobic waste treatment represents a renewable energy vector that can be used as a fuel to power vehicles or to generate electricity and heat for domestic and industrial applications, which can partially mitigate Europe's dependence on imported fossil fuels [1,2]. In this context, the number of biogas plants in Europe has increased from 6227 in 2009 to 17783 by the end of 2017, while biomethane production capacity has also increased from 752 GWh in 2011 to 19352 GWh by the end of 2017 [3]. An upgrading of biogas into biomethane is required prior use as a vehicle fuel or for the injection into natural gas grids due to the high concentration of impurities present in raw biogas: CO_2 (15-60%), CO (<0.6%), H_2S (0.005-2%), N_2 (0-2%), O_2 (0-1%), NH_3 (<1%), siloxanes (0-0.2%) and volatile organic compounds (<0.6%) [4]. Hence, most international biomethane standards require a composition of $CH_4 \geq$ 90-95%, $CO_2 \leq$ 2-4%, $O_2 \leq$ 1% and negligible amounts of H_2S [2,5,6].

Multiple technologies are nowadays commercially available or under validation phase to remove CO_2 and H_2S from biogas in order to fullfil with biomethane standards. Biological technologies are being succesfully scaled-up since the past decade and exhibit lower environmental impacts and lower operating costs. However, biotechnologies require either a cost-effective H_2 production from renewable energy surplus (in the case of hydrogenotrophic upgrading) or large areas and favourable environmental conditions (in the case of photosynthetic biogas upgrading) [2,7]. On the other hand, membrane separation, chemical/water/organic scrubbing, cryogenic separation or pressure swing adsorption can remove CO_2 from biogas, while *in-situ* chemical precipitation or adsorption onto activated carbon or metal ions provide an effective H_2S removal [2,7]. These physicochemical methods present high operating costs (2-5 ct€ kWh^{-1}) and environmental impacts as a result of their high energy demand, entail process operation at high temperatures and pressures, and can not support a simultaneous H_2S and CO_2 removal [8]. Therefore, there is an urgent need to develop cost-effective technologies operating under ambient conditions capable of supporting an integral biogas upgrading

(H_2S and CO_2 removal in a single step process), which will increase the environmental and economic sustainability of biogas upgrading and boost biomethane industry.

In this context, the use of an absorption-stripping process based on an aqueous solution of Fe-EDTA-carbonate represents an innovative physicochemical technology capable of simultaneously removing H_2S and CO_2 from biogas [9]. Highly carbonated aqueous solutions at high pH mediate a rapid and effective CO_2 capture at ambient pressure and allow an air-aided CO_2 desorption. The absorption and dissociation of CO_2 is described by equations (1) to (4):

$$CO_{2_g} \rightarrow CO_{2_L} \tag{1}$$
$$CO_{2_L} + H_2O \rightarrow H_2CO_3 \tag{2}$$
$$H_2CO_3 + H_2O \rightarrow HCO_3^- + H^+ \tag{3}$$
$$HCO_3^- \rightarrow CO_3^{2-} + H^+ \tag{4}$$

The mass transfer of CO_2 from the biogas to the aqueous chemical solution can be described as a function of a volumetric mass transfer coefficient (k_La), multiplied by the concentration gradient in the liquid phase ($\frac{CO_{2g}}{H} - CO_{2_L}$), where H is the dimensionless Henry`s law constant. At this point it should be stressed that the high pH of the scrubbing solution maintains the value of CO_{2L} very low, and therefore, the gas-liquid concentration gradient as a maximum value. In addition, the high ionic strength of the scrubbing solution prevents the coalescence of biogas bubbles, which enhances k_La.

On the other hand, Fe^{3+}-EDTA solutions support a cost effective H_2S oxidation to elemental sulphur. According with Wubs and Beenackers [10], the absorption and oxidation of H_2S with Fe-EDTA is described by equations (5) and (6):

$$H_2S_{(g)} \leftrightarrow H_2S_{(aq)} \tag{5}$$
$$H_2S_{(aq)} + 2Fe^{3+}/EDTA \rightarrow S_{(s)} + 2H^+ + 2Fe^{2+}/EDTA \tag{6}$$
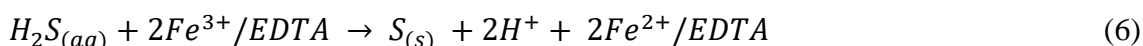
The Fe^{2+}/EDTA resulting from H_2S oxidation to S can be regenerated into its active ferric form (Fe^{3+}/EDTA) by oxidation with the air used for CO_2 stripping (equations 7 and 8).

$$O_{2\,(g)} \leftrightarrow O_{2\,(aq)} \tag{7}$$

$$O_{2\,(aq)} + 4Fe^{2+}/EDTA + 2H_2O \rightarrow 4Fe^{3+}/EDTA + 4OH^- \tag{8}$$
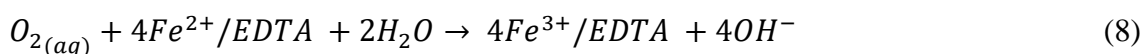
Several studies have investigated the potential of Fe^{3+}/EDTA to remove H_2S from biogas. In this sense, Horikawa et al., [11] studied the purification of biogas and reported a 90% removal of H_2S from biogas using a 0.2 M Fe/EDTA aqueous solution in a system composed of an absorption and a regeneration column with a total volume of 0.82 L. Similarly, Schiavon Maia et al., [12] observed a 91% removal of H_2S in a similar absorption-regeneration system using a 0.2 M Fe/EDTA solution, at biogas and liquid flow rates of 340 mL min^{-1}. Finally, Frare et al., [13] investigated the absorption efficiency of H_2S in a similar absorption-regeneration system using a 0.4 M Fe/EDTA solution at a biogas flow rate of 265 mL min^{-1} and at different liquid flow rates (22, 48, 61, 70, 80, 122, 162, 207, 250 mL min^{-1}). Despite the promising results obtained in terms of H_2S removal, the use of Fe/EDTA solutions has been exclusively studied for H_2S and NO_x removal [14]. In this context, the performance of novel Fe/EDTA solutions enriched with carbonates must be tested in order to support a simultaneous removal of CO_2 and H_2S from biogas at ambient pressure and temperature, which is expected to decrease both the investment and operating costs (the latter by one order of magnitude compared to conventional physical/chemical biogas upgrading technologies).

This study investigated, for the first time, the use of a chemical scrubbing process based on a Fe/EDTA/carbonate solution for the simultaneous removal of CO_2 and H_2S from biogas in a single step process composed of a biogas absorption column interconnected to an air-aided regeneration column. A Taguchi $L_{16}(4^5)$ experimental design was used in order to evaluate the influence of Fe/EDTA molarity, carbonate concentration, and biogas, air and liquid flow rates on biogas upgrading and to elucidate the optimal values of the parameters.

2. Materials and methods

2.1 Biogas and Fe/EDTA solution

The synthetic gas mixture used as a model biogas was composed of CH_4 (70%), CO_2 (29.5%) and H_2S (0.5%) (Abello Linde; Spain). The Fe/EDTA/carbonate solution was

prepared using iron (III) monosodium ethylenediaminetetraacetic (Alfa Aesar, Germany), sodium carbonate and sodium bicarbonate (Cofarcas, Spain).

2.2 Experimental set-up

The experimental lab scale set-up was located at the Institute of Sustainable Processes of Valladolid University (Spain). The lab scale set-up consisted of a biogas absorption column with a working volume of 1.8 L (internal diameter = 4 cm; height = 150 cm) and a regeneration column with a working volume of 2.0 L (internal diameter = 4 cm; height = 198 cm). Both columns were interconnected by a recirculation pump using a degassing chamber of 0.45 L (internal diameter = 8 cm; height = 9 cm). Biogas was injected in the absorption column under counter-current flow operation using a metallic diffuser of 2 μm pore size installed at the bottom of the column. Similarly, air was injected in the regeneration column under counter-current flow operation using a metallic diffuser of 2 μm pore size installed at the bottom of the column (Fig. 1). The air and biogas flow rates were controlled via rotameter and mass flow controller, respectively (Aalborg, USA).
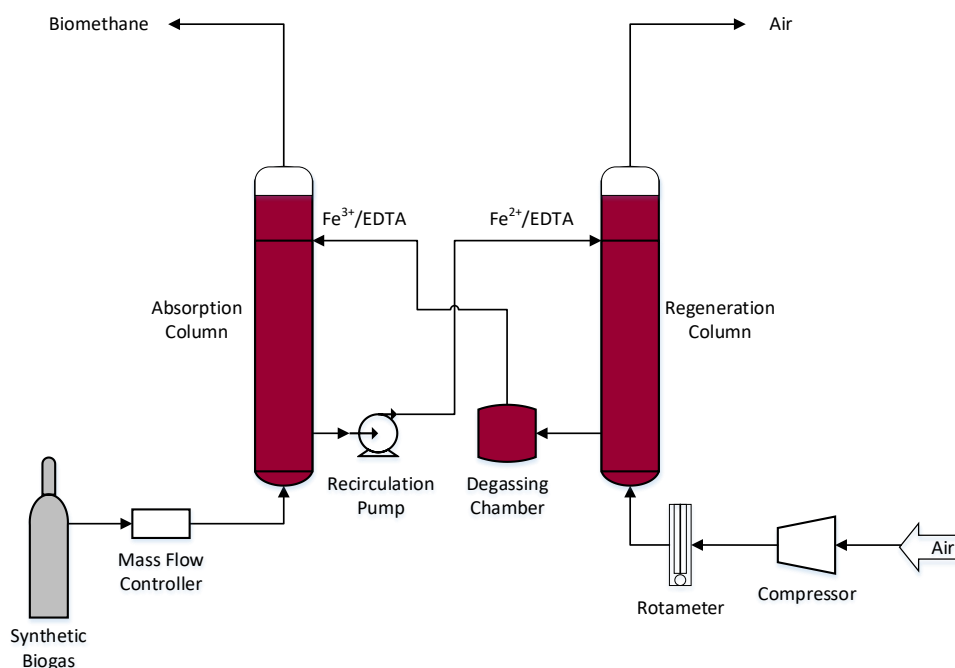
Figure 1. Schematic diagram of the experimental plant used for the integral upgrading of biogas.

2.3 Optimization of operational conditions by Taguchi's parameter design

Five operational parameters (control factors) were selected in order to optimize the simultaneous removal of CO_2 and H_2S from biogas, while preventing a negative O_2 and

N$_2$ stripping from the scrubbing solution to biomethane: Fe/EDTA molarity (M), inorganic carbon concentration (IC), biogas flow rate (B), air flow rate (A) and recirculating liquid flow rate (L). M is an important factor determining the absorption of H$_2$S, while IC mediates the absorption of CO$_2$ from biogas. B, L and A were selected in order to study the influence of the recycling liquid/biogas ratio in the absorption column on biomethane quality and the efficiency of CO$_2$ desorption in the regeneration column. Four different levels were established for each control factor based on literature (Table 1). The selection of such a high number of factor levels aimed at elucidating the behavior of the parameters within the tested range by identifying quadratic and sinusoidal effects [15]. The main objective of this work was the minimization of the concentration of CO$_2$, H$_2$S, O$_2$ and N$_2$ and the maximization of the concentration of CH$_4$ in the upgraded biogas.

Table 1. Factors and levels for the optimization of biogas upgrading.

Factor	Acronym	Levels			
		1	2	3	4
Fe/EDTA Molarity (M)	M	0.00	0.05	0.01	0.03
Inorganic Carbon Concentration (mg L^{-1})	IC	10000	4000	6000	8000
Biogas Flow rate (mL min^{-1})	B	20	10	30	40
Air Flow rate (mL min^{-1})	A	800	200	500	1000
Recycling Liquid Flow rate (mL min^{-1})	L	10	5	20	30

The optimization of these five factors at the four different levels was carried out using a Taguchi's orthogonal array L$_{16}$(4^5) design [16]. The selected orthogonal array was a highly fractional factorial design that reduced the number of experiments from 4^5=1024 (required by a full factorial design) to 16, while still obtaining statistically meaningful results. The experimental design matrix resulted in a set of 16 experiments whose factor level combinations are depicted in Table 2. The order of execution of the 16 experiments was randomized and each test accounted for triplicate measurements of the upgraded biogas under steady state in order to be able to estimate the residual error of the analysis of variance (ANOVA). Each experiment lasted eight hours and a new solution was prepared for each replica. The pH value in each was set at 9.25 in order to allow an effective CO$_2$ and H$_2$S capture from biogas at ambient pressure, while allowing a cost-

effective air-aided CO_2 desorption. The investigation of the influence of pH on CO_2 and H_2S removal was not necessary since its beneficial effect has been previously proved in many publications [17,18]. Mean results of the 16 experiments are shown in Table 2 and the results for each triplicate measurement are included in Table S1.

Table 2. Taguchi's $L_{16}(4^5)$ orthogonal array and mean results.

Trial	M	IC	B	A	L	CO$_2$ (%)	H$_2$S (%)	O$_2$ (%)	N$_2$ (%)	CH$_4$ (%)
	Control factors and levels					Mean results of biomethane concentration				
1	1	1	1	1	1	4.5	0.035	0.27	0.85	94.4
2	1	2	2	2	2	2.7	0.046	0.37	1.65	95.3
3	1	3	3	3	3	5.6	0.034	0.21	0.66	93.5
4	1	4	4	4	4	4.3	0.025	0.14	0.83	94.7
5	2	1	2	3	4	4.0	0.000	0.21	0.93	94.8
6	2	2	1	4	3	17.8	0.000	0.16	0.64	81.4
7	2	3	4	1	2	24.9	0.000	0.25	0.78	74.0
8	2	4	3	2	1	17.9	0.000	0.11	0.84	81.2
9	3	1	3	4	2	3.2	0.011	0.12	0.96	95.7
10	3	2	4	3	1	19.7	0.007	0.08	0.45	79.8
11	3	3	1	2	4	3.1	0.025	0.10	0.30	96.5
12	3	4	2	1	3	1.7	0.038	0.25	1.78	96.2
13	4	1	4	2	3	6.3	0.014	0.16	0.56	93.0
14	4	2	3	1	4	12.2	0.023	0.14	0.61	87.0
15	4	3	2	4	1	1.6	0.006	0.51	0.74	97.2
16	4	4	1	3	2	2.5	0.016	0.20	0.39	96.9

At this point it should be highlighted that the $L_{16}(4^5)$ design has 15 degrees of freedom, (*d.f.*), which were all consumed by the use of five four-level control factors ($5×(4−1)=15$ *d.f.*). No degrees of freedom were left to evaluate the interactions between control factors and therefore, interactions were integrated with the main effects according with the triangular interactions table of the design [19]. The L_{16} array was initially designed for two-level experiments. However, sets of mutually interactive columns of the $L_{16}(2^{15})$ array were merged to accommodate five four-level factors in order to use it for four-level experiments. The merging of mutually interactive columns minimized the above mentioned interactions [20].

The influence of the control factors on the performance of biogas upgrading was evaluated using ANOVA. The interactions between the most influential control factors, although integrated with the main effects, were graphically represented to evaluate their

contribution. A Duncan´s multiple range test was carried out in order to identify significant differences amongst factor levels and therefore to select those levels providing the optimum response during biogas upgrading [21].

All statistical calculations (ANOVA, Duncan's test and predictive models) were performed using Excel (Microsoft, USA).

2.4 Analytical procedures

The concentrations of CH_4, CO_2, H_2S, O_2 and N_2 in the biogas and biomethane were determined using a gas chromatograph coupled with a thermal conductivity detector (Varian CP-3800 GC-TCD, Palo Alto, USA) and equipped with a CP-Molsieve 5A (15 m × 0.53 mm × 15 μm) and a CP-PoraBOND Q (25 m × 0.53 mm × 15 μm) columns. The injector and detector temperatures were maintained at 150 and 175 °C, respectively. Helium was used as the carrier gas at 13.7 mL min^{-1}. The pH was determined with an Eutech Cyberscan pH 510 (Eutech Instruments, The Netherlands). IC concentration was analyzed using a Shimadzu TOC-VCSH analyzer (Japan).

3. Results and discussion

3.1 Influence of the control factors on biogas upgrading

The ANOVA of the experimental results (Table 3) demonstrated that the molarity of the Fe/EDTA solution was a significant factor influencing the concentration of all five biogas components according to the significance level used in all statistical calculations ($p < 0.05$). The concentration of inorganic carbon in the solution directly impacted on the concentrations of CO_2, N_2 and CH_4, while the concentrations of CO_2, O_2, N_2 and CH_4 were affected by the biogas and recycling liquid flow rates. Finally, the air flow rate in the stripping column also influenced the CO_2, H_2S, N_2 and CH_4 content.

Table 3. ANOVA for the regular analysis.

Factor	p Value				
	CO_2	H_2S	O_2	N_2	CH_4
M	$5.51 \times 10^{-35*}$	$2.50 \times 10^{-7*}$	$8.52 \times 10^{-3*}$	$4.26 \times 10^{-3*}$	$2.21 \times 10^{-36*}$
IC	$1.01 \times 10^{-29*}$	7.04×10^{-1}	7.77×10^{-2}	$2.92 \times 10^{-2*}$	$3.55 \times 10^{-31*}$
B	$2.62 \times 10^{-33*}$	1.39×10^{-1}	$1.41 \times 10^{-5*}$	$5.24 \times 10^{-7*}$	$6.21 \times 10^{-34*}$
A	$3.72 \times 10^{-20*}$	$2.58 \times 10^{-2*}$	2.63×10^{-1}	$9.43 \times 10^{-3*}$	$1.75 \times 10^{-22*}$
L	$6.75 \times 10^{-22*}$	2.48×10^{-1}	$4.36 \times 10^{-2*}$	$3.48 \times 10^{-2*}$	$1.02 \times 10^{-23*}$

*A significance level $p < 0.05$ was used to identify significant factors

The effect of each factor level on the mean values of the concentration of the target components in the upgraded biogas is shown in Fig. 2. The CO_2 concentration values obtained at the four different levels of M (0, 0.01, 0.03, 0.05) were 4.3, 6.9, 5.6 and 16.1%, respectively. At this point, it is important to stress that this increase in CO_2 concentration recorded at the highest molarity was not likely influenced by the increase in the molarity of the Fe/EDTA solution but related to the interactions of the different levels of each control factor assessed in the test at 0.05 M of Fe/EDTA. A decrease in CO_2 concentration was observed at increasing inorganic carbon concentration, from 13.1% at 4000 mg IC L^{-1} to 4.5% at 10000 mg IC L^{-1}. The pH values recorded in each experiment in the absorption column are collected in Table S2. A higher inorganic carbon concentration in the absorption solution entailed a higher pH and buffer capacity, which provided an enhanced transfer of CO_2. The increase in biogas flow rate brought about an increase in CO_2 concentration of the upgraded biogas, from 2.5% at 10 mL min^{-1} to 13.8% at 40 mL min^{-1}, as a result of the corresponding reduction in the biogas residence time in the absorption column. Air flow rates of 200, 500 and 1000 mL min^{-1} in the desorption column supported CO_2 concentrations of 7.5, 8.0 and 6.7%, respectively, while a higher CO_2 concentration value of 10.8% was recorded at 800 mL min^{-1}. Finally, CO_2 concentrations of 8.3 and 7.9% were achieved at recycling liquid flow rates of 5 and 20 mL min^{-1}, respectively; while a higher CO_2 concentration of 10.9% was recorded at 10 mL min^{-1}. A liquid flow rate of 30 mL min^{-1} provided a CO_2 concentration of 5.9% (Fig. 2a).

A decrease in H_2S concentration was observed as the Fe/EDTA molarity increased, from 0.035% at 0.00 M to 0.000% at a concentration of 0.05 M. These results can be explained by the capacity of the Fe/EDTA solution to partially oxidize the H_2S present in biogas. No clear correlation between the H_2S concentration and the air flow rate in the upgraded biogas was observed, with values of 0.021, 0.014, 0.024 and 0.011% at air flow rates of 200, 500, 800 and 1000 mL min^{-1}, respectively (Fig. 2b). The IC concentration, biogas and liquid flow rates did not exert a significant effect on the elimination of H_2S according to the statistical analysis at $p > 0.05$ (Table 3). The increase in biogas flow rate induced a slight decrease in H_2S levels, which suggests the interference of other factors since a decrease in biogas residence time in the absorption column should entail a reduction in H_2S removal efficiencies.
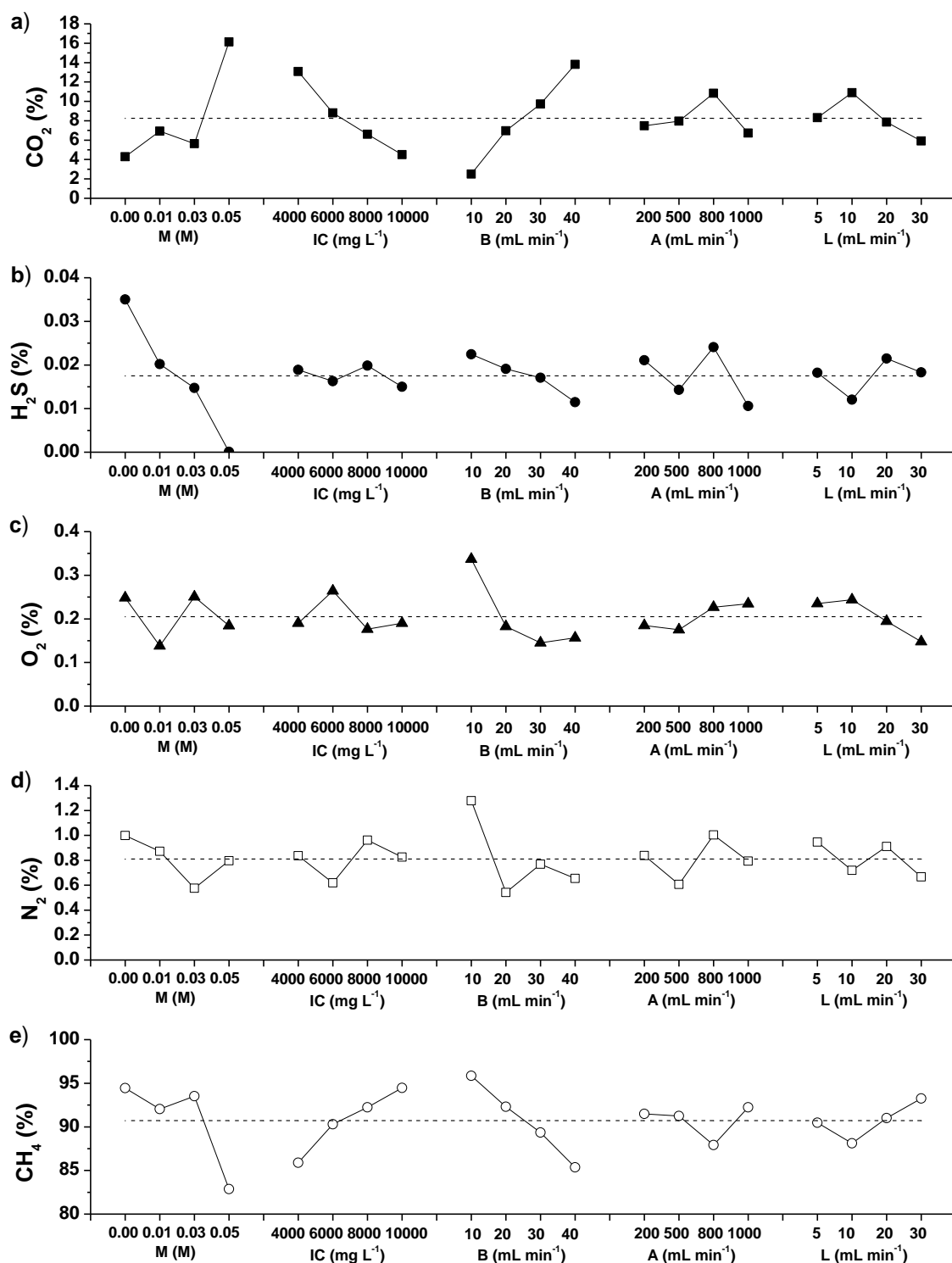
Figure 2. Influence of the control factors on the mean response of (a) CO_2 (■), (b) H_2S (●), (c) O_2 (▲), (d) N_2 (□) and (e) CH_4 (○) concentration in the upgraded biogas.

O_2 concentrations of 0.25, 0.14, 0.25 and 0.18% were recorded at Fe/EDTA molarities of 0.00, 0.01, 0.03 and 0.05 M, respectively. A decrease in O_2 concentration was observed at increasing biogas flow rates, from 0.34% at 10 mL min^{-1} to 0.16% at 40 mL min^{-1}, as a result of the enhanced dilution of the stripped oxygen. Finally, the decrease in O_2

concentration at increasing liquid flow rates, from 0.24% at a flow rate of 5 mL min^{-1} to 0.15% at a flow rate of 30 mL min^{-1}, suggests the interference of other factors, since a higher recycling liquid flow rate should entail a higher O_2 stripping (Fig. 2c). The IC concentration and air flow rate did not exert a significant effect on O_2 content (ANOVA test at p>0.05, Table 3).

Although all the parameters significantly influenced the elimination of N_2 (p < 0.05, Table 3), no clear correlations between N_2 concentration in the upgraded biogas and the experimental parameters were observed. The N_2 concentrations recorded at a Fe/EDTA molarity of 0.00, 0.01, 0.03 and 0.05 M were 1.00, 0.87, 0.58 and 0.80%, respectively. N_2 concentrations of 0.84, 0.62, 0.96 and 0.83% were recorded at IC concentrations of 4000, 6000, 8000 and 10000 mg L^{-1}, respectively. Similarly, N_2 concentrations of 1.28, 0.54, 0.77 and 0.65% were achieved at biogas flow rates of 10, 20, 30 and 40 mL min^{-1}, respectively, and of 0.84, 0.61, 1.00 and 0.79% at air flow rates of 200, 500, 800 and 1000 mL min^{-1}, respectively. Finally, recycling liquid flow rates of 5, 10, 20 and 30 mL min^{-1} supported N_2 concentrations of 0.95, 0.72, 0.91 and 0.67%, respectively (Fig 2d).

CH_4 concentrations in the upgraded biogas at Fe/EDTA molarities of 0.00, 0.01, 0.03 and 0.05 M were 94.4, 92.0, 93.5 and 82.9%, respectively. It is important to stress that the decrease in CH_4 concentration recorded at 0.05 M of Fe/EDTA was due to the high CO_2 concentration in the upgraded biogas likely caused by the interactions of the different levels of each control factor assessed in the tests at 0.05 M of Fe/EDTA. An increase in CH_4 concentration was observed at increasing IC concentrations, from 85.9% at 4000 mg IC L^{-1} to 94.5% at 10000 mg IC L^{-1}. The increase in biogas flow rate mediated a decrease in the CH_4 concentration of the upgraded biogas, from 95.9% at 10 mL min^{-1} to 85.4% at 40 mL min^{-1}. On the other hand, air flow rates of 200, 500 and 1000 mL min^{-1} in the stripping column supported CH_4 concentrations of 91.5, 91.2 and 92.2%, respectively, while a lower CH_4 concentration of 87.9% was observed at 800 mL min^{-1} when the medium contained the lowest IC concentration. Finally, recycling liquid flow rates of 5, 10, 20 and 30 mL min^{-1} corresponded to CH_4 concentrations of 90.5, 88.1, 91.0 and 93.3%, respectively (Fig. 2e).

In the particular case of CO_2, N_2 and CH_4 concentrations, the five control factors tested were decisive in order to fulfill any biomethane standard. The Fe/EDTA molarity and air flow rate were significant to minimize H_2S concentration, while the most relevant factors determining the O_2 concentration in the upgraded biogas were the liquid and biogas flow rates and the Fe/EDTA molarity.

3.2 Process optimization

A Duncan's multiple range test was performed in order to verify the optimal level for each control factor and to obtain the operational conditions optimizing the upgrading of biogas. The test was applied to the factors with a significant effect on the concentration of the different gases measured in the upgraded biogas. According to the test results, the combination of levels of each control factor that minimized the concentration of CO_2, H_2S, O_2 and N_2 in the upgraded biogas and maximized the concentration of CH_4 was M_4-IC_1-B_2-A_4-L_4, which corresponds to 0.03 M Fe/EDTA, 10000 mg IC L^{-1}, 10 mL min^{-1} of biogas flow rate, 1000 mL min^{-1} of air flow rate and 30 mL min^{-1} of liquid flow rate.

A visual analysis of the interaction between Fe/EDTA molarity and the inorganic carbon concentration was also performed by jointly representing the mean responses obtained for CO_2 and H_2S at the tested levels of Fe/EDTA molarity and IC (Fig. 3). According to this analysis, a change in Fe/EDTA molarity from 0.03 M to 0.05 entailed an increase in CO_2 concentration above 15% for IC levels ranging from 4000 to 8000 mg L^{-1}, but the impact is negligible if the maximum 10000 mg L^{-1} IC level is used, at which CO_2 concentration is around 5% independently of the Fe/EDTA concentration. On the other hand, a change in Fe/EDTA molarity from 0.03 to 0.05 M corresponded to changes in H_2S concentrations from 0.023, 0.006, 0.016 and 0.014% (at IC concentrations of 4000, 6000, 8000 and 10000 mg L^{-1}, respectively) to 0.000% regardless of the IC concentration level (Fig. 3b). Therefore, the optimum combination resulting from the Duncan's multiple range test (M_4-IC_1-B_2-A_4-L_4) can be changed to the optimum combination resulting from the analysis of interactions, M_2-IC_1-B_2-A_4-L_4: 0.05 M Fe/EDTA - 10000 mg L^{-1} IC- 10 mL min^{-1} biogas - 1000 mL min^{-1} air - 30 mL min^{-1} liquid.

The model equations for each design response, calculated with Excel using multiple linear regression (MLR) [22], can be represented by equations (9) to (13). The confidence

intervals of the coefficients were calculated as the product of the standard deviation of the coefficient and the student-t statistic for 0.05 significance level and n - k degrees of freedom, were *n* is the number of experiments (16) and *k* the number of model coefficients (6).
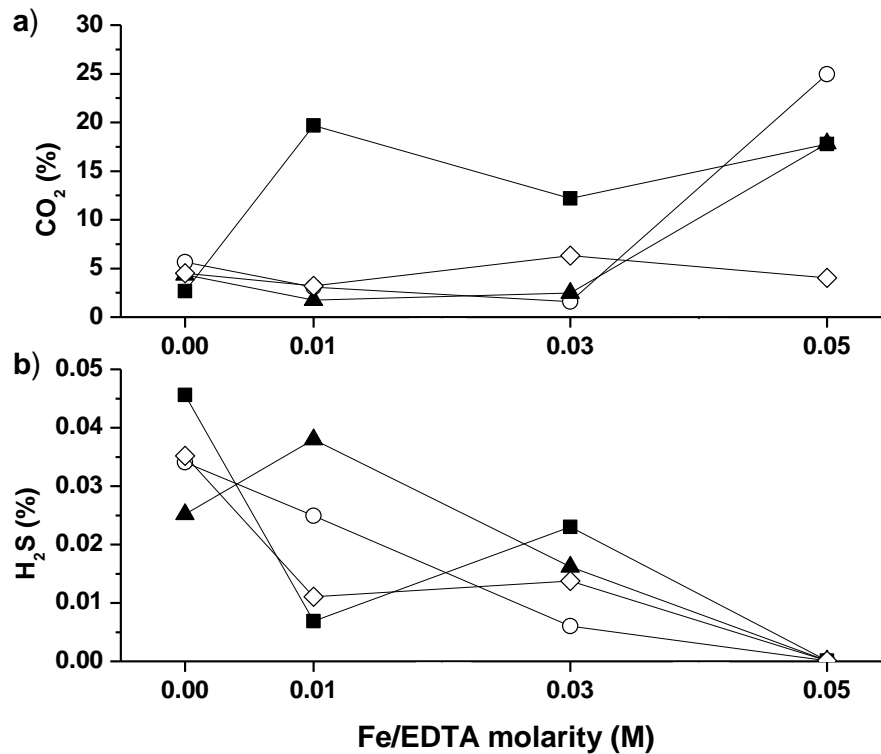
Figure 3. Effect of interactions between Fe/EDTA molarity and inorganic carbon concentration ((■) 4000, (○) 6000, (▲) 8000 and (◇) 10000 mg L^{-1}) on the concentrations of (a) CO_2 and (b) H_2S in the upgraded biogas.

$$CO_2 \ (\%) = 8.25 + 2.57M - 2.09IC + 2.75B + 0.13A - 0.86L \quad\quad (9)$$
$$R^2 = 81.0\%$$
$$H_2S \ (\%) = 0.0175 - 0.0079M - 0.0006IC - 0.0026B - 0.0014A + 0.0009L \quad (10)$$
$$R^2 = 77.8\%$$
$$O_2 \ (\%) = 0.205 - 0.003M - 0.007IC - 0.043B + 0.015A - 0.024L \quad\quad (11)$$
$$R^2 = 53.6\%$$
$$N_2 \ (\%) = 0.811 - 0.060M + 0.023IC - 0.123B + 0.023A - 0.043L \quad\quad (12)$$
$$R^2 = 32.3\%$$
$$CH_4 \ (\%) = 90.72 - 2.50M + 2.08IC - 2.58B - 0.17A - 0.93L \quad\quad (13)$$
$$R^2 = 79.1\%$$

where R^2 is the coefficient of determination. Low R^2 values may result from uncontrolled influencing factors (noise factors) or unconsidered quadratic interactions or effects. The biomethane composition predicted by the model under the operational conditions optimized according to the analysis of the effect of interactions (M_2-IC_1-B_2-A_4-L_4) was: $CO_2 = 2.6\%$, $H_2S = 0.004\%$, $O_2 = 0.25\%$, $N_2 = 0.92\%$ and $CH_4 = 96.3\%$. These values comply with the requirements of most international biomethane standards ($CH_4 \geq 90$-95%, $CO_2 \leq 2$-4%, $O_2 \leq 1\%$ and negligible amounts of H_2S) [2,5,6].

Models with interactions and quadratic terms can be described by equations S1 to S5, which have been included in the supplementary material document, seem to fit better to the experimental data derived from the design of experiments (improving the coefficient of determination). However, the prediction of the concentration of CO_2, H_2S and CH_4 (7.0%, 0.000% and 92.1%, respectively) derived from these models for the experiment performed under the selected optimal conditions did not match the results obtained experimentally. The prediction from the models that only included the main effects was much closer to the experimental results, which ultimately supported the use of linear regression instead of quadratic interactions.

3.3 Continuous biogas upgrading operation

The optimal combinations of factor levels identified in the Duncan's multiple range test and in the analysis of the effect of interaction M × IC were not tested in any of the 16 experiments of the Taguchi´s $L_{16}(4^5)$ orthogonal array. Thus, both combinations were subsequently tested under continuous operation in order to confirm the expected results and to evaluate the stability of the process over time. The optimum Duncan test combination M_4-IC_1-B_2-A_4-L_4 (0.03 M - 10000 mg L^{-1} - 10 mL min^{-1} - 1000 mL min^{-1} - 30 mL min^{-1}) was tested from days 0 to 9, and the optimum combination derived from the analysis of the effect of interaction M × IC (M_2-IC_1-B_2-A_4-L_4: 0.05 M - 10000 mg L^{-1} - 10 mL min^{-1} - 1000 mL min^{-1} - 30 mL min^{-1}) was tested from days 9 to 19.

The CO_2 concentration in the biomethane using the optimum Duncan's test combination (stage I) was $1.5 \pm 0.3\%$, corresponding to CO_2 removal efficiencies (REs) of 95.1%. Biogas upgrading under the optimum combination from the analysis of the effect of interactions (stage II) entailed a CO_2 concentration of $1.4 \pm 0.2\%$, which corresponded to

CO_2-REs of 95.5% (Fig. 4a). These CO_2-REs were higher than those previously reported by Horikawa et al., [11], who recorded CO_2-REs ranging from 4.0% to 16.0% using an aqueous solution of 0.2 M Fe/EDTA in a system composed of an absorption and a regeneration column with a total volume of 0.82 L, and operated with a biogas flow rate of 1000 mL min^{-1} and a liquid flow rate of 83 mL min^{-1}. CO_2 absorption at industrial scale can be increased by operating at a high pH value in the scrubbing solution and by increasing the liquid to biogas ratio without compromising O_2 and N_2 levels in biomethane. The former would increase the gas-liquid concentration gradient in the biogas absorption column, while the latter would increase both the overall mass transfer coefficient between the liquid and the biogas and the total absorption capacity of the column.

H_2S concentration during stage I was 0.013 ± 0.004%, corresponding to H_2S-REs of 96.8%, while the increase in Fe/EDTA concentration from 0.03 to 0.05 M applied in stage II resulted in a complete removal of H_2S from biogas (Fig. 4b). These results confirmed that the analysis of the effect of interactions provided the best combination of operational parameters due to its capacity to completely remove H_2S from biogas. These results were superior than those previously reported by Horikawa et al., [11], who recorded H_2S-REs of 90.0% in a similar experimental set-up operated at 0.2 M Fe/EDTA, a biogas flow rate of 1000 mL min^{-1} and a liquid flow rate of 83 mL min^{-1}. Likewise, Schiavon Maia et al., [12] reported H_2S-REs of 91.4% in a similar system configuration operated at 0.2 M Fe/EDTA, with biogas and liquid flow rates of 340 mL min^{-1}.

The O_2 concentration in the upgraded biogas remained roughly constant in both stages, the recorded values being 0.37 ± 0.11% and 0.29 ± 0.03% for stages I and II, respectively (Fig. 4c). On the other hand, the N_2 concentration recorded during stage I was 1.17 ± 0.24% and 0.97 ± 0.08% during stage II (Fig. 4d).
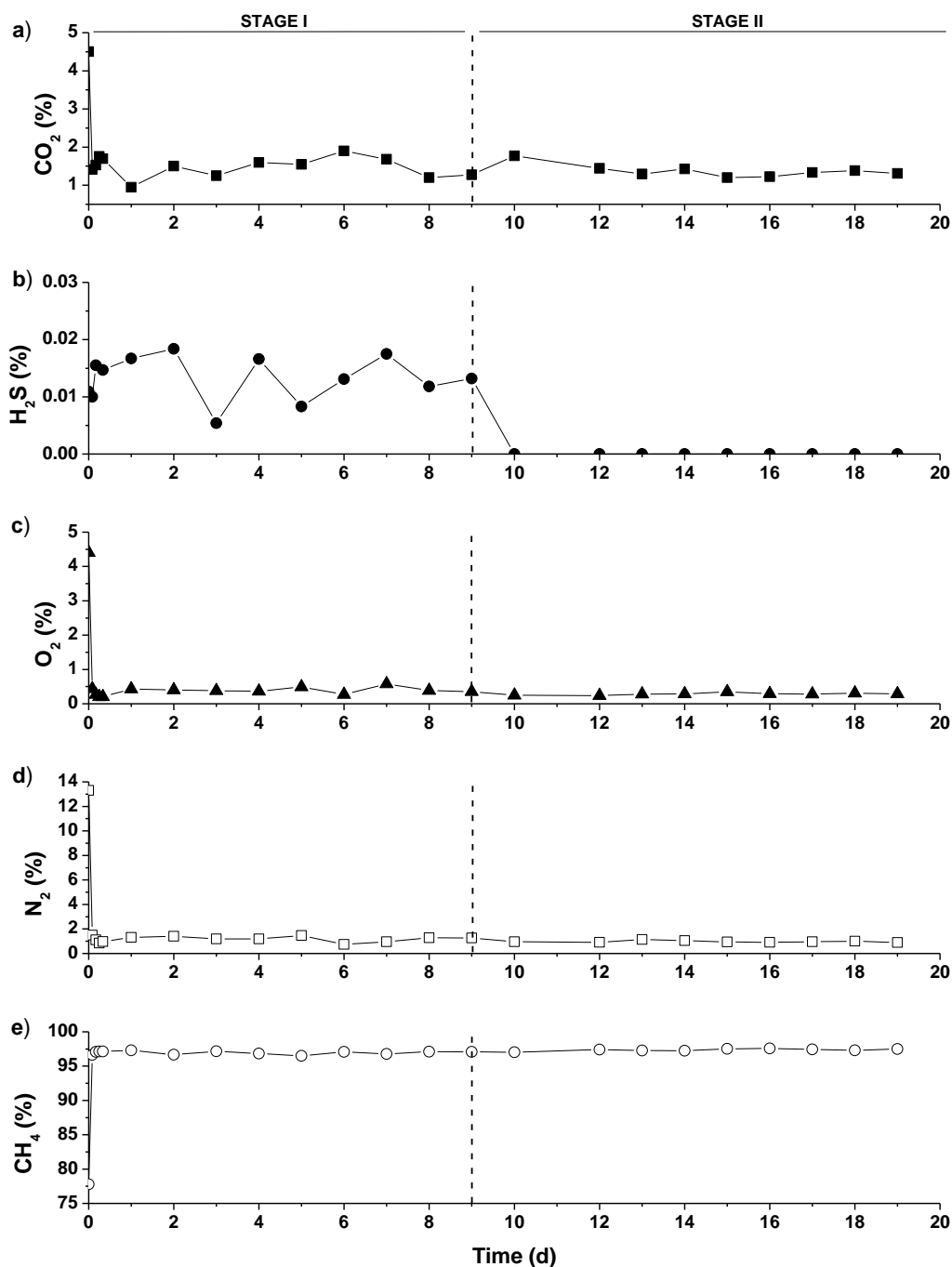
Figure 4. Time course of the concentration of (a) CO_2 (■), (b) H_2S (●), (c) O_2 (▲), (d) N_2 (□) and (e) CH_4 (○) in the upgraded biogas.

Finally, CH_4 concentrations in the upgraded biogas of $97.0 \pm 0.3\%$ in stage I and $97.4 \pm 0.2\%$ in stage II were achieved (Fig. 4e). These high CH_4 concentration values together with the high CO_2-REs and H_2S-REs confirmed that this innovative technology represents a superior option for the upgrading of biogas compared with conventional biological or physicochemical technologies. These results confirmed that the use of this single step technology at ambient temperature and pressure, and without continuous chemical

addition, was feasible since the biomethane obtained during stage I and II complied with the European Biomethane Standard EN 16723 for injection into natural gas grids or use as a vehicle fuel ($CH_4 \geq 90\text{-}95\%$, $CO_2 \leq 2\text{-}4\%$ and $O_2 \leq 1\%$) [2,5,6]. A siloxane and water removal would be however required to fulfill the above mentioned biomethane Standard. The results also confirmed the values predicted by the model equations resulting from the experimental design and support the use of fractional factorial experimental designs in optimization of multifactor processes.

Despite a new chemical solution was prepared for each replica when assessing the upgrading capacity of each series of operational conditions, the Fe/EDTA/carbonate solution herein proposed can be used during long operational periods. Thus, the absorbed CO_2 decreases the pH of the scrubbing solution, which is further restored as a result of the air-aided CO_2 stripping. Similarly, H_2S is oxidized using Fe^{3+} following equation 6, and the resulting Fe^{2+} is regenerated in the stripping column according to equation 8.

The main limitation encountered during the continuous operation of this technology was foam formation in the regeneration column due to the high air flow rate used (1000 mL min^{-1}). To overcome this problem, 10.0 mL of antifoam 204 (Sigma-Aldrich, USA) were added on day 6 and 2.0 mL were added on days 7, 8 and 13. For the design of the absorption and stripping columns at industrial scale it is important to consider the fact that the air flow required in the regeneration column is significantly higher than the biogas flow pumped into the absorption column. This results in the need of larger regeneration columns compared to the absorption column. The sulphur produced from H_2S oxidation throughout the continuous operation was easily recoverable from the bottom of both columns at the end of the process.

3.4 Energy study

An energy analysis was conducted in order to obtain the power consumption of this technology for the upgrading of 300 Nm^3 h^{-1} of biogas. Power consumption for biogas sparging in the absorption column and air sparging in the regeneration column were calculated according to Eq. (14), and the power required for liquid recirculation between both columns was calculated according to Eq. (15).

$$E_{gas} = \frac{Q_{gas} \times \Delta P}{0.7} \tag{14}$$

$$E_{liq} = \frac{Q_{liq} \times \rho \times g \times H}{0.7} \tag{15}$$

where Q_{gas} is the flowrate of biogas or air (m^3 s^{-1}), ΔP is the pressure drop (kPa), Q_{liq} is the flowrate of liquid between both columns (m^3 s^{-1}), H is water column height (m), ρ is the water density (kg m^{-3}), g is the Earth gravity constant (m s^{-2}).

The electricity demand of the system accounted for 0.02 kW-h $(Nm^3)^{-1}$ of biogas treated. This low value of the Fe/EDTA/carbonate-based scrubbing process compare positively with the 0.2 – 0.3 kW-h $(Nm^3)^{-1}$ of biogas treated of conventional processes such as water or organic solvent scrubbing, pressure swing adsorption and membrane separation.

4. Conclusions

This study demonstrated the effectiveness and stability of Fe/EDTA/carbonate-based scrubbing for the simultaneous removal of H_2S and CO_2 from biogas. This innovative process was able to operate at ambient pressure and temperature, and without external chemical addition, which supported an energy demand 10 times lower than their physical/chemical counterparts. The experimental Taguchi´s design revealed the significant influence of Fe/EDTA molarity, inorganic carbon concentration, biogas flow rate, air flow rate and recirculating liquid flow rate on biomethane quality. An effective optimization via a Duncan's multiple range test and an analysis of the effect of interactions provided the optimal conditions for each control factor in order to maximize the CH_4 content and minimize CO_2, O_2, N_2 and H_2S content in biomethane. Continuous biogas upgrading in this innovative absorption-stripping system at 0.05 Fe/EDTA, 10000 mg IC L^{-1}, 10 mL biogas min^{-1}, 1000 mL air min^{-1} and 30 mL liquid min^{-1} supported concentrations of $CH_4 > 97\%$, $CO_2 < 2\%$ and $O_2 < 1\%$, which complied with most international biomethane regulations.

Acknowledgements

References

[1] D. Andriani, A. Wresta, T.D. Atmaja, A. Saepudin, A review on optimization production and upgrading biogas through CO_2 removal using various techniques, Appl. Biochem. Biotechnol. 172 (2014) 1909–1928. https://doi.org/10.1007/s12010-013-0652-x.

[2] R. Muñoz, L. Meier, I. Diaz, D. Jeison, A review on the state-of-the-art of physical/chemical and biological technologies for biogas upgrading, Rev. Environ. Sci. Bio/Technology. 14 (2015) 727–759. https://doi.org/10.1007/s11157-015-9379-1.

[3] European Biogas Association, EBA Statistical Report 2018, (2018). https://www.europeanbiogas.eu/eba-statistical-report-2018/ (accessed December 2, 2019).

[4] E. Ryckebosch, M. Drouillon, H. Vervaeren, Techniques for transformation of biogas to biomethane, Biomass and Bioenergy. 35 (2011) 1633–1645. https://doi.org/10.1016/j.biombioe.2011.02.033.

[5] European Committee for Standardization, UNE EN 16723-2:2018 Natural gas and biomethane for use in transport and biomethane for injection in the natural gas network - Part 2: Automotive fuels specification, (2018). https://www.en-standard.eu/une-en-16723-2-2018-natural-gas-and-biomethane-for-use-in-transport-and-biomethane-for-injection-in-the-natural-gas-network-part-2-automotive-fuels-specification/ (accessed December 10, 2019).

[6] European Committee for Standardization, UNE EN 16723-1:2017 Natural gas and biomethane for use in transport and biomethane for injection in the natural gas network - Part 1: Specifications for biomethane for injection in the natural gas network, (2017). https://www.en-standard.eu/une-en-16723-1-2017-natural-gas-and-biomethane-for-use-in-transport-and-biomethane-for-injection-in-the-natural-gas-network-part-1-specifications-for-biomethane-for-injection-in-the-natural-gas-network/ (accessed December 10, 2019).

[7] I. Angelidaki, L. Treu, P. Tsapekos, G. Luo, S. Campanaro, H. Wenzel, P.G. Kougias, Biogas upgrading and utilization: current status and perspectives, Biotechnol. Adv. 36 (2018) 452–466. https://doi.org/10.1016/j.biotechadv.2018.01.011.

[8] B. Stürmer, F. Kirchmeyr, K. Kovacs, F.H. Gba, D.C. Rea, I. Atee, J.S. Eba, S. Proietti, Technical-economic analysis for determining the feasibility threshold for tradable biomethane certificates, (2016) 1–24. http://www.ergar.org/wp-content/uploads/2018/07/BIOSURF-D3.4.pdf (accessed June 1, 2020).

[9] O.W. Awe, Y. Zhao, A. Nzihou, D.P. Minh, N. Lyczko, A review of biogas utilisation, purification and upgrading technologies, Waste and Biomass Valorization. 8 (2017) 267–283. https://doi.org/10.1007/s12649-016-9826-4.

[10] H.J. Wubs, A.A.C.M. Beenackers, Kinetics of H_2S absorption into aqueous ferric solutions of edta and hedta, Ind. Eng. Chem. Res. 32 (1993) 2580–2594. https://doi.org/10.1021/ie00023a022.

[11] M.S. Horikawa, F. Rossi, M.L. Gimenes, C.M.M. Costa, M.G.C. Da Silva, Chemical absorption of H_2S for biogas purification, Brazilian J. Chem. Eng. 21 (2004) 415–422. https://doi.org/10.1590/S0104-66322004000300006.

[12] D.C. Schiavon Maia, R.R. Niklevicz, R. Arioli, L.M. Frare, P.A. Arroyo, M.L. Gimenes, N.C. Pereira, Removal of H_2S and CO_2 from biogas in bench scale and the pilot scale using a regenerable Fe-EDTA solution, Renew. Energy. 109 (2017) 188–194. https://doi.org/10.1016/j.renene.2017.03.023.

[13] L.M. Frare, M.G.A. Vieira, M.G.C. Silva, N.C. Pereira, M.L. Gimenes, Hydrogen sulfide removal from biogas using Fe/EDTA solution: Gas/Liquid contacting and sulfur formation, Environ. Prog. Sustain. Energy. 29 (2010). https://doi.org/10.1002/ep.

[14] W. Li, J. Zhao, L. Zhang, Y. Xia, N. Liu, S. Li, S. Zhang, Pathway of FeEDTA transformation and its impact on performance of NOx removal in a chemical absorption-biological reduction integrated process, Sci. Rep. 6 (2016) 18876. https://doi.org/10.1038/srep18876.

[15] R. Roy, Design of experiments using the Taguchi approach: 16 steps to product and process improvement, John Wiley & Sons, New York, USA, 2001, p. 560.

[16] G. Taguchi, S. Chowdhury, Y. Wu, Taguchi's quality engineering handbook, John Wiley & Sons, New York, USA, 2004, p. 1696.

[17] E. Tilahun, E. Sahinkaya, B. Çalli, Effect of operating conditions on separation of H_2S from biogas using a chemical assisted PDMS membrane process, Waste and Biomass Valorization. 9 (2018) 2349–2359. https://doi.org/10.1007/s12649-018-0226-9.

[18] E. Tilahun, E. Sahinkaya, B. Çalli, A hybrid membrane gas absorption and biooxidation process for the removal of hydrogen sulfide from biogas, Int. Biodeterior. Biodegradation. 127 (2018) 69–76. https://doi.org/https://doi.org/10.1016/j.ibiod.2017.11.015.

[19] N. Logothetis, H.P. Wynn, Quality through design: experimental design, off-line quality control, and Taguchi's contributions, Oxford University Press, Michigan, USA, 1994, p. 464.

[20] S.H. Park, J. Antony, Robust design for quality engineering and six sigma, in: World Scientific, Danvers, USA, 2008, p. 545.

[21] P.J. Ross, Taguchi techniques for quality engineering: loss function, orthogonal experiments, parameter and tolerance design, McGraw-Hill, New York, USA, 1988, p. 329.

[22] B.G.M. Vandeginste, D.L. Massart, L.M.C. Buydens, S. De Jong, P.J. Lewi, J. Smeyers-Verbeke, Handbook of chemometrics and qualimetrics: Part B, Elsevier Science, Amsterdam, The Netherlands, 1998, p. 867.

Supplementary material

Optimization of a chemical scrubbing process based on a Fe-EDTA-carbonate based solvent for the simultaneous removal of CO_2 and H_2S from biogas

David Marín[1, 2, 3], Marisol Vega[2, 4], Raquel Lebrero[1, 2], Raúl Muñoz*[1, 2]

[1] Department of Chemical Engineering and Environmental Technology, School of Industrial Engineering, Valladolid University, Dr. Mergelina, s/n, 47011, Valladolid, Spain.

[2] Institute of Sustainable Processes, Dr. Mergelina, s/n, 47011, Valladolid, Spain.

[3] Universidad Pedagógica Nacional Francisco Morazán, Boulevard Centroamérica, Tegucigalpa, Honduras.

[4] Department of Analytical Chemistry, University of Valladolid, Campus Miguel Delibes, Paseo Belén 7, 47011 Valladolid, Spain.

* Corresponding author: mutora@iq.uva.es

Table S1. Biomethane composition for the orthogonal array

a)

	Control factors and levels					Biomethane composition in steady state replicate 1				
Trial	**M**	**IC**	**B**	**A**	**L**	**CO_2 (%)**	**H_2S (%)**	**O_2 (%)**	**N_2 (%)**	**CH_4 (%)**
1	1	1	1	1	1	4.2	0.025	0.24	0.84	94.7
2	1	2	2	2	2	2.7	0.063	0.28	1.72	95.3
3	1	3	3	3	3	5.1	0.033	0.22	0.73	93.9
4	1	4	4	4	4	3.8	0.017	0.22	0.69	95.3
5	2	1	2	3	4	3.8	0.000	0.31	1.27	94.6
6	2	2	1	4	3	18.4	0.000	0.16	0.60	80.8
7	2	3	4	1	2	25.3	0.000	0.21	0.65	73.8
8	2	4	3	2	1	17.8	0.000	0.07	1.29	80.9
9	3	1	3	4	2	3.0	0.011	0.15	0.77	96.1
10	3	2	4	3	1	18.7	0.021	0.18	0.84	80.3
11	3	3	1	2	4	2.8	0.031	0.07	0.42	96.7
12	3	4	2	1	3	1.9	0.039	0.46	1.97	95.6
13	4	1	4	2	3	6.2	0.041	0.16	0.55	93.0
14	4	2	3	1	4	11.4	0.028	0.16	0.67	87.8
15	4	3	2	4	1	1.6	0.006	0.32	1.11	97.0
16	4	4	1	3	2	2.6	0.000	0.10	0.25	97.1

b)

Trial	Control factors and levels					Biomethane composition in steady state replicate 2				
	M	IC	B	A	L	CO$_2$ (%)	H$_2$S (%)	O$_2$ (%)	N$_2$ (%)	CH$_4$ (%)
1	1	1	1	1	1	4.3	0.039	0.28	0.90	94.5
2	1	2	2	2	2	2.4	0.031	0.48	1.72	95.3
3	1	3	3	3	3	5.9	0.037	0.19	0.63	93.3
4	1	4	4	4	4	5.0	0.035	0.10	0.40	94.5
5	2	1	2	3	4	3.6	0.000	0.25	1.12	95.0
6	2	2	1	4	3	17.6	0.000	0.16	0.62	81.6
7	2	3	4	1	2	25.0	0.000	0.16	0.47	74.3
8	2	4	3	2	1	18.4	0.000	0.16	0.56	80.9
9	3	1	3	4	2	3.3	0.006	0.10	1.06	95.6
10	3	2	4	3	1	20.1	0.000	0.01	0.13	79.8
11	3	3	1	2	4	3.6	0.022	0.12	0.33	96.0
12	3	4	2	1	3	1.4	0.044	0.16	1.68	96.7
13	4	1	4	2	3	6.4	0.000	0.15	0.55	92.9
14	4	2	3	1	4	12.8	0.026	0.11	0.55	86.5
15	4	3	2	4	1	1.5	0.006	0.61	0.56	97.3
16	4	4	1	3	2	2.3	0.000	0.21	0.49	97.0

c)

Trial	Control factors and levels					Biomethane composition in steady state replicate 3				
	M	IC	B	A	L	CO$_2$ (%)	H$_2$S (%)	O$_2$ (%)	N$_2$ (%)	CH$_4$ (%)
1	1	1	1	1	1	4.9	0.042	0.29	0.80	93.9
2	1	2	2	2	2	2.9	0.042	0.36	1.52	95.2
3	1	3	3	3	3	6.0	0.032	0.20	0.63	93.2
4	1	4	4	4	4	4.3	0.024	0.11	1.41	94.2
5	2	1	2	3	4	4.6	0.000	0.08	0.40	95.0
6	2	2	1	4	3	17.3	0.000	0.018	0.69	81.9
7	2	3	4	1	2	24.5	0.000	0.36	1.21	74.0
8	2	4	3	2	1	17.4	0.000	0.11	0.67	81.8
9	3	1	3	4	2	3.3	0.017	0.12	1.06	95.5
10	3	2	4	3	1	20.3	0.000	0.06	0.37	79.3
11	3	3	1	2	4	2.9	0.022	0.10	0.13	96.8
12	3	4	2	1	3	1.9	0.031	0.14	1.70	96.3
13	4	1	4	2	3	6.3	0.000	0.16	0.59	92.9
14	4	2	3	1	4	12.3	0.016	0.14	0.61	86.9
15	4	3	2	4	1	1.6	0.006	0.60	0.57	97.2
16	4	4	1	3	2	2.6	0.049	0.29	0.44	96.6

Table S2. Mean steady state pH for each experiment in the absorption column

Trial	M	IC	B	A	L	Initial pH	Final pH
1	1	1	1	1	1	9.25	8.80
2	1	2	2	2	2	9.24	8.75
3	1	3	3	3	3	9.24	8.96
4	1	4	4	4	4	9.24	8.73
5	2	1	2	3	4	9.23	8.80
6	2	2	1	4	3	9.26	7.60
7	2	3	4	1	2	9.22	7.91
8	2	4	3	2	1	9.22	8.01
9	3	1	3	4	2	9.25	8.90
10	3	2	4	3	1	9.23	8.04
11	3	3	1	2	4	9.23	8.79
12	3	4	2	1	3	9.25	9.00
13	4	1	4	2	3	9.22	8.67
14	4	2	3	1	4	9.22	8.21
15	4	3	2	4	1	9.22	8.87
16	4	4	1	3	2	9.22	8.91

The header "Control factors and levels" spans the columns M, IC, B, A, L.

Models with interactions and quadratic effects

The model equations for each design response using quadratic effects can be represented by equations (S1) to (S5).

$$CO_2\ (\%) = 4.621 + 1.752M - 1.938IC + 2.680B - 0.536L - 0.309M \times C + 0.645M \times B - 1.765B \times IC + 0.981M \times M + 1.141A \times A - 0.555L \times L \quad \text{(S1)}$$
$$R^2 = 98.7\%$$

$$H_2S\ (\%) = 0.0265 - 0.0072M - 0.0027B - 0.0012A + 0.0030L - 0.0002M \times IC + 0.0022M \times B + 0.0030IC \times B - 0.0042A \times A + 0.0002L \times L \quad \text{(S2)}$$
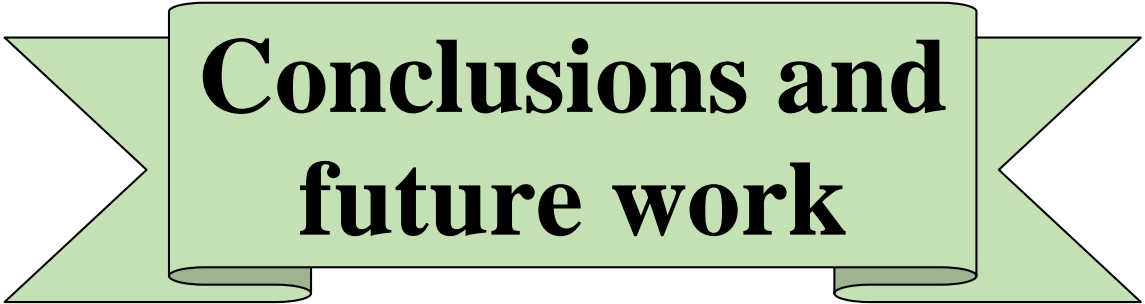$$R^2 = 96.5\%$$

$$O_2\ (\%) = 0.220 - 0.003IC - 0.037B + 0.055A - 0.014L + 0.028M \times IC + 0.013M \times B + 0.013IC \times B - 0.006IC \times IC \quad \text{(S3)}$$
$$R^2 = 71.5\%$$

$$N_2 \text{ (\%)} = 0.600 - 0.089M + 0.039IC - 0.119B + 0.002L + 0.021IC \times IC +$$
$$0.069M \times M + 0.017M \times IC + 0.065M \times B + 0.006IC \times B \qquad \text{(S4)}$$
$$R^2 = 52.2\%$$

$$CH_4 \text{ (\%)} = 94.34 - 1.66M + 1.91IC - 2.52B + 0.54L + 0.29MIC - 0.70M \times B +$$
$$1.70IC \times B - 1.06M \times M - 1.08A \times A + 0.57L \times L \qquad \text{(S5)}$$
$$R^2 = 98.2\%$$

Conclusions and future work

Conclusions and Future Work

The potential of innovative technologies that allow a simultaneously removal of H_2S and CO_2 from biogas in a single step process was evaluated in this thesis.

A preliminary evaluation of the performance of photosynthetic biogas upgrading outdoors under favorable environmental climatic conditions (summer period) was conducted. **Chapter 1** constitutes the first proof of concept of the bioconversion of biogas to biomethane coupled to centrate treatment during summer time in an outdoors pilot scale HRAP interconnected to an external AC via settled broth recirculation. In this work, the feasibility of a zero-effluent process operation was also demonstrated. The results herein obtained demonstrated that temperature played a key role on the efficiency of biogas upgrading at low-to-medium alkalinities, while high alkalinities enhanced process robustness against daily temperature variations.

In **Chapter 2** the influence of the diffuser type and L/G ratios on biogas upgrading performance in an outdoor pilot scale HRAP was evaluated. This study demonstrated the statistically significant influence of the type of biogas diffuser and the L/G ratio in the AC on the quality of the biogas obtained. L/G ratios > 1.0 supported a significant decrease in CO_2 concentration in the upgraded biogas along with a superior stripping of O_2 and N_2 from the scrubbing solution regardless of the type of diffuser used. The use of a 2 μm metallic diffuser provided the highest CH_4 concentration in the upgraded biogas regardless of the L/G ratio (94.6-95.2%), which complied with most international regulations for biomethane injection into natural gas grids.

Chapters 3 and 4 described for the first time the influence of seasonal variation on biogas upgrading coupled with digestate treatment in an outdoors pilot scale HRAP. The high alkalinity and pHs of the cultivation broth were identified as key parameters to maintain a constant biomethane composition during the daytime. The CO_2, H_2S and CH_4 concentrations recorded in the biomethane complied with most international regulations for biogas injection into natural gas grids during most of the year. Hence, this study confirmed the year-round feasibility of outdoors algal-bacterial processes for the

simultaneous removal of CO_2 and H_2S from biogas coupled to nutrient removal from digestates.

The validation of the potential of photosynthetic biogas upgrading under outdoors conditions finally involved the evaluation of three innovative operational strategies to improve the quality of biomethane under unfavorable environmental conditions and to increase the sustainability of the process by operating the process without external alkalinity supplementation (**Chapter 5**). This study confirmed that the use of a greenhouse, the direct CO_2 stripping in the photobioreactor via air stripping during winter conditions, and the use of digestate as a make-up water during summer conditions can provide a biomethane that fulfilled most international biomethane standards.

In **Chapter 6**, a validation of photosynthetic biogas upgrading at semi-industrial scale was carried out. This work constitutes, to the best of our knowledge, the first validation of photosynthetic biogas upgrading in a pilot-scale semi-closed photobioreactor interconnected to an AC under outdoors conditions. The L/G ratio and the alkalinity in the AC were identified as key parameters influencing the quality of the final biomethane at pilot scale, with optimum values of 0.5 and 634 ± 48 mg L^{-1}, respectively. The implementation of the optimum operating parameters during continuous operation resulted in a biomethane with CO_2 concentrations of <0.1%-1.4%, H_2S<0.5ppm$_v$ and CH_4 contents of 94.1-98.9%, which complied with most international regulations for methane injection into natural gas grids.

Chapter 7 confirmed that PPB represent an innovative biological platform for the simultaneous treatment of PWW and upgrading of biogas under photo-anaerobic conditions. Dilution of PWW with tap water plays a key role on the efficiency of wastewater treatment and biogas upgrading. CH_4 concentrations of 93.3% along with TOC removals of 90% can be achieved using PPB under infrared radiation, which complied with most international regulations for biogas use as a vehicle fuel.

In **Chapter 8**, an absorption-stripping process based on an aqueous solution of Fe-EDTA for the simultaneous removal H_2S and CO_2 from biogas with minimum O_2 and N_2 desorption was optimized. This work revealed the influence of parameters such as Fe-

EDTA molarity, carbonate concentration, and biogas, air and liquid flow rates on the biogas upgrading process. Continuous biogas upgrading in this innovative absorption-stripping system at 0.05 Fe/EDTA, 10000 mg IC L^{-1}, 10 mL biogas min^{-1}, 1000 mL air min^{-1} and 30 mL liquid min^{-1} supported concentrations of $CH_4 > 97\%$, $CO_2 < 2\%$ and $O_2 < 1\%$, which complied with most international biomethane regulations.

An energy assessment was herein conducted in order to compare the power consumption of the different technologies investigated in this thesis. In this sense, the power consumption required for the upgrading of 300 Nm^3 h^{-1} of biogas in algal-bacterial photobioreactors accounts for 0.08 kW-h (Nm^3)$^{-1}$ of biogas treated. On the other hand, the upgrading of biogas in the absorption-stripping process required an energy demand of 0.02 kW-h (Nm^3)$^{-1}$ of biogas treated. This lower energy consumption of absorption-stripping process compared with photosynthetic upgrading represents a key advantage of this physical/chemical technology and stands 1 order of magnitude lower than conventional water or organic solvent scrubbing. Unfortunately, a realistic evaluation could not be conducted for the upgrading of biogas with PPB due to the fact that this technology has only been tested batchwise in gas-tight photobioreactors at laboratory scale and no consistent data under continuous operation is available.
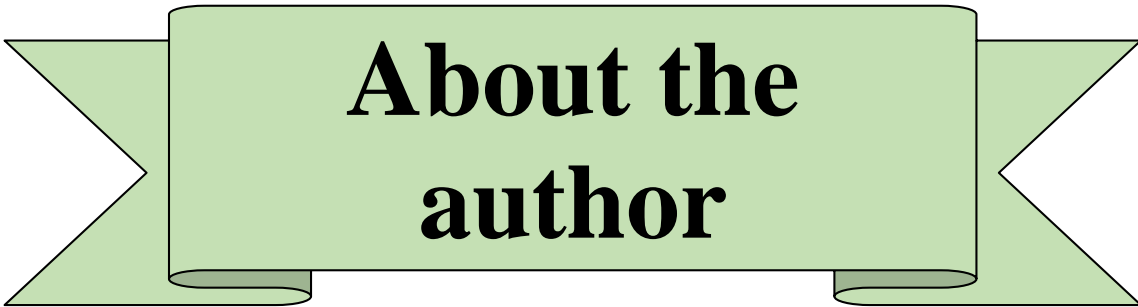
The ability of the different technologies to support a simultaneous treatment of wastewater and nutrient recovery represents also a key indicator. Algal-bacterial systems are able to recover nutrients from agricultural wastewaters and digestate from wastewater plants, without generation of effluents. Similarly, PPB have the ability to perform a simultaneous upgrading of biogas and treatment of piggery wastewater, which entails a significant environmental advantage due to the high pollutant load of this type of wastewater. The novel absorption-stripping process here developed does not support any treatment or nutrient recovery from wastewaters.

Finally, the production of biomass is an important indicator based on its potential valorization as a feedstock for multiple industries. Algae-bacterial systems generate a biomass that can be used as fertilizer due to its high content of nitrogen, phosphorous, phytohormones and fungicides. On the other hand, biomass from PPB systems can be used as fertilizer in agricultural sector, or feed additive in animal husbandry sector. In

addition, PPB biomass can be used as a pigments source due to the presence of carotenoids and bacteriochlorin, which serve as a raw material for the manufacture of red, purple or orange dyes and color additives in the food industry.

Despite the advances carried out in the present thesis in the simultaneous removal of H_2S and CO_2 from biogas in outdoors algal-bacterial photobioreactors, in PPB photobioreactors and in absorption-stripping systems based on an aqueous solution of Fe-EDTA, future research should focus on:

1. The optimization of continuous biogas under outdoors conditions at semi-industrial scale using other configurations of photobioreactors and in the semi-closed photobioreactor with other type of wastewaters

2. The validation of PPB-based biogas upgrading in continuous photobioreactors under indoor and outdoor conditions, and its subsequent scale-up.

3. The validation of biogas upgrading use of an absorption-stripping process based on an aqueous solution of Fe-EDTA at pilot-scale.

About the author

Biography

David Fernando Marín De Jesus (Tegucigalpa, Honduras, 1989) studied Chemical Engineering at Universidad Nacional Autónoma de Honduras. In September 2014, David was awarded with a scholarship from Universidad Pedagógica Nacional Francisco Morazán in order to conduct a Master degree at the University of Valladolid. In September 2014, he started a Master´s degree in Chemical Engineering at University of Valladolid, with a Final Master Thesis focused on the study of pharmaceutical and personal care products biodegradability in a completely mixed aerobic activated sludge reactor under the supervision of Dr. Rubén Irusta and Dr. Pedro García in September 2016.

In September 2016, David joined the Biological Gas Treatment and Microalgae Technology Research Group headed by associate professor Raquel Lebrero and associate professor Raúl Muñoz Torre within the Environmental Technology Group of the Department of Chemical Engineering and Environmental Technology – University of Valladolid. In July 2017, David was awarded with a PhD contract by the Regional Government of Castilla y León. His PhD thesis was focused on biogas upgrading in algal-bacterial photobioreactors under outdoors conditions, biogas upgrading using an innovative physical/chemical process based on Fe/EDTA and biogas upgrading in purple phototrophic bacteria photobioreactors (September 2016 - February 2021). During his PhD, David carried out a research stay of seven months at Universitat Politècnica de Catalunya-BarcelonaTech (2018, Spain).

Publications in International Indexed Journals

David Marín, Alessandro A. Carmona-Martínez, Saúl Blanco, Raquel Lebrero, Raúl Muñoz (2021) *Innovative operational strategies in photosynthetic biogas upgrading in an outdoors pilot scale algal-bacterial photobioreactor*. Chemosphere 264: 128470.

David Marín, Marisol Vega, Raquel Lebrero, Raúl Muñoz (2020) *Optimization of a novel chemical scrubbing process based on a Fe-EDTA-carbonate based solvent for the simultaneous removal of CO_2 and H_2S from biogas*. Journal of Water Process Engineering 37: 101476.

David Marín, Alessandro A. Carmona-Martínez, Raquel Lebrero, Raúl Muñoz (2020) *Influence of the diffuser type and liquid-to-biogas ratio on biogas upgrading performance in an outdoors pilot scale high rate algal pond*. Fuel 275: 117999.

David Marín, Antonio Ortíz, Rubén Díez-Montero, Enrica Uggetti, Joan García, Raquel Lebrero, Raúl Muñoz (2019) *Influence of liquid-to-biogas ratio and alkalinity on the biogas upgrading performance in a demo scale algal-bacterial photobioreactor*. Bioresource Technology 280: 112–117.

David Marín, Esther Posadas, Dimas García, Daniel Puyol, Raquel Lebrero, Raúl Muñoz (2019) *Assessing the potential of purple phototrophic bacteria for the simultaneous treatment of piggery wastewater and upgrading of biogas*. Bioresource Technology 281: 10–17.

David Marín, Esther Posadas, Patricia Cano, Víctor Pérez, Saúl Blanco, Raquel Lebrero, Raúl Muñoz (2018) *Seasonal variation of biogas upgrading coupled with digestate treatment in an outdoors pilot scale algal-bacterial photobioreactor*. Bioresource Technology 263: 58–66.

David Marín, Esther Posadas, Patricia Cano, Víctor Pérez, Raquel Lebrero, Raúl Muñoz (2018) *Influence of the seasonal variation of environmental conditions on biogas upgrading in an outdoors pilot scale high rate algal pond*. Bioresource Technology 255: 354–358.

Rebeca López-Serna, **David Marín-de-Jesús**, Rubén Irusta-Mata, Pedro Antonio García-Encina, Raquel Lebrero, María Fdez-Polanco, Raúl Muñoz (2018) *Multiresidue analytical method for pharmaceuticals and personal care products in sewage and sewage sludge by online direct immersion SPME on-fiber derivatization – GCMS*. Talanta 186: 506–512.

Esther Posadas, **David Marín**, Saúl Blanco, Raquel Lebrero, Raúl Muñoz (2017) *Simultaneous biogas upgrading and centrate treatment in an outdoors pilot scale high rate algal pond*. Bioresource Technology 232: 133–141.

Publications in Preparation

Sara Cantera, Peter Q. Fischer, Irene Sánchez-Andrea, **David Marín**, Diana Z. Sousa, Raúl Muñoz (2021) *Impact of the algal-bacterial community structure, physio-types and biological and environmental interactions on the performance of a high rate algal pond treating biogas and wastewater*. Algal Research (Under revision).

Book Chapters

María Rosario Rodero, Roxana Ángeles-Torres, **David Marín**, Israel Díaz, Alexandre Colzi, Esther Posadas, Raquel Lebrero, Raúl Muñoz (2018) *Biogas purification and upgrading technologies*. In: Biogas: Fundamentals, Process, and Operation. Edited by Meisam Tabatabaei. Springer-Nature. pp. 239-276. ISBN: 978-3-319-77335-3

Roxana Ángeles-Torres, **David Marín**, María del Rosario Rodero, Celia Pascual, Armando González-Sanchez, Ignacio de Godos, Raquel Lebrero, Raúl Muñoz (2020) *Biogas treatment for H$_2$S, CO$_2$ and other contaminants removal*. In: From Biofiltration to Promising Options in Gaseous Fluxes Biotreatment: Recent Developments, New Trends, Advances, and Opportunities. Edited by: Dumont E, Soreanu G. Elsevier. ISBN: 978012819064

Conference Participation

Oral Presentation

David Marín, Esther Posadas, Dimas García, Daniel Puyol, Raquel Lebrero, Raúl Muñoz (2019) *Assessing the potential of purple phototrophic bacteria for the simultaneous treatment of piggery wastewater and upgrading of biogas*. IWA Conference on Algal Technologies and Stabilization Ponds for Wastewater Treatment and Resource Recovery - IWAlgae2019. 01-02 July 2019. Valladolid, Spain.

David Marín, Esther Posadas, Raquel Lebrero, Raúl Muñoz (2017) *Biogas treatment with recovery of nutrients from centrate in an outdoors high rate algal pond through algae-bacteria systems*. IV Conferencia Internacional sobre Gestión Olores y COVs en el medio ambiente. 20-21 September 2017, Valladolid, Spain.

Raúl Muñoz, Esther Posadas, **David Marín**, Saúl Blanco, Raquel Lebrero (2017) *Biogas upgrading coupled with centrate treatment in an outdoors pilot scale high rate algal pond*. 1st IWA conference on Algal Technologies for Wastewater Treatment and Resource Recovery. 16-17 March 2017, Delft, The Netherlands.

Esther Posadas, **David Marín**, Raquel Lebrero, Raúl Muñoz (2016) *Simultaneous biogas upgrading and centrate treatment in outdoors algal-bacterial photobioreactors*. II Jornadas Nacionales de Bioprocesos para el tratamiento de aire. 17 November 2016, Valencia, Spain.

Poster Participation

David Marín, Raquel Lebrero, Raúl Muñoz, Rubén Díez-Montero, Joan García, Ivet Ferrer (2019) *Biogas production and upgrading in a microalgae-based system treating agricultural runoff: a pilot-scale study*. 16th World Congress on Anaerobic Digestion. 23-27 June 2019, Delft, The Netherlands.

David Marín, Antonio Ortíz, Enrica Uggetti, Joan García, Raquel Lebrero, Raúl Muñoz (2018) *Influence of Liquid/Gas ratio and alkalinity on photosynthetic biogas upgrading efficiency in an outdoors tubular photobioreactor*. 3rd International Conference on Alternative Fuels, Energy and Environment (ICAFEE): Future and Challenges. 28-31 October 2018, Nanjing, China.

López Serna R, Pérez Elvira S, Bolado S, Irusta R, Ortiz S, **Marín-de-Jesús D**, Martínez Paramo S, Hernando N, García Guzmán D, Posadas E, Pérez Lemus N, Díaz Curbelo A, Muñoz R, García-Encina P.A (2018) *Tratamiento de contaminantes emergentes en sistemas de tratamiento de aguas residuales y lodos*. XIII Congreso Español de Tratamiento de Aguas, 18-20 June 2018, León, Spain.

Rodero R, Lebrero R, **Marín D**, Lara E, Arbib Z, Muñoz R (2017) *Innovative technologies for a cost-effective biogas upgrading in wastewater treatment plants*. AlgaEurope 2017 Conference. 5-7 December 2017, Berlin, Germany.

David Marín, Esther Posadas, Patricia Cano, Raquel Lebrero, Raúl Muñoz (2017) *Daily evaluation of biogas upgrading in an outdoors pilot scale high rate algal pond*. International Conference on Alternative Fuels: Future and Challenges. 23-24 October 2017, Daegu, South Korea.

Esther Posadas, **David Marín**, Kumar G, Raquel Lebrero, Raúl Muñoz (2016) *Simultaneous biogas upgrading and centrate treatment in outdoors algal-bacterial photobioreactors*. International Conference on Alternative Fuels – ICAFEE 2016, 2-4 December Kayseri, Turkey.

Research Stays

Universitat Politècnica de Catalunya-BarcelonaTech (Spain) February 2018 – August 2018. Supervisor: Dr. Enrica Uggetti and Dr. Joan García. Scope: During this stay David investigated the biogas upgrading potential of an outdoors pilot-scale hybrid (semi-closed) horizontal tubular photobioreactor interconnected to an external absorption column. The influence of the liquid-to-biogas ratio and the alkalinity of the cultivation medium in the absorption column on the quality of the upgraded biogas was assessed and optimized. In addition, the photobioreactor was operated continuously under optimized process parameters.

Conferences Committee

Member of the Organizing Committee of the "IWA Conference on Algal Technologies and Stabilization Ponds for Wastewater Treatment and Resource Recovery - IWAlgae2019". 01-02 July 2019, Valladolid, Spain.

Member of the Organizing Committee of the "IV Conferencia Internacional sobre Gestión Olores y COVs en el medio ambiente". 20-21 September 2017, Valladolid, Spain.

Teaching and student mentoring

Lecturer in the cord course "Tecnología Ambiental y de Procesos" at the Industrial and Automatic Electronics Engineering degree of Valladolid University (14 h of teaching load in the academic year 2019-2020).

Co-supervisor of an undergraduate student Final Degree Project from the Chemical Engineering Degree at Valladolid University (2018). Student: Patricia Cano Arroyo. Title: Biomethane production and digestate nutrient recovery in High Rate Algal Pond photobioreactors.